Master thesis
MSc Applied Earth Sciences

Review and validation of settlement prediction methods for organic soft soils, on the basis of three case studies from the Netherlands

By

Christian Bernhard Houkes

14 July 2016

This page is intentionally left blank

Review and validation of settlement prediction methods for organic soft soils, on the basis of three case studies from the Netherlands

By

Christian Bernhard Houkes

Written in partial fulfilment of the requirements for the degree of

Master of Science
in Applied Earth Sciences
track Geo-Engineering

At the department of Geoscience and Engineering
faculty of Civil Engineering and Geosciences
Delft University of Technology

Graduation committee

Prof. Dr. C. Jommi	Delft University of Technology Faculty of Civil Engineering and Geosciences Department of Geoscience and Engineering Geo-Engineering Section
Dr. Ir. D.J.M. Ngan-Tillard	Delft University of Technology Faculty of Civil Engineering and Geosciences Department of Geoscience and Engineering Geo-Engineering Section
Ir. K.J. Reinders	Delft University of Technology Faculty of Civil Engineering and Geosciences Department of Hydraulic Engineering Hydraulic Structures and Flood Risk
Ir. A. Kleinjan	Sweco Nederland Department of Coasts and Rivers Geotechnical Engineering Group

A digital version of this thesis is available at: http://repository.tudelft.nl/.

This page is intentionally left blank

Preface

The completion of this thesis marks the end of eight months of intensive research, with the ultimate personal goal of graduating from university – thus this document also marks the end of a chapter in life. It has been a chapter full of interesting but also rather complex contents, which challenged me and never made me feel bored for even just a single moment.

The past eight months have increased my interest and curiosity for the many aspects and topics related to engineering geology and to applied earth sciences in general, but also made me aware of the fact that even after more than five years of study there is still so much to learn in this field of science. Therefore I am very happy to have gotten the opportunity to perform this practically relevant research in commission and with support of Sweco Nederland. I have not only been able to gain a lot of new skills and knowledge, but along the way also to get some exciting insight in engineering practice, which so far I hardly have been able to get due to the rather busy study schedules at Delft University of Technology. The latter is definitely not meant in a negative way, since I am convinced that I got the best possible education in my field of interest that I was reasonably able to follow, equipping me with an invaluable and worldwide acknowledged set of skills and knowledge that will certainly prove to be useful during the rest of my provisional career in engineering geology.

Even though the findings presented in this thesis are not very spectacular, I still hope and do believe that they can and will be of advantage to geotechnical engineering decisions in practice and/or to subsequent academic research.

Acknowledgements

Although this thesis is the final product of an individual research project, it was only with the indispensable support of many people that this was realised. First of all, I would like to thank the members of my graduation assessment committee: Prof. Dr. C. Jommi, Dr. Ir. D.J.M. Ngan-Tillard and Ir. K.J. Reinders from Delft University of Technology, and Ir. A. Kleinjan from Sweco Nederland, who were patient oracles for my burning questions. Their valid criticism, suggestions, helpful answers to questions and general guidance kept me on track to meet the research goal and objectives and to successfully finalize this research.

Dr. Ir. D.J.M. Ngan-Tillard deserves to be acknowledged additionally for the fact that primarily thanks to her interesting lectures, starting already in the first undergraduate year, my initial interest and final study choice in the direction of engineering geology was solidified.

I should not forget to thank Dr. E. Ponzoni from Delft University of Technology, who assisted in selecting and providing the data for the case Leendert de Boerspolder, and who answered also various questions specifically with regard to soil compressibility parameter determination.

Furthermore, I would like to thank my colleagues at Sweco Nederland, most notably but not limited to Ir. E. van der Putte, Ir. N. van Leeuwen and Ing. G. van Doornik, who made me feel welcome from the very beginning and who were also supportive by answering my daily practical questions.

Last but not least, I would like to thank my close family members, i.e. my parents and my sister, who have supported and encouraged me throughout all the stressful years of study, providing me with comfort and love.

Christian Bernhard Houkes
Nieuwerkerk aan den IJssel, the Netherlands
7 July 2016

Abstract

Organic soft soils pose technical challenges in construction industry due to their extraordinary compressibility and deformability, which is an issue of particular relevance in the densely populated Netherlands, of which more than half of the land surface is covered by such soft soils. Uncertainty and variability in settlement predictions for constructions on soft soils are large, however: in the order of tens of percent. Therefore this research was performed, reviewing and validating one-dimensional settlement prediction methods for organic soft soils, in particular peat, with focus on long-term settlements. Special interest for validation concerned relatively unknown and uncommon, but seemingly simple and easy to use, empirical settlement prediction methods or compressibility parameter correlations.

The main goal was to designate the best performing 1D settlement prediction method with an optimum balance between accuracy, usability and time investment, taking also into account the soil parameter determination including preceding sampling and testing procedures. This goal was met in part based on thorough literature review of seven different settlement prediction methods or models: Terzaghi, Buisman, Koppejan, Bjerrum, Fokkens, De Glopper, Den Haan (a,b,c-Isotachs), and in part based on subsequent validation of the latter four of those methods. Validations were performed on the basis of soil test data and field measurements, collected in the course of three actual field research or construction projects in the Netherlands.

The literature review additionally comprised a critical review and comparison of different soil compression test methods: incremental loading (IL) oedometer, constant-rate-of-strain (CRS) and K_0-CRS tests. Furthermore, previous studies regarding the reliability of settlement predictions, addressing many error sources including sample disturbance, were reviewed and summarised.

In one case, soil compressibility characteristics had to be determined from raw IL and CRS compression test data, for which various methods of soil parameter determination were studied and performed. This includes in particular the determination of the preconsolidation pressure, for which four different methods were applied and mutually compared: Casagrande's method, Butterfield's method, the work-per-unit-volume method [Becker et al., 1987] and the pore pressure method.

The main conclusions from the settlement prediction methods validations are that the soil compressibility parameter correlations and the method of Fokkens are best to be disregarded for use in engineering practice because of their unreliability or their considerable practical limitations. Of the remaining settlement prediction methods, the a,b,c-Isotachs model theoretically provides the most sound and versatile description of soil behaviour upon compression as well as unloading. However based on the data available and the results obtained, the Bjerrum model yielded the most accurate results in practice, with final settlement estimations for a more than 350 years old dike within 12% of the actual settlement.

Table of contents

1 Introduction

The findings presented in this thesis are the result of a Master (MSc) graduation research project regarding settlement predictions for soft organic soils in general. More specifically, the research comprises a comparative analysis of different settlement prediction methods by means of a validation with field measurements, as well as an assessment of the suitability of different laboratory test methods, the quality of data and interpretation of the test results. This research was performed at the request of *Sweco Nederland* (formerly *Grontmij*), part of Europe's largest architecture and engineering consultancy company.

The next chapter provides an introduction to the research topic in the form of a problem statement, from which the relevance of this study will become clear. Following thereafter, in chapter 1.2 the main goal and objectives of the research are stated, after which in chapter 1.3 its scope is narrowed down. Then, in chapter 1.4, a concise overview of the available data resources is provided. Finally, the outline of the thesis is elucidated in chapter 1.5.

1.1 Problem statement

In March 2016 the population of the Netherlands surpassed the number of 17 million. These 17 million people live on a land surface area totalling no more than 33,900 km^2, resulting in an average population density of about 500 inhabitants/km^2. As a result, the Netherlands rank amongst the top 30 of most densely populated countries in the world, being outranked only by geographically exceptional microstates and island nations [CBS, 2016; CIA, 2016]. Providing housing and ensuring mobility for such an amount of people on such a small area poses a challenge not just to public authorities, but also to the engineers who have to design and realise the solutions for the questions and problems related hereto.

However more than half of the Dutch subsurface – particularly in the most densely populated western provinces – is made up of soft soils like clay and peat; at some places down to a depth of more than 20 metres (view Figure 1-1, and refer to Appendix A for soil maps). Therefore, problems due to the high deformability and compressibility of such soils are likely to be expected, which includes not just uniform vertical settlements, but even more so differential settlements, resulting for instance in cracking masonry walls and wavy rails or road surfaces. Indeed, many of these problems (especially on the long term) have occurred – and still occur. No need to say that such failures can cause enormous financial damages in terms of restoration or reconstruction works. So the Dutch construction industry inevitably has to deal with these settlement-related problems, which are preferably to be avoided, or at least desired to be controlled and limited as much as possible during the construction and lifetime of any kind of (infra)structure.

In order to limit these problems, special construction methods have been developed. Whereas buildings are usually founded on piles reaching down into the firm Pleistocene sand below the Holocene soft soils, this practice would be simply too costly for the thousands of kilometres of roads and railway infrastructure in the country. A possible solution might seem to use lightweight fill materials. However there are limits to the amounts that are reasonably applicable, again mainly from a financial viewpoint since these materials often have to be imported from far abroad or have to be fabricated artificially. As a most commonly applied alternative, earth fills and embankments are erected and left to rest, i.e. to settle, for several months in order to limit the residual settlements occurring during execution of the above-ground works and the subsequent lifetime of the structure. Residual settlements can be further limited by application and – after a waiting period – removal of a so-called "extra surplus height", thus increasing the amount of settlement in an early (non-critical) phase of construction. In order to decrease the waiting period, drainage may be applied in addition, thus allowing a sooner start or continuation of above-ground construction works.

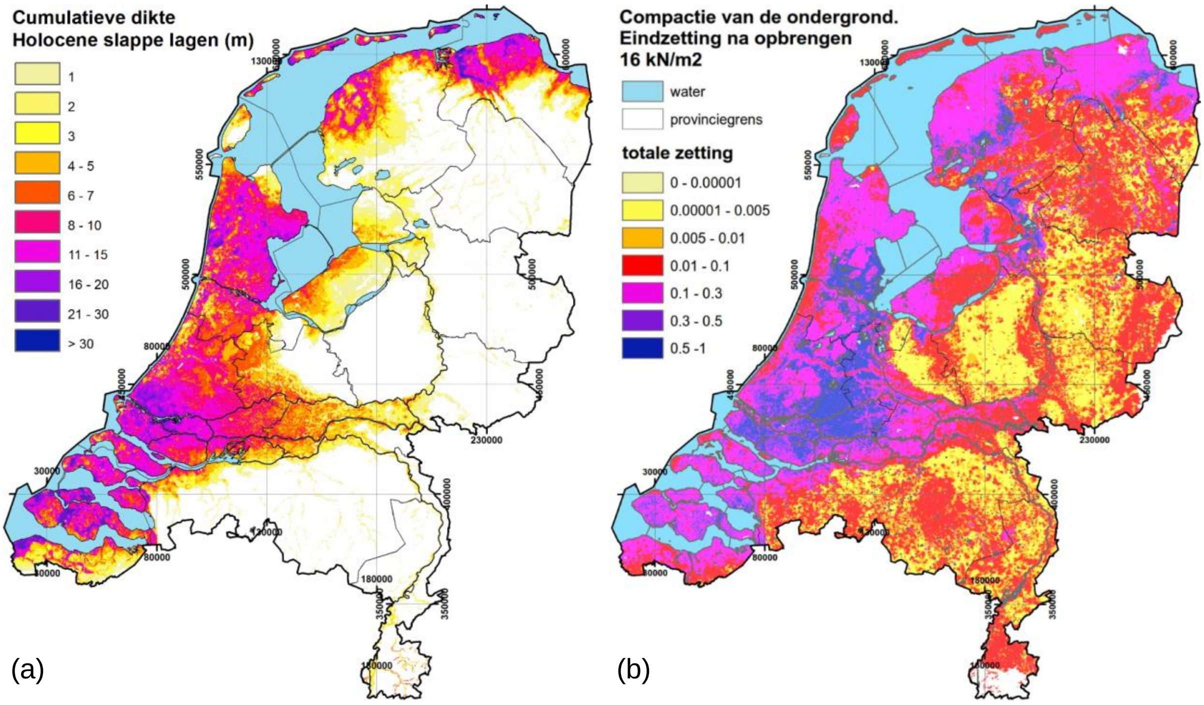

Figure 1-1: Maps depicting the thickness and the compressibility of soft soils in the Netherlands, where:
a) shows the spatial distribution and cumulative thickness of Holocene soft soils [TNO, 2014a], and
b) presents an estimation of the final settlements that would hypothetically occur if a uniform surcharge of 16 kPa (approx. 1 m of dry sand) would be applied at the surface [TNO, 2014b].
A detailed representation of soil types occurring in the Netherlands, presently as well as historically, and the changes therein over time, can be found in Appendix A.

However all of these special construction techniques are laborious, costly and time consuming, so it is very undesirable to over-dimension the mitigation measures, or to apply such techniques when they would not be necessary at all. In order to choose the most appropriate construction method and/or mitigation measures, first of all a good understanding of the settlement process in general, as well as the ability to accurately *predict* settlements, is required. The importance of accurate settlement predictions is highlighted by the fact that usually the executing party has to meet contractually agreed settlement requirements as per client's request: if these requirements are not fulfilled, the executer will not get paid for that part of the job, or he has to return for maintenance and revision in case of a DBM (Design, Build and Maintain) contract form.

Many different methods exist to predict settlements: analytical as well as numerical, but all using empirical soil compressibility parameters. However even after almost a century of research in soil mechanics, the accuracy of settlement predictions still leaves a lot to be desired: actual settlement measurements of construction projects are often found to deviate from predictions considerably, not only with regard to the final settlements, but likewise with regard to the development of the settlement over time, i.e. the shape of the time-settlement curve. Just for example, a general rule of thumb for the uncertainty margin of settlement predictions is a startling 30% [CROW, 2004].

The cause for this poor performance of settlement prediction models is sometimes readily attributed to the large uncertainty and spread in test results for soil parameter determination. However it is premature to conclude that this is the main source of uncertainty, since multiple potential error sources and uncertainties in the entire process chain from ground investigation, to calculation and modelling, up until the actual construction works, have an influence on the reliability and accuracy of a settlement prediction (refer to chapter 3.3). Moreover, performing more tests and/or thorough statistical analysis is expensive and maybe not effective at all, since the ground itself already is intrinsically variable. Therefore quantitative attribution of uncertainty to a particular action or parameter is very difficult.

Furthermore, different prediction models require different soil parameters, some of which might be more complicated and/or costly to obtain than others, whilst their value in terms of a (possibly) higher accuracy of the resulting prediction is unclear. In Dutch geotechnical engineering practice, still the Koppejan method (refer to section 3.2.3) is often applied, due to its ease of use, the large amount of experience gained in using it, and the relatively simple and standardised methods of parameter determination. Nevertheless there are multiple reasons to believe that this method is not the most accurate one, although some improvements have been adopted over time. However the accuracy of multiple settlement prediction methods has rarely been analysed comparatively in detail by means of validation with field measurements: so far only one recent attempt of such a field validation is known, namely in the case of the Bloemendalerpolder as part of the Geo-Impuls research programme, which is elucidated further in section 4.1.1.

Whereas the primary phase of soil compression, i.e. consolidation, is considered to be understood and predictable sufficiently well, much less certainty exists about the processes and causes that underlie the phase of secondary compression, or creep. In this regard, peat is a particularly troublesome material, since not only the short term (primary) compressibility is amongst the largest of all soils, but even after 40 years embankments on peat often continue to settle at rates in the order of 1 cm per year [A. Kleinjan, pers. comm.]. Similar rates are also achieved by ground *subsidence* (to be distinguished from settlement; refer to section 2.2.3) in peat areas, which even adds to the settlement. Peats owe their high compressibility to their unique physical properties such as, amongst others, exceptionally high porosity, water content and organic matter content (refer to chapter 2.1 for more information with regard to material characteristics).

So it may become clear that several questions and practical problems concerning the prediction and mitigation of settlements are still unanswered or unsolved, as well as there is plenty of room for improvement of predictions. Therefore, *Sweco Nederland* requested to investigate and shed some more light on the above mentioned issues related to the prediction of settlements, specifically for one of the most problematic of soft soils: peat.

1.2 Research goal and objectives

Based on the experiences gained by geotechnical engineers employed at *Sweco*, a main research goal was formulated, further subdivided into a number of objectives, which together incorporate the topics or problems of most interest concerning the prediction of settlements in peat soil.

1.2.1 Main goal

Designate the best performing 1D settlement prediction method, with an optimum balance between accuracy, usability and time investment, taking also into account the soil parameter determination including preceding sampling and testing procedures.

1.2.2 Objectives

1) Obtain a good understanding of the applicability, advantages and possible shortcomings or limitations of the (historically) most important or distinctive settlement prediction models, namely: Terzaghi, Keverling Buisman, Koppejan, Bjerrum, Fokkens, De Glopper and Den Haan (a,b,c-Isotachs).
2) Select the most practically interesting methods (namely: Koppejan, Bjerrum, Fokkens, De Glopper, Den Haan) and find out which one is most accurate in practice, especially on the long term, by validation with actual field settlement measurements.
3) Try to assess which of these models is most effective and efficient considering also the time and complexity of obtaining or interpreting the required soil parameters. Particular interest concerns Fokkens and De Glopper because of their presumed simplicity.

4) Identify the probable causes for uncertainty and variability in these models: think for instance about sampling techniques, preparation & testing procedures, data interpretation, model geometry etc.
5) Critically review and compare the different contemporary laboratory test methods incremental loading (IL), constant rate of strain (CRS) and K_0-CRS for soil compressibility parameter determination, and assess their suitability and reliability to provide input to the different settlement prediction models.
6) Provide recommendations on how to reduce the uncertainty and to improve the accuracy of settlement predictions, regarding the entire process from site investigation to modelling results.

1.3 Scope

This research project comprises an extensive literature study regarding settlement prediction models as well as a quantitative comparison and validation of different such models. Furthermore, different laboratory soil compression test methods are reviewed and assessed with regard to their suitability to obtain soil compressibility parameters, which includes the interpretation of soil compression test results and a subsequent data quality assessment.

Although the settlement prediction models and underlying theory that are reviewed in this study are generally applicable for multiple types of soft soils, the current research will focus on the vertical settlement behaviour of *organic* soils, and of those *peat* in particular. Note, that settlement is to be distinguished from subsidence, as explained in section 2.2.3. Stability-related issues of dikes or embankments will not be regarded in this study.

The accuracy of settlement prediction methods will be assessed mainly with regard to their long-term performance, which is dominated by secondary compression. However it is not intended to apply the technique of settlement curve fitting and hence make a better estimation of the local soil properties and/or expected final settlement. Instead it is desired to evaluate specifically *initial* settlement predictions, based on *initially* available soil parameters.

Finally, all models investigated are one-dimensional (1D). Several of those are implemented in the computer programme *D-Settlement* developed by *Deltares*, which is the most often used settlement prediction software by engineering consultancy companies in the Netherlands. This is mainly because it is fairly easy to learn, quicker and therefore cheaper to use when compared to more complex 2D or even 3D finite element modelling (FEM) software packages. The *D-Settlement* software was also used for multiple settlement predictions and subsequent validations in the course of the current research, if possible, depending on the particular model being investigated.

1.4 Available data

The data resources that were used in the course of this research comprise multiple ground investigation reports, geotechnical laboratory test data as well as various field monitoring data, produced and collected in the context of actual construction projects or field and lab tests. Monitoring data consist inter alia of periodic measurements of settlement beacons and hydrostatic profile gauges, contained in tables or spreadsheets. The laboratory test results were either in the form of unprocessed raw data sheets, as for case No. 3, or in the form of technical laboratory test reports containing already interpreted tabulated test results for the other cases. The data are either publicly available (case No. 1), or were provided either by *Sweco* (case No. 2) or by TU Delft (case No. 3).

In total three different cases were investigated in the course of this research, each being introduced and described in much more detail in chapter 4.1, namely:

1) Bloemendalerpolder: “Proefterpen” (trial mounds) project;
2) Amstelhoek: N201 road bypass construction project;
3) Leendert de Boerspolder: induced dike collapse trial site.

1.5 Thesis outline

This thesis is divided into five main parts, which are indicated by the first digit in the headings numbering format, and named as follows: **1** Introduction, **2** Background knowledge, **3** Literature review, **4** Data analysis, and **5** Summary and conclusions. Each one of these main parts is subdivided into chapters, which are further subdivided into sections, which may be subdivided once more into subsections.

The first and current part provides the essential introduction to the current research by means of a problem statement, goal and objectives, scope and an overview of the available data.

The second part is intended to act as a general reference regarding peat as a material and settlement analysis. It may provide the less knowledgeable reader with basic knowledge, or else refresh one's memory with regard to the specific terminology in the actual field of study. This part starts with a chapter (2.1) regarding the general physical properties, formation, classification systems and geotechnical engineering aspects of peat. After that, chapter 2.2 addresses more specifically the theory of consolidation and settlement analysis.

The third part comprises an extensive literature review regarding different phases in the prediction of settlements. Starting with chapter 3.1, the most common laboratory test methods for the determination of soil compressibility characteristics will be critically reviewed and compared. Chapter 3.2 provides in chronological order a thorough review of the most important or distinctive 1D settlement prediction methods, with special emphasis on their respective limitations or advantages. Chapter 3.3 finally presents a complete summary of the findings of a previous study concerning the reliability and accuracy of settlement predictions.

The fourth part is dedicated to the results of the analysis, comparison and validation of the settlement prediction models based on the case studies. It starts with project descriptions of the cases that were investigated (4.1). Following in chapter 4.2 the specific methods of research including data acquisition, calculations, modelling and validation are explained in detail. Chapter 4.3 subsequently presents the results, which are then analysed and discussed in chapter 4.4.

The fifth and last main part contains a general summary of the work done and the findings obtained, followed by the conclusions and recommendations, after which a list of references can be found. The appendices attached at the very end of the thesis contain chiefly maps, plans, tabular data overviews, calculation results and graphs, which are referred to in the body text of the thesis.

2 Background knowledge

2.1 Geological and geotechnical characteristics of peat

This chapter will introduce to the basic but unique geological and geotechnical characteristics of organic soils in general and peat in particular, namely its general physical properties, origin and formation (genesis), classification and specific engineering aspects.

The information presented in the following sections is a synthesis of numerous sources including soil mechanics textbooks, namely: Berendsen (2008), Den Haan & Kruse (2007), Huat et al. (2014), Knappett & Craig (2012), Mesri & Ajlouni (2007), Neher (2008), STOWA (2012), TAW (1987), TAW (1996) and Verry et al. (2011). In favour of overall readability, repeated references to any of these will be omitted, except for figures and quotations.

2.1.1 Definition and classification of organic soils

Although technically any substance containing carbon is called "organic", in geoscience and geotechnics an organic soil is one that contains a significant amount of organic matter of *biogenic* nature, mostly vegetable. By the latter conditions any carbon in mineralised form, such as carbonate precipitate or cement (e.g. calcite or dolomite), is intentionally excluded.

This might raise the question what a "significant amount" is. About a dozen different scales or systems for the classification of organic soils, based solely on organic matter content, are described in literature. Their only commonality is that peats are defined at the high end of the organic content scale and other organic soils at the lower end. However the boundaries in between are set at widely varying values of organic content.

According to the European standard [NEN-EN-ISO 14688-2], in order to call a soil (slightly) organic, a minimum organic matter content of 2% is required: refer also to Table 2-1. The dry gravimetric organic matter content is most commonly determined on the basis of the "loss on ignition" (LOI) after combustion in an oven, with use of equation (4-3). Soils with more than 20% organic matter content may be called strongly organic, however there does not seem to exist one standardised value of organic content to distinguish peat: neither in ISO nor in ASTM. In international literature soil is usually indicated as peat when it has an organic content of more than 50%, sometimes even more than 75%, however according to the dated Dutch standard [NEN 5104] a soil can already be called peat when it has an organic matter content of more than 15%, depending on the relative amounts of inorganic fines, silt and sand. The according classification diagram for organic soil is shown in Figure 2-1 on the next page.

Table 2-1: Classification of organic soils with grain size ≤ 2 mm.
[NEN-EN-ISO 14688-2, 2016: Table 3]

Soil	**Organic matter content** [% of dry mass]
Slightly organic	2-6
Organic	6-20
Highly organic	>20

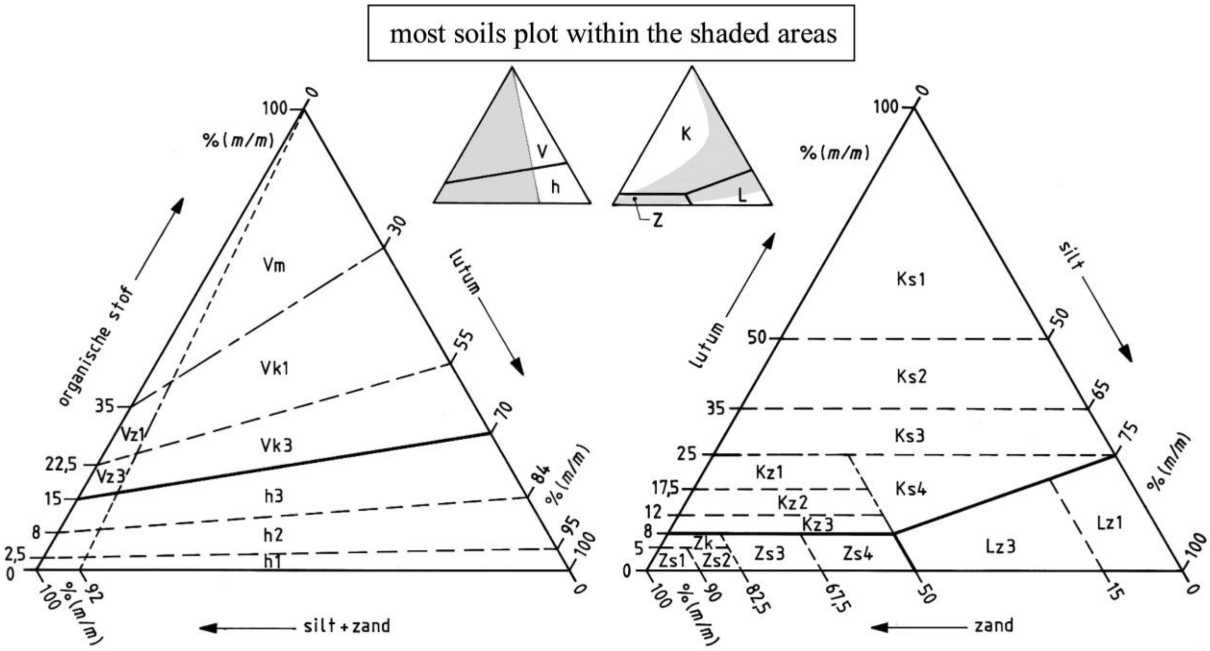

Figure 2-1: Soil classification diagrams for fine grained (≤ 2 mm) soils with and without organic content. Adapted from [NEN 5104: Fig. 3 & 4], by [Den Haan & Kruse, 2007].
Translation of terms: “organische stof” = organic matter; “lutum” = fines < 2 μm;
Translation of soil type abbreviations: V = peat; K = clay; Z = sand; L = loam;
Translation of affixes: m = low mineral matter content; k = clayey; h = “humeus” = organic; s = silty; z = sandy; Numbers 1 to 3 indicate an increasing relative amount of substance, from slightly to highly, e.g. “Vk1” = slightly clayey peat.

2.1.2 Physical properties, genesis and use of peat

In this section it is explained what peat is and how it is formed. In general geological terms, peat is a biogenic sediment. More specifically, peat is a soil that is primarily composed of partly or completely decomposed *plant* remains. It may have a light brown colour when freshly cut or excavated, however its colour will be (almost) black in a more decomposed or oxidised state. Peat typically has a spongy consistency and a mouldy organic odour. Plant fibres and even woody parts can sometimes be distinguished, but in more advanced stages of decomposition these might not be visible and the material might even have a mud- or gel-like consistency (“gyttja”; refer also to Table 2-2).

Due to their porous vegetable composition and wet depositional environment (to be detailed further below), peats exhibit extraordinarily high gravimetric water contents, sometimes in excess of one thousand percent. In other words, solid matter constitutes only a minor fraction of the total volume and weight of peat. As a result, the wet bulk unit weight of peat is very low; commonly about the same as water (≈ 10 kN/m^3). In case of incomplete saturation, for instance due to trapped gas bubbles, peat may be even lighter and thus float on water. So the low unit weight, the high water content and the previously mentioned high organic matter content may together be considered to be the most characteristic physical properties of peat. Other properties of peat with specific relevance for engineering are addressed in section 2.1.4.

The genesis, or formation, of peat simply requires that the rate of accumulation of vegetable matter is higher than the rate of decomposition. Since organic matter generally will decompose quickly by microbial activity and by chemical processes such as oxidation, however, another prerequisite is that the depositional environment is anaerobic. This is particularly the case in water-saturated or drenched environments like swamps, marshes, bogs and fens, all of which are types of *wetland* ecosystems. The rate of biological and chemical decomposition is further limited by a high degree of acidity of the water as well as by low temperatures.

Such environmental conditions prevail mainly in regions with humid temperate or boreal climates. That is why vast surficial peat deposits can be found especially in the north of the USA and Canada, on the British Isles, across Scandinavia, in the Baltic states and in Russia. In recent geological history, i.e. after the end of the last glacial period, environmental conditions promoting peat formation also prevailed in more central parts of Europe, including but not limited to the Netherlands, Germany and Poland (refer also to Appendix A1). However due to natural climate change and even more due to human intervention (refer to the last two paragraphs of this section), most surficial peat deposits in these countries have become fragmented or have disappeared. Still, though, peat can be encountered there widespread in the subsurface, often having a thickness of several metres. Lastly also in the tropics and subtropics, where abundant rainfall can sustain still-water marshes and swamps, extensive peat deposits can be formed despite the high temperatures.

In the historical and current boreal climatic conditions of North-Western Europe, peat primarily formed and still forms in *mires*, which are wetlands dominated by low-growing peat-forming vegetation with little or no tree cover. There are two types of mires: bogs (Dutch: “hoogveen”) and fens (Dutch: “laagveen”). These types of mires are mainly distinguished by their water source and water chemistry, which is related to, amongst other things, the terrain characteristics or geomorphology, subsurface mineralogy and the type of vegetation.

Fens are mainly rheotrophic, i.e. groundwater-supplied, characterised by relatively high concentrations of dissolved minerals (eutrophic) and by a neutral to high pH (alkaline), allowing a fairly large vegetation biodiversity. Typical fen vegetation comprises reeds (Phragmites), sedges (Carex) and other grasses, various flowering plants and some small tree species like willows, alders and birches. Bogs, on the other hand, are ombrotrophic, i.e. rain-supplied, characterised by a scarcity of dissolved minerals (mesotrophic and oligotrophic) and a low pH (acidic), allowing only limited plant biodiversity. Typical bog vegetation comprises mainly moss (Sphagnum), heather (Ericaceae) and some carnivorous plant species such as sundew (Drosera). Transitional types of mires exist as well, moreover it can happen that a mire starts as a fen and by continuous growth and peat accumulation gradually transforms into a (raised) bog.

Peat has been exploited extensively during past centuries to find use – after drying – as a fuel for residential and industrial heating purposes. This was the case in large parts of North-Western Europe until about a century ago and it still is the case in large parts of Russia and far Eastern Europe. In its dried form peat is called “turf” in Dutch. However partly because surficial peat reserves became depleted and more importantly because the mining and burning of peat led to considerable environmental damage and air quality problems, large-scale exploitation of peat has come to an end in western countries.

Acknowledgement of the importance of wetlands has strongly increased worldwide in the past two to three decades, not just ecologically but also economically and politically. That is because intact peat-forming wetlands naturally act as carbon *sinks*, whereas when damaged (such as by exploitation and/or drainage) they will act as carbon *sources* by the release of large amounts of the greenhouse gas carbon dioxide (CO_2). Moreover, wetlands act as natural water buffers and thus can play a supportive role in flood protection and drinking water supply.

2.1.3 Classification of peat

Peat can be classified by different means, for instance on the basis of its botanical composition, or on the basis of its structure and consistency. The former is more common in biology, agriculture and soil science, whereas the latter is more common in geotechnical engineering.

Regarding the botanical classification, usually the following classes of peat can be found and are distinguished in the Netherlands:

- Reed peat: consisting largely of remains of reeds (Phragmites);
- Sedge peat: consisting largely of remains of sedges (Carex);
- Woody peat: consisting largely of remains of woody plants and trees including willows, alders and birches;
- Moss or Sphagnum peat: consisting largely of bog moss (Sphagnum).

However often, due to advanced decomposition, the original botanical composition cannot be determined any more. Since knowing the botanical composition is of little value in engineering anyway, the geotechnical classification of peat is rather based on its structure and consistency. For this, three different, mostly visual and haptic perceptual methods can be used.

First of all, the widely known “Von Post” classification system provides a classification of peat by the degree of humification, or decomposition, on a scale ranging from H1 to H10. The assessment is done by visual analysis of the macroscopic structure and texture of a peat sample, as well as by manually squeezing it and looking at the turbidity and colour of the expelled water. Intact plant fibres and yellowish but clear expelled water indicate completely intact, undecomposed peat, to which the value H1 is assigned. The less vegetable fibres can be recognised, the weaker the material and the more turbid and dark the expelled water becomes, the higher its H-value will be: H10 ultimately indicates a completely decomposed peat without any recognisable traces of plant remains, behaving as a gel-like or muddy mass when squeezed, without expulsion of free water. A full written English description of this classification system is given by Verry et al. (2011).

Secondly, in Dutch geotechnical engineering practice, especially for borehole logging, usually the classification according to NEN 5104 is applied, which was presented already in Figure 2-1. However this requires a close visual and haptic investigation along with particle size analysis and determination of the organic content, in order to accurately determine relative amounts of substances.

Alternatively, a much simpler and more internationally used classification scheme for peat is suggested in the European standard [NEN-EN-ISO 14688-1], which is reproduced in Table 2-2. The aforementioned classification systems, with exception of NEN 5104, are illustrated in Figure 2-2 on the next page.

Table 2-2: Peat classification and description, translated and adapted from [NEN-EN-ISO 14688-1, 2016: Table 2].

Term	**Description**
Fibrous peat	Fibrous structure, well-recognisable intact plant remains, has some strength.
Pseudo-fibrous peat	Recognisable plant remains, has no strength.
Amorphous peat	No recognisable plant remains, spongy consistency.
Gyttja	Completely decomposed organic matter, mud- or gel-like consistency, may contain inorganic (mineral) matter.
Humus	Recent plant and animal remains, living organisms and their excrements, together with inorganic matter: topsoil.

2.1.4 Geotechnical engineering aspects

Identification of organic soils is very important because of the specific problems and challenges that these soils pose in engineering. Generally speaking, organic soils are weaker and more compressible than inorganic granular soils. In particular peats are highly compressible – in fact they have the highest compressibility of all natural soils. This concerns the primary compressibility as well as the secondary compressibility, which terms are further explained in subsection 2.2.3.2. The high compressibility is a direct result of their high porosity and water content in combination with a soft and easily deformable soil skeleton. The high porosity or void ratio is not only due to the loose packing of the solid particles or fibres, but also due to the hollow cellular structure of the vegetable components themselves.

Peat is a very special material any way, due to its strongly *anisotropic* nature as a result of both its sedimentary origin and its fibrous structure. The fibres in peat are namely arranged mostly parallel to each other, after having been deposited horizontally, which causes the bulk material properties and behaviour to be different depending on the direction or orientation of testing or loading. This anisotropy mainly affects the shear strength and hydraulic conductivity.

Not only anisotropy but also *heterogeneity* and (related hereto) spatial variability are exceptionally pronounced in peat deposits. Properties measured at one location can differ significantly from the properties just a short distance away, on micro- as well as on macro-scale. Moreover, peat is often interlayered with clastic sediments such as clay, silt and sand, sometimes in the form of isolated lenses or buried channels, which further increase the overall subsurface heterogeneity. These spatial variations in soil types and soil properties are particularly likely to cause non-uniform, or *differential*, settlements, which are very undesirable and potentially damaging for line infrastructure and shallowly founded buildings.

When furthermore regarding the shear strength that was mentioned just before, fibrous peat can be considered to be slightly beneficial as compared to soft and organic clays, since the vegetable fibres improve the soil's angle of internal friction and hence its shear strength. This effect is analogous with reinforcement by glass fibres in man-made construction materials. However note, again, that the shear strength of peat is anisotropic and that it moreover depends on the nature and the amount of vegetable fibres, which in turn depend on the botanical composition and the degree of humification, respectively.

Continuing with humification, it must be emphasised that the sensitivity of peat to decomposition poses substantial practical problems. Whenever peat soil is drained for any future land development and exposed to air, the rate of both biological and chemical decomposition will greatly increase, thus decreasing the strength and the volume of the exposed soil.

Some final remarks concern the previously addressed bulk unit weight of peat, which is of relevance in engineering in several ways. Firstly, the low unit weight causes the effective stress profile (refer to subsection 2.2.1.2) as a function of depth inside a peat layer to remain more or less constant. For peat with little or no overburden, this means that the effective stress throughout the layer is close to zero. Secondly, when peat dehydrates its bulk unit weight decreases even more, which can be critical particularly for water-retaining embankments. Since the material will become so light and effectively floating, it can fail easily due to being pushed away by the water it ought to retain. This risk is further increased by the formation of dehydration cracks, allowing water to intrude and possibly undermine the dehydrated peat body. This has last happened in the Netherlands fairly recently; namely in Wilnis in 2003. Thirdly and lastly, the unit weight has been found to be a useful index property for correlation with several compressibility parameters, several of which are investigated in more detail in the further course of the current research.

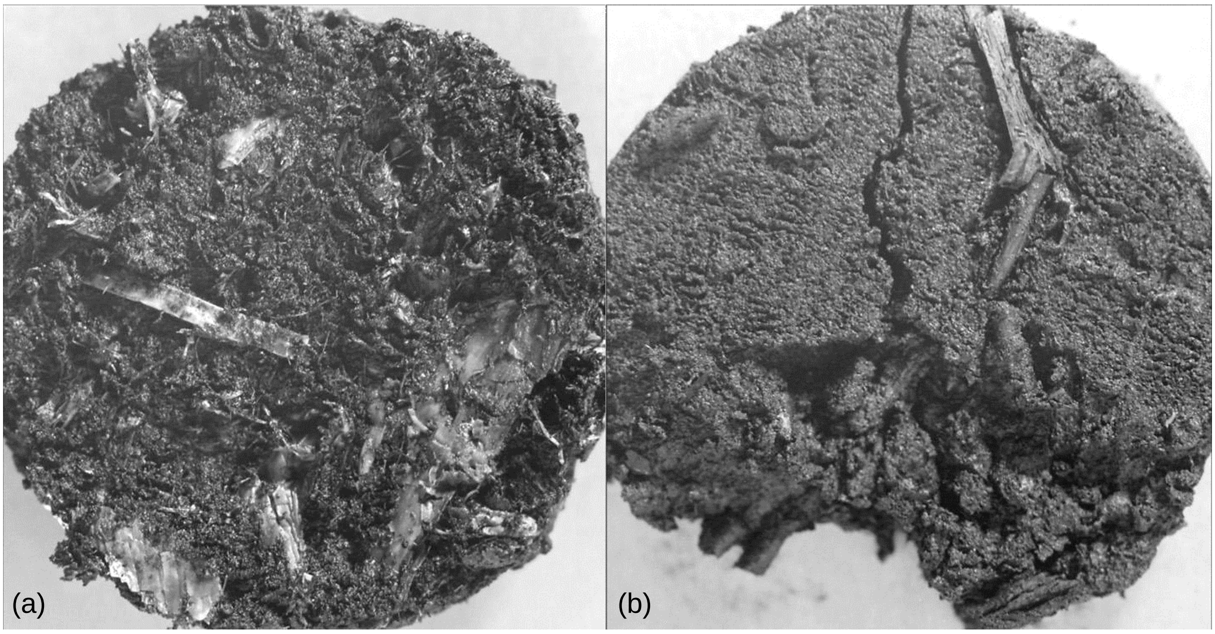

Figure 2-2: Photographs of disc-shaped peat samples in unsaturated condition, illustrating differences in structure, composition and degree of humification. Adapted from [Den Haan & Kruse, 2007: Fig. 10].

(a) Largely intact *fibrous* peat (reed peat), Von Post: H1-H2.

(b) More decomposed and almost amorphous *pseudo-fibrous* peat (woody peat), Von Post: H5-H6.

2.2 Summary of consolidation and settlement theory

This chapter is intended to provide a mostly brief and fundamental, yet comprehensive overview of the theory underlying vertical soil compression and settlement analysis, also acting as a reference for according terminology that may be used later on in this report.

2.2.1 Basic principles of effective stress and consolidation

It is still less than a century since the first comprehensive reference book on the mechanics of soils, titled *Erdbaumechanik auf bodenphysikalischer Grundlage*, was published [Terzaghi, 1925]. The author, Karl von Terzaghi (1883-1963), was an Austrian engineer who eventually was nicknamed “father of soil mechanics” after the practical relevance and importance of his findings and theories were acknowledged internationally. In particular his formulation of the Effective Stress Principle – later to be called Terzaghi’s Principle – established the science of soil mechanics in the first place and revolutionized the way in which strength, deformation and general behaviour of soil were approached in engineering.

2.2.1.1 Compressibility of soil in general

Soil generally is considered as a porous medium, comprising a skeleton of solid particles enclosing interconnected voids that contain a fluid, i.e. either a gas or a liquid. A soil element as a whole can change its shape (deformation) as well as its volume (compression or expansion) due to rearrangement of the solid particles.

The actual compressibility of a soil depends strongly on the structural arrangement of the solid particles, on the relative amount of voids (porosity or void ratio) and on the contents of those voids. Regarding the latter, for practical purposes water may be considered incompressible just as the individual solid particles; however air is highly compressible. Therefore a dry or only partially saturated soil can relatively easily change its volume due to compression of the gas in the voids, whereas a completely saturated soil can only do so when the liquid is allowed to escape (drain) from the voids.

Shear stress can be resisted only by the skeleton of solid particles of a soil due to the inter-particle contact reaction force. Normal stresses will be similarly carried by the soil skeleton. However in a closed (undrained) environment, any liquid inside the voids can also carry normal stress, which will result in an increase of the pore water pressure. The amount of pore water pressure above its hydrostatic value is usually called “excess pore water pressure”.

2.2.1.2 Effective stress

The resistance and transmission of forces through the soil skeleton was studied by K. von Terzaghi who eventually introduced the “Principle of Effective Stress” in 1925. This principle is based on the reasoning and observation that any stress carried by the pore water decreases the remaining stress on the soil skeleton, which proved to be essential for the understanding of soil mechanics. In short, the relationship is commonly formulated as follows [Knappett & Craig, 2012]:

$$\sigma = \sigma' + u \qquad (2\text{-}1)$$

Where:

σ = total stress, sometimes denoted as σ_t [units of force divided by area: e.g. kN/m^2 or kPa]
σ' = effective stress, sometimes denoted as σ_{eff} [kPa]
u = pore water pressure, sometimes denoted as σ_p [kPa]

Hence the effective stress can be found by subtracting the pore water pressure from the total (applied) stress. Any quantity of “pressure” in older formulations emerging in the further course of this thesis, without further specification, is supposed to correspond with *effective* stress.

Although the effective stress is considered to represent the stress transmitted through the soil skeleton, note that it is not the same as the inter-particle contact stress in a strictly physical sense. Instead, effective stress is the sum of all inter-particle contact forces divided by the gross specimen area, of which the actual inter-particle contact area only makes up a *very* small part. Therefore the inter-particle contact stresses in a strictly physical sense can be orders of magnitude higher than the effective stress.

The effective stress principle has direct consequences for the determination of the in-situ effective vertical stress in the subsurface due to the natural self-weight of the soil. According to the aforementioned principle, the effective vertical stress can be found by subtracting the pore water pressure from the total natural self-weight of the soil, assuming fully saturated and hydrostatic conditions:

$$\sigma'_v = \sigma_v - u = (\gamma_{sat} - \gamma_w)z \tag{2-2}$$

Where several variables were already defined previously, except:
γ_{sat} = unit weight of the soil in saturated condition [kN/m^3]
γ_w = unit weight of water = 9.81 kN/m^3
z = regarded depth inside the saturated soil layer [kPa]

In case the ground surface does not coincide with the phreatic water level, which is most often the case, the saturated soil layer is overlain by an unsaturated or dry topsoil layer, adding weight to the soil below. Then the effective vertical stress at the regarded depth is to be complemented by simply adding the stress due to the self-weight of this overlying topsoil.

2.2.1.3 Consolidation theory in short

Consolidation theory relies strongly on the just explained principle of effective stress and provides a description of the soil response due to an initial change in total stress and subsequent delayed development of effective stress. This subsection is intended just to provide a very brief description of the principle of consolidation and its *practical* application for reference. It is considered to be beyond the scope of this thesis to provide the full derivation of the partly Fourier-transformed differential equations that the consolidation theory is based upon. In this and following subsections therefore only the practically most relevant equations for application of consolidation theory in settlement analysis will be provided. For a more mathematical approach, one is kindly referred to any advanced soil mechanics textbook.

As described in a previous subsection, a water-saturated soil sample will be compressible only if the incompressible pore water is allowed to drain. Since pores and their interconnections are often microscopically small, however, a fluid flowing through the pores will experience a significant resistance to flow. This depends amongst other things on the permeability of the soil and on the viscosity of the fluid. Thus when a saturated sample is subjected to a load (increase of total stress), in practice the pore water will not drain from the soil immediately, but rather needs some time to escape by seepage. As a result, according to Terzaghi’s effective stress principle, initially a large part of the applied total stress will be carried by the pore water, resulting in excess pore water pressures that are (almost) equal to the increase of total vertical stress.

The initial excess pore water pressure will cause a hydraulic pressure gradient, resulting in flow of pore water towards a free-draining boundary of the soil sample or layer. This flow will continue until hydrostatic conditions are re-established. This process of excess pore water pressure reduction by drainage, is called “dissipation”. As dissipation proceeds, the applied total stress is gradually transferred from the pore water to the soil skeleton: consequently the soil skeleton experiences an increase of effective stress and the soil will be compressed. When dissipation has completed, the applied increment of total stress will be carried entirely by the soil skeleton.

The whole process described in the preceding two paragraphs is referred to as "consolidation". Consequently, a one-sentence definition of consolidation may read as follows, adapted from Knappett & Craig (2012):

Consolidation is the gradual reduction of volume of a saturated soil due to an increase in effective stress following after dissipation.

Note that a change in effective stress does not necessarily have to result from an applied load, but can also be due to direct drainage of pore water, e.g. by groundwater pumping. Any ground settlement that is the result of consolidation, is referred to as "consolidation settlement".

Consolidation is a time-dependent process, the rate of which is governed by the hydraulic properties of the soil and pore fluid (e.g. permeability, viscosity, density) and by the distance to the nearest free drainage boundary (drainage path length). One parameter that relates several of these properties is the coefficient of consolidation (c_v), which will be elucidated in subsection 2.2.2.2.

2.2.2 Specific soil compressibility characteristics

Before proceeding with specific consolidation-related soil properties, it is deemed appropriate to provide a brief and graphic-supported description of the process of soil compression and its main characteristics. After all, the soil compression curve as a function of time and stress exhibits some particular characteristics, which are observed for almost all soils and which are repeatedly referred to in the further course of this thesis.

Compression of soil in a laboratory test setup (refer to chapter 3.1 for according test methods) is graphically represented by plotting a measure of relative specimen volume or axial deformation on the vertical axis, versus the logarithm of effective stress on the horizontal axis. The relative specimen volume is traditionally expressed by means of the void ratio, although nowadays more often more directly measurable quantities of deformation such as strain are preferred to use.

A schematic but fairly typical soil compression curve is presented in the diagram of Figure 2-3. The typical curve characteristics are as follows:

- A gently sloping curve at the start;
- A bending point;
- A steeply sloping linear section;
- Another gently sloping section upon unloading and reloading.

A gentle slope indicates relatively high resistance to compression, whereas a steep slope indicates a relatively low resistance to compression. The unload-reload line, for instance, has a relatively gentle slope, which is typically due to the fact that the soil has been compressed and subjected to a higher stress level before. Thus its behaviour is dominated by elasticity, rather than plasticity that causes larger and irreversible deformations.

One thing that might strike, is the fact that the compression curve initially also has a relatively gentle slope, which implies reloading behaviour. Indeed, a common property of natural soils is a so-called preconsolidation stress, which is possible due to the fact that the soil may have been subjected to a higher effective stress in the past. This preconsolidation stress is *theoretically* to be found at the bend or kink in the compression curve – although in practice it is not that straightforward as it seems. More information about preconsolidation and the determination of its magnitude can be found in the next subsection (2.2.2.1).

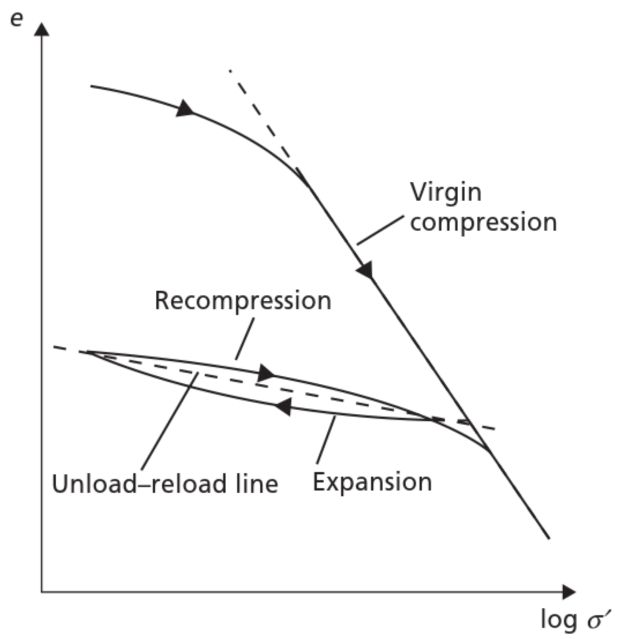

Figure 2-3: Schematic typical soil compression curve, representing void ratio (*e*) vs. the logarithm of effective stress (*σ'*). Adapted from [Knappett & Craig, 2012].

After the bend, the compression curve continues more steeply and becomes approximately linear, provided that the stress is plotted on a logarithmic scale. This part of compression is called "virgin compression", which indicates a stress range that the soil has never been subjected to before. Deformations in this range are both elastic as well as plastic in nature. The value of the slope of this line is traditionally referred to as "**compression index**", or alternatively as "virgin compression coefficient", which can be simply formulated as follows:

$$C_c = \frac{e_1 - e_2}{\log\left(\sigma'_2/\sigma'_1\right)} = \frac{\Delta e}{\Delta \log \sigma'} \tag{2-3}$$

Where:
C_c = compression index [-]
e_1 = void ratio at the beginning of the regarded slope section [-]
e_2 = void ratio at the end of the regarded slope section [-]
σ'_2 = effective stress at the end of the regarded slope section [kPa]
σ'_1 = effective stress at the beginning of the regarded slope section [kPa]
Δe = change, i.e. decrease, in void ratio [-]

Many other compressibility parameters can be defined on the basis of compression curves such as depicted above, depending on the particular part of the curve that is regarded as well as on the quantities that are represented along the axes. These different parameters, or coefficients, find use in different settlement prediction models and will all be discussed in the course of chapter 3.2. One other measure of compressibility that is useful to define already at this moment, since it will be used in one of following subsections, is the **coefficient of volume compressibility**. This coefficient can be formulated in terms of either void ratio or strain, knowing that these quantities are related by $\varepsilon = \Delta e / (1 + e_0)$:

$$m_v = \frac{1}{1+e_0} \cdot \frac{\Delta e}{\Delta \sigma'} = \frac{\Delta \epsilon}{\Delta \sigma'} \tag{2-4}$$

Where several variables were already defined previously, except:
m_v = coefficient of volume compressibility [m^2/kN]
e_0 = initial void ratio [-]
$\Delta\varepsilon$ = change in (linear) strain [-]

As a final remark, it is important to realise that in the diagram above, as well as in the further course of this report and in soft soil compression testing in general, exclusively *saturated* soils are considered. Dry soil specimens are much more compressible than saturated ones, as explained before, and hence one will measure unrealistic compressibility characteristics, since soft soils in the Netherlands generally occur in (almost) completely saturated state. The presence of small quantities of air in a soil specimen can already strongly influence the test results, which can be discovered when the compression curve exhibits a large amount of initial compression whereas initial compression behaviour is expected to be relatively stiff.

2.2.2.1 Preconsolidation pressure, OCR and POP

Preconsolidation is a commonly encountered compressibility characteristic of soil. Since the compressibility of a soil below and above the preconsolidation pressure can be very different, preconsolidation pressure is an essential parameter in virtually every settlement prediction model.

As was briefly indicated before, the preconsolidation pressure or –stress represents the maximum effective stress that a soil has been subjected to in the past. This maximum stress level may be equal to, is often larger than, but cannot be smaller than the present in-situ effective stress. If the maximum stress is equal to the present in-situ effective stress, the soil is said to be *normally consolidated*. If, on the other hand, the soil has ever experienced an effective stress level larger than the present-day level, the soil is said to be *overconsolidated*.

An (apparent) preconsolidation pressure may result from different physical processes. This may include for instance, but is not limited to, ground water level fluctuations, aging [Bjerrum & Lo, 1963] and mechanical loading. Regarding the latter, one should also take into account natural sediments and glaciers that have been eroded or melted away again, respectively.

Note that depending on the regarded source, the preconsolidation pressure can be found to be indicated by a wide variety of different letters or symbols, such as: p_g, p_c, p_m, σ'_{max}, σ'_p, σ'_{vp}, σ'_c and even σ'_y (“yield stress” [Becker et al., 1987]). P_g (where *‘g’* relates to “grensspanning”) is encountered most often in Dutch literature dating from before the 2000s, whereas σ'_p or σ'_{vp} is more commonly used nowadays. In international literature, on the other hand, preconsolidation pressure is most often indicated by the subscript *c*.

The most common and recommended [NEN 5118] method of determining the pre-consolidation pressure is **Casagrande’s method**, which is described and illustrated (Figure 2-4) as follows:

- Plot a compression curve of void ratio (vertical) vs. logarithm of effective stress (horizontal);
- Draw the tangent (A) to the virgin compression line;
- Determine by eye the point of maximum curvature and draw a horizontal line (B) through it;
- Draw the tangent to the curve (C) at the point of maximum curvature;
- Draw the bisector (D) between line B and C;
- Read the preconsolidation stress at the intersection point (o) of lines A and D.

Although Casagrande’s method is internationally most well-known, most used and even recommended by standards such as NEN, still several variations or alternatives to this method exist. Some of these alternative methods have been reviewed in more detail and are further explained in subsection 4.2.2.7.

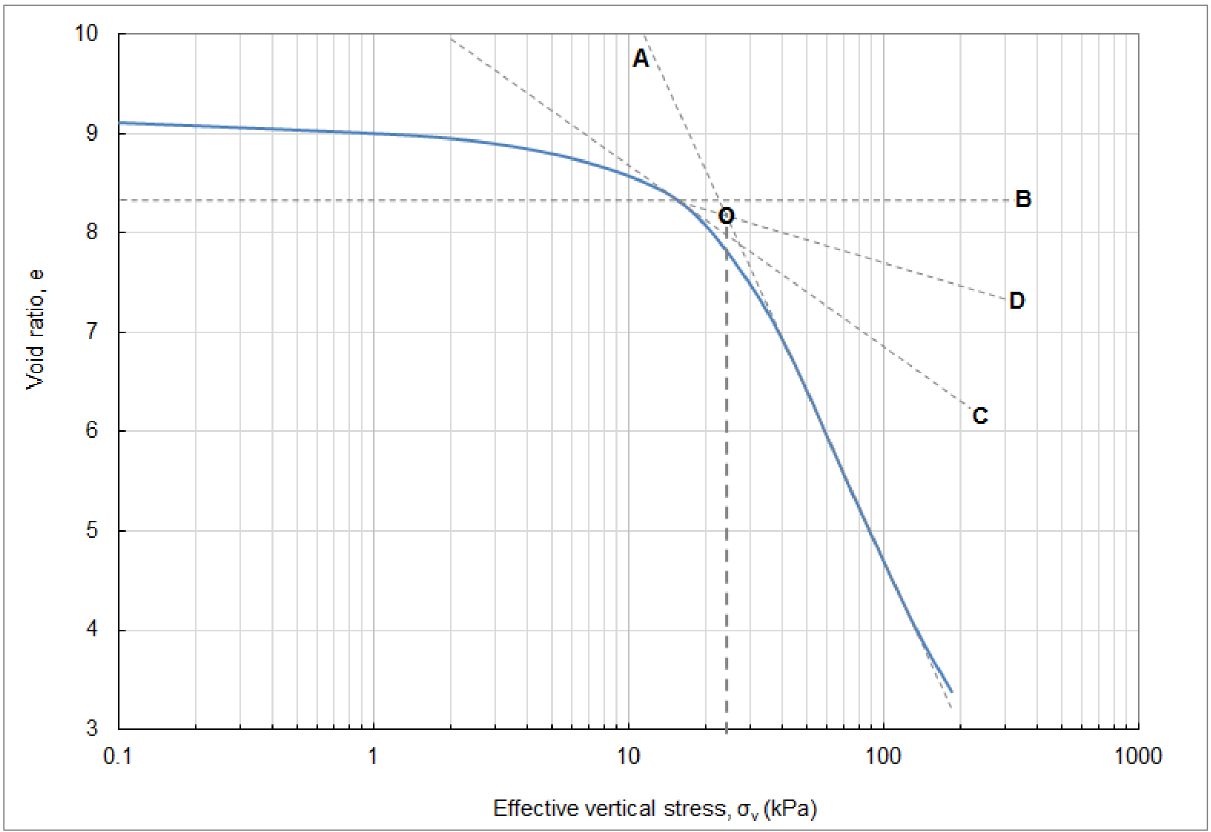

Figure 2-4: Personal illustration of Casagrande's method to determine the preconsolidation pressure. From the example, the resulting value would be approx. 24 kPa.

Note, that the preconsolidation pressure varies with depth and thus also per soil sample. In order to make incorporation in a settlement prediction model practically applicable, there are two different ways of taking account of the preconsolidation pressure, namely:

- **OCR** (overconsolidation ratio);
- **POP** (pre-overburden pressure);

the first of which is used as a multiplication factor, whereas the second is used as an addend, as graphically represented in Figure 2-5.

$$OCR = \frac{\sigma'_{vp}}{\sigma'_{v0}} \tag{2-5}$$

$$POP = \sigma'_{vp} - \sigma'_{v0} \tag{2-6}$$

Where:
σ'_{vp} = preconsolidation pressure [kPa]
σ'_{v0} = present in-situ effective vertical stress [kPa]

However both ways are in fact just a simplified representation of the real preconsolidation pressure profile, which usually is not linear with depth and also depends on the process causing the preconsolidation. In general, the OCR may be considered to be more representative of preconsolidation due to groundwater level decrease, whereas the POP may be considered to be more representative of preconsolidation due to mechanical preloading.

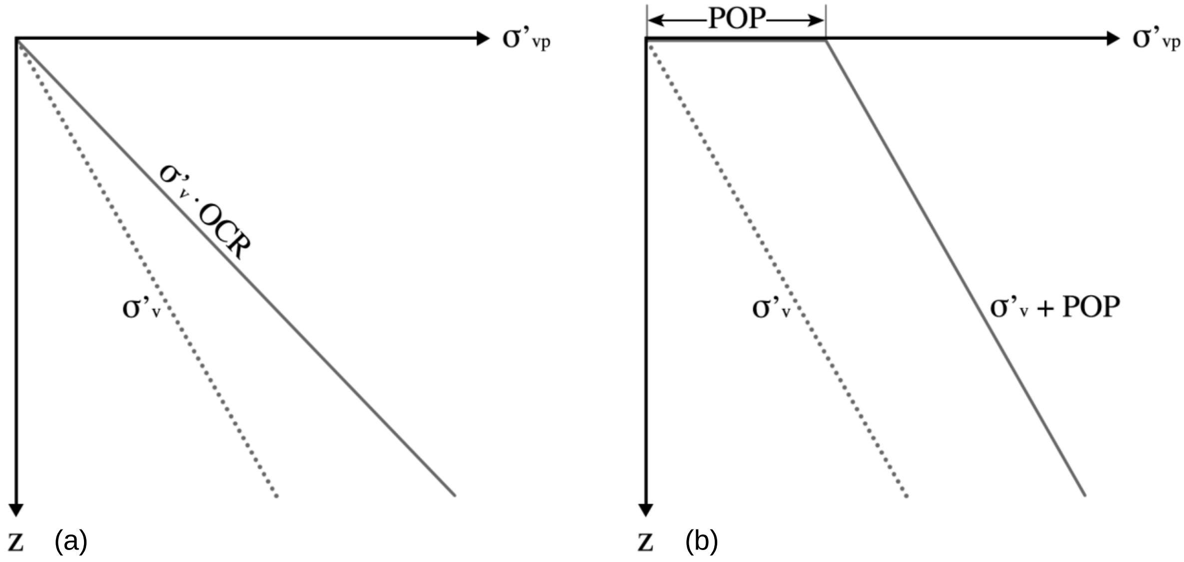

Figure 2-5: Schematic graphs [personal illustration, 2016] illustrating the difference between the two possible ways of taking account of preconsolidation pressure (σ'_{vp}), namely:
a) OCR (overconsolidation ratio), and
b) POP (pre-overburden pressure).
Where σ'_v is the effective in-situ vertical stress.

2.2.2.2 Coefficient of consolidation and hydraulic conductivity

Since consolidation plays a key role in soil compression and thus settlement prediction, it is important to have a parameter that can describe the consolidation characteristics of the soil. For this purpose, there is the coefficient of consolidation (denoted c_v) that emerges from underlying consolidation theory and that relates permeability and/or hydraulic conductivity, volume compressibility, drainage path length and consolidation time with each other.

The coefficient of consolidation can be determined by two similar graphical methods: the **log-time method** (after Casagrande) and the **root-time method** (after Taylor). Both methods in principle rely on curve-fitting with a theoretical consolidation curve. Since the log-time method was found to not be applicable to very soft organic soils due to a very steep onset of the compression curve, only the root-time method was used and will be described and illustrated here. Note on beforehand, that c_v is stress- and strain-dependent and therefore should be determined at an appropriate stress level and state of compressibility (at least in-situ stress level, or perhaps better around half of the expected final surcharge load).

Depending on the geometry and confinement of the soil sample, there is a theoretical consolidation curve relating the degree of consolidation (U_v) to a time factor (T_v). The degree of consolidation is an expression for the progress of consolidation with time and is defined by equation (2-7). The time factor is defined by equation (2-8). The according theoretical consolidation curve is represented in Figure 2-6.

$$U_v = \frac{e_0 - e}{e_0 - e_1} \tag{2-7}$$

Where:
U_v = degree of consolidation at a certain moment in time [-]
e_0 = initial void ratio before the start of consolidation [-]
e = void ratio at the time in question during consolidation [-]
e_1 = void ratio at the end of consolidation [-]

$$T_v = \frac{c_v t}{d^2} \tag{2-8}$$

Where:
T_v = time factor [-]
c_v = coefficient of consolidation [m^2/s]
t = time [s]
d = drainage path length, i.e. half the sample thickness in an oedometer test [m]

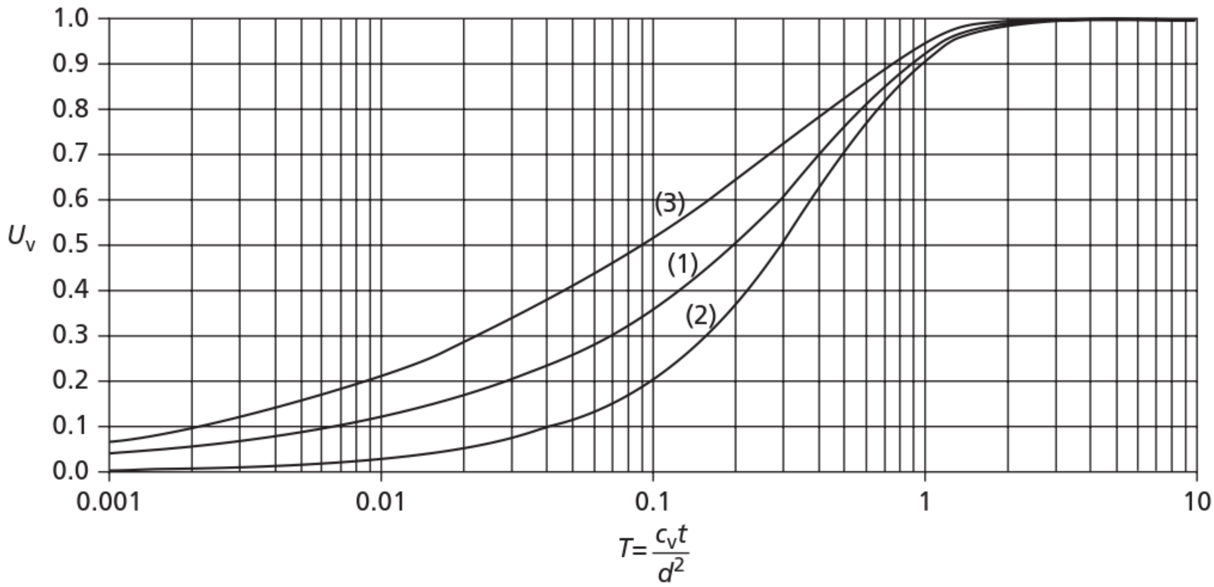

Figure 2-6: Theoretical consolidation curves to assist with the determination of c_v [Knappett & Craig, 2012]. Curve numbers 1,2,3 represent the consolidation process for different boundary conditions. In practice, however, curve No. 1 will nearly always be used, which covers all common pore pressure distributions due to loading in a two-sided drained system, as is the case in any conventional oedometer test apparatus (refer to section 3.1) that is used to determine the consolidation characteristics.

With these tools, the value of c_v can be found by means of the **root-time method** (refer to Figure 2-7). This method is required to find the time at which 90% consolidation (U_v = 0.9) has taken place, by comparison with the inset of the “Theoretical curve” in Figure 2-7, as follows:

- Plot an experimental compression curve of settlement (vertical) vs. the square root of time (horizontal);
- Draw a tangent to the linear part of the experimental curve. The point where consolidation practically starts, corresponding with U_v = 0, is found at the level of a_s;
- The theoretical curve is linear up to about 60% of consolidation. So the point of 90% consolidation may be found at a level of (90/60)·(a_{60} – a_s) below a_s;
- Alternatively it can be made use of the fact, that at 90% consolidation the abscissa AC of the consolidation curve is 1.15 times the abscissa AB of the extrapolation of the linear section.

Once t_{90} has been determined, c_v can subsequently be calculated after rewriting equation (2-8), in which the time factor (T_v) for a given degree of consolidation (U_v = 0.9) can be read from curve No 1. in Figure 2-6, such that:

$$c_v = \frac{0.848\, d^2}{t_{90}} \tag{2-9}$$

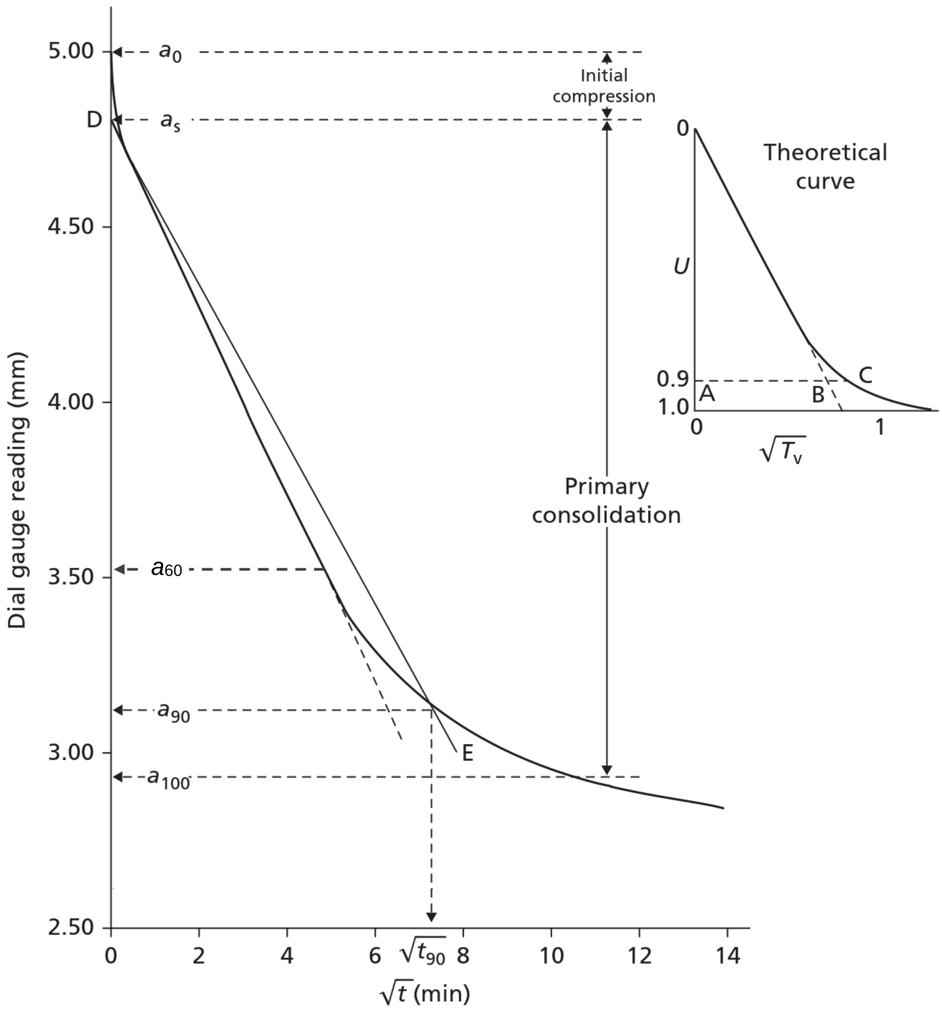

Figure 2-7: Schematic illustration of the root time method for determining c_v, adapted from [Knappett & Craig, 2012].

The settlement-root-time diagram does not necessarily have to start at time 0 min, in which case the reading of t_{90} should be corrected by subtracting the time at the onset of the compression curve. Just keep in mind that readings taken from a root-time axis always first have to be squared in order to obtain the real time values for further calculations.

Ultimately, by recalling the coefficient of volume compressibility (m_v) from equation (2-4) and the unit weight of water (γ_w = 9.81 kN/m^3), the hydraulic conductivity k_v [m/s] can be calculated as follows:

$$k_v = c_v \, m_v \, \gamma_w \tag{2-10}$$

2.2.3 Settlement analysis

In this section an introduction to settlement analysis and prediction will be provided, mainly intended to define some basic terminology and to eliminate some common misconceptions.

2.2.3.1 Settlement vs. subsidence

First of all, the distinction has to be made between soil settlement (Dutch: “zetting”) and subsidence (Dutch: “bodemdaling”). Although both phenomena lead to downward movement of the ground surface and both even can take place simultaneously, they are not the same and should be considered independently.

The essential difference is that in the case of settlement the soil is being compacted by external (surficial) force, whereas in the case of subsidence the ground surface reduces in level autonomously. In other words, when soil compression is the result of an increased and/or maintained level of effective stress due to some kind of surcharge load, it is called settlement, whereas when the ground surface level decreases by itself without any additional surcharge load, it is called subsidence.

Settlement consequently is a mostly local phenomenon that typically occurs during and right after construction works, be it the construction of a building, a road or railway embankment, or a dike, for example. It is this phenomenon that is studied in the course of the current research.

Subsidence, on the other hand, generally is a more regional phenomenon and has a wider range of possible causes. It can be the result of hydrological changes (e.g. groundwater abstraction, groundwater table fluctuations), extraction of natural resources (e.g. oil, natural gas or salt), soil shrinkage due to evapotranspiration, collapse of subsurface cavities (either natural, such as karst, or man-made, such as mine drifts and shafts) and possibly even tectonics (graben formation). Furthermore, when considering organic soils in particular, organic matter can decompose due to microbial activity or due to chemical oxidation when exposed to air, as described already in chapter 2.1, thus naturally leading to a decrease in volume as well.

The effect of both above described phenomena is to be seen complementarily. In large parts of the Netherlands, *subsidence* alone already causes a continuous lowering of ground surface level in the order of 1 cm per year [Den Haan, 2008]. Den Haan attributes this mainly to oxidation of organic matter above the phreatic water level and less to fluctuations of the groundwater table, the latter of which would affect the in-situ effective stress. Den Haan's opinion is supported by other researchers, such as Pons & Zonneveld (1965) and Schothorst (1977), who found that the relative contribution of oxidation of organic matter to subsidence is between 50% and 85%. However there is still much debate and research going on regarding the precise causes of subsidence in the Netherlands, which is beyond the scope of this research regarding *settlements*.

2.2.3.2 Primary vs. secondary settlement

In the previous section (2.1) already the process of consolidation settlement was explained. A schematic stress-compression diagram (Figure 2-3) as well as a schematic time-settlement diagram (Figure 2-7) were shown. The (theoretical) time-settlement curve has so far appeared to become horizontal after consolidation has ended. Indeed, the process of *consolidation* (i.e. dissipation of pore pressures) will end – however it has been observed and proven that the process of *compression* in general does not. This discrepancy was first investigated in detail by A.S.K. Buisman around 1940 (refer to section 3.2.2).

It happens to be that the compression of a soil continues eternally under a constant effective stress, albeit usually at a very small rate. This eternal phase of compression is commonly referred to as "**secondary compression**", since it becomes apparent or dominant *after* consolidation. Secondary compression is a visco-plastic, or "creep" deformation process that is thought to be due to rearrangement of fine-grained particles in combination with slow expulsion of highly viscous particle-adsorbed water, becoming even more viscous as particles move closer together over time [Knappett & Craig, 2012].

In order to keep a simple distinction between different compression phases, consolidation settlement has been named accordingly also "**primary compression**", since it is the most apparent or dominant process in the earliest phase of soil compression. Note however that it is not said that consolidation is the *only* process occurring during primary compression: in fact, it is generally believed that secondary, or creep effects take place already from the start of and during consolidation, however the former are negligible with respect to the latter.

For relatively coarse-grained mineral soils such as sand, secondary compression can be considered negligible. However in clays and even more in *organic* clays and peat, secondary compression can be very significant and on the very long term might even become larger than the primary (consolidation) settlement.

In addition to the previous, in practice one might initially also observe a nearly instantaneous amount of compression upon loading. This is referred to as "**initial compression**", which is likely to occur in particular in unsaturated conditions due to compression of the more easily compressible air-filled voids [Huat et al., 2014]. Furthermore, soil also has elastic (reversible) deformation properties, which are included in initial compression.

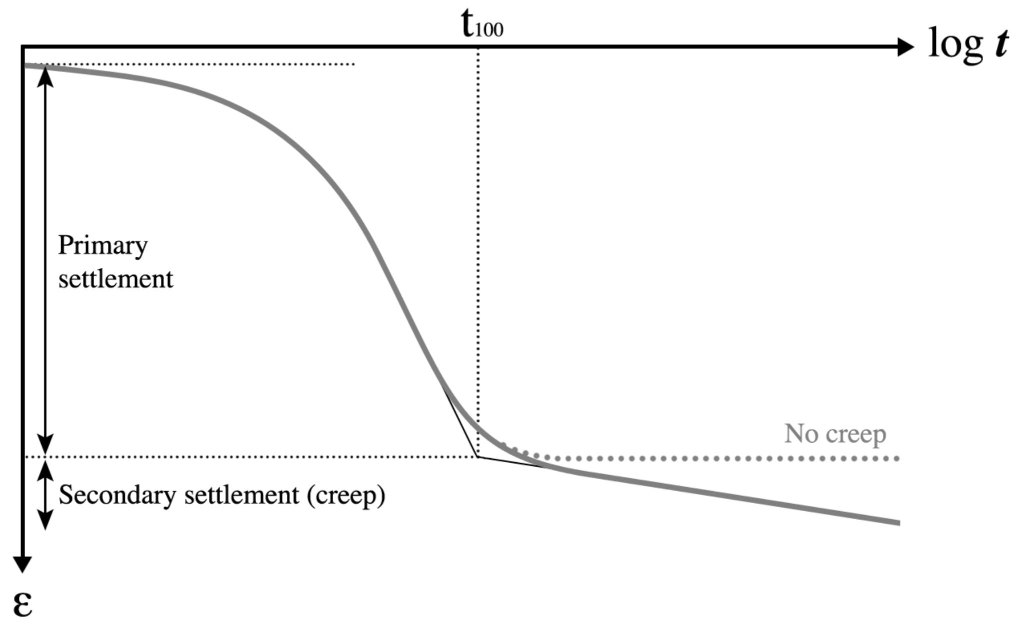

Figure 2-8: Personal schematic illustration of a typical compression curve representing *strain* (*ε*) as a function of the logarithm of *time* (*t*). The two main phases of settlement, or compression, are distinguished as well as the end time of consolidation (t_{100}). The initial 'gap' at the top of the curve may be regarded as initial compression.
The compression curve development *without* creep settlement is indicated as well, as could be the case for sand.

2.2.3.3 Settlement prediction

Numerous models have been developed to predict vertical deformation or settlement of soils. Contemporary models provide a description of a soil's compression behaviour as a function of both stress and time, possibly taking into account differences in compressibility due to stress history or preconsolidation. Different models and their parameters are discussed in much detail in chapter 3.2. In very general terms, a settlement prediction model is supposed to be built up as follows:

$$S = s_0 + s_p(\sigma') \cdot U(t) + s_s(t) \tag{2-11}$$

Where:
S = total settlement
s_0 = initial compression
s_p = primary compression as a function of effective stress (σ')
U = degree of consolidation as a function of time (t)
s_s = secondary compression as a function of time (t)

Note, that sometimes the secondary compression is considered to be stress-dependent as well (e.g. Koppejan, 1948). In any case, the total compression or settlement is a sum of different components, of which the magnitude is defined by their own soil-specific compressibility parameters. Graphical and analytical methods for determining these parameters are explained in section 4.2.2, whereas the laboratory test methods with which the required test data are to be obtained will be introduced in the next chapter (3.1).

3 Literature review

3.1 Soil compression test methods

Because natural materials are intrinsically variable, every soil type has its own particular properties and therefore every settlement prediction formula or model relies on locality- and soil-specific empirical input parameters.

In settlement prediction these parameters are not limited to only soil physical or index properties such as for instance unit weight, porosity or water content. In particular, it is required to know as precisely as possible the *compressibility* of the soil when subjected to loading, as well as its stress history (preconsolidation pressure). These properties are expressed by parameters that exist with different names and symbolic notations, depending on the formula or model that is used, as will become more clear in the course of chapter 3.2. In any case, however, compressibility parameters are to be determined experimentally in a soil mechanical laboratory test setup. Different testing methods and equipment can be used to do so, the most common of which will be elucidated in the following sections.

3.1.1 Conventional oedometer with incremental loading (IL)

Being the oldest and probably the simplest soil compression test device, the oedometer is used already since the early 20th century and, with minor adaptations, it still is. Although the oedometer is supposed to have been developed and first used by J. Frontard around 1910 in France, the oldest retrievable documented description of this device is by Terzaghi (1925), who built and used this device around 1920 for his research on soil compression, swelling and consolidation.

Figure 3-1 schematically depicts a conventional oedometer in cross-section. The soil specimen is disc-shaped, typically 20 mm in height and with a diameter/height ratio of at least 3, held inside a confining (stainless) steel ring. The top and bottom are enclosed by porous stones to allow drainage of pore water. The upper porous stone can move inside the steel ring and is covered by a loading cap through which pressure can be applied onto the sample. The entire assembly is situated inside an open cell filled with water so that the specimen remains saturated but the pore water is still allowed to drain.

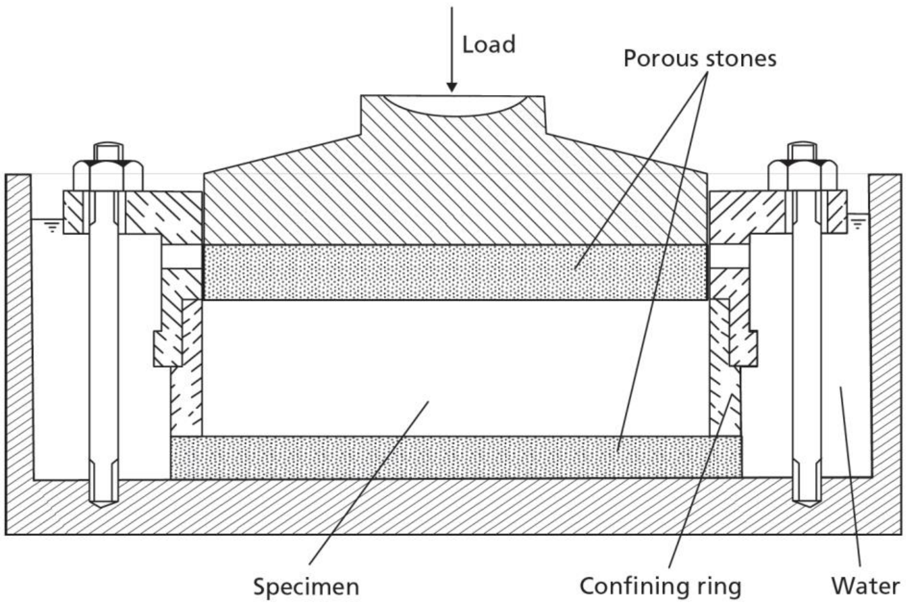

Figure 3-1: Schematic cross-section of an oedometer [Knappett & Craig, 2012].
Note that the confining ring does not necessarily have to be fixed with screws.

The confining ring imposes a condition of zero lateral strain on the soil sample. In order to minimize wall friction, the inside of the confining ring has to be polished very smoothly. The compression of the specimen under stress is measured by means of a dial gauge or electronic displacement transducer on the loading cap. Although sample preparation and testing can be laborious and time consuming, the general working procedure and operation of the device is fairly straightforward. Oedometer sample requirements and test procedures have been standardized; in the Netherlands for instance by NEN 5118 (1991).

During a conventional, i.e. incrementally loaded, oedometer test, the soil sample is subjected to discrete increments of vertical axial stress. Loading is traditionally done manually by adding weights directly on top or by means of a lever beam. However systems with electronically controlled compressed air loading presently exist as well [Head, 1994; Clayton & Hight, 2007]. The initial stress applied will depend on the type of soil and its original in situ conditions; usually it is chosen to amount to half of the (estimated) in situ stress. Subsequent stress increments are generally twice the previous level. At the end of every loading step, the excess pore water pressures should have dissipated completely, such that the applied total stress equals the effective vertical stress in the sample. Therefore each stress level is normally maintained for a period of 24 hours, although more time may be required in exceptional cases, which depends on the consolidation period that is to be estimated in advance. Additional to loading, also an unload-reload cycle ought to be performed in the virgin compression range of stress, in order to determine the respective reloading compression coefficient.

Presentation of the results can be done in several different ways, depending on what particular compressibility parameters are desired to be determined. In general, the void ratio or the strain of the sample at the end of each increment period is plotted versus the corresponding effective stress and versus time: the strain can be either linear or natural (refer to subsection 3.2.7.1) and the stress and time must have a logarithmic scale. From the resulting data and graphs the following compressibility parameters can be determined, amongst others: virgin compression coefficient or compression index, unloading-reloading coefficient, secondary compression or creep coefficient, and the preconsolidation pressure, all being defined and determined slightly differently depending on the settlement prediction method that is used (refer to chapter 3.2). Furthermore, the oedometric or constrained modulus, the coefficient of consolidation and hence the hydraulic conductivity can be derived (the latter provided that detailed time-deformation measurements are available).

There are some potential pitfalls in oedometer tests, however, as well as there are several disadvantages of this testing method. First of all, oedometer test results can only be considered to be reliable and interpretable in accordance with consolidation theory when the tested samples were fully saturated. But the main pitfall in oedometer tests concerns just the degree of saturation of soil samples [Chakrabarti & Horvath, 1986]. Incomplete saturation can be due to inappropriate storage conditions or sample preparation, but can also occur naturally in soil samples taken from the vadose zone. Moreover, organic soils are known to often contain methane or carbon dioxide gas bubbles as a product of anaerobic microbial activity feeding on the organic matter [Den Haan & Kruse, 2007]. Regardless of the exact cause, incomplete saturation of soil samples will lead to inaccurate compression test results if not taken into account – more specifically an *overestimation* of compressibility, since gas is by orders of magnitude more compressible than liquid. In addition, gas bubbles will also affect the hydraulic conductivity.

On the other hand, when a soil is initially unsaturated and being wetted or submerged in an oedometer cell, some unexpected behaviour could occur, such as initial swelling due to suction [Clayton & Hight, 2007]. Some types of clay are particularly prone to swelling, but in general all soils can swell upon wetting under low load. Swelling may become unexpectedly pronounced in case the soil contains soluble salts, which increases water absorption due to the osmotic effect. The accuracy and overall representativeness of test results can become highly doubtful, at least, when testing unsaturated and/or swelling soils in an oedometer.

The fact that only relatively thin soil samples are tested in an oedometer has the advantage of reducing wall friction, but at the same time has the major disadvantage of introducing scale effects as well as increasing the sensitivity to natural inhomogeneity and also to sample disturbance [Clayton & Hight, 2007]. Scale effects and inhomogeneity are particularly relevant for many (fibrous) peats, since coarse woody parts and fibres can make up the majority of such a peat soil sample. This fibrosity and coarseness also complicates sample preparation and increases the risk of disturbance [Den Haan & Kruse, 2007]. And sample disturbance in turn is known to affect the test results, which is why for soil compression and strength tests soil specimens always should be in an undisturbed state. More information on the significance and effects of sample disturbance are provided in subsection 3.3.3.1.

Furthermore, in a conventional oedometer pore water is only allowed to drain vertically, which neglects the anisotropic nature of many soils due to their sedimentary origin, affecting various mechanical and hydrological properties such as the permeability [Clayton & Hight, 2007]. Especially peat and clay, because of their horizontally oriented fibres or mineral particles, respectively, are strongly anisotropic. Generally speaking, the horizontal permeability is much larger, sometimes by more than two orders of magnitude, than the vertical. Since the former dominates drainage in practical geotechnical problems, oedometer test results concerning permeability will thus have limited value of use.

Penultimately, it has to be realised that the laterally confined and enforced vertical deformation will only provide useful information on the vertical (1D) compressibility characteristics of the soil. However in practice, depending on the problem geometry, the drainage capability of the soil and the loading rate, multi-dimensional deformation may occur. For instance fast loading of limited width compared to the thickness of the stratum will rather lead to an initial change in shape (by lateral expansion) without volume change, followed by volumetric strain when excess pore pressures slowly start to dissipate. Refer to subsection 3.3.3.3 for more elucidation with regard to multi-dimensional soil deformation effects in practice.

Lastly, considering the fact that usually between 6 [Knappett & Craig, 2012] and 14 [Reddy et al., 2015] loading steps including an unload-reload cycle are applied, and every step is maintained for at least 24 hours, the total duration of a single conventional oedometer test consequently requires between one and two weeks. No need to say that this may be regarded as a disadvantage.

3.1.2 Constant rate of strain (CRS) oedometer

The constant rate of strain (CRS) test is a more advanced alternative method of determining the compressibility characteristics of soils. Thanks to several advantages over the conventional (incremental loading) method, it has gained popularity especially in Canada, the U.S.A., Japan and Hong Kong [Reddy et al., 2015]. The primary advantage of the CRS method is that it can perform the same measurements as the conventional oedometer test during a much shorter time, rarely requiring more than two days in total [Den Haan et al., 2001], with the exception of tests on very low permeability (clay) soils. Moreover, it offers a direct way of determining the permeability of the soil and so the device can be classified as a permeameter as well [Adams, 2011].

As the name already implies, the CRS test is strain-controlled, contrary to the IL test that is stress-controlled. Since the former requires continuous operation, the device is controlled automatically and measurements are registered automatically (digitally) as well. Thanks to the automated registration, measurement intervals can be very short and the resolution accordingly high. Although all this automation decreases the need for human intervention during both the testing process and the registration of measurements, still the strain rate has to be set or adjusted manually in order to meet certain requirements for the excess pore water pressure, as explained further below. Nevertheless the overall human intervention and hence the probability of human errors during CRS tests is relatively low as compared with IL tests.

Furthermore, the shorter total test duration can increase productivity and at the same time decrease the unit labour costs [Adams, 2011]. However it should be remarked that the CRS oedometer as a whole is more complex (mechanically as well as electronically) and therefore much more expensive than the conventional oedometer. This will be further clarified in the following paragraph.

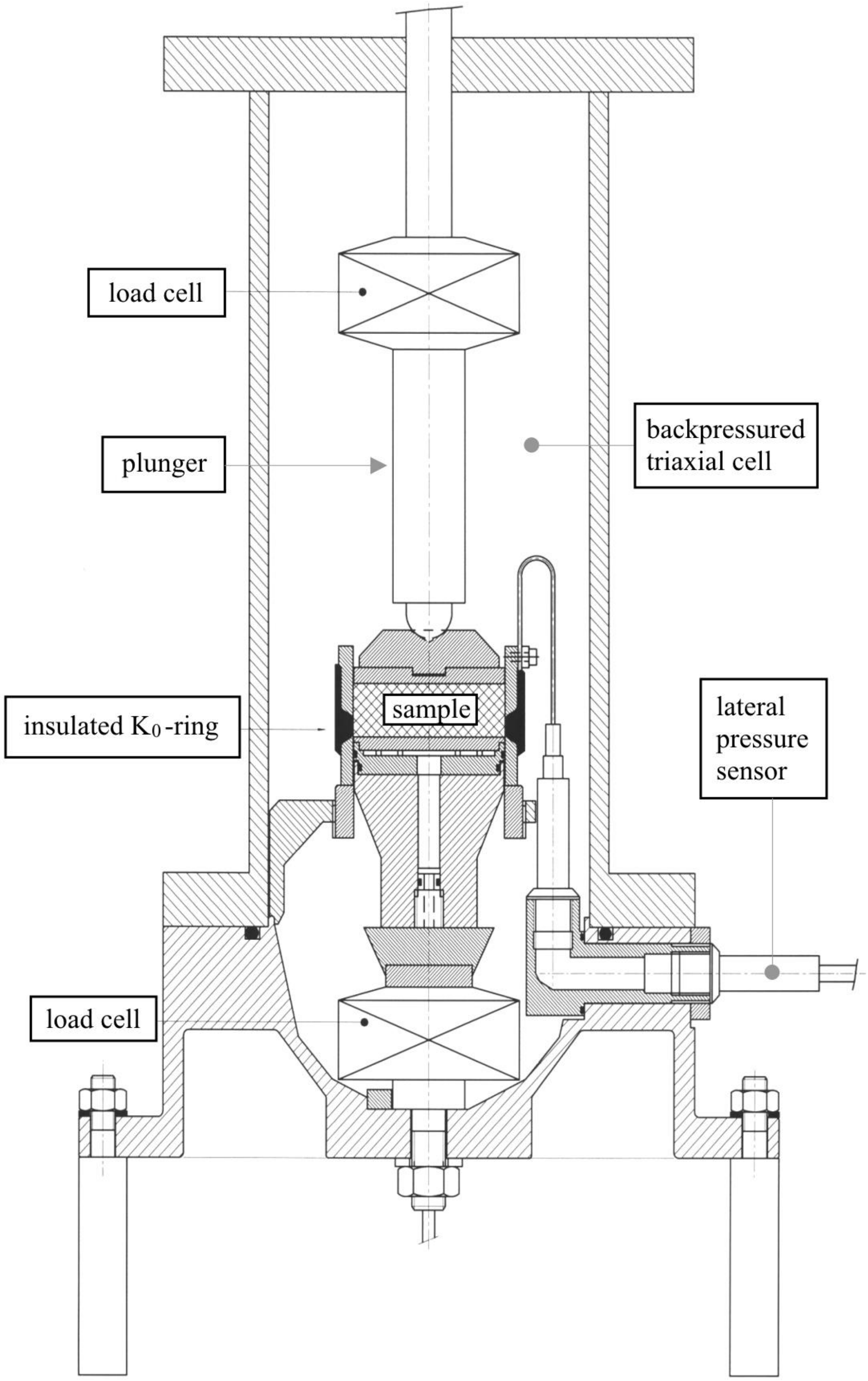

Figure 3-2: Schematic cross-section of a (K_0-)CRS test apparatus [Den Haan et al., 2001]. The currently used K_0-CRS apparatus at *Deltares* has no back pressure control, however [D.J.M. Ngan-Tillard, pers. comm.]. A regular (non-K_0) CRS apparatus merely lacks the K_0-ring and lateral pressure sensor.

Although the sample is also held inside a confining steel ring and the one-dimensional fashion of compression principally is the same as in a conventional oedometer, the CRS apparatus as a whole is very different (for a schematic representation, see Figure 3-2). First of all, the sample is more isolated from the environment by being situated in a closed cell, much like a triaxial cell. Consequently, the device offers the possibility to control the cell backpressure and thus the effective stress in the specimen. Apart from the total vertical pressure, which is measured by an external load cell, also the (excess) pore water pressure is measured by means of a pressure transducer located at or close to the bottom of the sample. The latter allows for direct calculation of the hydraulic conductivity or permeability [Adams, 2011], which may be regarded as a major advantage over a conventional oedometer.

However there are also some limitations and disadvantages of the CRS test. First of all it is nearly impossible, or at least technically very difficult, to maintain a constant load in order to determine the secondary compression or creep characteristics of the soil [Den Haan et al., 2001; Adams, 2011]. For long-term settlement predictions especially in organic soft soils, though, this is a very important characteristic and not being able to determine its value is deemed inacceptable. Fortunately there are alternative approaches to determine these characteristics from CRS tests, as suggested and described in [Den Haan et al., 2001]: either by means of applying a discrete strain *rate change*, or by maintaining a constant strain (i.e. rate = 0) and analysing the subsequent viscous relaxation behaviour. Both approaches require a very detailed set of measurement data based on tests that include either such a strain rate change or a phase of constant strain. The constant strain-relaxation method for creep parameters determination is applied in the further course of the current research as well and is detailed in subsection 4.2.2.4.

Furthermore, the choice of an appropriate strain rate ($\dot{\epsilon}$) for the soil to be tested is very important since dissipation of pore pressures must be ensured. However this can be quite difficult to do reliably *in advance* of the test that provides the required consolidation and permeability characteristics. Gorman et al. (1977) report that the chosen strain rate should generate at least 7 kPa of pore pressure but should not generate pore pressures in excess of 50% of the applied total vertical stress at any time during the test. The choice of strain rate may be based on the liquid limit (*LL*) of the soil to be tested, which is accompanied by the following indicative recommendation for clayey soils [Gorman et al., 1977]:

- if *LL* > 60, use $\dot{\epsilon} \approx 8.33 \cdot 10^{-7}\ s^{-1}$;
- if *LL* < 60, use $\dot{\epsilon} \approx 1.67 \cdot 10^{-6}\ s^{-1}$.

However Reddy et al. (2015) conducted series of CRS tests at several different strain rates on organic clays with *LL* > 60%, and they found that strain rates up to $8.0 \cdot 10^{-6}\ s^{-1}$ still satisfied the aforementioned excess pore pressure requirements. So the strain rates recommended by Gorman et al. are likely conservative values. Indeed, Den Haan et al. (2001) mention a value of $2 \cdot 10^{-6}\ s^{-1}$ as a common and appropriate strain rate regardless of the soil type.

Reddy et al. (2015) furthermore proved that the soil parameters determined from CRS tests, including preconsolidation pressure, coefficient of consolidation, hydraulic conductivity etc., are unfortunately strain rate-dependent. However at higher vertical effective stresses, the strain rate dependence diminishes.

Finally it must be noted that neither the CRS test procedure, nor the subsequent parameter determination, is described in any Dutch (NEN) or EU (Eurocode) standard. For CRS test execution and interpretation one therefore has to rely on foreign standards such as ASTM D4185 for instance.

3.1.2.1 K_0-CRS oedometer

A further development on the CRS test as described above, is the K_0-CRS test. This device was developed by *GeoDelft* (now *Deltares*) around the year 2000 and its main difference with respect to the “regular” CRS test is that it offers the possibility of measuring lateral stresses and hence the determination of the neutral lateral earth pressure coefficient, K_0 [Den Haan et al., 2001]. This parameter is especially of use in certain multi-dimensional finite-element geotechnical computer models, but not in 1D settlement prediction models as investigated in the current research. Its measurement is realised by means of an adapted confining ring with a thin titanium membrane equipped with strain gauges and/or hydraulic pressure sensors (Figure 3-3). Titanium is used rather than steel because it is less stiff than steel, so that it can be thicker and more robust, but still sufficiently deformable and sensitive. Because the device has been designed for application on very soft soils commonly encountered in the Netherlands, such as clay and peat, the Deltares K_0-ring can endure lateral stresses of no more than 250 kPa.

Besides this added functionality of lateral stress measurement, a method of determining the effect and magnitude of wall friction has been incorporated too, by measuring the vertical stress independently both on top and at the bottom of the soil specimen. The difference between these vertical stresses is considered to correspond with losses due to wall friction [Den Haan et al., 2001]. The (combined) influence of wall friction and excess pore pressure has been assessed analytically as well, by dr.ir. E.J. Den Haan in cooperation with dr.ir. J.B. Sellmeijer, which resulted in a set of fairly complex equations and derivations that were presented in chapter 5 of [Den Haan, 2001].

As for the rest, the K_0-CRS test in general has the same features and therefore also the same benefits and limitations as the "regular" CRS test. It may be added that the Koppejan compression coefficients (refer to section 3.2.3) cannot be determined with constant rate of strain-devices, but must be determined by means of conventional (IL) oedometer tests.

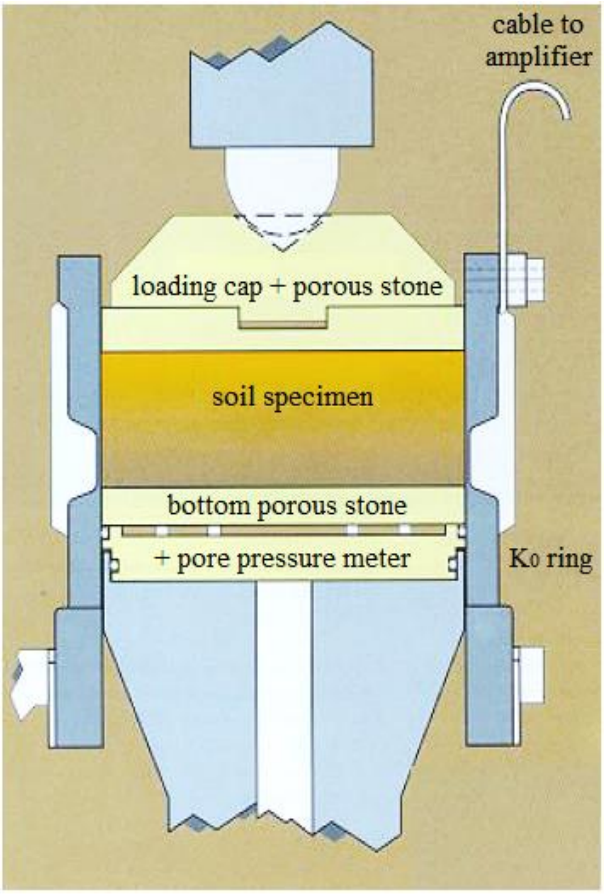

Figure 3-3: Close-up schematic cross-section of a K_0-CRS test apparatus, zoomed in on the sample container with the K_0-ring and its thin membrane [Den Haan et al., 2001].

3.2 Chronological review of settlement prediction methods

This chapter comprises a comprehensive review of the most important or most distinctive one-dimensional settlement prediction methods that have been developed in the course of the past century. It has been tried to remain to the point as much as possible by describing just the essential background and features of each method, and highlighting the most significant differences and (dis)advantages with respect to other methods. Regarding the equations shown, the choice is made to adhere to the original notation and use of symbols as much as possible in order to illustrate the variety encountered in literature, as well as to accentuate their differences in a historical developmental perspective.

3.2.1 **Terzaghi** (1925)

Karl von Terzaghi, who was already introduced in chapter 2.2, is considered to have proposed the first coherent consolidation theory by combining his effective stress principle with hydrological principles following from Darcy's law. Accordingly, his book *Erdbaumechanik* (1925) also provides a well-founded attempt at describing and formulating the compression and swelling behaviour of – especially cohesive – soils, albeit in a different form than it is known nowadays. This might be due to the fact that Terzaghi focused more on the hydrodynamic processes in relation to soil compression and particularly expansion, rather than on the implications for the settlement of embankments and structures.

Nevertheless Terzaghi was the first to infer from laboratory tests conducted on laterally confined clay and sand samples, that a logarithmic relationship was appropriate to describe one-dimensional soil deformation. Graphically he displayed this in a "Druck-Porenziffer-Diagramm" (English: pressure-void ratio diagram), comprising a so-called "Hauptast" (English: main branch) and a so-called "Schwellkurve" (English: swelling curve), representing virgin compression/loading and expansion/unloading, respectively. His formula for the main branch, or virgin compression curve, which empirically relates void ratio to vertical pressure, originally reads as follows [Terzaghi, 1925]:

$$e = -\alpha \ln (p_s + p_c) - \beta \ln (p_s + p_c) + c \tag{3-1}$$

Where:

- e = void ratio[(1)] = volume of voids / volume of solid soil particles [-]
- α = empirical constant, as a measure of the compressibility of the material [-]
- β = empirical constant, generally negligible [-]
- p_s = applied pressure (supposedly *effective* pressure, although not explicitly stated) [kPa]
- p_c = empirical constant, depending on the material and its water content, in order to avoid that e will go to infinity if $p_s \rightarrow 0$ [kPa]
- c = empirical constant, essentially representing the void ratio at a reference stress of 1 kPa [Fröhlich, 1934].

Although some further elucidation of this relationship (3-1) with regard to settlement prediction was provided in *Theorie der Setzung von Tonschichten* [Terzaghi & Fröhlich, 1936], still that publication did not present the formulation as it is commonly known nowadays. Instead, the current "logarithmic compression law" or "load-settlement law", being attributed to Terzaghi, did not appear in literature until around 1940 and is generally formulated as follows [e.g. Buisman, 1940; Koppejan, 1948]:

---

[1]) Terzaghi used to represent void ratio by the symbol *ε* (epsilon), which in this report however was decided to be replaced by the nowadays more commonly used letter *e*, in order to avoid any possible confusion with strain.

$$\frac{z}{h} = \frac{1}{C} \ln\left(\frac{p_0 + \Delta p}{p_0}\right) \tag{3-2}$$

Which, however, is also known to exist in a different but equivalent form [Heemstra, 2013]: (2)

$$\epsilon = \frac{C_c}{1 + e_0} \log\left(\frac{p_0 + \Delta p}{p_0}\right) \tag{3-3}$$

Where:
z = compression of the soil layer [m]
h = total (initial) thickness of the compressible soil layer [m]
C = compression coefficient [-]
p_0 = initial effective overburden pressure [kPa]
Δp = increase of effective pressure due to loading [kPa]
ε = linear strain(2) = z / h [-]
e_0 = initial void ratio [-]
C_c = compression index [-]

The quotient $C_c / (1 + e_0)$ in equation (3-3) is also known as the “compression ratio” and denoted as *CR*, which would be used later again in the formulation of Bjerrum’s isotache model (1967). The compression index itself can be found by determining the slope of the virgin compression line in an *e*-log(*p*) diagram, according to equation (2-3): $C_c = \Delta e / \Delta\log(p)$.

Similarly, the compression coefficient (*C*) that appears in equation (3-2) is related to the slope of the virgin compression line in an ε-ln(*p*) diagram, although in this case representing the *inverse* of the slope. This coefficient may as well be expressed in terms of the more often used compression index by: $C = \ln(10)\cdot(1 + e_0) / C_c$.

Since Terzaghi’s compression law is based on the principles posed within the framework of his consolidation theory (1925), consequently it is also limited by its associated assumptions, namely [Knappett & Craig, 2012]:

1. The soil is homogeneous;
2. The soil is fully saturated;
3. The solid particles and water are incompressible;
4. The compression and flow are one-dimensional;
5. Strains are small;
6. Darcy’s law is valid for all hydraulic gradients;
7. The permeability and the coefficient of volume compressibility remain constant throughout the process;
8. There is a unique and time-independent relationship between void ratio and effective stress.

According to Knappett & Craig, the main limitations of Terzaghi’s theory (apart from its one-dimensional nature) arise from assumption 8: experimental results show that the relationship between void ratio and effective stress is not independent of time. As well, Terzaghi’s compression law implies that a final compression is reached for any finite load, which is known to not be the case [Koppejan, 1948]. These time-related issues have been addressed by subsequent settlement prediction methods, starting with Keverling Buisman (refer to section 3.2.2).

2) Heemstra (2013) mistakenly wrote the void ratio (*e*) left of the equals sign, whereas he meant and should have written strain: $\varepsilon = \Delta e / (1 + e_0)$.

Furthermore, Terzaghi's compression law is only valid for virgin compression, i.e. for stress levels higher than the preconsolidation pressure, or normally consolidated soils. Also it has to be kept in mind that it is based on elastic compression principles, implying full recoverability of strains (note the small strain assumption), which is known to be unrealistic for highly deformable soils like peat in particular.

Lastly, when just considering strains in peat, one more quite inconvenient problem has to be addressed. As effective stresses in peats are most often very low (in fact, close to zero) due to their exceptionally high water content and low unit weight, p_0 may be so small with respect to Δp that the value of the argument of the logarithm will increase dramatically and therefore the calculated strain or settlement will become unrealistically large – possibly even larger than the initial layer thickness [Soudijn & De Kock, 1977].

3.2.2 **Keverling Buisman** (1940)

In subsequent years after Terzaghi (1925) it was experienced that the soil compression process does not end within times of observation, but in fact continues in a way that could not be explained by the existing theory of consolidation. Prof. ir. A.S.K. Buisman found, based on settlement measurements of embankments and structures and on test results of undisturbed soil samples, that soil compression must be distinguished in two different phases: namely a "direct" (consolidation) phase, and a "secular"[(3)] phase being approximately linear with the logarithm of time. In his book titled *Grondmechanica* (1940), his "secular time-settlement law" is formulated as follows [Buisman, 1940]:

$$s_t = h_0 \cdot p \cdot (\alpha_p + \alpha_s \cdot \log t) \tag{3-4}$$

Where:

s_t	=	settlement of the soil layer at time t [m]
h_0	=	total initial thickness of the compressible soil layer [m]
p	=	increase of effective pressure due to loading [kPa]
α_p	=	direct compression constant, indicating compression at $t = t_0$ (usually 1 day) [-]
α_s	=	secular compression constant, indicating the increase of compression with ten-fold increase of time [-]
t	=	time [days]

The compression constants are to be calculated per unit thickness and unit pressure, which can be achieved either by reading the settlement s_t at appropriate times from a time-settlement diagram and dividing s_t by ($h_0 \cdot p$), or by reading directly from a time-settlement diagram where the vertical axis is already scaled by $1/(h_0 \cdot p)$, such as indicated schematically in Figure 3-4.

Note that after some time the terms "direct" and "secular" synonymously became known as "primary" and "secondary", respectively. The first might be due to the *p* in the subscript, in combination with the fact that it is the first phase taking place. Renaming secular to secondary might be a logical consequence after the former. However some experts in the field [e.g. Heemstra, 2013] urge to not mix up the terms "secular" and "secondary", since they are defined slightly differently: secondary compression refers to the deformation process occurring after consolidation has completed in general, whereas the secular effect specifically is defined as a time- and stress-dependent deformation characteristic being zero at t = 1 day and being applicable only after that moment in time.

[3]) Secular: derived from Latin "saeculum", meaning: (life)time, age or century. Hence "secular" may be interpreted as "perpetual" or "endless".

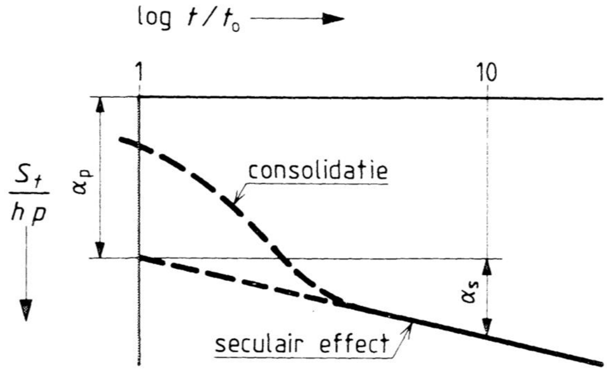

Figure 3-4: Schematic semi-logarithmic time-settlement diagram, illustrating the definition of the direct and secular compression constants [NEN 5118: Fig. 12].

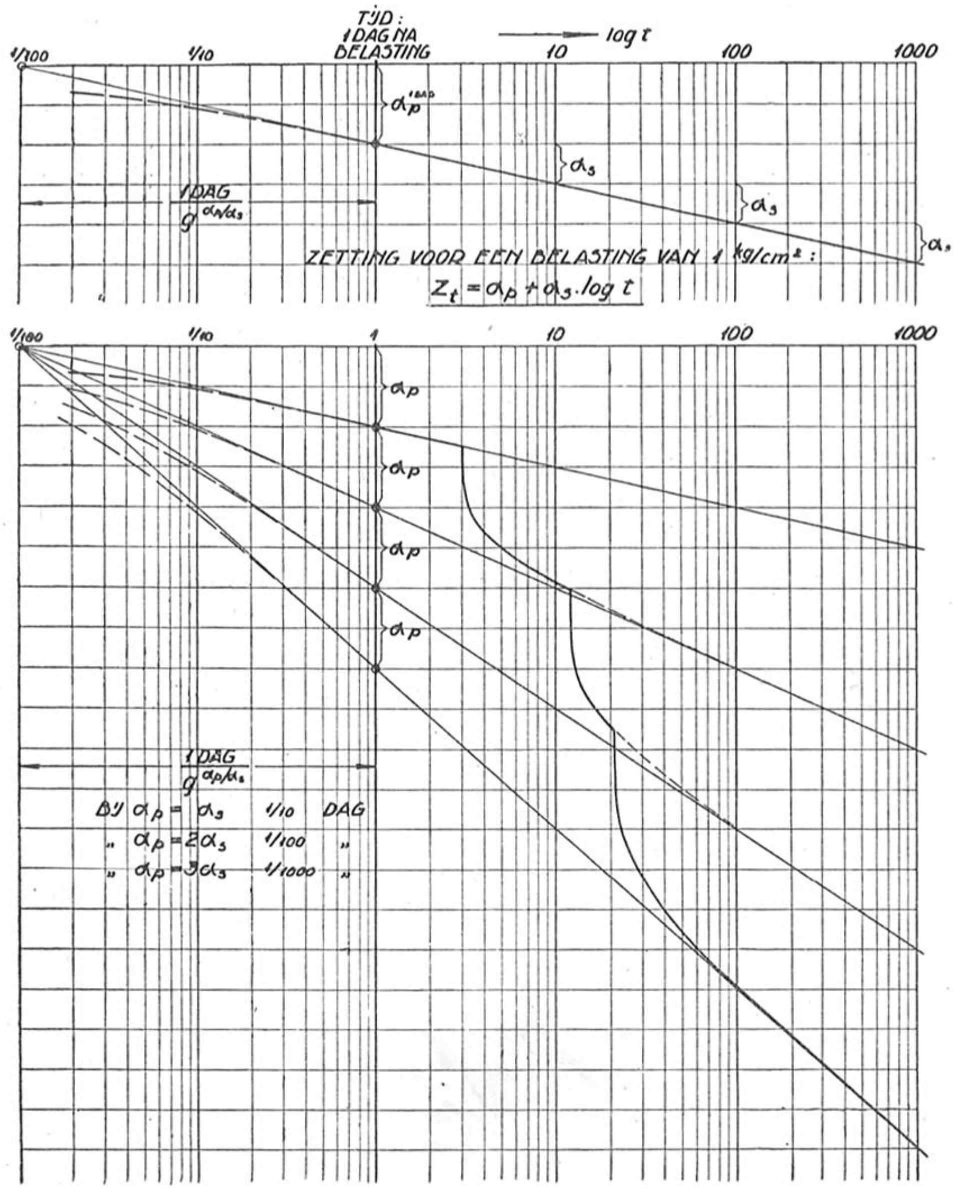

Figure 3-5: Schematic and hypothetic semi-logarithmic time-settlement diagram, illustrating Buisman's principle of superposition for soil compression due to staged loading [Buisman, 1940: Fig. 68].

In §45 of *Grondmechanica* (1940), Buisman treats the special case of soil compression due to step-wise, or staged, loading. He provides an interpretation of some staged compression test results, along with a proposed approach of how to deal with such problems in settlement prediction. He suggested that a sequential load increase could be considered to be superposable on the previous and/or still ongoing compression process, which implies that the slope of every new settlement asymptote is larger than the previous one. This can be best illustrated by means of a time-settlement diagram, as provided schematically in Figure 3-5.

In the course of the following decades, however, it was found that the application of Buisman's superposition principle led to substantial overestimations in settlement predictions: every superposition step introduces an error, cumulating with each loading stage considered. This error may be caused by the fact that the previous loading stage is not completely consolidated yet when the next stage is applied already, which is a common practice [Van Baars, 2003]. Therefore the superposition principle must be regarded as incorrect. Instead, every loading stage should be considered to be independent of the previous stages, such that the slope of the settlement asymptotes remains constant on the long term and independent of the load applied [Den Haan, 2003; Heemstra, 2013]. Be aware that this problem is also relevant for the later Koppejan method (1948), in which the superposition principle was originally applied as well. However outside of the Netherlands both methods, let alone the superposition principle, are rarely applied anyway [Den Haan, 2003].

Another limitation of Buisman's method is that it implicitly assumes that secular compression does not occur before t = 1 day: for t < 1 day, the contribution of secular compression would become negative, which is physically impossible and therefore incorrect. Furthermore, Buisman's formula is only valid for virgin compression and therefore cannot take into account preconsolidation, just as Terzaghi's load-settlement law. And finally, it is known that the compression constants, α_p and α_s, are not really constant but depend on time and stress state [NEN 5118].

3.2.3 **Koppejan** (1948)

Because Terzaghi's load-settlement law has the shortcoming of not considering time-dependent (secular) soil compression, and Buisman's secular time-settlement law does not take into account the stress dependence of secular compression, ir. A.W. Koppejan combined Terzaghi's law with Buisman's law, so that he obtained the following formula [Koppejan, 1948]:

$$s = h_0 \left(\frac{1}{C_p} + \frac{1}{C_s} \cdot \log_{10} t \right) \log_e \frac{p_0 + p}{p_0} \tag{3-5}$$

Where:
s = settlement of the soil layer [m]
h_0 = total initial thickness of the compressible soil layer [m]
C_p = Koppejan primary compression coefficient [-]
C_s = Koppejan secondary compression coefficient [-]
t = time after loading [days]
p_0 = initial overburden pressure [kPa]
p = pressure increase due to loading [kPa]

According to Koppejan (1948) "*the use of logarithms of different bases in the formula has been accepted in order to adhere to the basic formulas as much as possible*" (p.37). If desired, however, this could be avoided easily by adding a factor of $\log_e(10) \approx 2.3$ and subsequently replacing the natural (base e) logarithm by a common (base 10) logarithm.

Although the original Koppejan formula could not handle preconsolidation, it was soon adapted in order to also cope with overconsolidated soils, by means of another set of compression coefficients. The adapted formula required that any load (step) that passes the preconsolidation pressure has to be split in a sub-step below and a sub-step above the pre-consolidation pressure [Deltares, 2014]. The according formula reads, according to CUR (1996):

$$\frac{\Delta h}{h} = \left(\frac{1}{C_p} + \frac{1}{C_s} \cdot \log \frac{\Delta t}{\Delta t_d}\right) \cdot \ln\left(\frac{p_g}{\sigma'_i}\right) + \left(\frac{1}{C'_p} + \frac{1}{C'_s} \cdot \log \frac{\Delta t}{\Delta t_d}\right) \cdot \ln\left(\frac{\sigma'_i + \Delta\sigma'}{p_g}\right) \tag{3-6}$$

Where:
Δh = compression of the soil layer [m]
h = total initial thickness of the compressible soil layer [m]
C_p = Koppejan primary compression coefficient below the preconsolidation pressure [-]
C_s = Koppejan secondary compression coefficient below the preconsolidation pressure [-]
Δt = time after loading [days]
Δt_d = time of one day = 1 [day]
p_g = preconsolidation pressure [kPa]
σ'_i = initial effective stress in the middle of the soil layer [kPa]
C'_p = Koppejan primary compression coefficient above the preconsolidation pressure [-]
C'_s = Koppejan secondary compression coefficient above the preconsolidation pressure [-]
$\Delta\sigma'$ = increase of effective stress after consolidation [kPa]

Note that in practice h is commonly placed at the right side (just as h_0 in the original formulation), leaving solely the settlement Δh at the left side of the equals sign. Furthermore, the quotient (p_g / σ'_i) essentially represents the overconsolidation ratio (OCR) and Δt_d (= 1) is sometimes omitted, since this is needed just for mathematical dimensional correctness.

Unfortunately the Koppejan formula still incorporates several limitations from its predecessors. Amongst these is the fact that the compression coefficients C_p and C_s are not really constant [NEN 5118]. Also, application of the superposition principle was proven incorrect (refer to the last paragraphs of section 3.2.2). Furthermore, the problem of unrealistically large strains remains when the initial effective stress is very small with respect to the load (refer to the final paragraph of section 3.2.1). And finally the formula is again based on the implicit assumption that secular or secondary compression occurs only at $t \geq 1$ day, which is incorrect.

Another serious limitation that emerged at later times, is that the Koppejan method as well as previous methods cannot cope with unloading [Ammerlaan, 2011]. This is relevant when trying to model the application and subsequent removal of extra surplus height in construction projects.

In spite of its known limitations, however, the Koppejan method has become very popular in the Netherlands. This might be because of its relative simplicity whilst still it was the most complete settlement prediction model available for quite a long time (about 20 years). Furthermore, over the years a lot of practical experience has been gained with using this model, as well as with the parameter determination methods and the resulting values that have become intuitive to many users. Due to it being so naturalised in the Dutch geotechnical engineering sector, even nowadays it is still regularly used for settlement predictions [Visschedijk, 2010; Ammerlaan & Hoefsloot, 2012].

However due to its popularity, the Koppejan method has also been subject to a lot of research over the course of decades, which has resulted in some notable improvements of the original model. First of all, the relationship has been adapted to take account of the fact that consolidation does not happen instantaneously but instead is a time-dependent process, since pore pressures need time to dissipate, which according to Terzaghi's effective stress principle (section 2.2.1) leads to a *gradual* increase in effective stress and hence primary compression. In order to incorporate this time-dependency of primary compression into the Koppejan formula, the first term (1 / C_p) is multiplied with the degree of consolidation, U, which is a function of, amongst others, the coefficient of consolidation (c_v) and time. The downside of this extension, however, is that the consolidation coefficient is a function of the stiffness and permeability of the soil: whilst these are often simply assumed to be constant, both in fact depend on the (changing) stress and strain state. Obviously this complicates calculations a lot, but at the same time it will make settlement predictions during the primary phase (i.e. on relatively short term) more accurate, if implemented correctly.

Furthermore, the problem of unrealistically large strains – i.e. strains close to or even larger than the initial layer thickness – was resolved after introduction of the concept of *natural* strain in settlement analysis by E.J. den Haan in 1994: a detailed explanation of this concept is provided in subsection 3.2.7.1. Strictly speaking though, the use of natural strain instead of linear (engineering) strain in calculations with the Koppejan method also requires a different way of determining the compression coefficients, namely based on settlement diagrams in natural strain representation [Van Baars, 2003; Deltares, 2014]. However that requirement usually seems to be neglected in practice, as follows from various ground investigation and/or laboratory test reports [e.g. Van der Valk, 2007; Alink, 2012]. Nevertheless, the Koppejan method with "natural strain correction" has become the preferred method in cases where the Koppejan method is used.

When just considering the compression coefficients, it should be remarked that the determination of those has proven to be prone to errors (refer to section 3.3.3). Multiple attempts have been made to simplify and/or improve testing procedures, or to follow an indirect approach by correlating soil physical or index properties to compression coefficients. Regarding the latter, for example the porosity of peat soil has been correlated with the Koppejan compression coefficients by R.J. de Glopper (1979), which is described separately in section 3.2.6.

Finally, another improvement, called the "incremental method", has been suggested by Prof. S. van Baars (2003). This method is reported to cope well with staged loading, also it takes into account the time-dependent degree of consolidation and it even does so for pore water pressures during the secondary compression phase. To account for the changing permeability and stiffness during consolidation, the change in pore pressure is related to a change in effective stress and strain via Darcy's law. This is formulated and solved in an incremental fashion, since the method was developed with implementation into a numerical or finite-element model in mind. The according formula is a second order differential equation that is impractical to solve analytically by hand.

$$\dot{p} = \dot{\sigma}_v + \frac{\sigma_v - p}{1/C_p}\left[\frac{k}{\gamma_w}\frac{\delta^2 p}{\delta z^2} + \varepsilon_p \frac{C_p}{C_s \ln(10)} \exp\left(-\frac{\varepsilon_s}{\varepsilon_p}\frac{C_s \ln(10)}{C_p}\right)\right] \tag{3-7}$$

This Koppejan incremental method has not been implemented in commercial software packages that are most commonly used for settlement predictions in the Netherlands (e.g. *D-Settlement* or *PLAXIS*). However it seems that the *Rocscience Settle*^{3D} software does have this functionality [Rocscience Inc., 2009], since its user manual refers to Van Baars (2003).

According to his article, Van Baars has programmed the incremental method himself for validation, which was confirmed after personal communication: apparently the incremental method was programmed in Pascal and compiled as a dynamic link library, to be utilised as a user-defined soil model (UDSM) in *PLAXIS*. Upon request, Van Baars not only was able to retrieve the UDSM, but also readily willing to make it available for use in the current research, which the author is very grateful for. However on try-out, unfortunately the UDSM was not recognised by *PLAXIS* 2D (v.2015). Communication with *PLAXIS* revealed that the script lacks nowadays required 64-bit support and, more importantly, depends on an external function or library that is not included with contemporary versions of *PLAXIS* anymore. In order to resolve the problems, the original Pascal script would have needed to be edited by removing and replacing the external library dependency and subsequently re-compiling with 64-bit support. However the time available for this research did not allow for doing so, especially considering the lack of required software and limited programming skills, which altogether also would be beyond the scope of this research.

3.2.4 **Bjerrum** (1967)

Since development of the Koppejan method, research went on and particularly the influence of time on soil compressibility was investigated in more detail, yielding new insights with regard to the so-called “aging” effect(4) [Bjerrum & Lo, 1963]. As a result, it had emerged that compression cannot be described by a single curve in an *e*-log(*p*) diagram. Instead, a different representation, consisting of a system of parallel lines or curves, was considered to be more appropriate (see Figure 3-6). Each of these lines represents the equilibrium void ratio for different values of effective overburden pressure at a specific time of sustained loading [Bjerrum, 1967].

Because each of those parallel lines represents in fact a line of equal creep rate, it could be called an “isotache” (from “iso”: equal, and “tachos”: speed). Therefore in subsequent years this model became known as the “isotache model”. An adapted formulation of this model (3-14) also became part of the governing Dutch NEN standard [NEN 6740], which usually is referred to as “NEN-Bjerrum model”. Especially outside of the Netherlands the Bjerrum model has become well known and even has become the present-day de facto standard for settlement predictions.

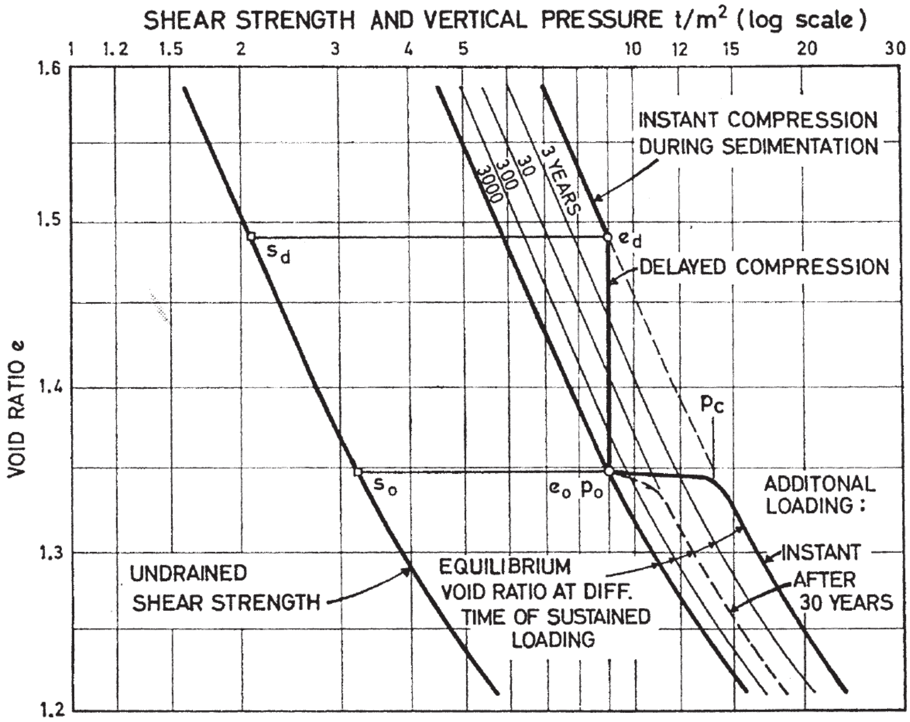

Figure 3-6: Schematic isotache diagram illustrating the compressibility as well as the shear strength development of a clay in compression [Bjerrum, 1967: Fig. 14].

On this occasion, however, it should be pointed out that Bjerrum was not the first to propose an isotache model: his findings were for a large part based on preliminary research by other researchers, amongst whom Šuklje (1957) was the first to use the term “isotache” in the context of soil mechanics. However the name Bjerrum became associated with this model, not only because he managed to comprehensively combine and integrate findings from multiple foregoing studies with own observations, but especially because he was the first to notice that creep rate depends on both overconsolidation ratio and age [Deltares, 2014].

4) Aging: the effect of cohesive soil, e.g. clay, exhibiting an increase of undrained shear strength and more brittle failure behaviour after longer times of sustained static loading. This is explained by the formation of cohesive bonds between the particles [Bjerrum & Lo, 1963].

At the same time, Bjerrum introduced a new terminology concerning the phase of compression, namely “instant” and “delayed” compression, which are differently defined than the more well-known primary and secondary compression phases: instant and delayed compression describe the reaction of the soil with respect to an increase of the effective stresses, whereas the primary and secondary compression are defined with respect to the point in time where pore pressures have dissipated.

Figure 3-7 is intended to clarify the definition of “instant” and “delayed” compression. It is shown how the compression of a clay layer develops with time if loaded with a suddenly-applied uniformly distributed pressure. The dashed curves represent the soil reaction that would occur if the applied pressure were transferred immediately to the clay structure as an effective pressure, and defines the instant and delayed compression. However in reality effective stresses will increase gradually since excess pore pressures dissipate slowly as well, so that the compression will follow the solid curve [Bjerrum, 1967].

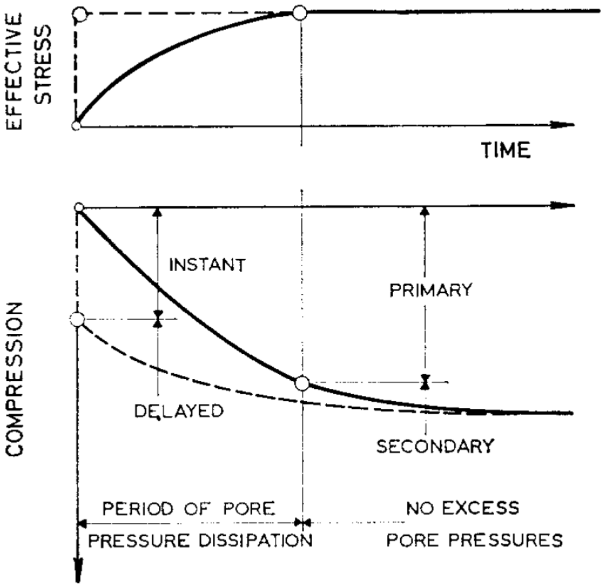

Figure 3-7: Schematic time-compression diagram illustrating the definition of “instant” and “delayed” compression compared with “primary” and “secondary” compression [Bjerrum, 1967: Fig. 15].

No complete mathematical formulation for the isotache model was provided originally by Bjerrum in 1967. Instead, the first one to do so was Garlanger (1972):

$$\Delta e = C_r \log \frac{p_c}{p_0} + C_c \log \frac{p_f}{p_c} + C_\alpha \log \frac{t_1 + t}{t_1} \tag{3-8}$$

Where:

Δe = change in void ratio [-]
C_r = slope of the compression line from p_0 to p_c (referring to Figure 3-6) [-]
C_c = slope of the “instant line” according to Garlanger (see remark just below), which in fact is the compression index as in equation (3-3) [-]
C_α = slope of the “delayed compression” curve in an e-log(t) diagram, i.e. the creep isotache separation in an e-log(p) diagram [-]
p_c = “critical pressure”, or preconsolidation pressure (see remark just below) [kPa]
p_0 = initial effective pressure [kPa]
p_f = applied effective pressure [kPa]
t_1 = time given to the “instant line” [days]
t = time variable [days]

Since only the third term, associated with coefficient C_α, describes the process of delayed compression, being a function of time, consequently both preceding terms *together* describe instant compression. When Garlanger (1972) uses the term “instant”, however, he seems to refer exclusively to the second term, associated with coefficient C_c. But the latter is just the elasto-plastic component of instant compression, whereas the very first term is the elastic component of instant compression.

The “critical pressure” (p_c) at the intersection point of the elastic and the elasto-plastic (instant) compression lines corresponds with the preconsolidation pressure. As follows from Figure 3-6, the preconsolidation pressure does not necessarily have to result from an actual overburden pressure, but can also be due to delayed compression under sustained loading, i.e. due to aging. So the (apparent) preconsolidation pressure will increase as time passes, although the load may remain constant.

In the course of time, the Bjerrum model formulation has been adapted to exist in several different forms, the two most common of which are presented in equations (3-9) and (3-11).

$$\epsilon(t) = RR\log\left(\frac{\sigma_p}{\sigma'_0}\right) + CR\log\left(\frac{\sigma'_n}{\sigma_p}\right) + C_\alpha\log\left(\frac{t-t_n+\theta_n}{t_{ref}}\right) \tag{3-9}$$

[Visschedijk, 2010; Deltares, 2014]

Where:
$\varepsilon(t)$ = linear strain as a function of time = $\Delta h / h$ as in equation (3-6) [-]
RR = primary compression coefficient below the preconsolidation pressure = $C_r / (1 + e_0)$ [-]
CR = primary compression coefficient above the preconsolidation pressure = $C_c / (1 + e_0)$ [-]
C_α = secondary compression, or creep, coefficient above the preconsolidation pressure [-]
σ_p = effective preconsolidation stress [kPa]
σ'_0 = initial effective stress [kPa]
σ'_n = effective stress after application of loading step n [kPa]
t = time variable [days]
t_n = moment in time of application of loading step n [days]
t_{ref} = reference time = 1 [day]
θ_n = equivalent age after application of loading step n [-]

The “equivalent age” was introduced here by analogy with the intrinsic time in the later developed a,b,c-Isotachs model [Den Haan, 1992]. Further explanation in that regard can be found in section 3.2.7.2: for now it is deemed sufficient to know that its value can be obtained with the following formula [Visschedijk, 2010; Deltares, 2014]:

$$\theta_n = \left(\frac{\sigma'_{n-1}}{\sigma'_n}\right)^{\frac{CR-RR}{C_\alpha}} \cdot (\theta_{n-1} + t_n - t_{n-1}), \qquad \theta_0 = t_{ref} \cdot \left(\frac{\sigma_p}{\sigma'_0}\right)^{\frac{CR-RR}{C_\alpha}} \tag{3-10}$$

In case stresses are higher than the preconsolidation pressure, or if the soil is normally consolidated, the term containing RR can be neglected and so the formulation becomes equivalent to the forms shown below, according to NEN 6740:

$$w_1 = \sum_{j=0}^{j=n} \frac{C_{c;j}}{1+e_j} \times h_j \times \log\frac{\sigma'_{v;z;0} + \Delta\sigma'_{v;z}}{\sigma'_{v;z;0}} \tag{3-11.1}$$

$$w_2 = \sum_{j=0}^{j=n} C_{\alpha;j} \times h_j \times \log\frac{t_\infty}{t_1} \tag{3-11.2}$$

Where:
w_1 = primary compression of the soil layer [m]
w_2 = secondary compression of the soil layer [m]
$C_{c;j}$ = primary compression index above the preconsolidation pressure [-]
$C_{\alpha;j}$ = secondary compression index above the preconsolidation pressure [-]
e_j = initial void ratio of the compressible soil layer *j* [-]
h_j = total initial thickness of the compressible soil layer *j* [m]
$\sigma'_{v;z;0}$ = vertical effective stress before loading, in the middle of the soil layer at depth *z* [kPa]
$\Delta\sigma'_{v;z}$ = vertical effective stress increase due to loading, in the middle of the soil layer at depth *z* [kPa]
t_∞ = end time of secondary compression, in days after loading = 10 000 [days]
t_1 = start time of secondary compression, in days after loading = 1 [day]

Consequently, in contrast to equation (3-9), the NEN formulation (3-11) is only valid for virgin compression, i.e. when stresses are higher than the preconsolidation pressure. In fact, NEN does not provide any information about how to deal with overconsolidated soil in settlement predictions using the Bjerrum model. This was not the only case where NEN was found to be very succinct and in fact incomplete. Fortunately, however, common settlement analysis software such as *D-Settlement* by *Deltares* does still offer this functionality when using the "NEN-Bjerrum" model.

It is deemed important to point out that the secondary compression index (C_α) can be defined in two different ways [CROW, 2004; Deltares, 2014]: namely an index with respect to strain ($C_{\alpha\varepsilon}$) and an index with respect to void ratio ($C_{\alpha e}$). Both indices appear in literature regarding Bjerrum's isotache model, but unfortunately often without a mention of which definition is used, although that may follow from the dependent variable being used (either strain or void ratio). Anyhow, it is important to be aware of this difference, since the indices are related as follows:

$$C_{\alpha\epsilon} = \frac{C_{\alpha e}}{1 + e_0} \tag{3-12}$$

Keeping in mind that the initial void ratio (e_0) of certain soils – peat in particular – can be as high as 10 and even higher [Bell, 2007; Mesri & Ajlouni, 2007], the indices' values can thus easily differ by an order of magnitude for the same soil. Both equations (3-9) and (3-11) make use of the strain-based secondary compression index ($C_{\alpha\varepsilon}$), however this is not explicitly stated in the corresponding publications. Confusion may increase even more when knowing that in most international literature [e.g. Garlanger, 1972] the void ratio-based index ($C_{\alpha e}$) is used, in which the subscript *e* is usually omitted just like in the aforementioned equations that use the strain-based index, however.

The isotache model has some constraints as well. First of all, just as for previous settlement prediction methods, the compression coefficients are not really constant [Den Haan et al., 2004]. This translates visually to the fact that the isotache lines are not exactly parallel but slightly curved, especially towards higher stresses and strains, or lower void ratios. Only the *ratio* of C_α / C_c may be considered constant for a particular soil, which has become known as the "C_α / C_c concept of compressibility" [Mesri & Godlewski, 1977]. As a side note, amongst all soils peats exhibit the highest values of this ratio, namely up to 0.10 [Mesri et al., 1997], although Dutch peats were found to have somewhat lower C_α / C_c ratios of about 0.06 [Den Haan, 1994].

According to Sipkema (2006), a further limitation is that secondary compression is not taken into account below the preconsolidation pressure although it should be. However this seems to be simply a matter of definition of the secondary compression index in equation (3-9): theoretically the model should be able to cope with secondary compression below the preconsolidation pressure since the corresponding term is merely time-dependent and not stress-dependent.

Lastly, Deltares (2014) explicitly points out that the accuracy of the isotache model strongly depends on the input parameters, but practice proves that the determination methods for NEN-Bjerrum parameters as well as the results can differ significantly from laboratory to laboratory. This remark is relevant for all empirical models, however, and will also be further addressed in section 3.3.3.

3.2.5 **Fokkens** (1970)

Ir. B. Fokkens was a lead engineer at *Grontmij N.V.* (acquired by *Sweco* in late 2015) when he developed his settlement prediction method based on Terzaghi's logarithmic compression law in combination with the empirical so-called "rijpingswet" (English: ripening law). Ripening, also known as "initial soil formation", comprises shrinkage and confirmation of soft soil as a result of pedogenetic(5) processes including, amongst others, dewatering due to evapotranspiration, and biological and geochemical processes [Pons & Zonneveld, 1965].

In brief, by combining both aforementioned laws, Fokkens inferred that it should be possible to relate empirically the quotient of organic matter content and water content to the effective overburden stress. He verified his supposition with laboratory test data on peat samples taken from below the phreatic level at 25 different but unknown locations, all with an organic matter content higher than 30%, tested at stresses ranging from 2 to 200 kPa.

Consequently, Fokkens was able to elaborate a relationship that describes compression of peat soil as a function of organic matter content, water content *and* pressure. Not only did he consider normally and overconsolidated peat soils separately, but for each he also provided two different formulas: one semi-analytical formula purely in terms of material parameters, and a second more empirical formula in which some of the parameters (namely n_1, C_v and p_m) are substituted by inter-relationships or by numbers obtained from empirical correlations.

The resulting formulas originally read as follows [Fokkens, 1970].

For normally consolidated soils:

$$\frac{\Delta Z}{Z} = \frac{n_1}{C_v \frac{H}{A_1} + \ln \frac{p_2}{p_1}} \cdot \ln \frac{p_2}{p_1} \tag{3-13.1}$$

$$\frac{\Delta Z}{Z} = \frac{A_1}{A_1 + 0.62H + 38} \cdot \frac{1}{25.3 \frac{H}{A_1} + \ln \frac{p_2}{p_1}} \ln \frac{p_2}{p_1} \tag{3-13.2}$$

For overconsolidated soils:

$$\frac{\Delta Z}{Z} = \frac{n_1}{C_v \frac{H}{A_1} + \ln \frac{p_2}{p_m}} \cdot \ln \frac{p_2}{p_m} \tag{3-14.1}$$

$$\frac{\Delta Z}{Z} = \frac{A_1}{A_1 + 0.62H + 38} \cdot \left(1 - \frac{\frac{H}{A_1}}{0.0395 \ln p_2 - 0.066}\right) \tag{3-14.2}$$

5) Pedogenesis: the natural process of soil formation, including a variety of subsidiary processes such as humification, weathering, leaching, and calcification. From: Oxford Reference, 2015.

Where:
ΔZ = compression of the soil layer [m]
Z = total initial thickness of the compressible soil layer [m]
n_1 = initial porosity of the soil, as a volume fraction [-]
C_v = compressibility constant = 1 / C_c , referring to compression index as in equation (3-3) [-]
A_1 = initial water content of the soil [g per 100 g of dry soil]
H = organic matter content of the soil [g per 100 g of dry soil]
= 1 – 1.04(1 – N) [Skempton & Petley, 1970]
N = loss on ignition (LOI), after heating at 550°C for 5 hours [g per 100 g of dry soil]
p_1 = initial effective overburden stress [gf/cm^2 ≈ 10^{-1} kPa]
p_2 = effective overburden stress after loading [gf/cm^2 ≈ 10^{-1} kPa]
p_m = maximum stress, or preconsolidation pressure [gf/cm^2 ≈ 10^{-1} kPa]

However the Fokkens method never found widespread use, which might be due to the lack of convincing proof of concept. According to TAW (1996) and Van et al. (1997) namely, attempts by E.J. den Haan in 1989 to validate Fokkens' theory were rather unsuccessful. Instead, based on own laboratory tests during his employment at *Grondmechanica Delft* (now *Deltares*), Den Haan proposed an adaptation, or update, of Fokkens' formula.

This updated formula was found to exist in literature [CUR, 1996; TAW, 1996; Van et al., 1997] in two different variations, however, which did cause quite some confusion – especially because of the absence of a proper explanation and mathematical derivation. Although all three publications refer to the same original technical report authored by Den Haan in 1989, unfortunately that report is nowhere to be retrieved anymore; not even upon direct request at *Deltares*.

Following are the two different variations of the updated Fokkens settlement prediction formula, both only for normally consolidated soil:

$$\frac{\Delta h}{h_0} = \frac{26.7 \cdot H \cdot (p)^{-0.437} - w_0}{\frac{100}{G} + w_0} \tag{3-15.1}$$

[TAW, 1996]

$$\frac{\Delta h}{h_0} = \frac{w_0 - 26.7 \cdot N \cdot (p)^{-0.437}}{w_0 + 37.1 + 0.362 \cdot N} \tag{3-15.2}$$

[CUR, 1996; Van et al., 1997]

Where several variables were already defined previously, except:
Δh = compression of the peat layer [m]
h_0 = initial thickness of the compressible peat layer [m]
p (6) = effective overburden stress after loading [kPa]
w_0 = water content of the peat [%]
G (7) = specific gravity of the dry solids of the peat soil [-]

6) Quantity p is denoted by TAW (1996) as p_m and defined as the *actual* maximum effective stress for normally consolidated soil; contrary to the notation and definition of p_m according to Fokkens (1970), being *historical* maximum stress for overconsolidated soil. In order to avoid confusion, p_m was therefore decided to be replaced by just p.
CUR (1996) and Van et al. (1997) use a different notation, namely (σ' / σ'_e). However its definition is equivalent with TAW, noting that σ'_e is just a unit stress of 1 kPa for strict dimensional correctness.
CUR (2003) on the other hand, whilst having the same notation as CUR (1996) and Van et al. (1997), appears to have a different *definition* though: σ' and σ'_e are defined as "effective stress normally consolidated peat" and "effective stress after loading", respectively. This makes no sense, however, and moreover it does not correspond with preceding publications. Therefore it is concluded that an error was made in CUR (2003).

It can be easily noticed that the numerators in the above formulas are in fact the same, but TAW chose to arrange the terms such, that the resulting settlement is negative. This does not at all clarify the more significant difference in the denominators, though, which became explicable only after more thorough investigation of both publications.

As it turns out, first the specific gravity (G) was alternatively expressed in terms of the LOI, the specific gravity of the organic matter (G_{org}) and the specific gravity of the inorganic particulate matter (G_{an}), by the following formula [TAW, 1996]:

$$G = \frac{100}{\frac{N}{1.04 \times G_{org}} + \frac{100 - N}{1.04 \times G_{an}}} \tag{3-16}$$

Then reference values of 1.365 and 2.598 were used for G_{org} and G_{an}, respectively [TAW, 1996], after which the quotient was elaborated and substituted into G in equation (3-15.1), subsequently yielding equation (3-15.2). The latter formulation therefore essentially is just a more empirical variation of the TAW formulation, thus potentially introducing an error since the actual soil physical properties will not necessarily correspond with the reference values used. Note again that this is neither explained by CUR (1996) nor by Van et al. (1997).

The general limitations of Fokkens' method are largely the same as for Terzaghi's compression law (1925), amongst which is especially the fact that no secular, or secondary, compression is taken into account. This is a pitiful shortcoming, considering that the Buisman (1940) and Koppejan (1948) relationships were known for a long time already. So the Fokkens method can merely yield a final settlement estimation without any time dependence.

Furthermore, some additional constraints and uncertainties arise from the empiricity of the formulas. Although an empirical formula might allow for faster and easier settlement prediction, it has the disadvantage of yielding an increased but hardly quantifiable uncertainty due to the use of correlations, assumptions and the like. Even more so, since in the case of Fokkens the correlations and subsequent numerical substitutions are not always clarified well, or not clarified at all [CUR, 1996; TAW, 1996]. For example, one rough assumption that was explicitly stated and used in a substitution for parameter n_1 by Fokkens (1970), is that the density of the organic matter was assumed to amount to 1.0 g/cm^3. Similarly, the density of the remaining (inorganic) matter was assumed to amount to 2.65 g/cm^3. Obviously, in particular the first assumption is highly doubtful, or at least cannot be universally true. Consequently, the empirical formula(s) might be applicable reliably solely to the particular type and location of origin of the soil samples that these assumptions and correlations were based on.

Another question that will inevitably come up when trying to use one of Fokkens' empirical formulas only with soil physical properties at hand, is whether the formula for normally consolidated soil or the formula for overconsolidated soil should be used – realising that the preconsolidation pressure is to be determined from soil compression tests. Alternatively trying to use correlations to do so might prove very difficult or unreliable, since such correlations are merely known to exist for clay soils (based on Atterberg limits) but not for peat [e.g. Bartlett & Alcorn, 2004; Kulhawy & Mayne, 1990; Solanki & Desai, 2008]. Similar is the case with sounding techniques such as CPT, for which OCR correlations are available only for other soils than peat. Hence another limitation of the Fokkens method has become apparent.

Nevertheless, Fokkens was the only one so far to attempt taking into account the organic matter content of the soil in settlement predictions. Although this has not been investigated extensively, this idea in general seems very legitimate, since organic matter and possible decomposition thereof definitely can influence the compressibility of organic soils, such as peat in particular.

---

[7]) Quantity G is described by TAW (1996) as "soortelijke massa", which ought to be translated literally as *density*, i.e. a substance's mass per unit volume [kg/m^3]. However TAW defines G as a dimensionless quantity, which implies that it is in fact a *relative* density. Indeed, after comparison with other examples in the concerning report, it was concluded that the latter is the case: G is the relative density, or specific gravity, of the dry solids (ideally to be determined with a pycnometer).

3.2.6 De Glopper (1979)

Based on his practical experiences as a civil engineer working at the *Rijksdienst voor de IJsselmeerpolders* (English: State Service for the IJsselmeer polders), ir. R.J. de Glopper identified several significant and recurring problems in the determination of soil parameters, influencing the costs and also the reliability of settlement predictions [De Glopper, 1979]:

- The compression coefficients have to be determined from tests conducted on undisturbed samples. Taking such samples requires relatively heavy and expensive equipment, and moreover much more labour time than simpler (disturbing) sampling methods, such that altogether undisturbed sampling is very expensive.
- Determination of compression coefficients by laboratory testing is very time consuming and expensive as well.
- Representativeness of compression test results on small samples taken at common intervals (1 m) is questionable, considering the heterogeneity of the in situ soil mass.
- Spread in test results (compression coefficients) is often very large, with a standard deviation around 50%.

Therefore De Glopper deemed it necessary to develop an easier, faster and cheaper way of determining the compression coefficients finding use in settlement predictions according to the Koppejan method (1948). He considered the pore volume fraction, or porosity, as the most promising soil property to be related to compressibility parameters, because he argued that a soil is more compressible when it has a higher porosity. This is in principle also what Terzaghi's logarithmic compression law (1925) was initially based on, recalling that void ratio is related to porosity. Moreover, Buisman (1940) had also found already that the compressibility of a soil is proportional to its porosity.

Subsequently De Glopper analysed laboratory test data of organic clays and peat originating from the IJsselmeerpolder, and presented graphs depicting the relationship between the porosity and the reciprocal of each of the compression coefficients C_p, C_s, C'_p and C'_s (Figure 3-8). The correlation coefficients of the linear fits are reportedly between 0.75 and 0.93 and are considered to be well within accepted range of soil parameter deviations for settlement predictions. Although he did not provide the according formulas, these can be easily derived from the graphs, which was done by the author of this thesis and can be found in subsection 4.2.2.2.

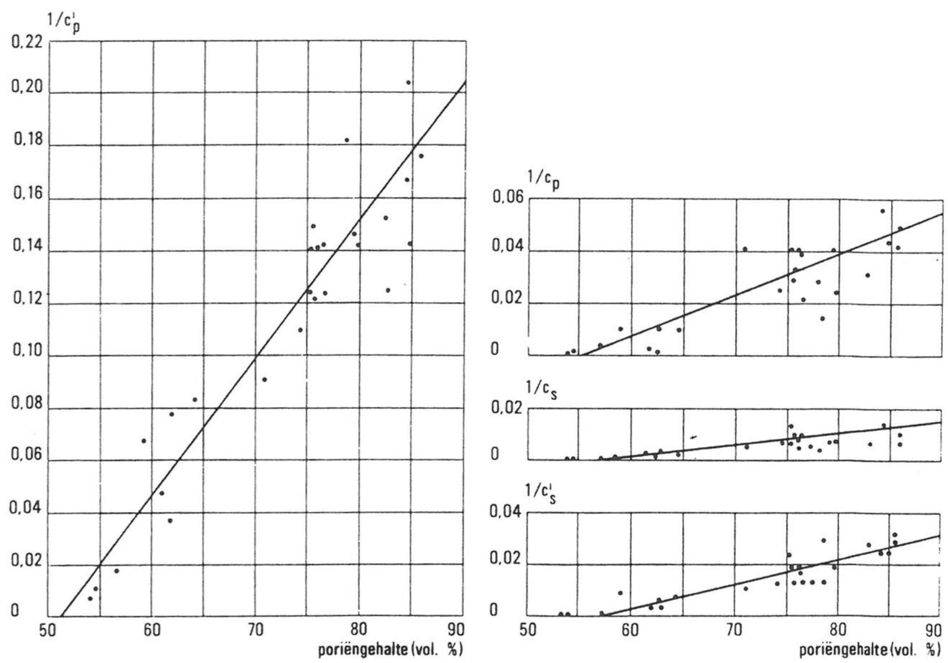

Figure 3-8: The relationship between the porosity and each of the Koppejan compression constants, for peats and clays from the IJsselmeerpolder [De Glopper, 1979: Fig. 1].

Furthermore, De Glopper compared predictions based on both parameter determination methods, i.e. compression coefficients obtained conventionally from laboratory tests and those derived from porosity values, with measured settlements. He found that the settlement predictions in both cases yielded very similar results. Although he did not provide quantitative or statistical data in this regard, his conclusions can be verified by analysis of the according graphs (see Figure 3-9). In fact, by precise comparison it might even be concluded that the predictions based on porosity-derived compression coefficients are more accurate than those based on the coefficients obtained from laboratory tests, although the difference is rather small.

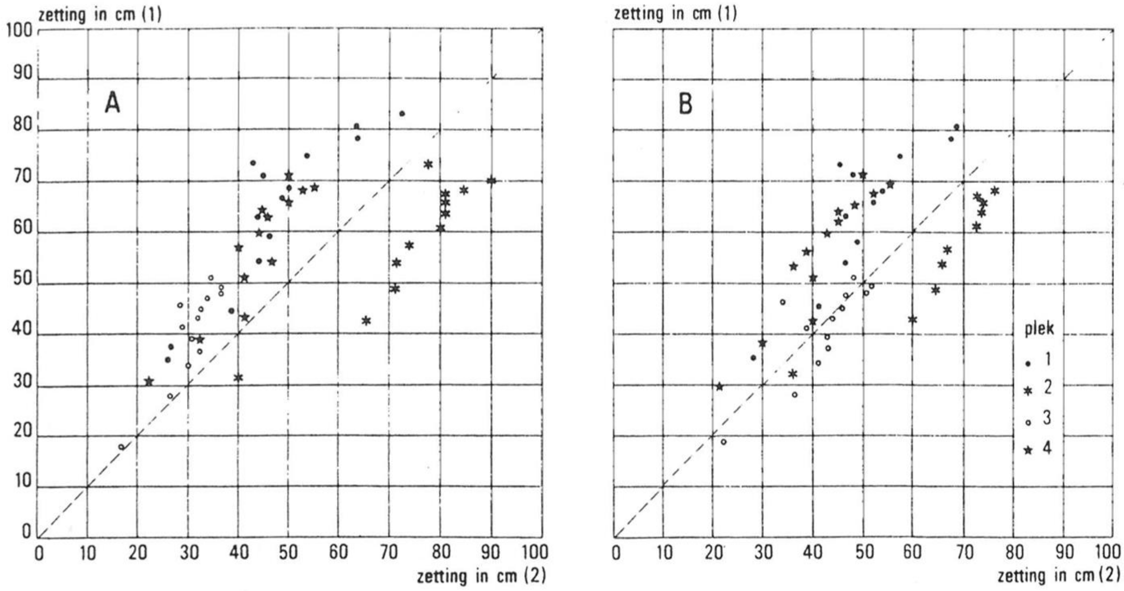

Figure 3-9: Scatter plots of the measured settlements (1) versus the predicted settlements (2), where:
A) uses predictions based on conventionally (i.e. laboratory tests) determined compression constants, and
B) uses predictions based on the porosity-derived compression constants.
[De Glopper, 1979: Fig. 4].

Perhaps even more interesting than the correlation and accuracy, however, are the consequences of this new approach for time and costs. Provided certain basic requirements for sampling, with regard to frequency, size and averaging as described in the article [De Glopper, 1979], the new method based on water content and/or porosity (which are practically equivalent) requires just 8% to 34% of the costs of conventional parameter determination by means of undisturbed sampling and subsequent laboratory testing. Furthermore, the effective labour time required for sampling with a regular gouge is only about one tenth as compared to undisturbed sampling techniques. Similarly, determination of the required soil properties takes less than two weeks, in contrast to the determination of compression coefficients from laboratory tests, which anno 1979 requires 6 weeks on average, according to De Glopper.

However any limitations related specifically to the use of the Koppejan settlement prediction method still remain (refer to section 3.2.3). Furthermore, De Glopper's relationship has one additional limitation, namely that the preconsolidation pressure, which is needed for settlement prediction by means of the Koppejan formula, remains unknown. Thus in its current form it can only be applied to normally consolidated soils. Otherwise the determination of the preconsolidation pressure would still require conduction of compression tests, since according correlations based on soil physical or index properties are not known for peat soil, as was already mentioned at the end of section 3.2.5. Finally – and perhaps most importantly – note that the relationship was developed on the basis of soil samples from a particular region in the Netherlands, and therefore might be less suitable for application at other locations.

So, in brief, De Glopper has not developed a new settlement prediction method, but instead proposed an easier, faster and cheaper way of determining the Koppejan compression coefficients. He suggested to relate the porosity of a soil to these compression coefficients and he found that the accuracy of this approach was no less than when using parameters determined by conventional (more laborious) methods. In any case, De Glopper's correlation in combination with the Koppejan method appears to be the simplest of all reviewed settlement prediction methods since it requires only one easily obtainable soil property.

3.2.7 **Den Haan** (1992)

Building forth upon Bjerrum's isotache model (1967), which slowly but steadily got adopted in international geotechnical practice, ir. E.J. den Haan made some further improvements to this existing model; most notably the use of natural strain and intrinsic time, which are explained separately further ahead in this chapter. Den Haan's isotache model is the latest development in settlement prediction and provides the most complete and sound theoretical description of one-dimensional soil compression.

Den Haan assumes that creep strain rate is uniquely defined by present stress and strain, whose interrelationship he describes by the parameters *b* and *c*. In correspondence with Bjerrum, this creep rate relationship can also be graphically represented by a system of parallel lines (isotachs), where *b* and *c* govern the slope and the vertical separation of the creep isotachs, respectively (see Figure 3-10). On the other hand, direct compression below the preconsolidation stress is described by a parameter *a*.

Although in literature the latter is sometimes referred to as "elastic compression", Den Haan expresses some doubts whether this compression is indeed fully recoverable upon unloading, and since this is not proven he rather avoids the use of the term "elastic" [Den Haan, 1994].

Note on this occasion, that Den Haan chooses to distinguish the different compression phases according to the definition first introduced by Buisman (1940), rather than using the "instant" and "delayed" phases as proposed by Bjerrum (1967), who developed the precursor to the a,b,c-Isotachs model. Indeed, Den Haan consistently uses the terms "direct" and "secular" also in later publications. The only important difference is, that Den Haan acknowledges that secular compression occurs already from the start of loading *together* with direct compression, which is supported by the a,b,c-Isotachs model.

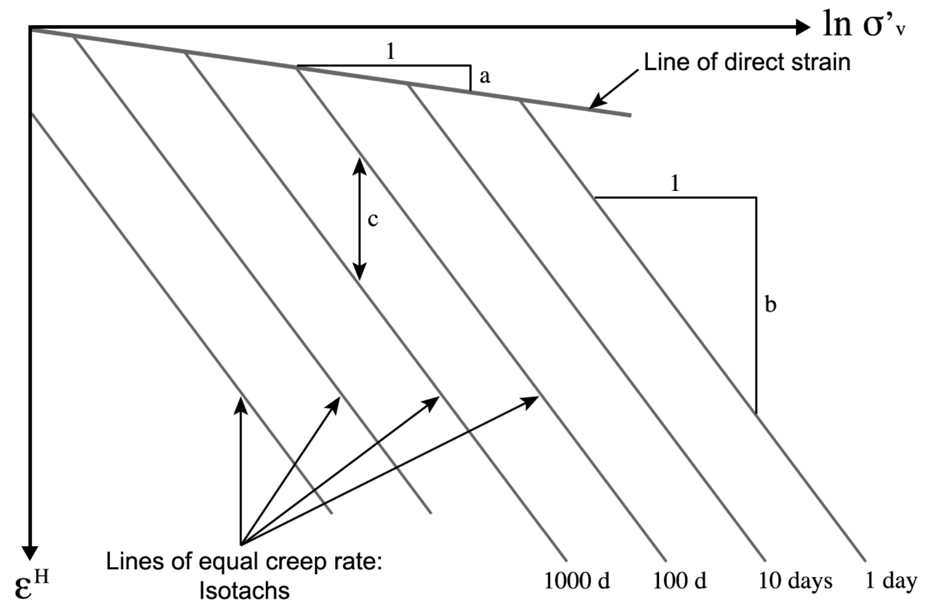

Figure 3-10: Simplified schematic isotache diagram [personal illustration, 2016].

The very first publication introducing the a,b,c-Isotachs model [Den Haan, 1992] provides two different (related) formulations, namely a logarithmic formula and a power law, however without a decent mathematical derivation in the mostly conceptual context of this first article. Whilst the power law is provided already right below, it is deemed more convenient to present the logarithmic formulation in a later subsection (2.3.7.3), in favour of a logical chapter structure in order to understand the model well.

The power law formulation of the a,b,c-Isotachs model reads as follows [Den Haan, 1992]:

$$\epsilon = 1 - \left(\frac{p_g}{p_0}\right)^{-a} \left(\frac{p}{p_g}\right)^{-b} \left(\frac{t}{t_0}\right)^{-c} \tag{3-17}$$

Where:

ε	=	linear strain, or compression [m]
p_g	=	preconsolidation pressure [kPa]
p_0	=	initial, or in situ effective stress [kPa]
p	=	effective stress after loading [kPa]
t	=	time after loading [days]
t_0	=	reference time = 1 [day]
a	=	direct, or unloading-reloading, compression parameter [-]
b	=	virgin compression parameter [-]
c	=	secular compression parameter [-]

Shortly after publication of the first article in the year 1992, he defended his PhD thesis [Den Haan, 1994] providing a much more detailed elucidation of the a,b,c-Isotachs model, which was published in *Géotechnique* another two years later [Den Haan, 1996]. Within these two more comprehensive publications, however, the model was presented in a different form and formulation, along with the introduction of two crucial new concepts: natural strain and intrinsic time. These concepts are first defined and explained in the next two subsections, after which in subsection 3.2.7.3 the final logarithmic model description along with its derivation is given. At last, in subsection 3.2.7.4, the practical use of the model will be illustrated.

3.2.7.1 Natural strain

Natural, or true strain is defined in terms of incremental deformation with respect to the current height, whereas linear, or engineering strain relates the deformation to the initial height [Papadaki, 2013; Van Baars, 2003]. For small values of strain (< 10%), these two strain types may be considered equivalent. However for larger deformations, as they often occur in soft soils, the natural strain is considered more realistic and more accurate. This is because calculations in terms of linear strain theoretically can yield values higher than 1, i.e. more than 100% compression, due to a finite level of stress, which is physically impossible. Linear strain on the other hand is not one-to-one related to deformation, as follows from equations (3-19) and (3-20), and may therefore exceed values of 1 whilst the actual compression remains below 100%. In fact, the deformation that can be back-calculated from the natural strain will reach asymptotically a minimum value, as illustrated in Figure 3-11.

Note that Den Haan did not develop the concept of natural strain himself; he just was the first one to use it in a soil settlement prediction model. In fact, natural strain is known and being used already since the early 20th century in other materials sciences [Freed, 1997] and appears to be introduced in soil mechanics in the late 1970s [Butterfield, 1979].

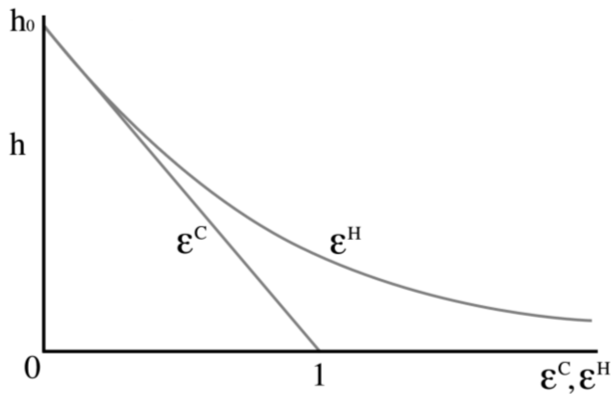

Figure 3-11: Schematic graph illustrating the difference between linear strain and natural strain, adapted from [Deltares, 2014].

The mathematical definitions for linear (ε^C) and natural (ε^H) strain(8) as well as their interrelationship are given in the equations (3-18) to (3-20), according to Den Haan (1994, 2003):

$$\epsilon^C = 1 - \frac{h}{h_0} = \frac{\Delta h}{h_0} \tag{3-18}$$

$$\epsilon^H = -\int_{h_0}^{h} \frac{\mathrm{d}h}{h} = -\ln \frac{h}{h_0} \tag{3-19}$$

$$\epsilon^H = -\ln\left(1 - \epsilon^C\right) \tag{3-20}$$

Where:
ε = strain [-]
h = height of the soil element after compression [m]
h_0 = initial height of the soil element [m]
Δh = height difference due to compression of the soil element [m]

Note finally that Den Haan sometimes defines strain equivalently in terms of specific volume (v), rather than in terms of height (h), as follows: $\varepsilon^H = -\ln(v / v_0)$, where $v = 1 + e$, and e = void ratio.

3.2.7.2 Intrinsic time

Intrinsic time (τ) is a somewhat less intuitive but essential feature of the a,b,c-Isotachs model, given for a certain strain and stress level. It can be considered as the time that would have been needed for the soil to reach its current state of compressibility, if only the present stress would have been acting from the end of sedimentation [Visschedijk, 2010; Papadaki, 2013].

Since this essentially is a description of the process of aging [Bjerrum & Lo, 1963], which after Bjerrum (1967) is known to affect the (apparent) preconsolidation pressure, hence the intrinsic time in the a,b,c-Isotachs model can be related to preconsolidation pressure as well. Indeed, these two quantities are interchangeable in the a,b,c,-Isotachs model [Den Haan, 2008]. The according relationship will be presented further below in equation (3-23).

First of all, Den Haan (1994; 2008) defines the intrinsic time as follows:

$$\tau = t - t_r \tag{3-21}$$

8) Superscript 'C' stands for Cauchy and 'H' for Hencky, who first described the corresponding strain.

Where:

- τ = intrinsic time [days]
- t = true time [days]
- t_r = time shift [days], depending on the choice of time origin such that $t_r = t - (c / \dot{\epsilon}_s^H)$ at any time during the creep, where $\dot{\epsilon}_s^H$ is the derivative of the secular natural strain with respect to time, i.e. the natural creep *rate* [s^{-1}].

And creep rate is related to intrinsic time through:

$$\dot{\epsilon}_s{}^H = \frac{c}{\tau} \tag{3-22}$$

Thus, any creep isotache is associated with one value of intrinsic time, and the isotachs may therefore as well be called intrinsic time lines [Den Haan, 1994].

Then finally, as mentioned before, in practice the intrinsic time is determined by relation with the preconsolidation pressure (p_g), the latter of which can be derived from compression tests. This relationship is equivalent with the previously presented equation (3-10) and reads as follows [Den Haan, 2008; Ammerlaan, 2011]:

$$\tau = \tau_1 \left(\frac{p_g}{p_0}\right)^{\frac{b-a}{c}} \tag{3-23}$$

Where all symbols have been defined already except τ_1, which is a reference time that usually is considered to be 1 day. Further explanation regarding τ_1 is provided in the next subsection.

3.2.7.3 Derivation and final formulation of the a,b,c-Isotachs model

The total (vertical) natural strain is the sum of the direct and the secular components of the natural strain, which applies to strain rates (derivatives) as well:

$$\epsilon^H = \epsilon_d{}^H + \epsilon_s{}^H \tag{3-24.1}$$

$$\dot{\epsilon}^H = \dot{\epsilon}_d{}^H + \dot{\epsilon}_s{}^H \tag{3-24.2}$$

When considering these strain components separately further on, in order to help understanding the origin of the formulas it might be helpful to have an annotated isotache diagram at hand, which can be found on the next page: Figure 3-12a displays the total strain isotache diagram, equivalent to the simplified diagram of Figure 3-10. Figure 3-12b, on the other hand, shows the separated strains isotache diagram.

From Figure 3-12b separate relationships for the direct and secular strain components can be derived. At this moment just the secular strain formula for the initial creep isotache ($\dot{\epsilon}_{s0}^H$) through σ'_{v0} will be given, which is positioned between the regular isotachs and so is not separated by a vertical distance c.

$$\epsilon_d{}^H = a \ln\left(\frac{\sigma'_v}{\sigma'_{v0}}\right) \tag{3-25}$$

$$\epsilon_{s0}^H = (b-a) \ln\left(\frac{\sigma'_v}{\sigma'_{v0}}\right) \tag{3-26}$$

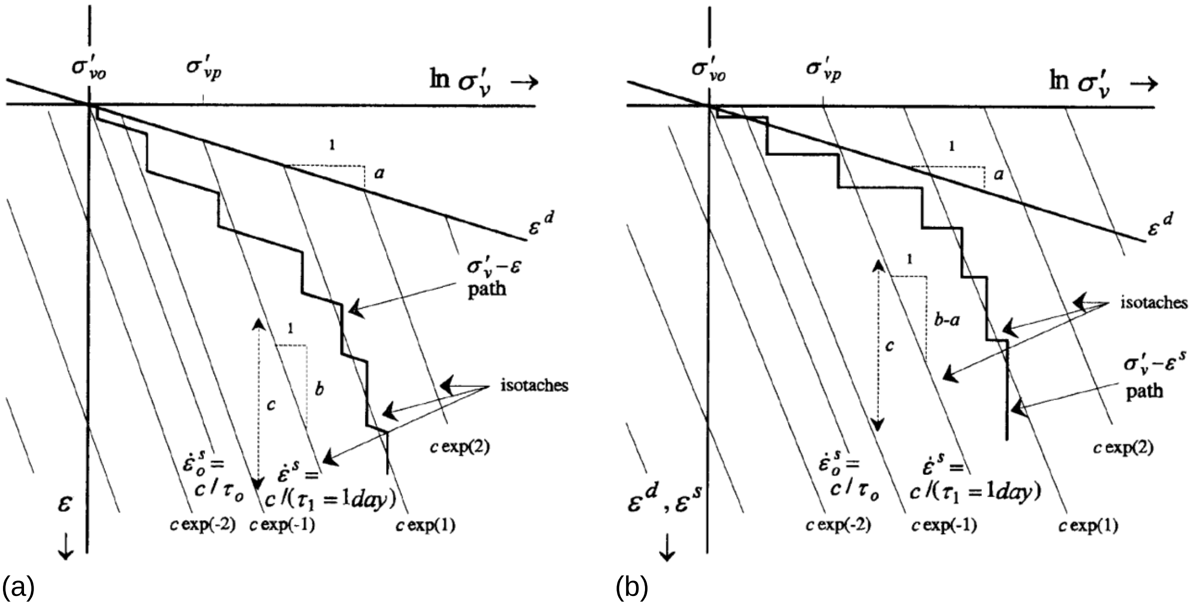

Figure 3-12: Annotated schematic isotache diagrams, in total strain representation (a) as well as in separated strains representation (b) [Den Haan & Kamao, 2003: Fig. 1].

There also is a reference isotache, τ_1, on which the intrinsic time τ is considered to be 1 day, so that according to equation (3-22): $\dot{\epsilon}_s{}^H = c$. In a separated strains diagram, the intersection of this reference isotache with the horizontal (σ'_v) axis gives the preconsolidation pressure (σ'_{vp}; previously p_g), whereas in a total strain diagram σ'_{vp} can be found at the intersection between the reference isotache with the direct strain line [Den Haan & Kamao, 2003; Den Haan, 2008]. This can also be verified from the graphs in Figure 3-12.

Ultimately it is desired to obtain a general formula for any isotache, including a term governing the creep time separation (Δ_c). Whilst being just a constant (c) in the logarithmic isotache diagram, mathematically this term thus depends on the logarithm of the creep strain rate:

$$\epsilon_s{}^H = \epsilon_{s0}{}^H - \Delta_c = (b-a)\ln\left(\frac{\sigma'_v}{\sigma'_{v0}}\right) - c\ln\left(\frac{\dot{\epsilon}_s{}^H}{\dot{\epsilon}_{s0}{}^H}\right) \tag{3-27}$$

In which, according to equation (3-22), $\dot{\epsilon}_s{}^H$ is closely related to intrinsic time and so the argument of the last logarithm may be substituted by (τ_0 / τ). When furthermore the sign of the last term is changed whilst the quotient in its argument is inverted, the following equivalent formula is obtained:

$$\epsilon_s{}^H = (b-a)\ln\left(\frac{\sigma'_v}{\sigma'_{v0}}\right) + c\ln\left(\frac{\tau}{\tau_0}\right) \tag{3-28}$$

The total natural strain can be found using equation (3-21), i.e. by summation of the equations (3-25) and (3-28). However by doing so, the direct strain component effectively cancels out in the resulting total strain formula. This is because the equation yet only regards virgin compression: indeed, the total strain formula written just in terms of *b* and *c* describes the creep isotachs alone [Den Haan, 1992], as can be verified from Figure 3-12. Since below the preconsolidation pressure predominantly reloading, i.e. direct compression, occurs, the general model description usually also includes the direct strain component that covers compression below the preconsolidation pressure. Consequently the direct strain component is added once more in order to obtain the final logarithmic formulation of the a,b,c-Isotachs model:

$$\epsilon^H = a\ln\left(\frac{\sigma'_v}{\sigma'_{v0}}\right) + b\ln\left(\frac{\sigma'_v}{\sigma'_{v0}}\right) + c\ln\left(\frac{\tau}{\tau_0}\right) \quad (3\text{-}29)$$

By now it will be clear that the direct strain is associated exclusively with parameter *a*, and the secular strain consists of a stress-dependent and an (intrinsic) time-dependent part associated with parameters *b* and *c*, respectively.

Although there is no conceptual distinction in the model between clay and peat, Den Haan (1994) remarks that fibrous peats may call for separate modelling, since such peats have two levels of structure, namely a macro- and a micro-pore network with different drainage characteristics. This is described by a process called “tertiary compression”, which is defined as steepening of the isobars after a prolonged period of loading. This would affect the a,b,c-Isotachs model such, that the creep isotachs show a tendency to diverge. Tertiary compression has been observed by several different researchers including Den Haan, however the effect is not well understood yet and calls for closer investigation.

As a meanwhile solution for the small contribution of tertiary compression, Den Haan (1994) proposed an adaptation of the a,b,c formula by incorporating an additional parameter *d* into the secular strain equation:

$$\begin{aligned}{\epsilon_s}^H &= b\ln\left(\frac{\sigma'_v}{\sigma'_{v0}}\right) + (c + d\ln\left(\frac{\sigma'_v}{\sigma'_{v0}}\right))\ln\left(\frac{\tau}{\tau_0}\right) \\ &= (b + d\ln\left(\frac{\tau}{\tau_0}\right))\ln\left(\frac{\sigma'_v}{\sigma'_{v0}}\right) + c\ln\left(\frac{\tau}{\tau_0}\right)\end{aligned} \quad (3\text{-}30)$$

To obtain the value of *d*, the above formula would need to be fit with isotachs determined experimentally at very high precision, however because the tertiary effect is so small with respect to the final strain and the relationship is too complex for practical purposes, the above formula has never been put to use in practice and even has not been found again in later literature.

Finally, according to Heemstra (2013), the a,b,c-Isotachs model may alternatively be formulated in terms of preconsolidation pressure. This can be done by substitution of ε from equation (3-17) at the position of ε^C in equation (3-20) and subsequent elaboration of the logarithms, yielding:

$$\epsilon^H = a\ln\left(\frac{p_g}{p_0}\right) + b\ln\left(\frac{p}{p_g}\right) + c\ln\left(\frac{t}{t_0}\right) \quad (3\text{-}31)$$

3.2.7.4 Practical description of the a,b,c-Isotachs model

The a,b,c-Isotachs model may be considered to be the most complete one-dimensional settlement prediction model available to date, integrating several decades of preliminary research on compression of soils. However its fundamental understanding and thus its usage lagged behind in geotechnical engineering practice [Visschedijk, 2010], especially in the first ten to fifteen years after its introduction. On this occasion, note that the a,b,c-Isotachs model is set up graphically very similar to Bjerrum’s isotache model (1967) and is to be used accordingly as well. However because a detailed practical description of that model was not provided in this report yet. For these reasons and because both models will be used in the further course of the current study, in this subsection its practical use will be explained and illustrated by means of a schematic isotache diagram, shown on the next page.

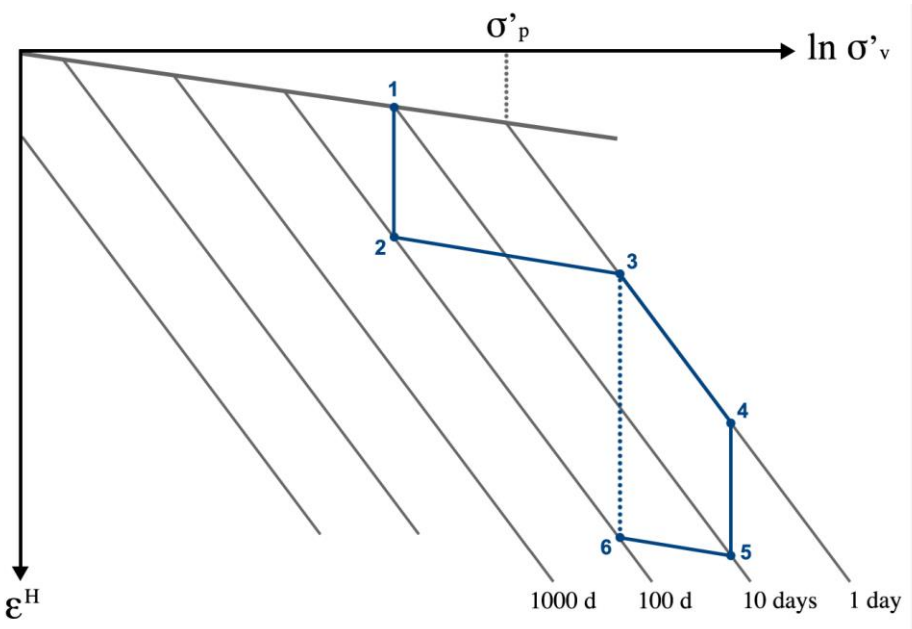

Figure 3-13: Schematic isotache diagram with a hypothetic load-compression path [personal illustration, 2016].

Referring to Figure 3-13, it is assumed that a soil sample has an initial compression state indicated by **1**. It lies on the isotache with an intrinsic time of 10 days. If this sample would be subjected to sustained loading (i.e. keeping the current load constant), pure creep will occur, represented by a vertical line. In the course of 90 days the soil will thus creep to the intrinsic time isotache of 100 days, marked by **2**.

Now suppose that a surcharge is applied. At low creep rates (or high intrinsic times) direct strain will be dominant, such that the compression state will move towards point **3** along a straight line with slope *a*. As the load continues to increase, the creep rate will also increase until the slope changes from a value *a* to *b* at point **3** on the isotache with an intrinsic time of 1 day. From this point onward, the creep rate will remain constant under continued load increase.

If at point **4** the load would be sustained (kept constant), then creep would occur again in the same fashion as at point **1**. Over a period of 9 days, for example, the soil would creep to a corresponding point on the intrinsic time line of 10 days, indicated by **5**. If at that moment the load would be decreased, however, something different will happen: since unloading is governed by the direct, or unloading-reloading, compression parameter *a*, the soil would unload and expand along a line with slope *a*.

Suppose the unloading process stops at a final compression state on the 100-days isotache, marked by **6**: the same situation could have also been reached directly from point **3**, by waiting 99 days at sustained loading. This is interesting as this implies that applying an extra surplus height and removing it again, following the path **3-4-5-6**, (theoretically) results in a substantial settlement over a shorter timespan than waiting for the creep process to finish during 99 days. Since the final state has a high intrinsic time and a low creep rate, future settlements will remain relatively small. It follows, that application of a preload surcharge in order to preconsolidate the soil for future construction works does make sense and may lead to a shorter construction time, or a shorter waiting time.

This practical model description, however, was based on a schematic diagram and has some limitations in practice. To begin with, the initial effective stress and strain state have to be known, which can be difficult to determine accurately. Moreover it should be kept in mind that the effective stress may vary as a function of time and will usually increase gradually after loading, since pore pressures need time to dissipate (consolidation).

Furthermore, the transition from slope *a* to slope *b* at the 1-day isotache will rarely be abrupt, but rather curved. This mainly depends on the consolidation period: soils with a very short consolidation period (more permeable and/or shorter drainage path) may indeed reach the 1-day isotache and have a distinctive kink at the *a*-*b* slope transition point. However most soft soils have longer consolidation periods (less permeable and/or longer drainage path) and will only approach, but probably not reach, the 1-day isotache following an increasingly curved downward path towards lower intrinsic time, or higher creep rate. This is because during the (longer) consolidation phase the creep process will continue as well and the time effect will become more dominant at higher creep rates. This also implies that application of preload surcharge in reality is limited in terms of applied load and resulting time gain.

3.2.7.5 How to obtain the parameters

At the end of this section, finally the acquisition of the a,b,c parameters themselves might still call for a brief clarification. Multiple ways exist to determine or estimate these parameters.

As described in [Den Haan & Kamao, 2003], [Den Haan et al., 2001] and [Den Haan et al., 2004], first of all the parameters can be determined from compression tests: both conventional (incremental loading) and CRS oedometer tests. Although Den Haan generally seems to advocate determining the compressibility parameters by means of (K_0-)CRS tests, the creep parameter (*c*) in contrast might be determined more easily and more reliably from conventional oedometer tests [Den Adel & Van, 2002]. Determination of a,b,c parameters has also been performed in the course of the current research, which is procedurally explained in more detail in subsection 4.2.2.4.

Otherwise, the a,b,c parameters *can* be calculated from the NEN-Bjerrum parameters *RR*, *CR* and C_α and hence they could even be related to the Koppejan parameters [Den Haan et al., 2004]. However this requires caution and is by no means straightforward without making several simplifying assumptions, partly because the a,b,c-Isotachs model uses *natural strain*-based parameters in contrast to the other mentioned models that use *linear strain*-based parameters [Deltares, 2014]. Strictly speaking, it is not possible to accurately convert the parameters without the availability of compression test data and thus in fact determining the parameters directly from these tests. More detailed information concerning the conversion to and from the a,b,c parameters, along with formulas, assumptions and limitations, can be found in §17.7 of the *D-Settlement* user manual [Deltares, 2014].

Furthermore, there are correlations with soil physical or index properties, such as unit weight [Den Haan & Molendijk, 2002; Den Haan et al., 2004]. In particular Den Haan & Molendijk found the unit weight to be a very suitable soil property from which the a,b,c parameters can be estimated with an acceptable level of accuracy. Some of these correlations are validated in the course of the current research and are further elucidated in subsection 4.2.2.3.

Lastly, it should be remarked that *b* and *c* are constants independent of stress and time, contrary to most compression coefficients used in preliminary models [Den Haan, 1994]. This is mainly due to the fact that the model as well as its parameters are based on natural strain. Moreover, the ratios of *b/a* and *b/c* can be considered constant for a particular soil as well [Den Haan, 2003; Den Haan et al., 2004].

3.2.8 Summary of settlement prediction methods and parameters

This section provides a concise tabular overview of all one-dimensional settlement prediction methods and their respective parameters that were reviewed in the previous sections.

Table 3-1: Tabular summary of settlement prediction methods and their respective parameters. The column of $\boldsymbol{p_g}$ indicates whether preconsolidation state-dependent compressibility is taken into account.

	Soil parameters				
	Primary	**Secondary**	$\boldsymbol{p_g}$	**Parameter determination**	**Special remarks**
Terzaghi + Fokkens	C_c or $1/C$ + n, A, H	-	-	Easy with conventional (incremental) oedometer test; + soil physical properties	Parameters not constant but stress/strain- and time-dependent; Only virgin primary compr.
Keverling Buisman	α_p	α_s	-	Easy with conventional oedometer test	Parameters not constant
Koppejan + Glopper	C_p, C'_p	C_s, C'_s	yes	Easy with conventional oedometer test; p_g more difficult (prone to error due to procedure and sample disturbance); + simple formula for correlation with porosity (n)	Parameters not constant; Natural strain correction available, but strictly requires different determination of parameters;
Bjerrum	C_r, C_c	C_α	yes (only primary compr.)	Easy with conventional oedometer test; p_g more difficult.	Parameters not constant
a,b,c-Isotachs (Den Haan)	a, b	c	yes (only primary compr.)	Possible with conventional oedometer test, but K_0-CRS test recommended; p_g or τ remains difficult.	Model and parameters based on natural strain; Parameters are constants; Theoretically more accurate predictions for large strains in very soft soils

3.2.8.1 Remarks on the conversion of parameters

The compression coefficients of Terzaghi, Koppejan and Bjerrum can be converted and related to each other [Den Haan et al., 2004; Deltares, 2014]. Only Buisman's coefficients are defined differently than others' – however Buisman's formula may be considered as obsolete anyway. More problematic is a correct conversion of the a,b,c parameters, though, as was already mentioned in subsection 3.2.7.5: caution should be taken when trying to convert *linear strain*-based parameters to *natural strain*-based parameters, or vice versa, which is hardly possible without making simplifying assumptions and which involves inconveniently complicated formulas. Therefore it is strongly recommended to determine the a,b,c parameters directly from compression test data. Please refer to §17.7 of the *D-Settlement* user manual [Deltares, 2014] for more detailed information and instructions concerning the conversion of a,b,c parameters.

3.3 Reliability of settlement predictions

Considering that, by rule of thumb, the uncertainty margin of settlement predictions amounts to about 30% [CROW, 2004], it may be apparent that there is room for improvement. Moreover, in the past two decades the Dutch construction industry has undergone changes that comprise, amongst others, increasing strictness of residual settlement requirements and shorter timeframes for construction works, whilst at the same time responsibilities are being shifted more and more from clients towards contractors. Hence the risks for contractors become almost unacceptably high and the strong need was felt to decrease the uncertainty and improve the reliability of settlement predictions.

Therefore in the year 2000 the *Werkgroep Gevoeligheidsanalyse Zettingsprognose* (English: Working Group on Sensitivity Analysis of Settlement Prediction) was established by CROW, the Dutch knowledge organisation for infrastructure, public space, transport and mobility. The goal of this working group, composed of experienced Dutch experts in the field of geotechnical engineering, was to identify and quantify uncertainties in settlement predictions and to give recommendations on how to reduce these. Accordingly, a number of studies was performed, culminating in a comprehensive publication titled *Betrouwbaarheid van zettingsprognoses* [CROW, 2004]. The research was focused on settlements related to *conventional* fills and embankments in Dutch line infrastructure projects. Not regarded on the other hand, are buildings or special structures like bridges and tunnels, hydraulic structures like flood barriers, offshore structures, soil improvement techniques and lightweight embankments. Note moreover, that their identification of uncertainties and error sources is qualitative rather than quantitative.

The following sections essentially provide a summary of this publication by CROW and also follow loosely its structure. For this reason, repeated references hereto will be limited in favour of overall readability, except when other sources of information were consulted and used by the author for additional detail.

3.3.1 Considerations on terminology and requirements

The CROW report starts with an extensive list of nomenclature and **definitions**. This is not just a service to the reader, but more importantly because already in a very early stage of the research misunderstandings occurred, which were caused by different use or definitions of technical terms. However the use of unambiguous and clearly defined terms was recognised to be essential for meeting the requirements and successful completion of any construction project. Therefore the first recommendation is to use clear terminology and to always include a glossary of terms in every report, which is promptly done by CROW on this occasion.

A primary source of **ambiguity** seems to lie especially in time-related terms, for example: the regarded total period of settlement might be stated by the client, or has to be presumed by the contractor, and reportedly can amount to 10 years, 12 years, 10,000 days (27.38 years) or 30 years, none of which have a particular physical meaning and thus are in fact arbitrary. Similar is the case for the start of the residual settlement period, which can be defined either as the time at which the ground works are completed, or as the time at which the (rail)road or structure is taken into use after completion of the above-ground works. In this report, an illustrated explanation of the most frequently used settlement-related terminology can be found in Appendix B.

Following, and partly related to the prior, the report treats the topic of settlement **requirements**, as it was found that these vary widely amongst different clients and projects. A cause for this might be the fact, that governing regulations or guidelines are often not decisive in this regard, so the choice is left with the client. The reasons for choosing certain requirements can vary between, amongst others, safety considerations, comfort, aesthetics and maintainability (affecting lifetime costs).

Furthermore, mostly it is not stated whether settlement requirements are set with respect to the serviceability limit state or the ultimate **limit state**. In most cases, presumably the serviceability limit state is intended. Moreover, neither it is stated whether requirements concern an expected value (50% exceedance probability) or an upper limit (5% exceedance probability).

In this case, the latter is likely the intended requirement, although settlement predictions themselves principally yield expected values (uncertainty margin ±30%). An upper limit is sometimes implicitly taken care of by “safely” using pessimistic parameters yielding a pessimistic prediction as well, however the statistical significance of this approach is doubtful at least.

In an attempt to standardise working procedures and to limit the chance of forgetting essential steps, an **action plan** for performing a settlement prediction is presented in chapter 4 of the CROW report. The action plan is accompanied by per-step points of attention and recommendations, as well as reference to existing standards (NEN) if relevant; particularly for site investigation, sampling and testing.

Special attention is given to the site investigation, data interpretation and subsequent subsurface schematisation, as further on these steps will turn out to form a significant factor influencing the reliability of settlement predictions (refer to section 3.3.3).

3.3.2 Assessment of spread in settlement predictions

By means of a “field test”, so to speak, the CROW working group has assessed the spread in settlement predictions in practice. This was done by assigning three independent Dutch geotechnical engineering firms with settlement predictions for three different real cases each. All firms were provided with the same set of soil investigation data and asked to use two settlement prediction methods per case: one being the still commonly used Koppejan method, and the other free of choice. Hence every company performed six settlement predictions in total. The assessment was not meant to validate the methods used, but only to identify the differences in outcomes and particularly their possible causes (error sources). Nevertheless, the outcomes were checked with respect to extrapolated real settlement measurements.

The anonymised assessment results are presented in chapter 5 of the aforementioned report. The spread in settlement predictions between different companies was found to be surprisingly large, even when using the same prediction model. For illustration, the settlement predictions are depicted in Figure 3-14.

The observed differences were identified to result mainly from the company’s choices of boundary conditions and parameters, including: material parameters, the current ground surface level, the application and amount of settlement-accelerating measures, and unclear residual settlement requirements (expected value or upper limit). More specifically, the CROW working group concludes that the chosen values of *compressibility parameters* can be considered to be the main cause for the observed differences. These parameters were to be derived from the provided soil investigation data by the companies themselves. The compression coefficients for the Koppejan method, for example, were found to differ already by a factor of 2 or more between companies, hence strongly affecting subsequent predictions. Other, though less influential, identified causes for differences are: the subsurface structure schematisation, the estimated unit weight of the fill material and the (average) phreatic water level.

When compared with actual settlement measurements, the relative difference between predictions and measurements was more than 30% in two out of three cases. As for the worst prediction, the NEN-Bjerrum method chosen by one company remarkably resulted in an overestimation of the final settlements by a factor of more than 2 with respect to the extrapolated measurements: namely 3.80, 7.80 and 7.75 m for the cases Pijnacker, Naaldwijk and Wijngaarden, respectively. The concerning company itself already indicated that these outcomes cannot be correct and thus should be disregarded. However it should not be concluded that the method itself is inaccurate, since in this case again the choice of soil parameters was identified by CROW as the main cause for the observed deviations. Unfortunately the chosen compressibility parameters are not presented in the CROW report, leaving no possibility for any verification or quantitative comparison.

Finally, it should be remarked that in practice usually monitoring is performed, based on which the surplus height is adjusted and/or other settlement accelerating measures are applied if necessary, in order to meet the contractual requirements (refer to subsection 3.3.3.4).

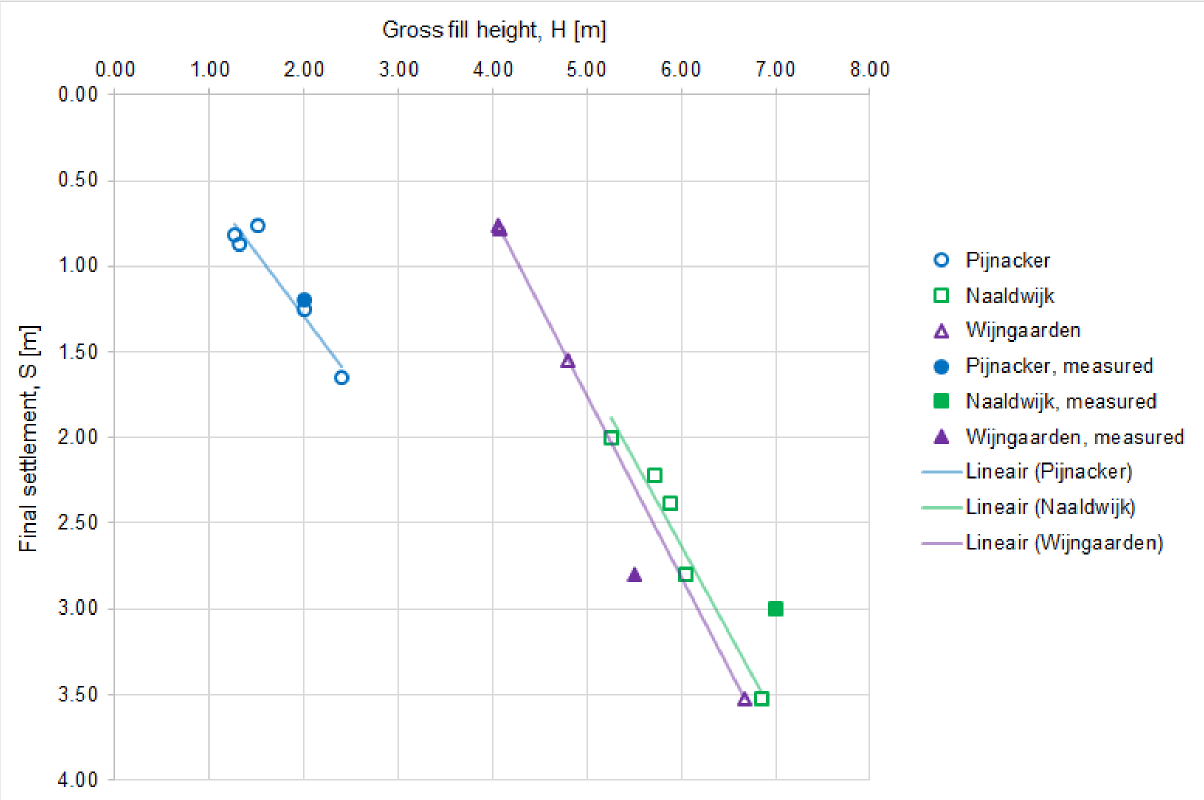

Figure 3-14: Graphical representation of the observed spread in settlement predictions (open shapes) with respect to extrapolated settlement measurements (filled shapes). NEN-Bjerrum predictions are disregarded, as explained in the main text. Adapted from [CROW, 2004: Fig. 10].

3.3.3 Identification of uncertainties and error sources

The CROW report continues in chapter 6 with an extensive overview of all uncertainties and error sources that the working group identified from experience, expert group discussions and case studies. Note, that the terms “uncertainty” and “error” might seem to become mixed up a little bit, not just in this thesis but also in the CROW publication, since a clear definition or distinction of the two terms is not provided by CROW. However it could be deduced that an uncertainty may generally be regarded to result from one or more possible errors.

CROW attempted to classify all uncertainties into two types: A or B. However the author considers this classification system to be ambiguous and impractical, due to the vague definitions and overlap between the two types, which is not further explained here. In fact, the working group itself acknowledges that “*Not always a strict distinction in types A and B is possible. Some uncertainties can comprise elements of type A as well as of type B*” [CROW, 2004, p.43]. Therefore, the use of this classification system is disregarded in the further course of this thesis.

In the following subsections all identified uncertainties and error sources are discussed: in accordance with the structure of the CROW report, the subsections represent the main project phases in which they occur. Whereas CROW describes all errors with a high level of detail, providing numerous examples and references and covering 18 pages in total, it is tried to present in this thesis a more concise summary, merely focussing on the key points.

3.3.3.1 Investigation phase

The first phase in the geotechnical design of a civil engineering project is the investigation phase, which includes the following subphases and their associated (indicative) components:

- Desk study: geological history and geomorphology, human history and land use, remains from previous constructions and (pipeline) infrastructure, contaminations, etc.
- Site investigation: geodetic survey, geophysical survey, probing and sounding, ground water level and pore pressures, etc.
- Sampling and testing: tools and methods, sample integrity, strength and compressibility tests, determination of physical properties, Atterberg limits, etc.
- Data interpretation: derivation of structural, hydrological and material compressibility and strength properties for further calculations or modelling.

CROW explicitly states that *"the **most important** source of uncertainty in the settlement prediction is formed by the exploration of the subsurface"* (p.45), which is an opinion that is shared amongst many other experts in geotechnical engineering. And for a good reason there also is a common saying: *You pay for a ground investigation whether you have one or not*. So a proper and extensive preliminary investigation is considered to be of utmost importance for obtaining a reliable basis for subsequent (geo)technical design and calculations. Wrong estimation or misinterpretation of any single component amongst the subphases listed above is known to have caused serious problems, not just once, in construction projects in the past.

Special attention is given to the increase of uncertainty due to an insufficient **number of investigation points** in a site investigation, resulting in interpolation errors and underestimation of spatial variability in general, including overlooking important man-made or natural geo-morphological features in the subsurface. The latter concern in particular filled ditches, which are ubiquitous in the Dutch polders, and buried river or tidal channels, which are very common in deltaic and coastal environments such as the Netherlands as well. Both features pose a high risk of causing large (differential) settlements when they remain undetected. Planning and design of an adequate site investigation campaign, with anticipation of such and other hidden hazards on the basis of thorough desk study, is the specialism of **engineering geologists**, whose applied geological knowledge can be considered to be of significant value during the entire site investigation and subsequent schematisation phase.

Similar notes concerning uncertainties related to **spatial variability** in the subsurface recur repeatedly in the CROW report. Subsequently, CROW provides several recommendations, along with references to relevant standards and guidelines, concerning the choice and execution of different site **investigation methods**, in particular regarding appropriate measurement intervals.

Furthermore, determination of the **hydrological conditions** (and possible variation thereof) in the subsurface is put forward as well, with a side note on the limited suitability of sounding tools to measure pore pressures in poorly permeable soils.

Then uncertainties due to **sampling** and, in close relation with that, laboratory **testing** are discussed. Errors in laboratory testing can be classified as either *systematic* or *random* errors. The former arise for instance from wrong calibration or systematic misuse or misinterpretation of testing equipment, as well as sample disturbance and the like. Sample disturbance was found to be a particularly extensive topic on itself and was therefore decided to address in a separate subsection (3.3.3.5). Systematic errors in general are very difficult to catch and cannot be simply eliminated by carrying out more tests. Random errors, on the other hand, arise for instance from accidental sample damage or misreading and could be eliminated by averaging or statistical analysis, provided a sufficient number of tests is performed.

Another uncertainty source being regarded are testing **procedures**. Amongst the procedural uncertainties is to be mentioned in particular the duration of compression tests, which concerns the total duration as well as the duration of any single loading step in incremental oedometer tests. Most often namely, the time available for laboratory research is limited, not least because of financial considerations. Den Haan (2008) discusses the possible consequences of saving on time, negatively affecting the accuracy of obtaining the compression coefficients as well as the preconsolidation pressure. If the compression tests are not conducted at sufficiently high loads and at sufficiently long time intervals (thus allowing full consolidation), no complete load-settlement curve can be obtained and hence especially the virgin compression parameters cannot be determined reliably [Den Haan, 2008].

Continuing with laboratory testing, CROW specifically brings the **degree of saturation** to attention. The importance of the degree of saturation in soil testing was already addressed in section 3.1.1 of this thesis, which is why this is not further detailed here again. One just should remain aware of the fact that the degree of saturation affects a wide range of material properties including compressibility and shear strength, and practice proves that full saturation is by far not always ensured.

Related to testing procedures, Van Essen (2014) criticises the incompleteness and outdatedness of **standards and regulations**, if existent or applicable at all. Whilst geotechnical investigation and calculation methods have developed and improved strongly over the past decades, the regulations lag behind considerably. This criticism is accompanied by a call for improvement of guidelines, in particular regarding new sampling and testing techniques, in order to standardise working procedures and subsequent data interpretation.

Finally, the subject of **data interpretation** is broached, although limited to some remarks concerning the determination of compression parameters in the laboratory. From the assessment of spread in settlement predictions (section 3.3.2), it had already emerged that in practice the interpretation of (the same set of) test results can differ considerably. Moreover, CROW acknowledges that compression tests on small samples generally yield insufficient information about the compressibility characteristics of the in situ subsoil as a whole. It is pointed out that settlement measurement data of nearby previous projects, or even of trial embankments, under certain conditions can provide valuable additional information.

Related hereto, the working group explicitly calls for caution when using **correlations** to determine soil parameters, since these often have a limited applicability and validity (for example based on clay, whilst being used to obtain peat parameters), resulting in a high but quantitatively unknown uncertainty. It will show in the further course of this research how well some correlations for the determination of compressibility parameters perform. Further remarks related to data interpretation are given in following subsections; specifically in 3.2.3.2 and 3.2.3.3.

3.3.3.2 Schematisation phase

The second phase in geotechnical design is the schematisation, i.e. the interpretation of the geological structure of the subsurface, including all relevant boundary conditions such as geometry (layer thicknesses and orientations), material properties, hydrological conditions and stress state. The latter concerns not just the natural (effective) self-weight of the soil strata, but also influences from neighbouring bodies (constructions, embankments, waterways etc.) and in particular stress history (preconsolidation). Whereas the influence of neighbouring bodies in a settlement prediction is believed to be relatively small, the preconsolidation pressure is deemed much more significant. More detailed information concerning the preconsolidation pressure and its determination is provided in subsection 2.2.2.1.

The **subsurface structure** has to be interpreted from (a combination of) borehole logs, probe or sounding test results (e.g. CPT) and/or geophysical (e.g. electromagnetic) methods. Moreover, regional geological information, such as from maps and archive data collected during the desk study, usually will also provide valuable clues about the existing structural geological features and trends, which are to be integrated with site investigation data. Overall, the data interpretation and subsurface schematisation requires expert knowledge and judgement, and is a partly *subjective* matter. Obviously, this phase is very prone to errors, most notably by misinterpretation or oversimplification of the subsurface structure, which may be due to the engineer's personal choices, a lack of information, or both. One way or another, once more the importance of adequate and extensive site investigation along with engineering geological expertise is highlighted, which was mentioned already in the previous subsection 3.3.3.1.

An oversimplification in the *horizontal* direction possibly leads to unexpected differential settlements, however an oversimplification in the *vertical* direction, for example by disregarding a thin layer of significantly more permeable soil such as sand, could strongly increase the rate of settlement due to a shorter drainage path.

Furthermore, the importance of choosing **representative cross sections** for settlement analysis is addressed: it should be taken care to virtually dissect a project site such, that the extremes of expected settlements and, most importantly, *differential* settlements are covered.

Finally, once more the significance of **hydrology** in the schematisation is emphasised, as water pressures most often are not linearly proportional with depth, but vary with time and per layer (e.g. artesian groundwater). Furthermore, the rise of the phreatic water level below an earth fill or embankment due to infiltration can also have a significant effect, since the effective stresses in the ground are directly related to pore water pressures according to Terzaghi's effective stress principle.

3.3.3.3 Calculation and modelling phase

The choice of a particular settlement prediction method, or model, will depend on various factors, such as the complexity of the project, the required level of accuracy and possibly also on the client's request. Of course several methods may nowadays be considered obsolete, though still they can be useful or sufficiently accurate depending on the requirements. However the *use* of any model – especially its input and the assessment of its outcomes – is definitely to be done by an experienced expert. Because nonsense input will yield nonsense output, even with the most advanced model. It may be noticed that this statement relates back to uncertainties in the investigation and schematisation phases.

The expert in charge is challenged all the more, since many things should be taken into account in the calculation or modelling, yet several of those are known to be frequently disregarded in practice, usually for reasons of simplification and time and cost saving. The main points of attention identified by CROW are as follows, not all of which have the same level of importance, depending on the project characteristics:

- Model limitations: see remarks below.
- Application of settlement-accelerating measures (e.g. drainage or extra surplus height).
- Staged loading and its development in time (sometimes (over)simplified to a single load step starting at half of the total loading time).
- Unit weight of the embankment or fill (depends on saturation, which can vary in time; often wrongly estimated).
- Possible settlement of the embankment or fill itself (depending on type of soil and unit weight; often neglected).
- Settlement of the embankment or fill below the phreatic water level (thereby decreasing its effective weight on the subgrade), also indicated as "submerging" [Deltares, 2014].
- Rise of the phreatic water level below fills or embankments due to infiltration (again changing the effective stress conditions).

Considering the limitations of the most common calculation models, CROW (2004) presents a decently explained overview thereof in its Appendix II. In this thesis though, model-specific limitations were discussed in detail in chapter 3.2.

As a general note, it is emphasised that **one-dimensional** (1D) models are intrinsically limited to 1D problems. Although design of 2D geometries is possible and commonly done in settlement prediction software like *D-Settlement*, this functionality is merely a tool assisting in visualising a geotechnical engineering project in cross section – however the settlement subsequently is still calculated using a 1D vertical settlement prediction model.

It is very important to understand the limitations of 1D settlement prediction models, though. Neglecting **multi-dimensional effects** such as stress spreading and especially lateral deformation can severely compromise the accuracy of settlement predictions, depending on the geometry of the project: the latter is of particular relevance for *narrow* earth fills or embankments. Due to not (being able) taking into account lateral deformations (e.g. squeezing), considerable underestimations of the settlement are known to occur. Ngan-Tillard et al. (2016) have performed and mutually compared 1D, 2D and 3D settlement predictions for the trial mounds in the Bloemendalerpolder (refer to section 4.1.1), by using the *PLAXIS* Soft Soil Creep model originally developed by Vermeer & Neher (1999). From this they found that, although all predictions underestimate the actual settlement during the time period considered, the 2D and 3D predictions yield very similar results approaching the real settlement most closely (-15%), whereas the 1D prediction is off by -20%. Thus they conclude that 2D effects should be considered in settlement predictions, whereas 3D effects yield merely an insignificant additional improvement.

Knowing that the trial mounds modelled by Ngan-Tillard et al. (2016) still have a considerable ground surface area (36×26 m), for narrower earth fills or embankments it is therefore all the more recommended to use a multi-dimensional (finite element) settlement prediction model, such as implemented in *PLAXIS*. Nevertheless it is reminded that the use of a more advanced model will only yield more accurate results if also the parameters were determined very accurately and moreover specifically for that model [CROW, 2004]. Regarding the latter, the parameter determination should be targeted as directly as possible at the calculation model that is intended to be used. This way, one can avoid the use of conversion formulas for model parameters, which may introduce additional uncertainty.

3.3.3.4 Execution phase

Uncertainties arising from the execution phase of a project naturally first of all depend on the care taken during and quality of the work. However this is a matter of integrity and of Quality Assurance and Quality Control (QAQC), which is not detailed further. Another – seemingly trivial, but unfortunately relevant – factor is **communication** and **administration**, being important at any time, starting already from the investigation phase. For example, reportedly it happens occasionally that an undefined or downright incorrect reference system for geodetic measurements is used, or a wrong scale on maps. A similar experience was gained personally by the author during the current research, in a case where North and South were erroneously switched on a map or cross section. Several other non-technical recommendations concerning communication and administration are not detailed further in this thesis.

Everything else that the CROW working group has to say about the execution phase, concerns **monitoring**. The working group clearly advocates the application of monitoring, since by doing so one can discover different-than-expected soil behaviour in an early stage of the execution and adjust plans and strategies accordingly. Monitoring and subsequent interpretation and interpolation of measurements is undoubtedly beneficial for the reliability of the final settlement prediction – though only possible after the works have already started. Accordingly, common software packages such as *D-Settlement* offer the possibility to fit soil parameters in a settlement prediction model to real measurements. Analysis and evaluation of monitoring data can provide holds in finding the cause of the deviations (e.g. boundary conditions, soil parameters, subsurface structure, calculation method, etc.), which information can be used not only to learn from, but also to improve the reliability of settlement predictions in future projects.

Choosing an adaptive execution based on monitoring (“observational method”) can furthermore help in meeting the contractual requirements, for example by implementing additional settlement-accelerating measures (e.g. drainage or extra surplus height) if necessary, or limit such efforts and save time and/or money in case the work proceeds better than expected.

As a particular point of attention, CROW highlights the importance of performing reliable baseline- or reference measurements before *any* excavation or construction activity has taken place, to which subsequent monitoring data will be compared. Furthermore, redundancy in the monitoring systems (double or backup equipment) is also deemed a practical necessity, since malfunction and loss of sensors or equipment, especially of settlement beacons, was found to be part of everyday practice.

3.3.3.5 Sample disturbance

This subsection regards separately a specific aspect of soil sampling and testing (refer back to subsection 3.3.3.1), namely **soil sample disturbance**, which is a particularly important and much-discussed topic in geotechnical engineering. It is undoubtedly acknowledged that sample disturbance affects the soil behaviour and thus can lead to unreliable laboratory test results and derived compressibility parameters, as detailed further below. Rightly so, the importance of soil specimen integrity throughout the process of sampling and testing is emphasised repeatedly in literature concerning the reliability of geotechnical testing methods and settlement predictions [e.g. CROW, 2004; Den Haan, 2008; Zwanenburg, 2013].

However the actual influence of sample disturbance on a settlement prediction has hardly been investigated *quantitatively*. This might be partly because so many different variables and processes play a role (sampling, transport, storage, cutting, testing, etc.). Moreover, research in this regard is also complicated by the fact that sample quality is a difficultly assessable quantity, not least due to the lack of a consistent and widely agreed measurement method or scale [Zwanenburg, 2013]. At least a dozen different methods of determining and quantifying the degree of sample disturbance have been proposed and are described in literature. Several of those are reviewed by Prasad et al. (2007), only to finally introduce their own – albeit easy to use – measure of sample disturbance called the "sample disturbance index", based on the pre- and post-yield compression indices. Zwanenburg (2013), on the other hand, describes again a different method that was introduced by Lunne, Berre & Strandvik in 1997 and that is reportedly used in Norway. It essentially expresses the amount of swelling that has occurred after sampling, by comparison of the void ratio at the in-situ stress level with the initial ("disturbed") void ratio.

In Dutch geotechnical investigation reports, however, any indication of sample disturbance is rarely encountered, with sole exception of laboratory test reports by Deltares, in which indeed often a certain "sample disturbance index" is given as a percentage. Deltares provides no indication whatsoever of how this index is determined, though. From personal verification attempts it has become clear that the Deltares index confusingly is *not* the same as the one proposed by Prasad et al. (2007). After trying several alternative ways, it was found that the Deltares index is similar to the method described by Zwanenburg: namely the percentage of *strain* at the in-situ stress level with respect to the initial state (0), as illustrated by Figure 3-15.

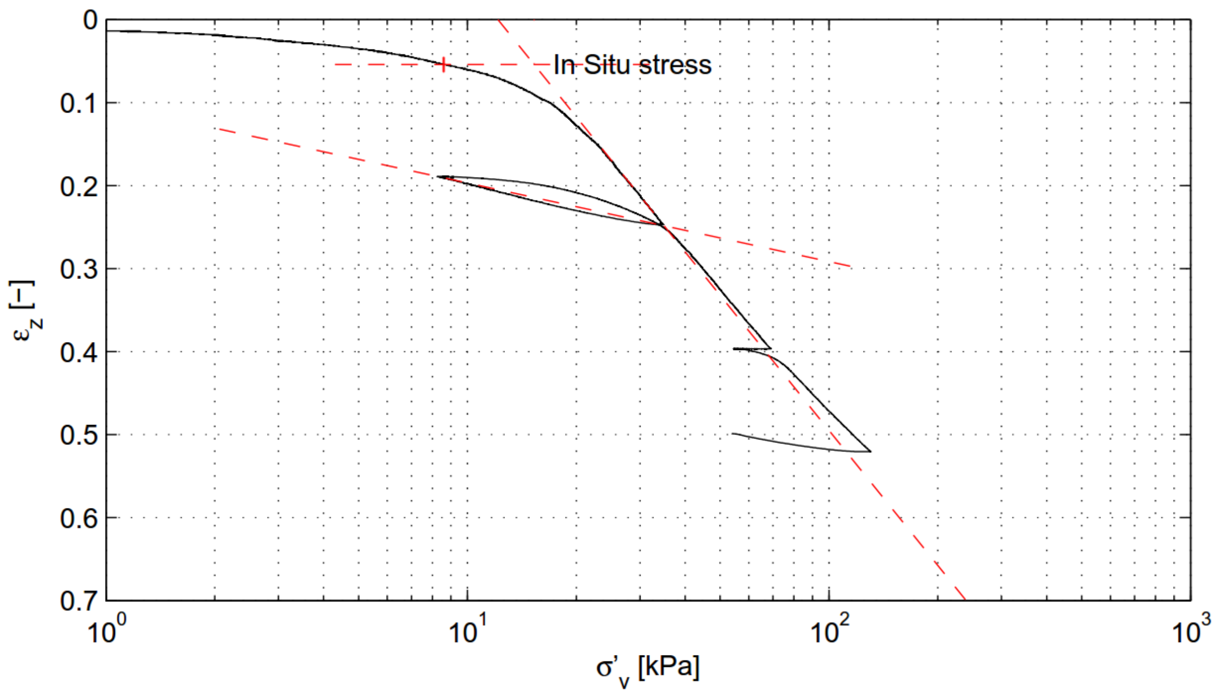

Figure 3-15: Compression curve of soil sample B102-t5-4 from the Leendert de Boerspolder, adapted from [Deltares, 2015]. The reported "sample disturbance index" is 6.2% (moderate quality), which closely corresponds with the strain at the in-situ stress. This verification holds for other test diagrams as well.

Regardless of the lack of convention in measurement and quantification, sample disturbance still is considered to form a significant factor contributing to the uncertainty in the reliability of soil parameters and hence settlement predictions. Consequently this also affects the quality and costs of geotechnical design and construction works in general. In order to shed some more light on this subject, CUR established an investigation commission named "Kwaliteit van grondonderzoek", co-financed by Rijkswaterstaat and actively supported by a multitude of industrial parties like, amongst others, Fugro GeoServices and Deltares. Investigations so far focused on boring and sampling methods, or more specifically a comparison of their resulting sample quality and subsequent influence on soil parameters [Van Essen, 2013; 2014]. A final report on that research does not seem to be published yet though. In any case, however, the influence of sample quality is to be seen in close relation with the calculation model that is being used: when the calculation model has an intrinsic uncertainty in its outcomes, or it is not suitable for the assigned job because it does not take into account certain essential soil behaviour or parameters at all, high-precision sampling and testing would simply be overdone and cost-inefficient [Zwanenburg, 2013].

One of the most important parameters in settlement analysis that is found to be strongly influenced by sample disturbance, is the apparent **preconsolidation pressure** (p_g) [Den Haan & Molendijk, 2002; Zwanenburg, 2013]. In practice, sample disturbance generally leads to an *underestimation* of p_g, as well as of b or CR [Den Haan, 2008; Van Essen, 2013]. View also Figure 3-16 for a visualisation. On the other hand, friction in laboratory test setups (most notably oedometer wall friction) is likely to lead to *overestimation* of p_g and b or CR [Den Haan, 2008]. This in turn might partially counteract the effects of sample disturbance.

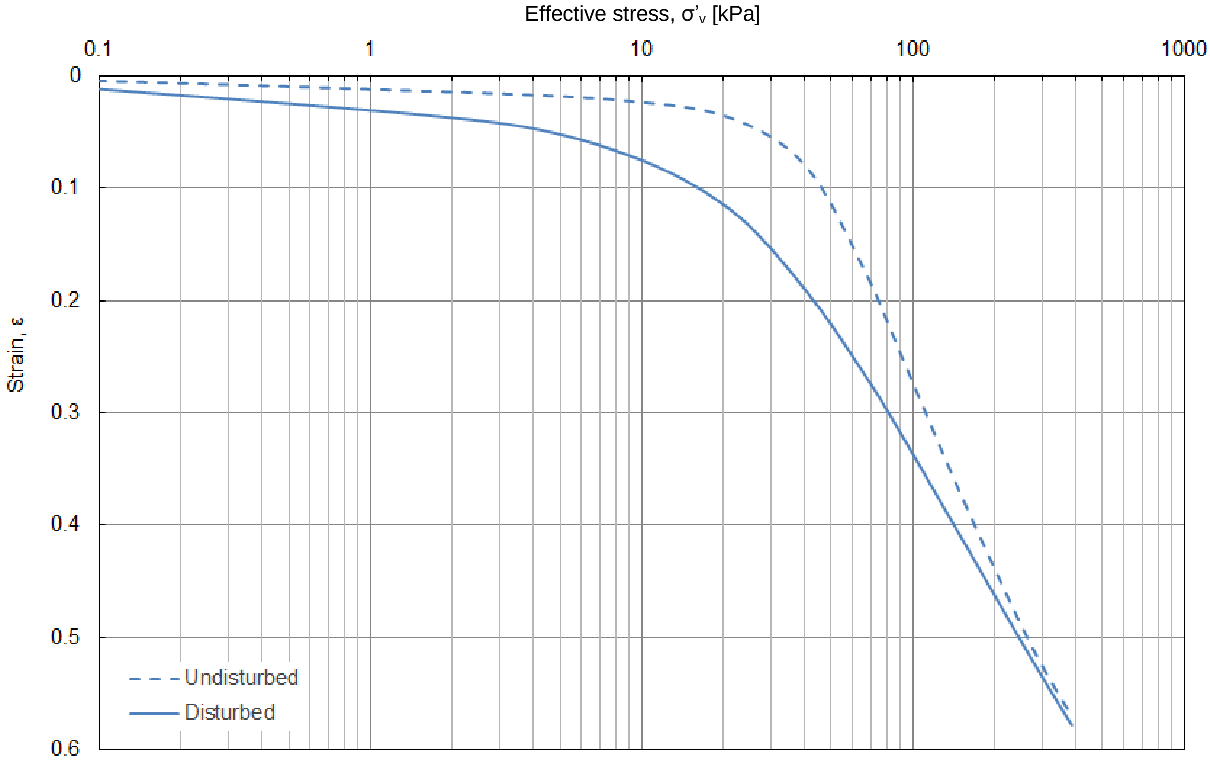

Figure 3-16: Hypothetical compression curve illustrating the difference in compression behaviour between a largely undisturbed soil sample and a more disturbed soil sample. From the diagram it is apparent that the slope of the virgin compression curve (yielding *b* or *CR*) will be underestimated due to sample disturbance. So will be the preconsolidation pressure as well, which according to Casagrande (subsection 2.2.2.1) and to several other graphical methods is dependent on the (tangent to the) virgin compression curve. Just for information, the response of a remoulded (i.e. completely disturbed) soil sample will approach a straight diagonal line.

Sample disturbance is generally not being corrected for in practice, which might be due to the fact that it further complicates test data processing and interpretation, and moreover it is unknown to what relative amount disturbance is counteracted by friction. Otherwise, a possible method to account for disturbance might be the long known “field virgin” or “in-situ” compression curve reconstruction method originally proposed by Schmertmann in 1955. Another possibility is the application of a sample disturbance correction factor as described in [Prasad et al., 2007].

3.3.4 Soil parameter sensitivity analysis

Ultimately, the CROW working group describes its performance of a parameter sensitivity analysis regarding the Koppejan method, which is still a frequently used settlement prediction methods in the Netherlands. This sensitivity analysis was done by means of the Monte Carlo method, comprising a total of 10,000 simulations of 10 different soil and geometry parameters, for 10 different problem geometries (regarding subsurface structure and amount of surcharge) to be indicated as “cases”.

The principal assumptions and conditions for the analysis were: all parameters are independent/uncorrelated, the earth fill is sufficiently wide and uniform (eliminating the possibility of horizontal deformations), pore water pressure is hydrostatic (linear increase with depth), and the effect of subsidence of the fill below the phreatic water level was neglected.

The results presented by CROW regard the *final* and *residual* settlements *separately* (refer to Appendix B for according terminology explanation). For every geometry, the α^2-values (i.e. the contribution of the variation of one parameter on the total variation of all parameters together, expressing sensitivity) were calculated. In this thesis only the three most complex and most realistic problem geometries (case numbers 7, 8 and 10) are considered, i.e. those consisting of two or more soil layers, with variation of all parameters, and all soil and stress parameters being stochastic. The Monte Carlo simulations yielded the following results for the final settlement (undefined symbols referring to Koppejan compression coefficients; section 3.2.3):

- For a 2-layer subsurface model with phreatic water level (z_w) at the ground surface (case 7), C'_p of the first layer was found to be most critical, i.e. to have the highest α^2-value.
- For a 2-layer model with z_w = -0.5 m (case 8), C'_s of the first layer was identified to be most critical.
- For a 4-layer model with z_w = -0.5 m (case 10), C'_s of the *second* layer was identified to be most critical.

And for the residual settlement:

- For a 2-layer model with z_w at the ground surface (case 7), C'_s of the first layer was identified to be most critical.
- For a 2-layer model with z_w = -0.5 m (case 8), C'_s of the first layer was again identified to be most critical.
- For a 4-layer model with z_w = -0.5 m (case 10), log(c_v) of the second layer was identified to be most critical.

A particularly interesting finding of the simulations is, that with the increase of the number of stochastic parameters (max. 34 in case of 4 layers, with 8 stochastic parameters per layer), from a certain point onward the coefficient of variation ($V = \sigma / \mu$) decreases. In other words, a sufficiently large number of uncertain parameters in the model causes the overall uncertainty of the result (settlement) to decrease. The suggested explanation is that the uncertainties in the different parameters cancel out each other, provided the number is large enough. However it is reminded that all parameters were assumed to be uncorrelated, which in reality is not true, so the practical significance of this observation remains difficult to assess and is not evaluated further by CROW.

Furthermore, some expectations were confirmed. For instance, a short hydrodynamic period minimises the influence of uncertainty in the consolidation coefficient on the final settlement. Vice versa, for a long hydrodynamic period the influence of uncertainty in c_v increases and at the same time the influence of uncertainty in C'_s decreases.

Also as expected, the uncertainty in the final settlement is mainly determined by C'_p and C'_s when the surcharge is larger than the preconsolidation pressure. And generally the contribution of the thickest layer dominates in the uncertainty of the final results.

Finally, the rule of thumb stating that the overall uncertainty of settlement predictions is approximately 30%, was also evaluated: for final settlements this turns out to be a fairly good estimate, corresponding with a limit exceedance probability (p-value) of around 5%, whereas for residual settlements this is a less good estimate corresponding with a limit exceedance probability of around 10%.

4 Data analysis

4.1 Introduction to the investigated cases

This chapter will provide an introduction to the cases that are analysed in more detail in the further course of this research. First of all, right below it is briefly explained why these particular cases were chosen. The selection of the cases was not just done randomly, but based in the first place on their difference in character, namely: a platform mound, a road embankment and a dike. Furthermore some more specific considerations were made as follows:

1) The Bloemendalerpolder (refer to section 4.1.1) was chosen because it was known that the subsurface consists mainly of peat. Just as important, however, was the availability of a large diversity and amount of site investigation and laboratory test data, as well as several years of monitoring data. Moreover it seemed convenient that the data are openly available, which makes verification and/or reuse of results easier also for the readers of this thesis.
2) The Amstelhoek case (section 4.1.2) comprises a real road construction project, of which all data were provided by *Sweco*. The composition of the subsurface is more diverse, which would allow for assessing especially the performance of some empirical settlement prediction methods in these particular conditions. Furthermore, it was considered to be a good learning experience for working with typical site investigation and monitoring data and to encounter its limitations. Last but not least, in the course of construction some peculiar deviations from original settlement predictions occurred, raising interest to investigate the possible causes for this. This concerns in particular location 1300 m (33% more settlement than predicted) and 2000 m (22% less settlement than predicted).
3) The Leendert de Boerspolder (section 4.1.3) was selected last, after it had become clear that the first case had been analysed already more thoroughly than expected and the second case posed more limitations than expected. So the Leendert de Boerspolder, with its ancient and manually constructed dike, seemed to provide an interesting opportunity to not only validate settlement predictions on the *very* long term, but also to compare different soil test and parameter determination methods based on a fairly extensive and diverse set of laboratory test data. The subsequent settlement predictions where to model the dike's settlement *in retrospect*, from about mid-17th century until present, in order to assess whether existing prediction models could yield accurate results on such long term and how well the different available soil test data could feed these models.

The following sections provide some general background information along with the most essential facts and figures for each case separately. This includes, amongst others, the purpose of the project, local geology, basic geotechnical design and an overview of available data.

4.1.1 Bloemendalerpolder

The first and foremost case that will be investigated, is the Bloemendalerpolder north of Weesp in the province of North Holland, the Netherlands (please refer to Appendix C1 for a map). This case is not a regular construction project, but part of a national research programme called "Geo-Impuls". The Geo-Impuls programme was set up in 2009 with the general intention to reduce failure costs in civil construction projects due to geotechnical causes, mainly by (a combination of) more consequent application of geo-risk management, increase of technical knowledge, and improvement of communication and cooperation between different project stakeholders [Cools, 2011; Geonet, 2016a]. More than 30 different parties were participating in the research programme, varying from (semi-)public authorities (e.g. municipalities, Rijkswaterstaat and ProRail) to engineering and contracting companies (e.g. Grontmij, Fugro, Boskalis and many more), as well as knowledge organizations, educational institutions and professional organizations (e.g. COB, Deltares, TU Delft and KIVI).

When around the same time as the initiation of the Geo-Impuls programme plans for urban development of the Bloemendalerpolder were announced, interest was aroused to couple this with the Geo-Impuls programme [Rohe, 2010; Hoefsloot, 2011]. After consultation, the property developer was found to be willing to provide the unique opportunity of using the area for practical research purposes for a total duration of 5 years: from 2010 until 2015.

Subsequently a full-scale field test was designed and performed in the Bloemendalerpolder, comprising the construction and long-term monitoring of two so-called “proefterpen” (English: trial mounds, or trial embankments). The goal of this field test was to improve general understanding of soft soil consolidation and creep settlement behaviour, as well as to validate common one-dimensional settlement prediction models. Furthermore, piles were installed near the edge of the mounds and monitored in order to investigate also the influence of lateral loading on foundation piles. However results from the latter experiment are not regarded in this thesis, in the first place because that is outside the scope of the current research, and in the second place because those results were already analysed in detail by Siderius (2011) and by Schadee (2012).

The essential facts, figures and available data of the Proefterpen Project Bloemendaler-polder are listed below, based on Hoefsloot (2011) and Alink (2012):

General / geometry

- The original polder ground surface level is on average -1.7 m NAP.
- The project comprises two trial platform mounds (“proefterpen”), each with a height of 3 m (staged construction; see Table 4-1), slopes of 1:2 (≈ 27°) and outer (bottom surface) dimensions of 36×26 m.
- The western platform mound (No. 1) is constructed without any settlement accelerating measures, whereas at the eastern platform mound (No. 2) drainage was applied, namely vertical strip drains in a triangular pattern with a centre-to-centre distance of 1 m.
- After a year, the top 0.5 m was removed from *half* of the surface area of each platform mound, in order to assess the effect of application and removal of an extra surplus height for reduction of residual settlements.
- At safe distance from the trial mounds a “reference location” was preserved to measure and monitor autonomous natural changes of the environment, such as ground water pressures and surface level (subsidence).
- Maps and plans of the project site are provided in Appendices C1 and C2.

Subsurface

- The subsurface is interpreted to consist primarily of peat, mostly fibrous, lying on top of a massive base layer of (most likely Pleistocene) silty sand. The thickness of the peat layer is at least 3.7 m (on average 4 m) underneath trial mound 1, gradually increasing to a maximum thickness of 6.3 m (on average 5.5 m) underneath trial mound 2. Manual borings indicate furthermore that the topsoil (40 cm) consists of dehydrated slightly organic clay.
- CPT profiles indicate a 0.5 to 1.0 m thick layer of silty clay at a depth between 1 and 2 m below ground surface.
- The phreatic ground water level is between -2.1 and -2.2 m NAP, i.e. at 0.4 to 0.5 m below ground surface.
- A schematic cross-section is provided in the site plan in Appendix C2.

Site investigation (executer between parentheses)

- Geodetic survey (*Fugro*)
- 17 Cone Penetration Tests (CPT) with friction sleeve and piezocone (*Fugro*)
- 1 CPTs with friction sleeve and piezocone (*Deltares*)
- 8 Cone Pressiometer (CPM) tests with friction sleeve and piezocone (*Fugro*)
- 4 Ball Penetration Tests (BPT) with piezometer (*Fugro*)
- 11 electronic field vane tests (*Fugro*)
- 3 continuous sampler, or “Begemann” borings (*Deltares*)

Laboratory testing (executer between parentheses)

- Soil classification according to NEN 5104, based on Begemann borings (*Deltares*)
- Unit weight, water content and degree of saturation (*Deltares*)

- Loss on ignition (*Fugro*)
- Koppejan compression coefficients by means of IL oedometer tests (*Fugro*)
- NEN-Bjerrum and a,b,c-Isotachs compression coefficients, K_0, preconsolidation pressure and hydraulic conductivity by means of K_0-CRS compression tests (*Deltares*)
- Undrained shear strength by means of Hand Vane tests (*Deltares*)
- Undrained shear strength by means of Torvane tests (*Fugro*)
- Shear strength by means of consolidated undrained (CU) single stage Triaxial tests (*Fugro*)
- Consolidation coefficient (c_v) by Casagrande *and* Taylor method (*Fugro*)

Monitoring (amounts for both mounds counted together; executer between parentheses)

- 12 settlement beacons (*Mourik Groot-Ammers*)
- 4 electronic settlement beacons (*BAM Infra*)
- 5 rod extensometers (*Deltares*)
- 4 inclinometer tubes for pile deformations (*Fugro*)
- 15 piezometers for pore water pressure (*Fugro*)
- 4 piezometers for pore water pressure (*Deltares*)
- 6 hydrostatic profile gauges for measurement of settlements of the original ground level underneath the mounds (*Mourik Groot-Ammers*)
- A plan of the monitoring equipment positions can be found in Appendix C2.

The final reporting on all geotechnical investigations, testing and monitoring was done by *Fugro GeoServices*. The site investigation and laboratory test results are contained in a report composed by Alink (2012), comprising over 200 pages, which also includes method descriptions and technical specifications of the equipment used. The monitoring results, on the other hand, are contained in a later published report composed by Hoefsloot & Schadee (2013). All reports concerning the Proefterpen Project Bloemendalerpolder are openly accessible on the internet [Geonet, 2016b].

A time log of all relevant activities performed for the Proefterpen Project is presented in Table 4-1.

Table 4-1: Time log of the Proefterpen Project Bloemendalerpolder. Adapted from [Alink, 2012: table 2-1].

Geotechnical site investigation	16 Sep - 29 Sep 2010			
Placement of monitoring equipment	24 Sep - 12 Oct 2010			
Construction phase	Week	Day	Trial mound 1	Trial mound 2
1st fill stage (28 Oct 2010)	1	1	1.0 m	1.0 m
Installation of vertical drains (2 Nov 2010)	1	6	none	1.0 m c.t.c.
2nd fill stage (22 Nov 2010)	4	26	0.5 m	0.5 m
3rd fill stage (14 Dec 2010)	7	48	0.5 m	0.5 m
4th fill stage (25 Jan 2011)	13	90	0.5 m	0.5 m
5th fill stage (17 Feb 2011)	16	112	0.5 m	0.5 m
Removal of extra surplus height (19 Dec 2011)	60	417	-0.5 m (half)	-0.5 m (half)
End of field test (Oct 2015)	260			

As mentioned briefly before, part of the Proefterpen Project was also a validation of common settlement prediction models, by comparison of predictions with actual field settlement measurements. The models considered in the course of that project were: Koppejan, NEN-Bjerrum and a,b,c-Isotachs. A notable amount of analysis in this regard has been performed already by experts at Fugro [Ammerlaan & Hoefsloot, 2012], whose results are also taken into consideration in the current research, however to be complemented by two more prediction methods, as explained in the next chapter (4.2).

4.1.2 Amstelhoek

The second case that will be investigated is the N201 provincial road bypass east of Uithoorn, in the provincial border area between North Holland and Utrecht, the Netherlands (refer to Appendix D1 for a map). Although the eye-catcher of this construction project is a new aqueduct crossing the Amstel river northeast of Uithoorn, this study will solely regard the road section within the province of Utrecht, i.e. south of the Amstel aqueduct and east of the village Amstelhoek, and more specifically the settlements associated with that road section.

The N201 is a particularly important and busy provincial road, not just because of the considerable amount of residential and commuter traffic, but even more because it is an access route to both the international airport of Amsterdam Schiphol as well as the Aalsmeer Flower Auction. The main reason for the construction of a bypass was, that this road used to cut through the middle of the residential areas of Aalsmeer, Uithoorn and Amstelhoek, thus negatively affecting the safety and quality of living in these towns. Moreover, the amount of traffic on the N201 had increased to such level that congestions had become a persistent problem and consequently the accessibility and overall functioning of the road were impeded considerably: already in 1992 every day on average 36,000 vehicles passed through Aalsmeer, with an average *annual* growth rate of 1.75% between 1992 and 1996 [Provincie Noord-Holland, 1999].

Ideas for redevelopment of the N201 road existed and were discussed for about 40 years, whilst the establishment of an agreement between the numerous stakeholders took its time [Booltink et al., 2005]. As the urgency of the traffic problems grew, however, the parties finally came to agreement in 1996, which resulted in a *Masterplan Corridor N201* containing amongst others the main goals, a proposed trace plan and the assignment of an Environmental Impact Assessment ("EIA"). Based on the results of the EIA [Provincie Noord-Holland, 2001], a preferred road trace was determined and approved. This was subsequently elaborated into a pre-design in 2001, which however due to financial limitations soon had to be reconsidered and adapted, resulting in a new, shortened and economised, trace plan. After approval, the final plan was recorded in the *Regioakkoord N201+* in late 2002 as well as in the *Bestuursovereenkomst II* in early 2003. Both (original and economised) trace plans are indicated on the map in Appendix D1.

Because of the trace change, a new EIA was required, which task was assigned to *Grontmij Nederland* (now *Sweco*). In the resulting EIA [Booltink et al., 2005] several options were evaluated, including most importantly three semi-parallel alternatives of the economised trace plan, which are all indicated on the maps in Appendix D1. Differences between the alternatives were considered to be negligibly small, except for the fact that a number of houses is located along the Tienboerenweg, in the way of trace alternative A. Since not only demolition of these buildings, but preferably any nuisance for the inhabitants ought to be prevented, the most environmentally friendly and therefore recommended alternative was alternative B [Booltink et al., 2005], which was accepted and realised finally [La Fors & Dercksen, 2006]. The technical design of this part of the N201 bypass, including the Amstel aqueduct, was performed by *Grontmij Nederland* [Meulblok & Forger, 2009].

By traffic flow modelling, construction of the bypass was estimated to result in an average traffic reduction of 40% on the old N201 road, based on an expected traffic intensity in 2015 in case no action would be taken [Provincie Noord-Holland, 2001]. The predictions took into account the general growth of traffic and in particular plans for future industrial developments in the area, which together are expected to cause the traffic intensity to increase by 35% on average, depending on the exact location. So after 2015 effectively no really significant reduction in traffic intensity will be achieved with respect to the baseline level (2000). Nevertheless this may still be considered as a positive result, since in case no action would be taken, an absolutely intolerable traffic situation would occur around 2015 and later.

As said, this study regards the settlements associated with the construction of the road embankment section within the province of Utrecht, south of the Amstel aqueduct and east of the village Amstelhoek. The essential facts, figures and available data of this part of the N201 bypass project are listed below, based on Meulblok & Forger (2009) and Van der Valk (2007):

General / geometry

- The original polder ground surface level is on average -5.3 m NAP.
- The main road surface level will be on average -3.80 m NAP, so that it is elevated about 1.5 m above the surrounding polder ground level. For a schematic overview of the road embankment and its dimensions, please refer to Appendix D4.
- In order to meet the total construction time limits and residual settlement requirements, settlement accelerating measures were applied, namely: vertical drainage in a triangular pattern with a centre-to-centre distance of 2 m, as well as an extra surplus height of 0.5 m.
- The road embankment contains a geogrid in order to ensure its stability.
- The road principally consists of two lanes (one in each direction), each with a width of at least 2.75 m and separated by a 0.80 m wide median strip. The total width of the road varies because of multiple crossings and associated sorting lanes and margins, however it amounts to at least 7.50 m including surface markings and side safety margins.
- To the west alongside the middle part of the main road, there is a parallel road for rural traffic, separated from the main road by a polder-dewatering ditch.
- Maps and plans of the project site are provided in Appendices D1 and D2.

Subsurface

- The subsurface is interpreted to consist mainly of peat and clay, the latter varying from organic to silty. The peat and clay together cover a more than 25 m thick base layer of Pleistocene sand, which is also graphically represented in Appendix D3. In general two different peat layers (sometimes clayey peat) can be distinguished, namely a 1.0-1.5 m thick layer starting between ground surface level and 1.5 m depth, and an approximately 1.0 m thick layer ("basisveen") laying directly on top of the sand. In between those peat layers, and partly encountered as topsoil, silty and organic clay is present. The sand starts at about 4.5 m below ground surface level, i.e. at an absolute depth of about -10 m NAP.
- The phreatic ground water level is between -5.9 and -6.0 m NAP, i.e. at 0.6 to 0.7 m below ground surface.
- A geological cross section of the middle part of the road trace of is provided in Appendix D3.

Site investigation (all performed by *Fugro*, except if stated differently)

- 82 Cone Penetration Tests (CPT) with friction sleeve
- 10 CPTs with friction sleeve and piezocone
- 7 CPTs with friction sleeve and piezocone (*MOS Grondmechanica*)
- 28 manual borings
- 19 mechanical borings
- 8 groundwater level monitoring wells

Laboratory testing (all performed by *Fugro*)

- Soil classification according to NEN 5104, based on manual and mechanical borings
- Unit weight, water content, degree of saturation and porosity (1)
- Loss on ignition
- Grain size distribution by dry sieving
- Koppejan compression coefficients by means of IL oedometer tests
- Shear strength by means of consolidated undrained ("CU") single stage Triaxial tests
- Consolidation coefficient (c_v) by Casagrande and Taylor method

[1]) For the porosity determination, the solid material density was reportedly assumed to be 2650 kg/m^3, which cannot be valid for every soil type and every sample. Since this likely raises a significant source of error, it is strongly recommended to manually calculate the porosity or void ratio from the water contents if necessary for any further calculations, rather than using directly the porosity values from the laboratory test reports.

Monitoring (all performed by *Combinatie Amstelhoek*) [Boekhorst, 2010]

- About 200 settlement beacons: 2 beacons on the crest and 2 beacons at the toe of the embankment at every 50 metres along the full length (2.8 km) of the road trace. (2)
- 41 additional settlement beacons at road crossings and culverts (not regarded in current research).
- 16 piezometers for pore water pressure monitoring; only at sensitive locations and structures around the Amstel river (not regarded in current research).
- 11 inclinometer tubes for horizontal deformations; only at risky or sensitive locations and structures around the Amstel river (not regarded in current research).
- 5 hydrostatic profile gauges; generally only at risky or sensitive locations, namely at 150 m (gas pipeline), 200 m and 300 m (pivot dike(3)), 950 m and 2000 m.

All construction and monitoring activities, including the installation of monitoring equipment and analysis of resulting measurements, were performed by the *Combinatie Amstelhoek*, which is a consortium of *KWS Infra* and *VWS Geotechniek* (both currently part of *VolkerWessels Group*) and *GMB Civiel*.

The construction of the Amstelhoek section of the N201 bypass was started in February 2011 and was finished on 16 May 2014 with the official opening of the Amstel aqueduct [De Ronde Venen, 2014]. However when considering the entire project, construction already started late 2006, so the total construction time amounted to almost 7 years.

The staged construction of the Amstelhoek road embankment itself was started in mid-October 2011 and finished at the beginning of February 2012, after which 250 days of consolidation and settlement time were reserved. The embankment was released ready for pavement construction as of 8 October 2012 [Luyten, 2011; Sipkema, 2012].

4.1.3 Leendert de Boerspolder

The third case to be investigated is the Leendert de Boerspolder northwest of Roelofarendsveen in the province of South Holland, the Netherlands (please refer to Appendix E1 for a map). The Leendert de Boerspolder has a total surface area of merely 6 hectares and is surrounded entirely by the shallow waters of the Ringvaart van de Haarlemmermeerpolder and the Hanepoel. As such, it can be classified as an island, albeit a man-made island.

According to the so-called Berging Rekening Courant agreement, it is required that any water storage basin being filled up has to be compensated by creation of an equal storage volume elsewhere. Around the year 2010 the water board Hoogheemraadschap Rijnland was looking for such a place to create new storage after filling of other locations. Around the same time it emerged that the water barriers and pumping stations of the Leendert de Boerspolder, which until that time had been in use for agricultural purposes, were in need of some profound maintenance. Since this would become a very costly affair, it was considered to redevelop the small and isolated polder into a water storage basin along with recreational functions. Therefore in the year 2011 Hoogheemraadschap Rijnland acquired this polder for redevelopment [STOWA, 2016; Van Veen, 2015].

In the course of plan making for the redevelopment, which would comprise flooding of the polder for the greater part, interest was raised to create an exclusive opportunity for learning more about dike stability and the validity of according stability calculation models by inducing a dike failure. This idea was elaborated and a unique dike failure research project, called "Dijkbezwijkproef", was set up in collaboration with several other water boards, provinces, STOWA and TU Delft. The dike failure field test was finally performed in the autumn of 2015.

---

2) Settlement beacon measurements are available as Excel datasheets, spanning the period from late March 2011 (baseline measurements) until August 2012. However available measurement intervals are irregular because some data sheets are missing.

3) Pivot dike (Dutch: "kanteldijk"): auxiliary dike surrounding the entrance(s) of a tunnel that crosses a waterway and/or water barrier. The pivot dike is an extra safety measure to prevent flooding of the polder in case of a calamity in the adjacent polder, or in case of leakage or failure of the tunnel itself.

In advance of this dike failure test, a lot of site investigations were performed in order to obtain data to predict and evaluate the later observed dike failure behaviour. These investigations included a multitude of different soil compression tests – which seemed to be of particular interest for the current research regarding long-term settlement predictions. Not just the availability of the test data, but also the fact that the data were collected from a very long existent polder and surrounding dike, made it seem very interesting to investigate this case in more detail.

This case study will solely regard the settlements that the dike has undergone, in particular on the southern side in area B (refer to Appendix E2). The polder seems to be first established already in the 11th century, however since then it has undergone several major changes and floods [Van Veen, 2015]. According to Prof. C. Jommi [pers. comm.], the part of the dike regarded in detail is estimated to exist since about the mid-17th century. When taking the year 1650 as the reference point, the total elapsed settlement time thus amounts to about 365 years.

The essential facts, figures and available data of the Leendert de Boerspolder and its dike are listed below, based mainly on Jommi et al. (2015):

General / geometry

- The polder ground surface level close to the dike toe is -1.7 m NAP, gradually decreasing down to -1.9 m NAP towards the centre of the polder.
- The dike's crest is at -0.4 m NAP, i.e. about 1.4 m above the average polder ground level.
- The dike has a base width of about 10.0 m, an inner (polder side) slope of approx. 1:3 and an outer (water side) slope of approx. 1:2.5.
- The water level outside the dike is -0.7 m NAP.
- Maps and plans of the project site are provided in Appendices E1 and E2.

Subsurface

- The dike itself has a very heterogeneous composition, with a remarkably high *average* unit weight of 18 kN/m^3.
- The subsurface is interpreted to consist from top to bottom of: 0.6-0.7 m of unsaturated sandy organic clay topsoil, followed by 2.0-2.2 m of peat and finally almost 8 m of slightly silty organic clay, until the Pleistocene sand is encountered at an absolute depth of -12.0 m NAP below the dike. Note that the top of the sand dips slightly in northern direction.
- The phreatic ground water level is on average at -2.4 m NAP in the polder, -2.2 m NAP below the toe of the dike and -1.5 m NAP below the crest of the dike, although especially below the dike it was found to vary locally.
- A schematic cross-section is provided in Appendix E3.

Site investigation (numbers per area (A,B,C,D); executer unknown)

- 15 Cone Penetration Tests (CPTu) with friction sleeve and piezocone
- 6 Manual borings
- 4 Standpipes
- 1 Electrical Resistivity Tomography (ERT) along the southern dike

Laboratory testing (executer between parentheses)

- Unit weight, water content and degree of saturation (*TU Delft & Deltares*)
- 6 Incremental loading oedometer tests, unprocessed (*TU Delft*)
- 5 CRS compression tests, unprocessed (*Gemeentewerken Rotterdam*)
- 11 K_0-CRS compression tests, processed for determination of NEN-Bjerrum and a,b,c-Isotachs compression coefficients, K_0, preconsolidation pressure and hydraulic conductivity (*Deltares*)

Where the numbers of laboratory tests only take into account those that were made available for the current research.

4.2 Methods

This chapter provides detailed descriptions of the methods or procedures that are followed to ultimately satisfy the objectives and the goal of the current research. First, the choice for the settlement prediction methods will be briefly elucidated. After that, sequentially the methods of data and parameters acquisition, modelling, calculation and analysis will be described in detail in order to clarify how the results were obtained.

4.2.1 Selection of settlement prediction methods

The settlement prediction methods that were chosen to assess and validate in detail, were mainly based on the desires of *Sweco Nederland*, following from practical questions and problems encountered by employed engineers in daily working practice. Special interest concerns the less well-known methods (i.e. De Glopper and Fokkens) that are presumed to be less time consuming and easier to use with regard to parameter determination and/or calculation than more commonly used methods, however with an unknown reliability or accuracy.

The selected methods were mentioned already briefly in the objectives (section 1.2.2) and comprise the following:

- Koppejan
- De Glopper (in combination with Koppejan)
- Fokkens (6 different versions)
- Bjerrum
- Den Haan (a,b,c-Isotachs)

In the course of the Bloemendalerpolder case study it turned out that Koppejan, Bjerrum and Den Haan have been validated already, which is why emphasis was put on the methods of Fokkens and De Glopper, which both are widely unknown despite being mentioned in broadly read geotechnical reference publications like CUR 162 (1996). Furthermore also several empirical correlations for obtaining a,b,c parameters are validated. Ultimately focus was shifted towards data interpretation from soil compression tests in the case of the Leendert de Boerspolder.

The methods of De Glopper and Fokkens were applied on the basis of data of the Bloemendalerpolder and Amstelhoek. Note that Fokkens' method exists in six different versions (refer to section 3.2.5), all of which were validated on the aforementioned two cases. The a,b,c parameter correlations were validated exclusively on the Bloemendalerpolder peat, rather than on the heterogeneous and more clayey soils at Amstelhoek.

For the case of the Leendert de Boerspolder, it was intended to derive the Koppejan, Bjerrum and a,b,c-Isotachs parameters and to use these three models for settlement predictions. As explained in the final remark of section 4.2.3, however, the lab test data proved to be sufficient only for direct determination of the Bjerrum and a,b,c parameters of *all* soil layers. So in this case the long-term settlement analysis was performed with just these two methods. An important part of this case study was the process of parameter determination itself though, besides the settlement analysis. The methods of data acquisition and soil parameter determination are explained in the next section.

4.2.2 Data acquisition and soil parameter determination

4.2.2.1 Data available

For the first two cases, Bloemendalerpolder and Amstelhoek, most data were available in the form of geotechnical lab reports (pdf), containing pre-processed soil compression test results together with according graphs and diagrams, as well as soil physical properties, which were described already in chapter 4.1. Of course, from these only the information directly relevant for subsurface interpretation and settlement analysis was used, which means that inter alia shear strength data from triaxial tests and the like were neglected. Still, a large amount of data was used, which had to be input manually into spreadsheets and organised for further use and analysis. Next to that, the necessary geospatial and geological information was derived in both cases from a combination of site plans, manual bore logs, CPT test diagrams and – in the case of Amstelhoek – even already available CPT-based geological cross sections (Appendix D3).

Regarding the last case, Leendert de Boerspolder, only the K_0-CRS test results were already pre-processed and interpreted. The other compression test results (i.e. incremental loading and regular CRS oedometer) were provided as raw test data sheets. These raw data sheets contained in general the following information or readings: initial sample dimensions, time since start of test, time since start of stage, axial load and axial displacement or deformation. The IL data moreover also contained detailed soil physical properties (e.g. initial water content, initial void ratio, density), whereas the CRS data instead contained measurements of the back pressure, back volume and pore pressure. Readings or measurements were taken automatically for both kinds of tests; only the application and registration of the load increments for the IL tests were done manually. The measurement time intervals for CRS tests were constant at once every 30 s, whereas the intervals for IL tests were variable (increasing with time from once per second to once per minute).

From these data regarding the Leendert de Boerspolder, soil compressibility parameters could be determined in a possibly most objective and unbiased way, in order to compare the different soil test and parameter acquisition methods with regard to their quality, suitability and usability for settlement predictions. Geospatial and geological information was obtained from site plans and CPT profiles that were contained in a preliminary site characterisation summary report by Jommi et al. (2015).

4.2.2.2 De Glopper

For the methods of De Glopper (yielding Koppejan coefficients) and Fokkens all required input parameters mostly consist of, or are to be determined from soil physical or index properties. Both methods were only applied to the cases Bloemendalerpolder and Amstelhoek, for which laboratory-obtained Koppejan coeffients were also available for direct comparison. In this subsection it is explained how the Koppejan coefficients were obtained according to De Glopper, followed by the method of Fokkens in the next subsection.

De Glopper's relationship (refer to section section 3.2.6) in combination with the Koppejan method appears to be the simplest of all considered settlement prediction methods since it requires just one easily obtainable soil property, namely the porosity. The formulas for the according porosity-compressibility relationships were derived on the basis of Figure 3-8, and are presented in the subsequent Figure 4-1.

Although the porosity (*n*) could be very easily calculated from the void ratio (*e*) by: $n = e \,/\, (1 - e)$, it was found that the given values for void ratio inexplicably deviate from own verification calculations by a few percent. Consultation with the research supervisor, Prof. C. Jommi, revealed that this fact had caught attention already before in other research projects. Therefore, it was decided to calculate the porosity of every sample by oneself from the saturated and dry unit weights as follows, also taking into account the degree of saturation if known:

$$n = \frac{V_v}{V_t} \tag{4-1}$$

$$V_v \text{ (if 100\% sat.)} = V_w = \frac{m_{wet} - m_{dry}}{\rho_w} \tag{4-2.1}$$

$$V_v \text{ (if partially sat.)} = \frac{V_w}{S_w} \tag{4-2.2}$$

$$V_t = h_0 \cdot \pi \cdot \left(\frac{d}{2}\right)^2 \tag{4-2.3}$$

Where:

n = porosity, as a fraction [-]
V_v = volume of voids or pores [m^3]
V_t = total volume of the soil sample [m^3]
V_w = volume of water in pores [m^3]
m_{wet} = mass of the sample in *wet* condition [kg]
m_{dry} = mass of the sample in *dry* condition [kg]
ρ_w = density of pore water, assumed to be 1000 kg/m^3
S_w = initial degree of saturation of the sample, as a fraction [-]
h_0 = initial height of the sample [m]
d = diameter of the sample

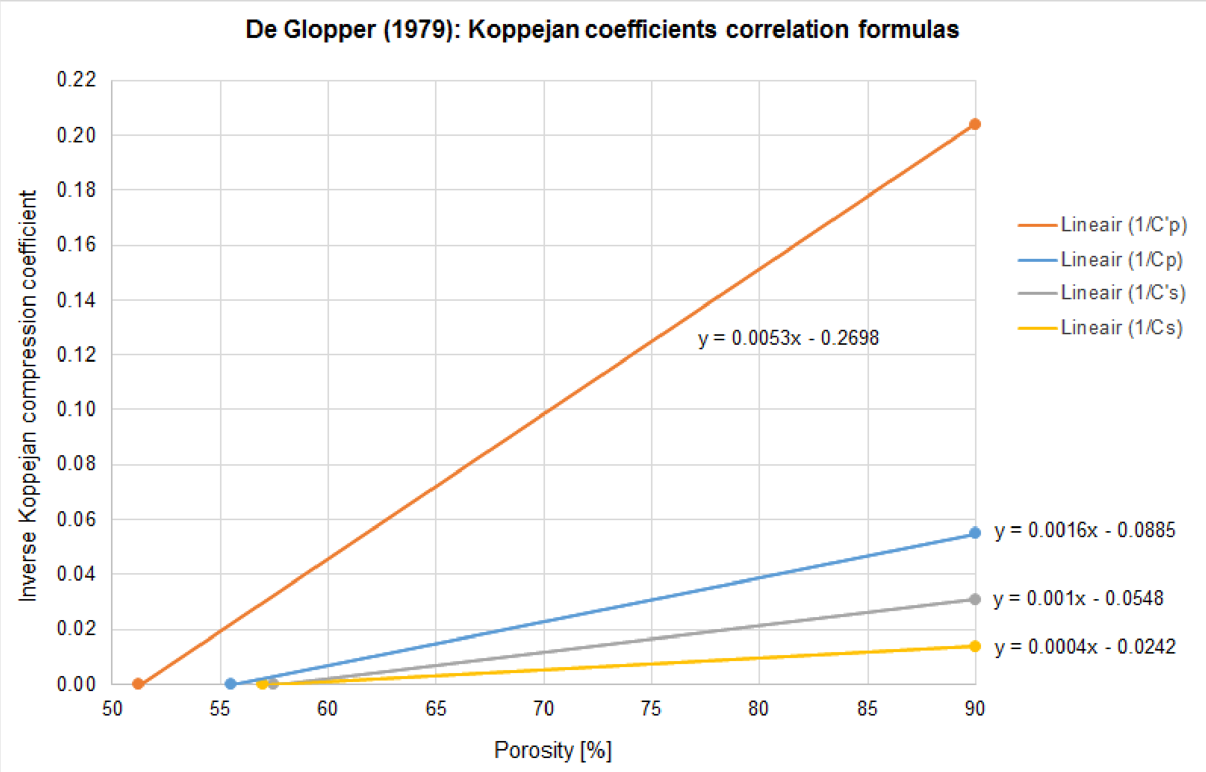

Figure 4-1: Formulas for the Koppejan coefficients by correlation with the porosity of peat, drawn and derived according to Figure 3-8 [De Glopper, 1979].

The above equations and soil properties provide all necessary input for using De Glopper's relationship in order to estimate the Koppejan compressibility coefficients. A fringe benefit is that the porosity is also needed for Fokkens' method, which will be regarded next. Note, however, that De Glopper's formulas require the porosity values to be percentages, whereas Fokkens' formulas require them to be fractions (< 1).

4.2.2.3 Fokkens

The Fokkens method comes in no less than six different versions (refer to section 3.2.5) that do not all require the same input parameters. In total 12 different quantities are required to know in order to use all six versions of the formula, namely: A_1 or w_0, γ_w, N, H, p_m, p_1, p_2, C_v ($<p_g$), C_v ($>p_g$), G, n_1 and Z or h_0.

One of the least complicated quantities seems to be the initial water content (A_1 or w_0), since it is usually provided in laboratory test reports. However it was found that the given values for water content in laboratory test reports deviate considerably from own verification calculations according to NEN 5112 (on the basis of saturated and dry soil unit weight), by up to 15%, despite the NEN 5112 being mentioned as reference in the reports. This caused some confusion and uncertainty, but finally it was argued that this might be due to the fact that the soil sample used for initial water content determination is probably taken from a slightly different part of the core than the actual oedometer test sample that should remain undisturbed. This may explain the observed difference and therefore it was decided to use the water contents that are given in the lab test reports without further hesitation.

The loss on ignition (*N*) could be found directly in the lab test reports, from which the organic matter content (*H*) can be calculated according to Skempton & Petley (1970):

$$H = 1 - 1.04 \cdot (1 - N) \tag{4-3}$$

The maximum, or preconsolidation pressure (p_m) is also given in the test reports, however this parameter has a catch in it because it depends on the depth that the sample originated from. Since Fokkens (1970) does not provide further detail on how to deal with this, it is assumed that the *average* preconsolidation pressure for the entire layer considered is appropriate.

The overburden stress (p_1) before loading was determined by estimating the effective overburden stress acting on top of the compressible soil layer(s), based on the wet and dry unit weights of the soil, according to equation (2-2). p_1 is easiest to estimate at the Bloemendalerpolder, since basically there is just one compressible soil layer (peat), covered by about 60 cm of unsaturated clayey topsoil that solely contributes to the initial effective overburden stress. p_1 at Amstelhoek is determined by the same principle, however there are more different soil layers in the subsurface, so their effective weights have to be estimated separately and then added together where relevant. Finally the overburden stress (p_2) *after* loading is simply the sum of p_1 and the load of the earth fill, the latter being sand with a unit weight that is commonly presumed to be 20 kN/m^3 (saturated) and 18 kN/m^3 (unsaturated).

Regarding the stress-related variables in Fokkens' formulas, it should be emphasised that Fokkens originally used units of gf/cm^2 in equations (3-13) and (3-14), whereas later adaptations defined stresses to be in units of kPa: 1 kPa = 10.1937 gf/cm^2 and 1 gf/cm^2 = 0.0981 kPa. It was experienced that forgetting this will yield nonsense results for equation (3-14).

Special attention should also be paid when using or deriving the value of C_v. First of all, recall that Fokkens' C_v has no relation with the coefficient of consolidation (c_v), but is defined as the inverse of the compression index: 1/C_c. Secondly, C_c will have a different value depending on the preconsolidation state of the soil and so whether Fokkens' formula (3-13) or (3-14) is used.

The only soil property that could not be determined directly from any of the available lab test reports, is the specific gravity of the dry solids (*G*) for use in the 'TAW' equation (3-15.1). For this, it was made use of previous pycnometer density measurements of the Bloemendalerpolder peat, performed and published by Papadaki (2013). The resulting average value for *G* is 1.50.

4.2.2.4 a,b,c parameters from correlations

As was already briefly mentioned in subsection 3.2.7.5, in the course of literature study also several correlations for the estimation of a,b,c parameters from soil physical or index properties were encountered. Based on the extensive set of laboratory test data and a,b,c parameters available for the Bloemendalerpolder, it was deemed of particular practical interest to assess the usefulness and validity of such empirical correlations by comparison with lab test results *and* by validation of subsequent settlement predictions with field measurements. The following correlations and approximations for *peat* have been found and used:

$$a = 0.0535 \cdot (\rho_{nat})^{-3.95} \tag{4-4}$$

[Den Haan & Molendijk, 2002]

$$a = \frac{b}{7} \tag{4-5}$$

[Deltares, 2014], rough estimate

$$b = 0.33 - 0.36 \cdot (\rho_{nat} - 1) \tag{4-6}$$

[Den Haan & Molendijk, 2002], for "Hollandveen" peat

$$b = 0.326 \cdot (\rho_{nat})^{-2.11} \tag{4-7}$$

[Den Haan et al., 2004; Den Haan & Kruse, 2007]

$$c = 0.029 - 0.05 \cdot (\rho_{nat} - 1) \tag{4-8}$$

[Den Haan & Molendijk, 2002], only for soil with $\gamma_{nat} < 1.5$

$$c = \frac{b}{12} \tag{4-9}$$

[Deltares, 2014], rough estimate

Where:
ρ_{nat} = bulk density of the soil in natural *wet* condition = γ_{nat} / 9.81 [t/m^3]

4.2.2.5 a,b,c and Bjerrum parameters from compression tests

Whereas in the cases of the Bloemendalerpolder and Amstelhoek the soil compressibility parameters were provided, in the case of Leendert de Boerspolder these parameters had to be determined by oneself, from raw data as outlined in subsection 4.2.2.1.

The methods for determining the compression parameters or coefficients of interest were in accordance with literature, such as in particular: Den Haan & Kamao (2003), Den Haan et al. (2001), Den Haan et al. (2004) and Deltares (2014). In general any of the compression coefficients is to be determined from the slope of a tangent line to a particular part of the stress-strain or time-strain curve, as shown in Appendices H2 and H3, namely:

- *a* and *RR* from the unload/reload part of the stress-strain curve;
- *b* and *CR* from the virgin compression part of the stress-strain curve;
- *c* and $C_{\alpha\varepsilon}$ from the tail of the time-strain curve during a constant load phase in the virgin range of stress (CRS tests require a different approach, as explained further below).

It might seem as if a,b,c and Bjerrum's coefficients are identical. However they are different, firstly due to the difference in use of natural strain (ε^H) versus linear strain (ε^C), and secondly due to the use of natural logarithms versus common logarithms:

$$a, b = \frac{\Delta \epsilon^H}{\Delta \ln \sigma'_v} = \frac{\epsilon_2^H - \epsilon_1^H}{\ln\left(\frac{\sigma'_{v2}}{\sigma'_{v1}}\right)} \tag{4-10.1}$$

$$c = \frac{\Delta \epsilon^H}{\Delta \ln t} = \frac{\epsilon_2^H - \epsilon_1^H}{\ln\left(\frac{t_2}{t_1}\right)} \tag{4-10.2}$$

$$RR, CR = \frac{\Delta \epsilon^C}{\Delta \log \sigma'_v} = \frac{\epsilon_2^C - \epsilon_1^C}{\log\left(\frac{\sigma'_{v2}}{\sigma'_{v1}}\right)} \tag{4-11.1}$$

$$C_{\alpha\epsilon} = \frac{\Delta \epsilon^C}{\Delta \log t} = \frac{\epsilon_2^C - \epsilon_1^C}{\log\left(\frac{t_2}{t_1}\right)} \tag{4-11.2}$$

Note, that merely the absolute vertical displacement, total vertical stress, pore pressure (only for CRS tests) and initial sample dimensions were contained in the raw data sheets, from which the useful quantities such as effective stress, linear strain and natural strain had to be calculated first. On the basis of those quantities compression curves are plotted as a function of effective stress as well as of time, which are indispensable in order to ascertain *visually* the exact points or sections of the curves where the tangents and slopes have to be determined (refer to Appendices H2 and H3). These points or sections are different for every single test. Some of these diagrams are also needed to determine graphically the preconsolidation pressure, which is further explained in subsection 4.2.2.7.

Recall from section 3.1.2 that during a **CRS** compression test it is not possible to maintain a constant load, so that the secondary, or creep compression coefficients cannot be determined from a time-strain curve as indicated above. However in the same section two alternative approaches are mentioned, of which the constant strain-relaxation method is used here because the CRS tests incorporated a phase of constant strain. Such a phase leads to a decrease of vertical effective stress, or relaxation, due to the viscous properties of the soil, which can be used to determine the creep parameter *c*. This method is proposed by Den Haan et al. (2001) and explained as follows.

From the literature review regarding the a,b,c-Isotachs model (section 3.2.7) it is known that the total strain rate is the sum of two components, namely the direct and the secular strain rates. In case the total strain remains constant, the sum of these two components must be zero. The strain rate components may be written as follows [Den Haan et al., 2001]:

$$\dot{\epsilon}_d^H = \frac{a\dot{\sigma}'_v}{\sigma'_v} \tag{4-12.1}$$

$$\dot{\epsilon}_s^H = \dot{\epsilon}_{sR}^H \left(\frac{\sigma'_v}{\sigma'_{vR}}\right)^{(b-a)/c} \tag{4-12.2}$$

Where the subscript addend *'R'* indicates the respective value at the *start* of relaxation. When the two components are added together, equated to zero and elaborated, according to Den Haan et al. (2001) one obtains:

$$\sigma'_v = \sigma'_{vR}\left(1 - \frac{(b-a)}{c}\ \frac{\dot{\sigma}'_{vR}}{\sigma'_{vR}}\ t\right)^{-c\,/(b-a)} \tag{4-13}$$

This formula can now be used directly to determine the value of *c* by manual curve fitting on the time-stress relaxation curve from the data (see for example Figure 4-2), since the values of the other variables are known or can be calculated otherwise. The initial stress rate ($\dot{\sigma}'_{vR}$) was found by means of the forward finite difference method over the first 180 seconds of every concerning relaxation phase.

Two final remarks have to be made concerning conventional (**IL**) oedometer tests. Firstly, note that for reliable parameter determination pore pressures should have dissipated completely at the end of every load step. In the case of the Leendert de Boerspolder's test data this condition was deemed to be satisfied by ensuring that the time-strain curve tails are linear, so that no direct/primary compression due to a change in effective stress is taking place.

Secondly, for correct determination of Bjerrum and a,b,c isotache parameters it is important that the duration of every load step is (close to) 24 hours, since the reference creep isotache is defined at 1 day. If this is not the case, both the creep and virgin compression coefficients have to be corrected by means of a time shift factor as described by Deltares (2014). The loading time durations for the IL tests conducted on material from the Leendert de Boerspolder were found to be sufficiently close to 24 h in order to neglect this correction.

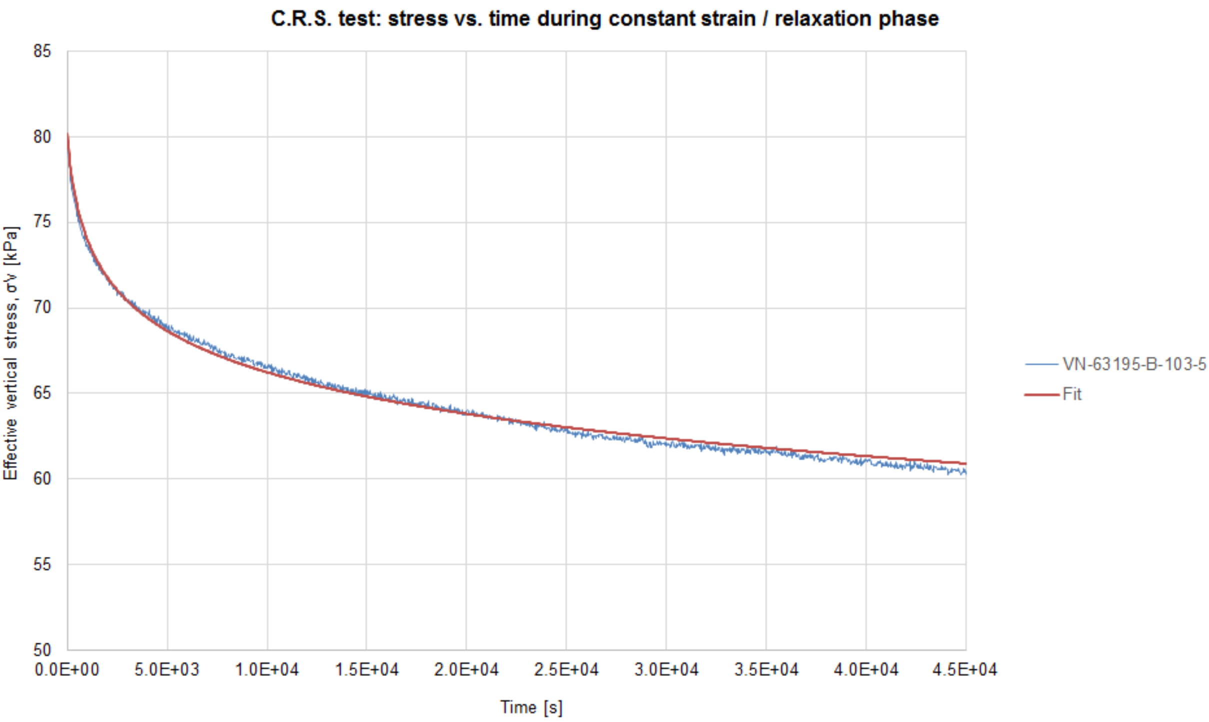

Figure 4-2: Example of a stress relaxation curve with manual curve fit according to equation (4-13) for determination of parameter *c*.

4.2.2.6 Koppejan coefficients from compression tests

The Koppejan compression coefficients can only be determined directly from conventional IL oedometer tests. Whereas the physical meaning of C_p and C'_p corresponds with reloading (*a*, *RR*) and virgin compression (*b*, *CR*), respectively, the Koppejan model has two different secondary compression coefficients: C_s and C'_s. Thus there is an additional secondary compression or creep coefficient in the Koppejan formula that is not present in the isotache models. However remember that the creep rate in the latter models is related to intrinsic time (refer back to subsection 3.2.7.2), which again can be related to preconsolidation pressure, therefore the isotache models theoretically still incorporate a preconsolidation state-dependent creep coefficient.

Recall from equation (3-6) that secondary compression in the Koppejan formula depends on time *and* stress. As a result, the observed total strain is made up of a primary and secondary component that both depend in part on the same quantity and that need to be disentangled when trying to determine the respective compression coefficients. This can be done as described below according to Deltares (2014), starting with a slightly adapted version of equation (3-6) regarding exclusively the particular load step (*n*) that is regarded for parameter determination. Hence the Koppejan formula becomes as follows:

$$\epsilon^* = \left(\frac{1}{C_p} + \frac{1}{C_s} \cdot \log t^*\right) \cdot \ln\left(\frac{\sigma'_n}{\sigma'_{n-1}}\right) \qquad (4\text{-}14)$$

Where:
ε^* = strain during the regarded load step = $\varepsilon(t) - \varepsilon(t_n)$ [kPa]
t_n = time at the start of the regarded load step [s]
t^* = time during the regarded load step = $t - t_n$ [s]
σ'_n = total stress applied during the regarded load step [kPa]
σ'_{n-1} = total stress applied during the preceding load step [kPa]

In order to find the value of both compression coefficients, either below or above the preconsolidation pressure, it is necessary to determine the secondary compression coefficient first, from the slope of the tail of the time-strain curve. Note that this is only allowed when pore pressures have dissipated completely and thus consolidation and primary compression have finished, so that the primary compression component may be neglected. Hence the secondary compression coefficient can be determined by means of the following formula, derived from equation (4-14):

$$C_s = \frac{\Delta \log t^*}{\Delta \epsilon^*} \cdot \ln\left(\frac{\sigma'_n}{\sigma'_{n-1}}\right) \tag{4-15}$$

After that the (inverse of) the primary compression coefficient can be determined from the slope of the stress-strain curve, and by subtraction of the contribution of secondary compression:

$$\frac{1}{C_p} = \frac{\Delta \epsilon^*}{\ln\left(\frac{\sigma'_n}{\sigma'_{n-1}}\right)} - \frac{1}{C_s} \log t^* \tag{4-16}$$

Based on visual assessment of the (quality of) the incremental loading test results as well as of the shape of the resulting stress-strain curves, it was deemed most appropriate to determine C_p and C_s (< p_g) from the second loading stage (≈ 4.5 kPa), and C'_p and C'_s (> p_g) from the seventh loading stage (≈ 75 kPa) for every test.

4.2.2.7 Coefficients of consolidation and hydraulic conductivity

In order to perform accurate settlement predictions especially on the short term, it is required to know the consolidation characteristics of the soil layer(s). These characteristics are described by means of the coefficient of consolidation (c_v [m^2/s]), hydraulic conductivity (*K or k* [m/s]) or intrinsic permeability (κ [m^2]). These can all be obtained from soil compression tests, regardless of the kind of test – just the method of determination will be different.

In section 2.2.2.2 already two different methods for determining c_v and k_v were described: Casagrande and Taylor. However these methods were and *can be* applied only for dissipation phases due to discrete load increments, i.e. for conventional IL oedometer tests. Thus for all CRS tests that were conducted on soil samples from the Leendert de Boerspolder a different method has to be used. Note that in the other investigated cases, the geotechnical lab test reports already listed the consolidation and hydraulic characteristics of the tested soil samples.

As experienced already before, NEN was found to fall short again in that it does not provide *any* information regarding the execution and interpretation of CRS compression tests. Therefore at first instance ASTM was consulted, which indeed provides a guideline for the CRS test procedure along with instructions for determining c_v [ASTM D4186]:

$$c_v = -\frac{H^2 \log\left(\frac{\sigma_{v2}}{\sigma_{v1}}\right)}{2\Delta t \log\left(1 - \frac{u_b}{\sigma_v}\right)} \tag{4-17}$$

Subsequently the vertical hydraulic conductivity could be calculated from c_v and m_v by means of equation (2-10), or preferably more directly as follows [Bartlett, 2005]:

$$k_v = \frac{0.434 r H^2 \gamma_w}{2\sigma'_v \log\left(\frac{\sigma_v - u_b}{\sigma_v}\right)} \tag{4-18}$$

Where:
k_v = vertical hydraulic conductivity [m/s]
H = average soil sample height during the regarded time period Δt [m]
σ_{v2} = total vertical stress at time t_2 [kPa]
σ_{v1} = total vertical stress at time t_1 [kPa]
Δt = regarded (short) time period = $t_2 - t_1$ [s]
u_b = average excess pore pressure over Δt at the bottom of the sample [kPa]
σ_v = average total vertical stress over Δt [kPa]
σ'_v = average effective vertical stress over Δt [kPa]
r = constant rate of strain = $d\varepsilon / dt$ [s^{-1}]
γ_w = unit weight of water ≈ 9.81 kN/m^3

However after applying these equations to the data, values of c_v were obtained in the order of 10^{-10} m^2/s and values of k_v in the order of 10^{-12} m/s, which both seemed much too low by at least two orders of magnitude, knowing that the soil samples consisted of peat. It was and still is not completely clear why these particularly low values were found. However further study of ASTM D4186 and Bartlett (2005) revealed that these equations are only valid provided some specific conditions, including steady state. A certain data reduction method is suggested in these publications to assess whether this condition holds, but this appeared to be needlessly complicated just to confirm that the obtained results are incorrect. So instead it was decided to rather use another set of equations that was found in literature, namely:

$$c_v = \frac{H_1 H_2 \, \Delta\sigma_v}{2 \, u_b \, \Delta t} \tag{4-19}$$

[Adams, 2011; Gorman et al., 1977]

$$k_v = \frac{\dot{\epsilon}}{(1-\epsilon)} \frac{\gamma_w}{2 \, u_b} H^2 = \frac{\mathrm{d}z}{\mathrm{d}t} \frac{\gamma_w}{2 \, u_b} H \tag{4-20}$$

[Adams, 2011; Den Haan, 2001]

Where several variables were already defined previously, except:
H_1 = soil sample height at time t_1 [m]
H_2 = soil sample height at time t_2 [m]
$\Delta\sigma_v$ = change in total vertical stress over the regarded time period Δt [kPa]
$\dot{\epsilon}$ = linear strain rate = $d\varepsilon/dt$ [s^{-1}]
dz/dt = rate of vertical deformation [m/s]

These equations (4-19) and (4-20) were found to yield much more realistic results, within the same order of magnitude as found by professional laboratories, and were deemed to suffice.

4.2.2.8 Preconsolidation pressure, OCR and POP

As already described in subsection 2.2.2.1, for determination of the preconsolidation pressure the graphical method of Casagrande is most common and recommended [NEN 5118]. Therefore Casagrande's method was applied to the Leendert de Boerspolder data as well. However this method requires the void ratio to be known as a function of stress, or at least the *initial* void ratio, which was not available for CRS tests. Moreover, it was experienced that Casagrande's method is by no means very exact and, in fact, can be quite ambiguous and imprecise for compression curves that are very gradual, i.e. having no distinctive bending point. The latter was especially often the case for the CRS compression curves: view Figure 4-3 below, for example.

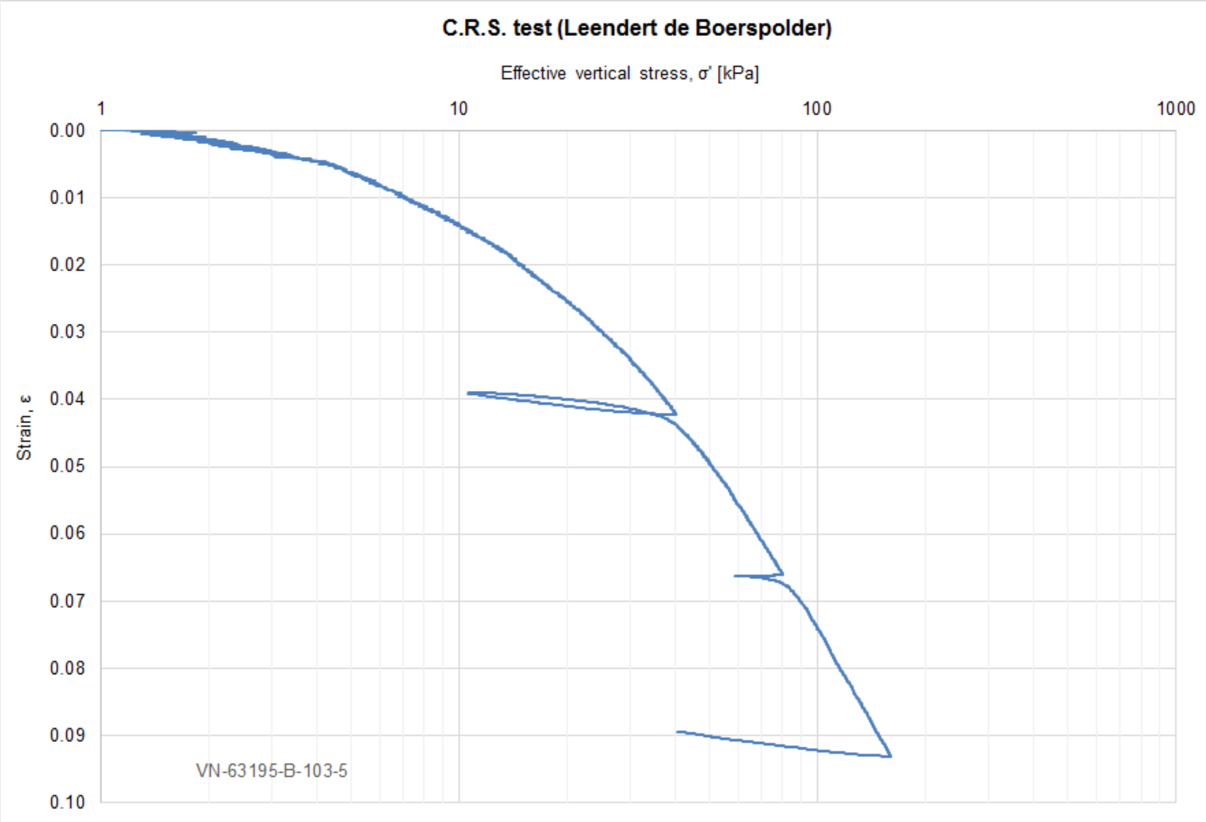

Figure 4-3: A gradual compression curve with an indistinct bending point, being illustrative for the difficulty experienced in trying to determine objectively and reliably the preconsolidation stress with Casagrande's method.

For these reasons, it was searched for alternative methods, several of which were helpfully suggested by E. Ponzoni and D.J.M. Ngan-Tillard [pers. comm.]. Based on a subsequent literature review regarding preconsolidation pressure determination methods, it was decided to try three of those, partly additional to Casagrande's method for IL oedometer tests, and to mutually compare the results. The alternative methods are described below.

The first alternative method considered has been presented by **Butterfield** (1979). He proposed to determine the preconsolidation pressure from a compression diagram in which the vertical axis represents the natural logarithm of the specific volume ($v = 1 + e$), instead of the void ratio (e) as according to Casagrande. The scale and quantity along the horizontal axis is left unchanged, representing the logarithm of effective stress. Butterfield suggested that this representation could improve the linearity of compression curves and thus could make determination of the preconsolidation pressure easier and less ambiguous, which he verified with some experimental data sets. Whereas back in 1979 this concept was still something new, at latest since the work of Den Haan (1994) it has become widely known that the natural logarithm of specific volume is equivalent with natural strain (refer to subsection 3.2.7.1).

The point at which exactly the preconsolidation stress is to be determined, is not explicitly indicated by Butterfield. However from his diagrams (view Figure 4-4 for example) it could be inferred that this has to be simply at the intersection point of the tangent lines along the beginning and along the end of the stress-compression curve, in contrast to Casagrande's more complicated bisector method. So just being simpler than Casagrande's method might already be regarded as an advantage of Butterfield's method.

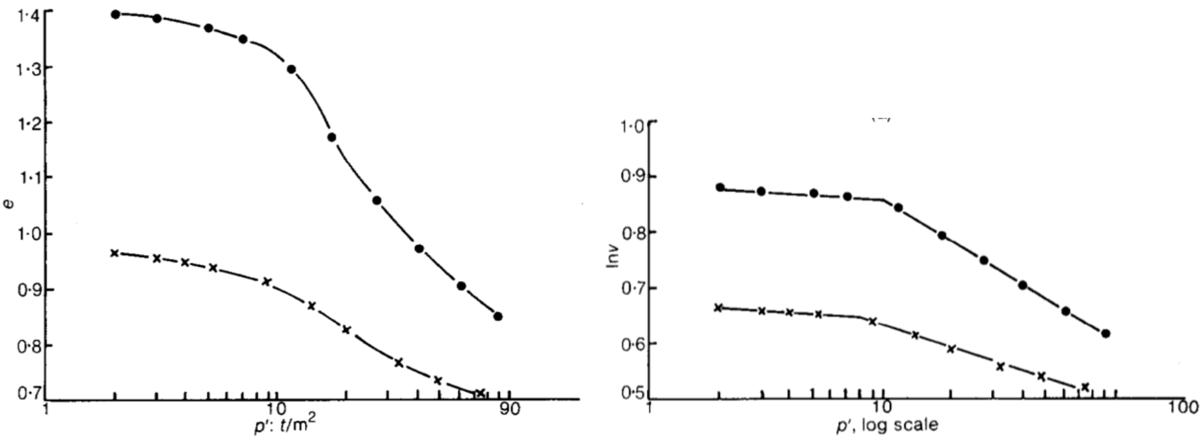

Figure 4-4: Set of graphs illustrating the improvement of compression curve linearity by plotting the natural logarithm of specific volume along the vertical axis (right), instead of the traditional void ratio (left). Both diagrams show compression curves of the same two Drammen clay soil samples, respectively [Butterfield, 1979: Fig. 4], on the basis of compression test data originally obtained by Bjerrum (1967).

The second alternative method considered has been developed by **Becker et al.** (1987). They proposed to use the work per unit volume as a criterion for determining the preconsolidation pressure, or *yield stress* as they call it. Therefore in this thesis this method will be referred to as the "**work method**". The incremental work per unit volume may be calculated as follows [Becker et al., 1987]:

$$\Delta W = \left(\frac{\sigma'_i + \sigma'_{i+1}}{2}\right)(\epsilon_{i+1} - \epsilon_i) \tag{4-21}$$

Where:
ΔW = incremental work per unit volume [kJ/m^3]
σ'_i = effective stress at the start of the load increment or measurement interval [kPa]
σ'_{i+1} = effective stress at the end of the load increment or measurement interval [kPa]
ε_{i+1} = *natural* strain at the end of the load increment or measurement interval [kPa]
ε_i = *natural* strain at the start of the load increment or measurement interval [kPa]

The diagrammatic representation (Figure 4-5) requires the use of the *cumulative* work per unit volume along the vertical axis, i.e. the sum of all preceding incremental work quantities. At the same time the horizontal axis must represent the effective stress on a *linear* scale. Subsequently the preconsolidation stress is to be determined at the intersection point of the tangent lines along the beginning and along the end of the stress-work curve.

A number of such graphs, based on various soil compression test data, were presented in their article. From this, the work method appears very promising at first glance. Only towards low stress levels the linearity sometimes seems to be less pronounced – which unfortunately is the main snag of this method. Their compression tests were namely performed on (firm) clays at stresses ranging from 0 to over 2 *Mega*pascal. So, when considering that the stress ranges of interest for most (earthen) structures on soft soils in the Netherlands hardly ever exceed 200 kPa, it remains doubtful whether Becker et al.'s work method indeed can give better approximations of the preconsolidation pressure.

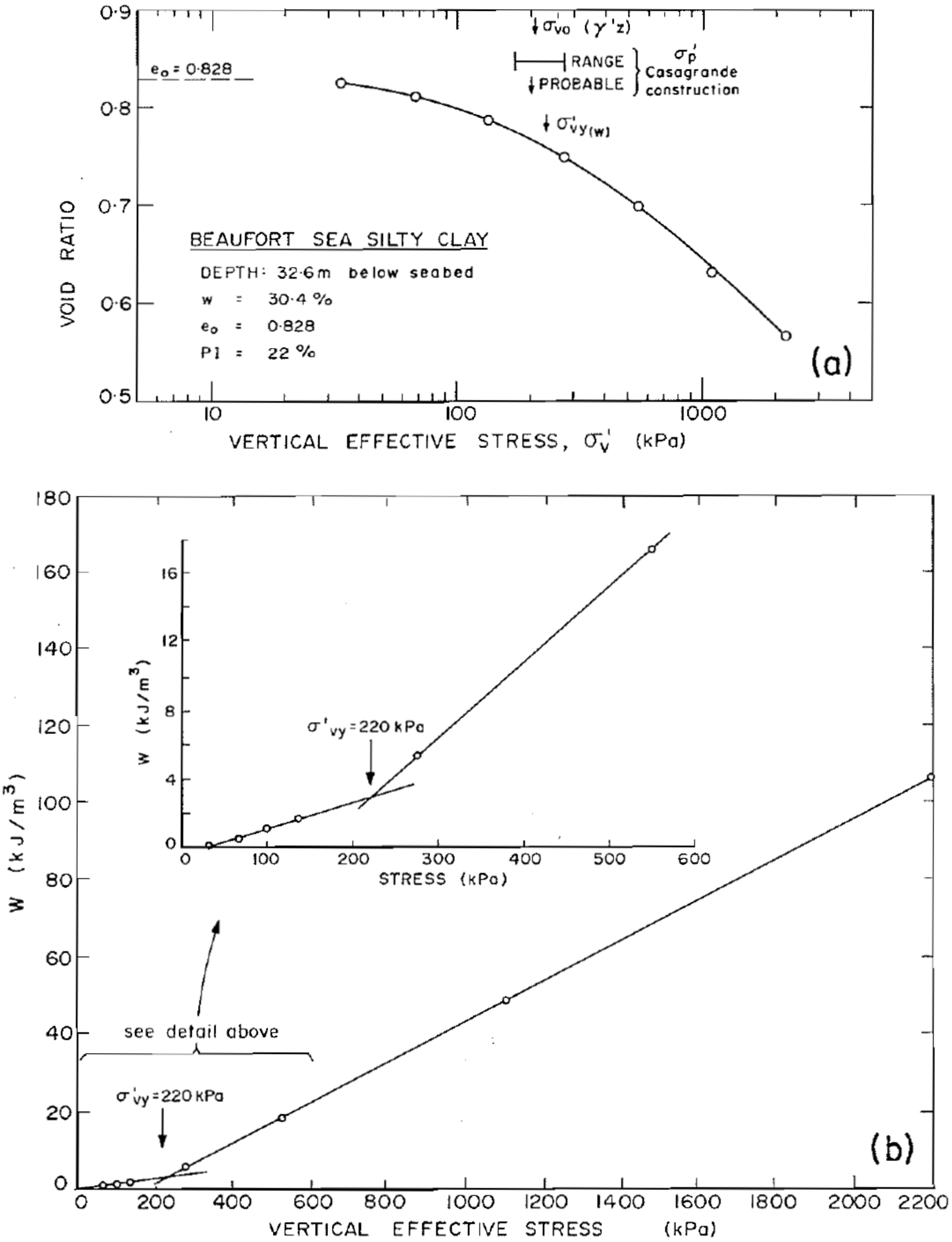

Figure 4-5: Set of graphs illustrating the differences between two representations for determining the preconsolidation pressure, on the basis of compression tests on firm Beaufort Sea clay, where:
a) shows a traditional compression curve representing void ratio vs. the logarithm of stress, as required for the application of Casagrande's method, and
b) shows a plot of the cumulative work per unit volume vs. stress, based on the same dataset as diagram (a), for application of the "work method".
[Becker et al., 1987: Fig. 2].

The third alternative method considered is based on the excess pore water pressure, which in this thesis will be referred to as the "**pore pressure method**". Although this method could not be attributed to a specific (group of) researcher(s), it was found to be applied and graphically explained well by Premchitt et al. (1995), but it certainly was first proposed well before that time.

The principle of the pore pressure method is simple: instead of the void ratio or another measure of compression, the excess pore pressure is plotted along the vertical axis, whilst the horizontal axis remains the common logarithm of effective stress. Pore pressures are reportedly found to stay at a low level and to increase only very slowly, or to not increase at all, until the preconsolidation stress is reached; after this stress level the pore pressure starts increasing considerably in an approximately log-linear fashion. Hence the preconsolidation pressure is to be found at the kink in the pore pressure curve, even if the void ratio compression curve does not exhibit such a distinct kink.

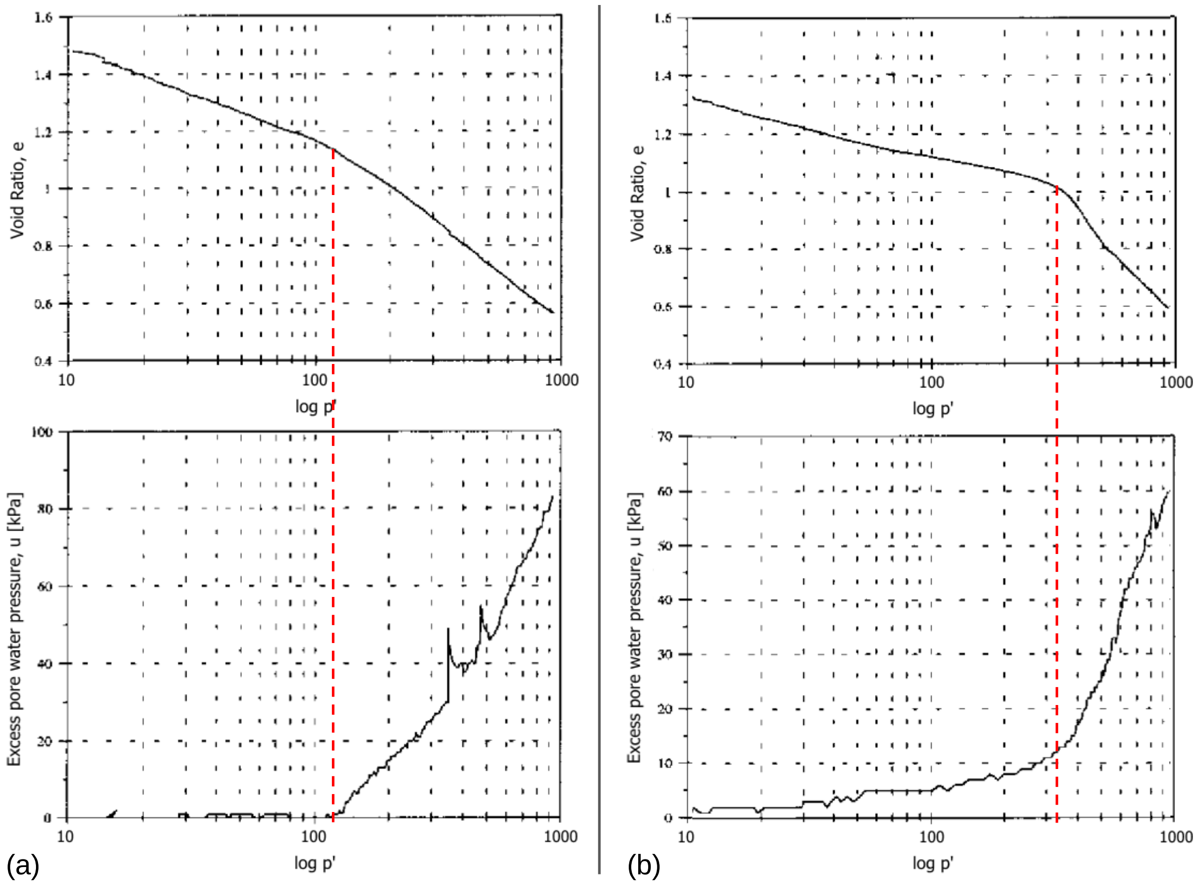

Figure 4-6: Set of CRS test graphs of two different samples, (a) and (b), for each of which the top graph presents the traditional void ratio curve vs. the logarithm of effective stress, and the bottom graph presents the excess pore pressure curve, respectively. The red dashed vertical lines indicate the preconsolidation stress that follows from the excess pore pressure curves. The diagrams are adapted from [Premchitt et al., 1995: pp. 78-79].

Once the preconsolidation pressure for a particular soil sample is known, after applying either one of the aforementioned methods, finally the overconsolidation ratio (OCR) and the pre-overburden pressure (POP) at that particular depth can be calculated. This is done by means of formulas (2-5) and (2-6) that were presented in subsection 2.2.2.1, on the basis of the (estimated) in situ stress.

4.2.3 Subsurface schematisation

After determination of all the required parameters for use in the settlement prediction models or formulas of choice, a subsurface schematisation has to be made for every case considered. For this, a combination of mainly bore logs and CPT diagrams is used. CPT data fortunately were already interpreted automatically. Otherwise, this could have been done manually in accordance with the widely known graphical method after Robertson [Robertson & Cabal, 2015], based on the cone resistance, sleeve friction and friction ratio, as shown in Figure 4-7 for reference.

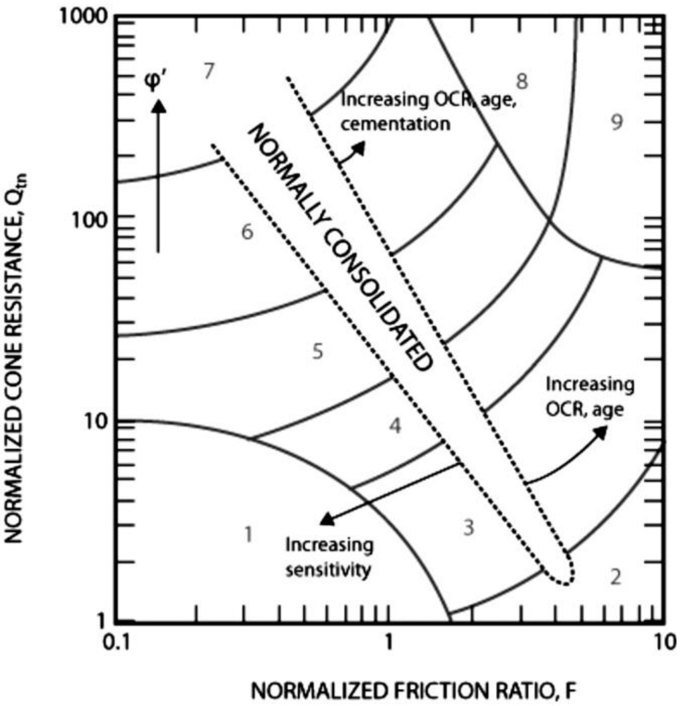

Figure 4-7: CPT Soil Behaviour Type chart [Robertson & Cabal, 2015: Fig. 23]. Quantities along the axes are *normalized*, i.e. corrected for depth or overburden pressure as well as for so-called "unequal end area" pore pressure effects. Since this chart is not used in the current research and shown just for reference, it is deemed irrelevant to explain its use here in full detail; instead, one is kindly referred to Robertson & Cabal (2015).

Sometimes it can – and did – happen that there are discrepancies between CPT data and bore logs, so that it might not always be straightforward to interpret ground investigation data. In such cases first it was tried to take an educated *average* between the different data sources, whereas for larger discrepancies (>25 cm of another soil type or difference in layer boundary depth) it was given more trust to bore logs (e.g. in the case of Bloemendalerpolder, where some CPT results inexplicably indicated a layer of silty clay between 1 and 2 m depth). Still this choice may remain a valid point of discussion, though.

However there is a certain limit to the value and usefulness of high precision of subsurface schematisation, specifically with regard to time-efficiency versus resulting gain of accuracy. This is particularly relevant for the manual settlement prediction calculations (Fokkens), where distinguishing many soil layers would increase complexity at lot whilst the formula itself can yield merely a rough estimation at best. Nevertheless, for the computer-modelled geometries, especially in the case of Amstelhoek, the subsurface was schematised with as much detail as reasonably possible. Below a written summary of the schematisations for every case is provided. In all cases the applied load is to be considered separately in addition.

- The stratigraphy at the Bloemendalerpolder is the simplest of all cases investigated, since it consists of just one massive peat layer on Pleistocene sand, increasing in thickness towards East, plus 40 cm of unsaturated organic clay topsoil above the phreatic level. Only trial mound No. 1 was modelled in *D-Settlement*. The Fokkens formulas were applied to the same vertical stratigraphy as well, moreover for both trial mound No. 1 and No. 2.
- In the case of Amstelhoek, in contrast, generally five soil layers are distinguished, namely two different layers of peat, organic clay and/or silty clay, as well as Pleistocene sand and 60 cm of clayey topsoil above the phreatic level. As indicated at the beginning of chapter 4.1, two locations were modelled, namely: 1300 m and 2000 m, which have different thicknesses and distribution of soil layers in the subsurface. This, however, altogether was deemed to become too complicated for manual calculation with Fokkens' method, in which case all middle clay layers were considered as a single layer and furthermore just one location

(2000 m) was analysed. The latter was chosen in order to assess the performance of Fokkens' formulas with regard to more clayey soil types.

- The Leendert de Boerspolder at last was schematised with four soil layers in total, namely from bottom to top: Pleistocene sand, silty organic clay, peat and slightly sandy organic clay as topsoil. Layer thicknesses can be derived from the geometries, as referred to right below.

The subsurface geometries in *D-Settlement* were designed as two-dimensional cross sections for every case, which are all included in Appendix J. Recall from subsection 3.3.3.2 that this does not mean that multi-dimensional deformations are taken into account, however.

Regarding Fokkens' method, no real "geometry" was used other than cells in a spreadsheet, representing the different soil layers as in a vertical borehole profile, which were arithmetically added together to obtain the total final settlement estimation. The respective layer thicknesses used for calculations according to Fokkens' method can be derived from the tables in Appendix I.

The next step is the attribution of representative soil physical and compressibility properties to every identified soil layer. For this, the interpreted test results were averaged per soil layer. On this occasion it is deemed important to note that soil layers were distinguished with regard to their soil classification *and* depth, because the same soil type is likely to have different compressibility characteristics at different depths. For example, peat is often encountered in the vertical soil profile more than once, e.g. the deep "basisveen" and the shallower "Hollandveen", separated by some other soil type. However the properties of these peats are likely to differ significantly from each other due to their difference in age and preconsolidation. Therefore it should be and was ascertained that never properties of two very different soil layers are combined or averaged.

A final remark concerns the parameter selection for use in the settlement predictions of the Leendert de Boerspolder. Compressibility parameters obtained from tests on samples taken from below the dike itself ought to be disregarded. This is because these soil layers have been compressed already and therefore will exhibit different behaviour than when in their original state. Unfortunately after complete lab test data analysis and interpretation this turned out to be the case for *all* IL oedometer test results (borehole B1002): these were taken from below the slope of the dike – although the map provided in the summary report [Jommi et al., 2015] indicates otherwise (refer to Appendix E2 Figure E-5). Moreover, these tests were conducted exclusively on peat and therefore could not provide sufficient data for all soil layers anyway. For these reasons, the IL test results were disregarded for use in the settlement predictions.

4.2.4 Settlement predictions

The computer-technical tools that were used for the actual settlement predictions comprise:

- Deltares D-Settlement 15.1 (2015): for predictions by means of the Koppejan, Bjerrum or a,b,c-Isotachs model;
- Microsoft Office Excel 2013: for predictions by means of Fokkens' method, as well as for all other data analysis, processing, calculations and graphing tasks.

D-Settlement, formerly named *MSettle*, is a relatively easy to learn and easy to use geotechnical computer programme aimed specifically at settlement prediction, offering "*accurate and robust models, capturing consolidation, creep, submerging, drains, staged loading, and unloading and reloading*" [Deltares, 2014]. This software is very commonly used by engineering consultancy companies in the Netherlands.

When regarding specifically the Leendert de Boerspolder case, two essentially different approaches of settlement prediction were followed. In the first approach, settlement predictions were performed by modelling the dike as a load with a thickness equal to the current dike height *relative to* the polder ground surface level, and making use of the "maintain profile" function in *D-Settlement*. This function maintains the load's desired top surface level with respect to zero (NAP) level and thus will incrementally add load to the geometry, in order to compensate for or equilibrate the settlement until the set end time. The calculated settlement of the dike consequently ought to closely approximate the settled bottom profile of the dike body in reality (≈ 1.6 m below ground level; refer to section 4.2.5) – provided that the used soil parameters were representative and the settlement prediction model is accurate. This is the way in which an initial settlement prediction would be performed when a certain final surface level of a fill is desired, so that the calculated settlement will provide an indication of the required surplus height.

In the second approach, the current *total* dike fill thickness was estimated from the CPT and borehole data (≈ 2.9 m; refer to section 4.2.5) and modelled as such in *D-Settlement*, this time without the "maintain profile" function. This approach should result in a final settlement such that the crest of the modelled dike corresponds with the currently observed dike crest level (≈ -0.4 m NAP) [Jommi et al., 2015] – again provided that the soil parameters were representative and the prediction model is accurate, which is the actual point of investigation.

The total settlement time period considered in *D-Settlement* was always in accordance with the original prediction for the case being regarded respectively: for the Bloemendalerpolder and Amstelhoek, this is 10,000 days, i.e. about 27.4 years. Only the Leendert de Boerspolder dike was modelled considering a time period from mid-17th century until present, i.e. 365 years, or roughly 133,000 days. In fact, the latter case comprised more a settlement *reconstruction* than a settlement *prediction*, which only is beneficial for the accuracy of the model validation, though.

The relationship of De Glopper was used to obtain alternatively the Koppejan compression coefficients, subsequently to be modelled in *D-Settlement* using the Koppejan model. The latter has been evaluated in linear strain as well as in natural strain mode.

Similar is the case for a,b,c parameters obtained by means of correlations: these parameters were, after soil layer-specific averaging, also used in a regular manner in *D-Settlement*. All settlement predictions in *D-Settlement* were done with the "submerging" function enabled, i.e. taking into account the effective stress reduction due to settlement below the phreatic water table.

The method of Fokkens finally was followed by first determining or calculating the 12 required soil parameters from the available data, which were then substituted into each of the six formulas presented in section 3.2.5 to obtain the according final settlement estimations. In case the subsurface consisted of more than one layer, the soil parameters were determined for every layer separately. In the latter case the total final settlement estimation is found by summation of the individual contributions of all layers.

4.2.5 Results analysis and model validation

Any compression parameters that were obtained by means of correlations, namely a,b,c parameters and also Koppejan coefficients by De Glopper's method, will be directly compared with the laboratory values for the same samples or soil types. Since it is acknowledged that laboratory values are not necessarily correct, the correlation-obtained parameters are subsequently used in settlement predictions as well, which are validated with actual field measurements as described below.

The validation of settlement predictions (including Fokkens) is done with respect to the final settlement estimation from *optimized* (curve-fitted) settlement predictions, based mostly on settlement beacon field measurements, as are available in the case of Bloemendalerpolder and Amstelhoek. Such settlement curve fits were already provided in geotechnical reports. Note, that it is not intended to perform extensive settlement curve fitting oneself, since solely the accuracy or reliability of *initial* settlement predictions, based on *initially* available soil properties, is to be evaluated.

For the Bloemendalerpolder, the best-fit final settlement of trial mound No. 1 is 1.60 m, and of mound No. 2 it is 2.40 m [Ammerlaan & Hoefsloot, 2012]. For Amstelhoek, the best-fit final settlement at location 1300 m is 0.96 m, and at location 2000 m it is 0.65 m [Sipkema, 2012].

In the case of the Leendert de Boerspolder, the final settlement was obtained from recent CPT profiles as shown for example in Appendix E3 [Jommi et al., 2015]. From these it followed that the final settlement of the dike in area B with respect to the adjacent polder ground level, is on average 1.6 m. The total thickness of the dike below its crest, which value was needed for predictions without the "maintain profile" function, could also be estimated from these CPT profiles and amounts to about 2.9 m.

Furthermore, the soil parameters obtained from compression tests will be reviewed critically with regard to their quality and usability for settlement predictions. Also any particular experiences or findings concerning the practical usability and applicability of the considered settlement prediction models will be discussed.

4.3 Results

This chapter presents all relevant results of the parameter determination and settlement predictions. Any particular observations and findings following from this, as well as critical review, are presented in the next chapter: Analysis and discussion of results. In order to keep the main report readable, the following sections will only briefly present final results in the form of tables or graphs, whereas all intermediate results are contained in Appendices G-J.

Appendix G contains the essential data that were *provided* in geotechnical laboratory test reports and used in calculations and validations in the course of this research. Appendix H contains all soil parameters that were *personally* determined from the raw test data of the Leendert de Boerspolder case, including in particular numerous diagrams used for this purpose. Finally Appendices I and J contain the relevant input and output of the settlement predictions, including the *D-Settlement* geometries and resulting settlement curves.

4.3.1 Soil parameter determination and validation

4.3.1.1 De Glopper: Koppejan coefficients

Table 4-2: Comparison of Koppejan coefficients for the case Bloemendalerpolder: laboratory values vs. De Glopper values (based on porosity), including relative errors with respect to lab values. Error values exceeding ±15% are highlighted in orange. 'T1' and 'T2' indicate trial mound No. 1 and No. 2, respectively.

Bloemendalerpolder	T1	T2	Average
Porosity [%]	87.5	92.2	89.8
Cp (lab)	10.9	8.7	9.8
Cp (De Glopper)	19.4	16.9	18.2
Relative error [%]	78.3	94.8	85.6
Cs (lab)	74.6	62.4	68.5
Cs (De Glopper)	92.7	78.9	85.8
Relative error [%]	24.3	26.5	25.3
C'p (lab)	4.9	5.3	5.1
C'p (De Glopper)	5.2	4.6	4.9
Relative error [%]	5.3	-13.8	-4.6
C's (lab)	45.6	22.8	34.2
C's (De Glopper)	30.6	26.7	28.7
Relative error [%]	-32.8	17.5	-16.0

Table 4-3: Comparison of Koppejan coefficients for the case Amstelhoek: laboratory values vs. De Glopper values, including relative errors with respect to lab values. Error values exceeding ±15% are coloured orange.

Amstelhoek	Clay top	Clay, organic	Peat, clayey	Peat, Hollandveen	Peat, basisveen
Porosity [%]	71.9	63.6	90.1	88.7	86.6
Cp (lab)	42.3	40.8	15.3	21.1	32.2
Cp (De Glopper)	37.7	75.6	17.9	18.7	20.0
Relative error [%]	-10.8	85.4	17.3	-11.4	-37.9
Cs (lab)	215.5	205.2	66.4	83.2	190.9
Cs (De Glopper)	219.4	812.6	84.4	88.6	95.9
Relative error [%]	1.9	296.0	27.1	6.6	-49.7
C'p (lab)	11.8	12.6	7.3	7.1	8.7
C'p (De Glopper)	9.0	14.9	4.8	5.0	5.3
Relative error [%]	-23.8	18.7	-34.1	-29.4	-39.4
C's (lab)	88.0	79.8	41.9	64.6	31.7
C's (De Glopper)	58.5	113.9	28.3	29.5	31.5
Relative error [%]	-33.5	42.8	-32.4	-54.3	-0.7

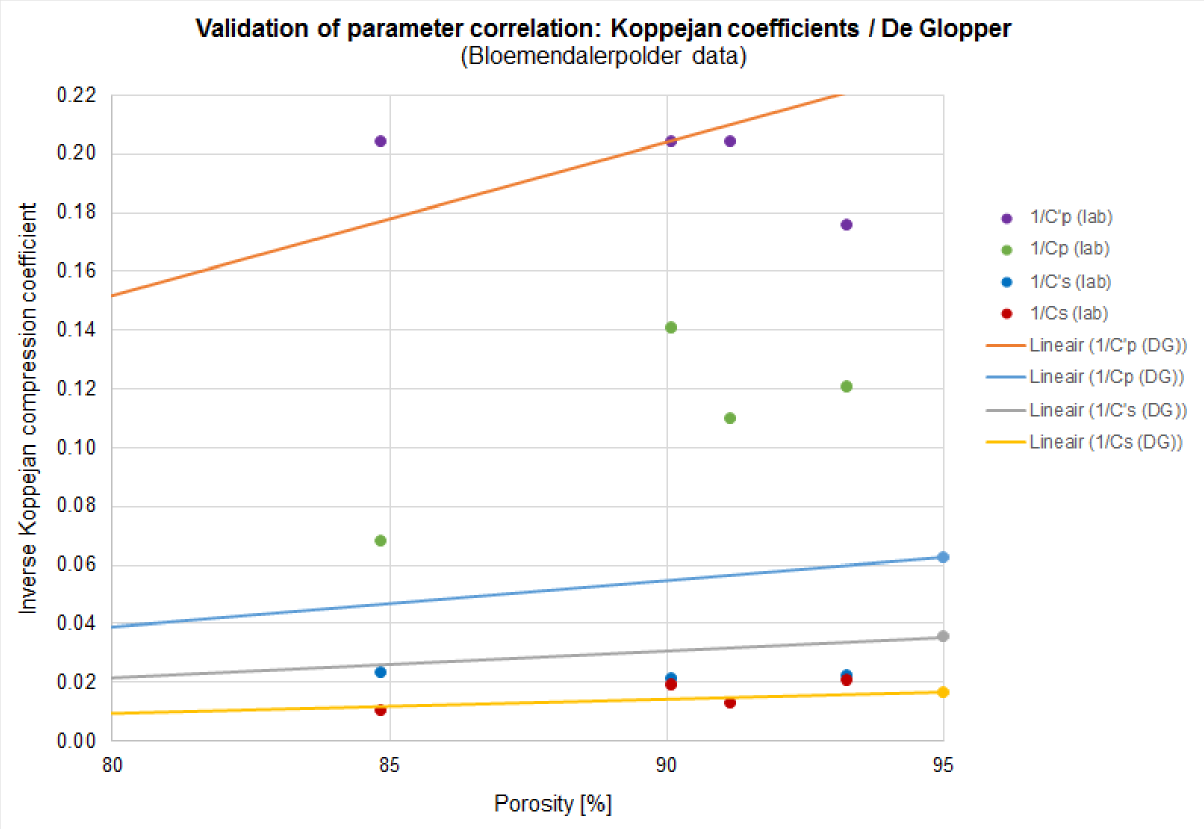

Figure 4-8: Graphical comparison of De Glopper's porosity-compressibility relationship (straight lines) and the respective actual laboratory values (dots) for the case Bloemendalerpolder (peat).

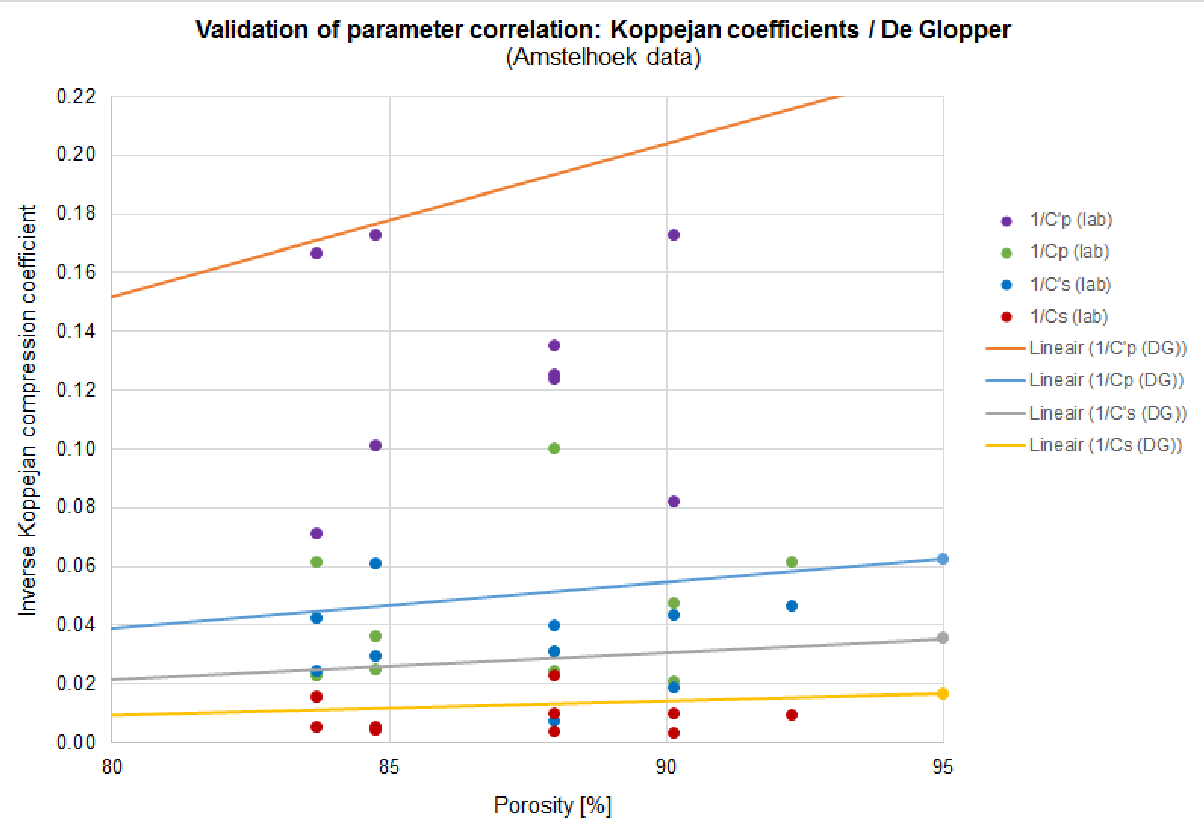

Figure 4-9: Graphical comparison of De Glopper's porosity-compressibility relationship (straight lines) and the respective actual laboratory values (dots) for the case Amstelhoek (peat and clay).

4.3.1.2 a,b,c parameters from correlations

Preliminary information concerning subsequent tables and graphs:

- a1: Determined by means of equation (4-4)
- a2: Determined by means of equation (4-5)
- b1: Determined by means of equation (4-6)
- b2: Determined by means of equation (4-7)
- c1: Determined by means of equation (4-8)
- c2: Determined by means of equation (4-9)

Note again, as mentioned already in subsection 4.2.2.4, that the a,b,c parameter correlations were only tested on Bloemendalerpolder data because their validity is limited to peat.

Table 4-4: Comparison of a,b,c parameters for the case Bloemendalerpolder: laboratory values vs. correlation-obtained values, including relative errors ('R.E.') with respect to lab values. Error values exceeding ±15% are highlighted in orange.

	B30 (2012) average	R.E. [%]	BT samples average	R.E. [%]	BT'*L*' samples average	R.E. [%]	Overall average	Overall R.E. [%]
	(K_0-CRS)		(K_0-CRS)		(IL)			
a (lab)	0.0330		0.0365		0.0455		0.0383	
a1	0.0502	52.3	0.0514	40.8	0.0597	31.1	0.0538	40.3
a2	0.0486	47.2	0.0459	25.8	0.0480	5.5	0.0475	24.2
b (lab)	0.3400		0.3215		0.3360		0.3325	
b1	0.3212	-5.5	0.3261	1.4	0.3395	1.1	0.3289	-0.7
b2	0.3132	-7.9	0.3189	-0.8	0.3453	2.8	0.3258	-1.8
c (lab)	0.0263		0.0256		0.0152		0.0223	
c1	0.0278	5.8	0.0285	11.3	0.0306	101.8	0.0289	26.7
c2	0.0283	7.9	0.0268	4.8	0.0280	84.8	0.0277	21.0

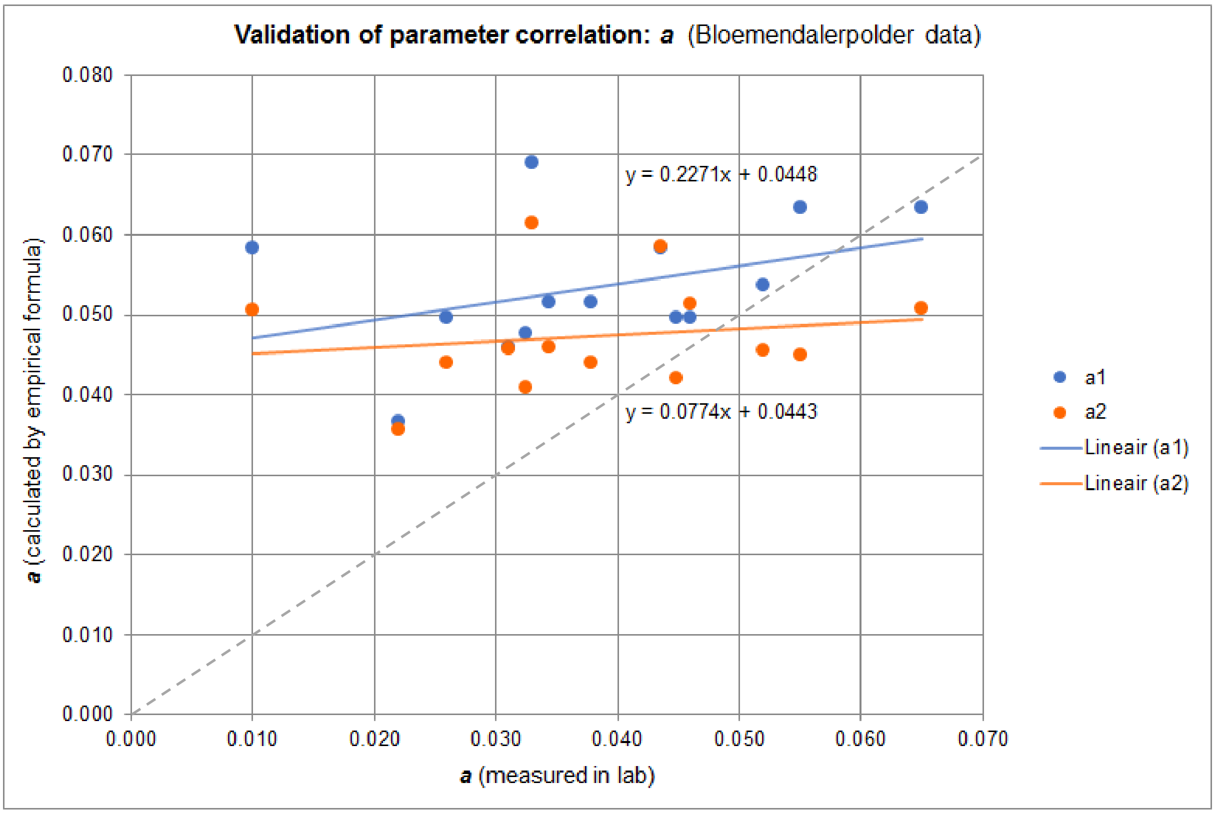

Figure 4-10: Scatter plot of empirical (correlation-obtained) values of ***a*** versus lab-determined values of ***a*** for the case Bloemendalerpolder (peat), including indicative approximate linear trends.

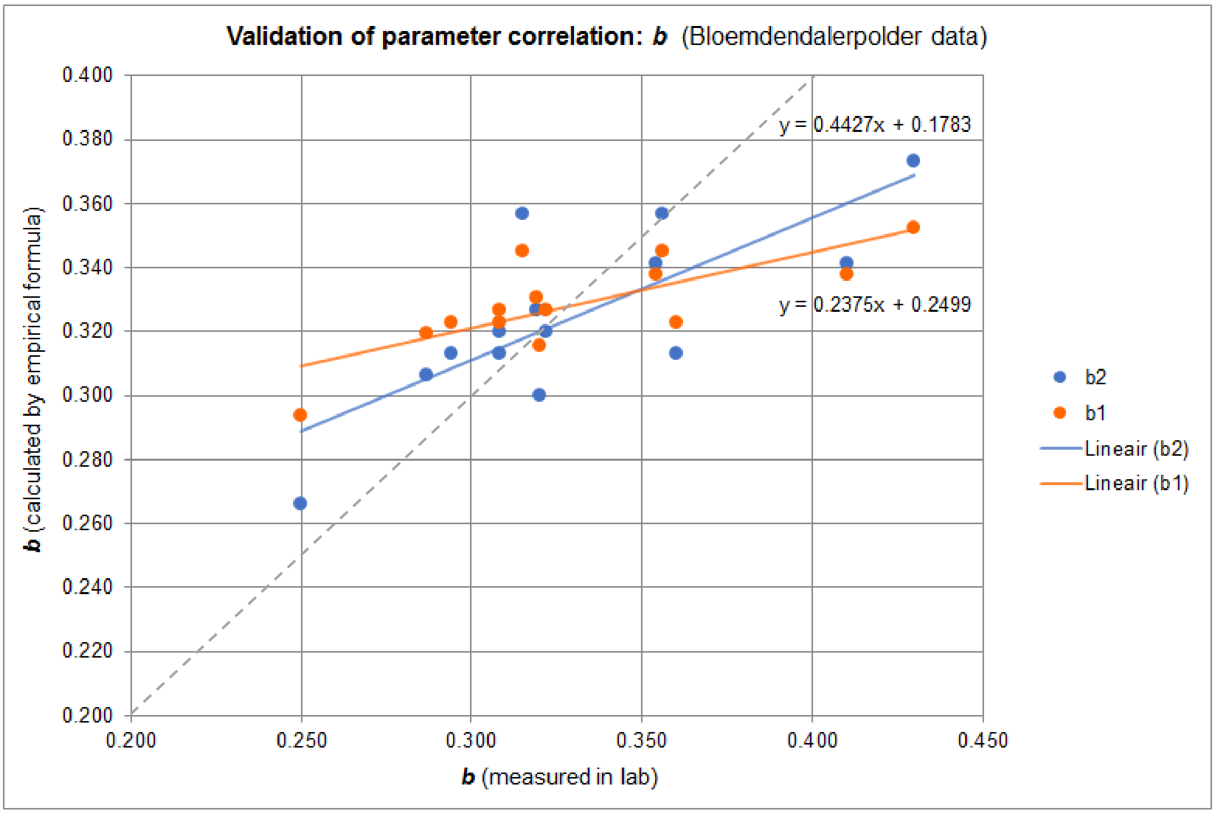

Figure 4-11: Scatter plot of empirical (correlation-obtained) values of ***b*** versus lab-determined values of ***b*** for the case Bloemendalerpolder (peat), including indicative approximate linear trends.

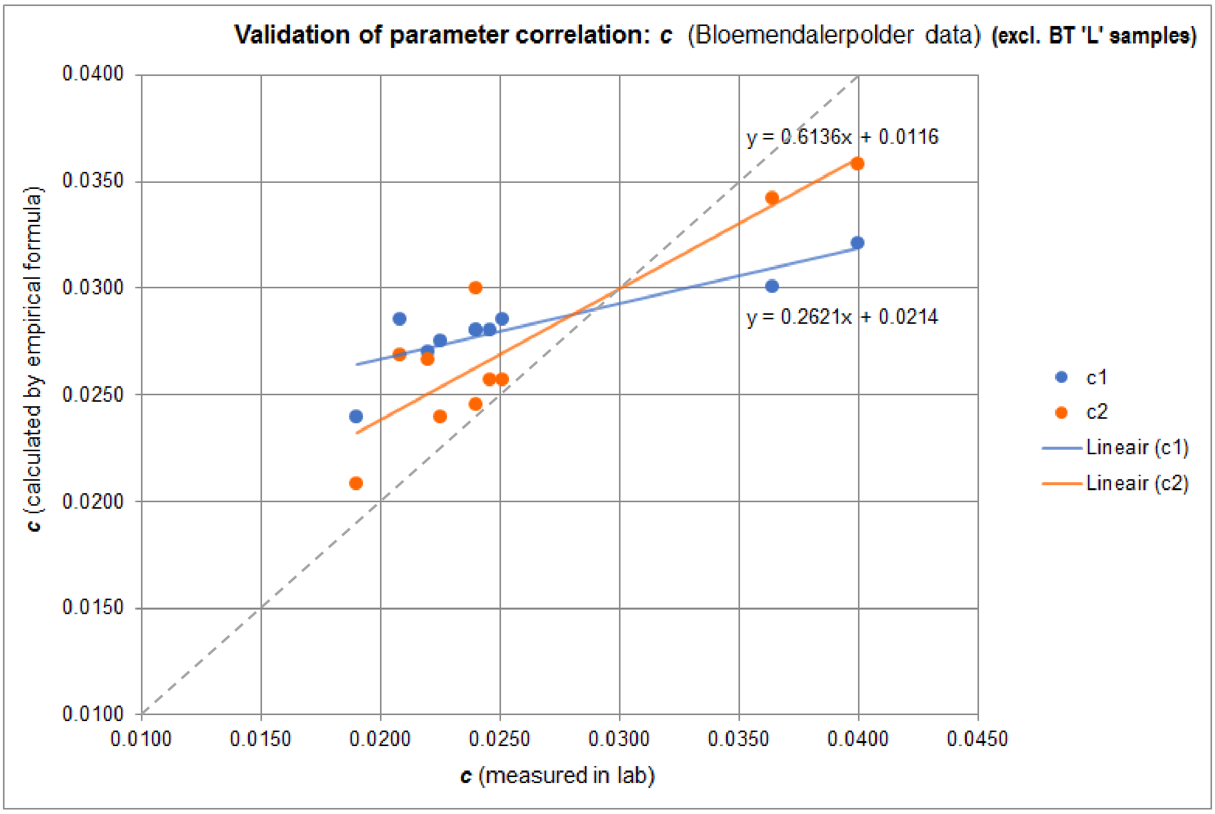

Figure 4-12: Scatter plot of empirical (correlation-obtained) values of ***c*** versus lab-determined values of ***c*** for the case Bloemendalerpolder (peat), including indicative approximate linear trends. BT 'L' samples were tested in conventional IL oedometer and yielded such peculiar results that they were disregarded in this validation graph.

4.3.1.3 Compressibility parameters Leendert de Boerspolder

Table 4-5: Overview of soil-specific *average* compressibility parameters for the Leendert de Boerspolder, based on multiple soil compression tests (refer to Appendix H1 for more detail and per-sample data). Recall that only parameters from IL and CRS tests were determined personally; K_0-CRS results were provided in the geotechnical laboratory test reports (Appendix G3).

Soil type	**Peat**	**Dike body fill**	**Silty clay**	**Silty clay**	**Peat**
Boring(s)	B1002 average	B103,B106 avg.	B104	B102 avg.	B101-B105 avg.
Location	dike slope	dike crest	polder	dike toe	polder & dike toe
Test method	(IL)	(CRS)	(CRS)	(K_0-CRS)	(K_0-CRS)
a	8.50E-02	3.48E-03	7.89E-03	8.00E-03	5.05E-02
b	3.55E-01	5.68E-02	1.75E-01	1.50E-01	3.61E-01
c	1.66E-02	2.96E-03	1.02E-02	8.70E-03	2.47E-02
b/a* | *b/c	4.2 | 21.4	16.3 | 19.2	22.2 | 16.9	18.8 | 17.2	7.2 | 14.6
RR	9.57E-02	7.65E-03	1.73E-02	1.80E-02	8.71E-02
CR	5.01E-01	1.18E-01	3.25E-01	2.90E-01	5.68E-01
$C_{\alpha\varepsilon}$	2.23E-02	6.43E-03	2.07E-02	1.70E-02	3.80E-02
C_p	75.3	-	-	-	-
C'_p	4.5	-	-	-	-
C_s	635.8	-	-	-	-
C'_s	22.6	-	-	-	-
OCR	1.2	1.1	4.0	4.6	2.9
POP	3.1	1.1	26.8	32.0	10.1
c_v	7.58E-06	9.99E-07	6.60E-07	-	-
k_v	3.41E-07	9.86E-06	7.52E-06	2.90E-08	2.49E-08

Table 4-6: Overview of all self-determined preconsolidation pressures, OCR and POP. 'Ca' = Casagrande; 'Bu' = Butterfield; 'Be' = Becker et al. Unrealistic values are coloured orange.
The work method by Becker et al. was disregarded for IL tests, and the pore pressure method was disregarded for all tests, for which the reasons are explained in subsection 4.4.2.3.

Boring No.	B1002						B103	B103	B104	B106	B106
Sample No.	6-2	6-4	6-7	7-2	7-4	8-1	5	6	8	4	5
Depth -surface	2.92	3.05	3.27	3.66	3.79	4.02	1.85	2.25	4.20	1.95	2.45
Location	dike slope						dike crest		polder	dike crest	
Test method	(IL)						(CRS)				
Pg (Ca)	23.0	26.0	23.0	25.5	22.0	17.5	-	-	-	-	-
Pg (Bu)	26.0	26.0	25.0	25.5	22.0	17.5	23.0	18.5	38.0	38.0	25.5
Pg (Be)	-	-	-	-	-	-	34	20	33.5	34	24
OCR (Ca)	1.2	1.5	1.1	1.4	1.1	0.6	-	-	-	-	-
OCR (Bu)	1.4	1.5	1.2	1.4	1.1	0.6	1.0	0.7	4.2	1.5	0.9
OCR (Be)	-	-	-	-	-	-	1.4	0.7	3.7	1.4	0.8
POP (Ca)	4.2	8.6	2.4	7.7	2.6	-9.5	-	-	-	-	-
POP (Bu)	7.2	8.6	4.4	7.7	2.6	-9.5	-0.8	-8.5	29.0	13.4	-3.2
POP (Be)	-	-	-	-	-	-	10.3	-7.0	24.5	9.4	-4.7

4.3.2 Settlement predictions

The following subsections group the final settlement prediction results per model or method. Predictions were performed with *D-Settlement*, except for Fokkens' method, as already explained in section 4.2.4). Every table subsequently lists the results for a particular case or location investigated. The settlement prediction results are analysed and discussed in section 4.4.3.

4.3.2.1 a,b,c-Isotachs with correlation-obtained parameters

Table 4-7: Overview of final settlement prediction results for **Bloemendalerpolder** trial mound No. 1 (T1), including relative errors ('R.E.') with respect to best fit extrapolation. Error values exceeding ±15% are highlighted in orange. These results are discussed exclusively in subsection 4.4.2.2.

T1 best fit extrapolation [Ammerlaan & Hoefsloot, 2012]:			**1.60**	**R.E. [%]**
abc	Original prediction (2011)		1.67	4.4
abc	Original parameters (verification)		1.73	8.4
abc	Peat parameter set 1 (a1,b1,c1)		2.02	26.3
abc	Peat parameter set 2 (a2,b2,c2)		1.98	24.1

4.3.2.2 De Glopper & Koppejan

Table 4-8: Overview of final settlement prediction results for **Bloemendalerpolder** trial mound No. 1 (T1), including relative errors ('R.E.') with respect to best fit extrapolation. Error values exceeding ±15% are highlighted in orange.

T1 best fit extrapolation [Ammerlaan & Hoefsloot, 2012]:		**1.60**	**R.E. [%]**
Koppejan	Original prediction (2011) + lin. strain	1.53	-4.4
Koppejan	Original prediction (2011) + nat. strain	1.30	-18.8
Koppejan	Original parameters (verification) + lin. strain	1.58	-0.8
Koppejan	Original parameters (verification) + nat. strain	1.34	-16.1
Koppejan	De Glopper (T1 data) + lin. strain	1.97	23.4
Koppejan	De Glopper (T1+T2 average data) + lin. strain	2.07	29.6

Table 4-9: Overview of final settlement prediction results for two different revisited locations at **Amstelhoek**, by means of the *Koppejan* method only. Relative errors ('R.E.') are with respect to best fit extrapolation. Error values exceeding ±15% are highlighted in orange.

1300 m ZB244 best fit extrapolation [Sipkema, 2012]:		**0.96**	**R.E. [%]**
1300 m/1400 m Koppejan original prediction		0.72	-25.0
1300 m Koppejan *revisited* prediction (more peat)		0.91	-5.2
2000 m ZB181 best fit extrapolation [Sipkema, 2012]:		**0.65**	**R.E. [%]**
2000 m/2100 m Koppejan original prediction		0.83	27.7
2000 m Koppejan *revisited* prediction (minor differences)		0.86	31.8

4.3.2.3 Fokkens

Preliminary note concerning predictions by means of Fokkens' method: 'NC' and 'OC' refer to the formula for normally consolidated and overconsolidated soil, respectively. The subsequent numbers between parentheses refer to the according equation number in this report.

Table 4-10: Overview of final settlement prediction results for **Amstelhoek** location 2000 m, including relative errors ('R.E.') with respect to best fit extrapolation. Error values exceeding ±15% are highlighted in orange.

2000 m ZB181 best fit extrapolation [Sipkema, 2012]:			**0.65**	**R.E. [%]**
2000 m Fokkens "analytical"		NC (3-13.1)	3.35	415.6
2000 m Fokkens "analytical"		OC (3-14.1)	3.75	477.0
2000 m Fokkens "empirical"		NC (3-13.2)	1.22	87.1
2000 m Fokkens "empirical"		OC (3-14.2)	0.83	27.6
2000 m Fokkens TAW		(3-15.1)	0.89	36.9
2000 m Fokkens CUR		(3-15.2)	0.98	51.5

Table 4-11: Overview of final settlement prediction results for **Bloemendalerpolder** trial mound No. **1** (T1), including relative errors ('R.E.') with respect to best fit extrapolation. Error values exceeding ±15% are highlighted in orange.

T1 best fit extrapolation [Ammerlaan & Hoefsloot, 2012]:			**1.60**	**R.E. [%]**
Fokkens "analytical"	T1 data	NC (3-13.1)	3.61	125.8
Fokkens "analytical"	T1 data	OC (3-14.1)	3.60	124.9
Fokkens "analytical"	T1+T2 average data	NC (3-13.1)	3.63	127.2
Fokkens "analytical"	T1+T2 average data	OC (3-14.1)	3.60	125.2
Fokkens "empirical"	T1 data	NC (3-13.2)	1.65	2.8
Fokkens "empirical"	T1 data	OC (3-14.2)	1.76	9.9
Fokkens "empirical"	T1+T2 average data	NC (3-13.2)	1.72	7.3
Fokkens "empirical"	T1+T2 average data	OC (3-14.2)	1.90	18.5
Fokkens TAW	T1 data	(3-15.1)	1.88	17.7
Fokkens TAW	T1+T2 average data	(3-15.1)	2.01	25.9
Fokkens CUR	T1 data	(3-15.2)	1.96	22.3
Fokkens CUR	T1+T2 average data	(3-15.2)	2.09	30.4

Table 4-12: Overview of final settlement prediction results for **Bloemendalerpolder** trial mound No. **2** (T2), including relative errors ('R.E.') with respect to best fit extrapolation. Error values exceeding ±15% are highlighted in orange.

T2 best fit extrapolation [Ammerlaan & Hoefsloot, 2012]:			**2.40**	**R.E. [%]**
Fokkens "analytical"	T2 data	NC (3-13.1)	5.03	109.5
Fokkens "analytical"	T2 data	OC (3-14.1)	4.95	106.3
Fokkens "analytical"	T1+T2 average data	NC (3-13.1)	5.00	108.3
Fokkens "analytical"	T1+T2 average data	OC (3-14.1)	4.95	106.4
Fokkens "empirical"	T2 data	NC (3-13.2)	2.46	2.5
Fokkens "empirical"	T2 data	OC (3-14.2)	2.79	16.1
Fokkens "empirical"	T1+T2 average data	NC (3-13.2)	2.36	-1.6
Fokkens "empirical"	T1+T2 average data	OC (3-14.2)	2.61	8.6
Fokkens TAW	T2 data	(3-15.1)	2.94	22.4
Fokkens TAW	T1+T2 average data	(3-15.1)	2.77	15.4
Fokkens CUR	T1+T2 average data	(3-15.2)	3.03	26.4
Fokkens CUR	T2 data	(3-15.2)	2.87	19.5

4.3.2.4 a,b,c-Isotachs & NEN-Bjerrum (Leendert de Boerspolder)

Table 4-13: Overview of final settlement prediction results for the dike at the Leendert de Boerspolder, including relative errors ('R.E.') with respect to the final settlement estimation based on recent CPT profiles. Error values exceeding ±15% are highlighted in orange. "mp" = "maintain profile".

Actual settlement after 365 years, based on CPT profiles [Jommi et al., 2015]:			**1.60**	**R.E. [%]**
abc	IL-based peat properties	"mp"	2.05	28.1
abc	K_0-CRS-based peat properties	"mp"	1.91	19.4
NEN-Bjerrum	IL-based peat properties	"mp"	1.76	9.7
NEN-Bjerrum	K_0-CRS-based peat properties	"mp"	1.80	12.3
abc	IL-based peat properties	without "mp"	1.89	18.4
abc	K_0-CRS-based peat properties	without "mp"	1.80	12.8
NEN-Bjerrum	IL-based peat properties	without "mp"	1.74	8.6
NEN-Bjerrum	K_0-CRS-based peat properties	without "mp"	1.74	8.6

4.4 Analysis and discussion of results

4.4.1 Site investigation and soil testing

To start at the beginning of any settlement prediction and, in fact, at the beginning of any construction project, let us first consider briefly the phase of site investigation and testing, as well as quality and representativeness of soil test results as a consequence. It has been emphasised already by CROW (2004) (referring back to section 3.3.3) that "*the most important source of uncertainty (…) is formed by the exploration of the subsurface*". When for a large infrastructural construction project, such as the N201 bypass in Amstelhoek, merely once every 100 m a CPT is performed and only once every 200 m a manual boring, that is already a relatively frugal amount of data, likely to lead to subsurface interpretation and schematisation errors. However when on top of that also the essential compressibility characteristics of the soil are tested and determined chiefly on just a small part of the whole road trace (namely around the Amstel river crossing and surrounding dikes), then it is highly probable that extrapolation of soil parameters to a distance of more than a kilometre away can lead to significant deviations and errors. In this light, it surprises that deviations from predictions in the case of Amstelhoek remained within ±30%. A more detailed case-specific analysis of the results for Amstelhoek is provided in section 4.4.3.3.

The process of soil *testing* is found to be prone to errors as well, which has emerged from literature review (e.g. CROW, 2004), but also during personal test interpretation and parameter determination. For example, consider the first loading stage of the conventional (IL) oedometer-tested sample No. B1002 6-2 (Leendert de Boerspolder):

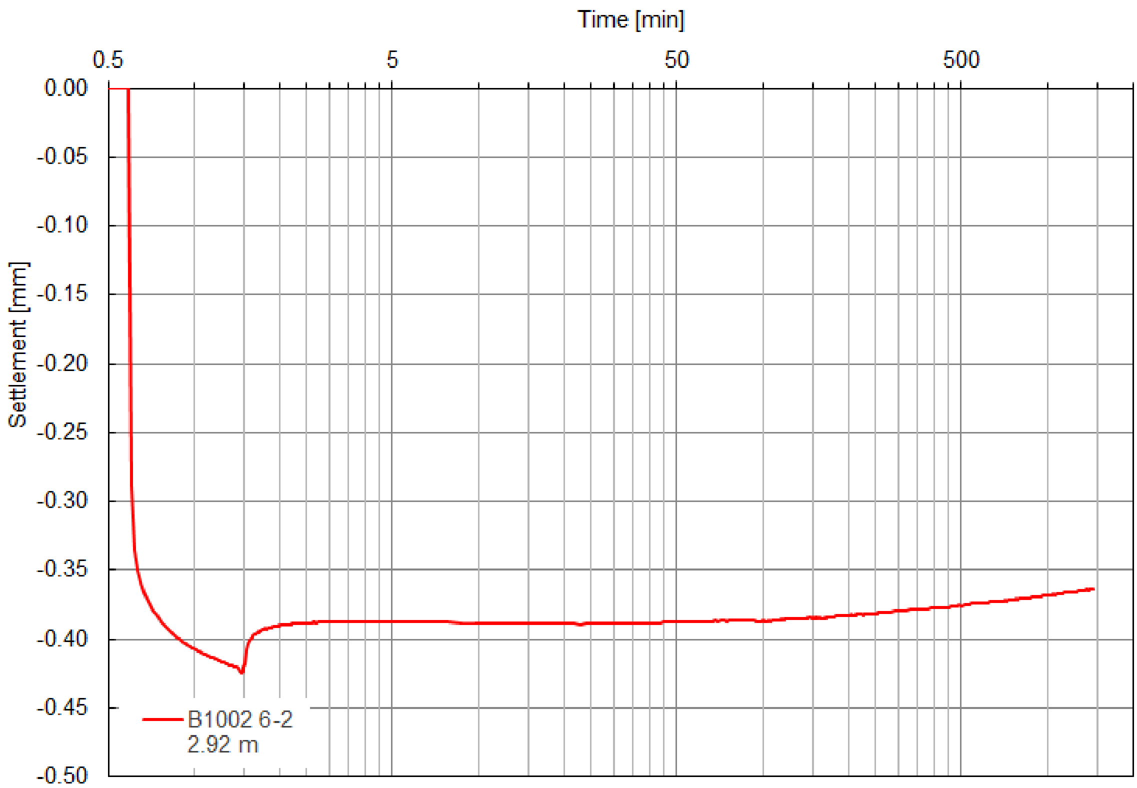

Figure 4-13: Peculiar time-settlement curve for the first loading stage of an IL-oedometer-tested sample.

A time-settlement curve bending upwards indicates unloading, which is certainly not to be expected nor to be desired in an early stage of oedometric compression. This behaviour has been observed more than once, though not for every sample, and only during early loading stages (aside from intentional unload-reload cycles at higher stress levels). Although being indicative of unloading, it is a puzzle *why* exactly this has happened. A human error is possible, however in case of “accidental” unloading is very unlikely to happen *repeatedly*, as observed. So the only reasonable alternative explanation that could be thought of, is that perhaps the soil samples initially were not completely saturated and then water was added, consequently causing the soil to swell. Such unexpected swelling due to wetting of unsaturated soil samples was already mentioned and warned for in section 3.1.1. What still remains inexplicable, however, is why the swell curve soon reaches a plateau, but after a considerable time delay continues to increase again (very gently though). Anyhow, it may be clear that this makes the first loading stage unrepresentative. For this reason the first incremental loading stage was consistently disregarded for the determination of any soil parameter in the current research.

In order to prevent such and similar peculiarities, first of all any sample disturbance (refer to subsection 3.3.3.5) and dehydration should be avoided as much as possible during the entire sample preparation process, from boring through transport and storage until testing. Reliable soil compressibility testing requires *undisturbed* and fully *saturated* soil samples. In case of oedometer testing in particular, it might be better to fill the oedometer cell and thus submerge the sample *before* applying the first load, so that no swelling *during* loading will occur. Furthermore, in order to decrease the probability of human errors during testing, automatically controlled test setups may be favoured in general to reduce the need for human intervention. Although this might be complicated to achieve for incrementally loaded (pressure-controlled) tests, it certainly can be and has been done [Head, 1994; Clayton & Hight, 2007].

Reduction of human intervention by automation not only decreases the probability of human errors, but also can decrease labour costs. Still the total time duration for incremental oedometer tests will remain long, however. In order to have an automatically controlled test *and* to limit the time duration as well, one can consider using CRS oedometers (refer to section 3.1.2). Just recall from the latter section that strain-controlled tests do not allow for determination of Koppejan compression coefficients.

4.4.2 Soil parameter determination

4.4.2.1 De Glopper: Koppejan coefficients

It has already been mentioned in the section concerning De Glopper’s method itself (3.2.6), that one of the primary limitations of empirical correlations is that their validity rapidly decreases outside of the area and the pedological conditions for which the relationship has been developed.

This is also likely to be the main cause for the observed large spread and deviations of Koppejan coefficients obtained via De Glopper’s relationship, as presented in subsection 4.3.1.1, in contrast to the strong correlation that De Glopper (1979) himself had found. When disregarding clay for the moment, since it was known in advance that De Glopper’s relationship is only valid for peat, the results are still poor. Because even for pure peat, such as especially in the Bloemendalerpolder but also in Amstelhoek, De Glopper’s method of obtaining Koppejan coefficients proved very unreliable with deviations up to 95% with respect to laboratory values. The sole exception is C'_p in the case of Bloemendalerpolder, which matched lab values fairly well to within ±14%.

Also when considering wariness with regard to the reliability of the laboratory reference values themselves, the deviations in De Glopper’s estimations of Koppejan coefficients are most likely too large to be useful. This was additionally validated by means of settlement predictions, which is discussed further in subsection 4.4.3.1.

Altogether, De Glopper’s relationship can be considered to be too unreliable for estimating the Koppejan compression coefficients of peat, let alone of other soils. A general trend (either overestimation or underestimation) can hardly be determined, since the spread in results is very large as well. Porosity alone thus appears to not be a universally sufficiently reliable property to estimate a soil’s compressibility characteristics from. Moreover, De Glopper’s relationship poses additional limitations in that it does not provide any way of estimating the magnitude of preconsolidation pressure, OCR or POP, which is per se required for a decent settlement prediction. As mentioned already at the end of section 3.2.5, alternative ways of estimating the preconsolidation pressure by correlation with soil index properties or from field tests were found to exist only for clay but not for peat. This moreover disregards the lack of consolidation properties, which would be needed as well especially for short term settlement predictions.

4.4.2.2 a,b,c parameters from correlations

To start with the most convincing finding: estimation of parameter ***b***, using either one of the proposed correlations (equation (4-6) or (4-7)), proved to correspond very well with laboratory values *on average*. Although the spread, or scatter, observed in Figure 4-11 is considerable, this is solely caused by the variability of the laboratory test results: averaging eliminates this spread and is deemed tolerable since the soil type is all peat at the Bloemendalerpolder. The correlations for the other parameters (*a* and *c*), on the other hand, seem to perform less well.

An important remark concerning the laboratory data has to be made here, though. It was noticed that the value(s) for *c* obtained from IL oedometer tests were significantly lower than values obtained from K_0-CRS tests: refer to the red coloured value in Table 4-4. Upon investigation where these low values came from, it was found that the IL-oedometer-obtained a,b,c parameters were only listed in a summary table without mention of their origin [Alink, 2012: p.188]. Since the original IL oedometer test data with determination of a,b,c parameters could not be retrieved anywhere else in the concerning geotechnical test report(s) and the values seem very peculiar in comparison with the results of other test methods, it is deemed justified to disregard the lab-value of *c* obtained from IL tests.

Neglection of IL test results (BT‘*L*’ samples) has been done in order to plot the graph of Figure 4-11. In that case, the correlation-based estimations of ***c*** (equations (4-8) and (4-9)) yield fair and practically usable results, with a deviation of less than +12% from laboratory values on average (refer also to Table 4-4). However a slight overestimation of the creep parameter can already have significant negative consequences for long-term settlement predictions, therefore a correction on the basis of the regression line equation provided in Figure 4-12 (after rewriting *x* in terms of *y*) might be considered.

Whereas parameter *c* still appears to remain within a fair margin, the empirical estimates for parameter ***a*** based on equations (4-4) and (4-5) in contrast may be considered to be too unreliable in any case. Note that laboratory values themselves already show a large variation when compared mutually. Hence it seems that parameter *a* is difficult to determine reliably in general: both by means of laboratory tests as well as from correlations.

Validation of the a,b,c parameter correlations by means of settlement predictions with *D-Settlement* (Table 4-7) confirms that the *overall* performance of the correlations is poor (large overestimation). However this includes the severely overestimated values of parameter *a*, which is strongly believed to be the main cause of the observed deviation in the final settlement prediction. If the correlations are planned to be used in practice, one should therefore very cautiously handle parameter *a* and consider at least applying a correction by means of the according regression line equation provided in Figure 4-9 (after rewriting *x* in terms of *y*). As with every correlation, however, this correction is also aimed at a particular location and soil, and so has a limited validity at other locations or for other soils.

A final remark concerns the same limitations as for De Glopper’s relationship: the correlations cannot be used standalone, since they provide neither a way of estimating the magnitude of preconsolidation stress, nor of determining hydraulic or consolidation properties.

4.4.2.3 Compressibility parameters from compression tests

Whereas the determination of the actual compression coefficients for the Leendert de Boerspolder did not pose special problems apart from being very laborious and time-consuming, the determination of the **preconsolidation pressure** was found to be more difficult. The difficulty arose from the fact that compression curves sometimes are very gradual (refer to Figure 4-x3), which makes determining the point of maximum curvature, and subsequently the preconsolidation pressure, according to Casagrande’s method ambiguous and subjective.

Interestingly, such gradual curvature was particularly pronounced for CRS tests, whereas incremental loading (IL) tests were generally found to yield compression curves with more distinctive bending points, making application of Casagrande's method slightly easier and less ambiguous. It cannot be said whether this is due to the different procedure of testing itself, or due to the soil samples having been subjected to different treatment in advance of testing (i.e. different level of disturbance).

Anyhow, three other methods were taken into consideration in hopes of decreasing obscurity and improving the reliability of the results, namely: Butterfield's method, the work method and the pore pressure method, all which were described already in subsection 4.2.2.8. The resulting preconsolidation stress values of these different methods were presented in Table 4-6. Following, the findings of this review and try-out of different preconsolidation pressure determination methods are analysed and discussed.

First of all, the methods of Casagrande and **Butterfield** yield very similar results when applied to IL oedometer test data, despite their slightly different approach and graphical representation. According graphs for example can be found in Appendix H2: Fig. 1 and 2. Taking into account that Butterfield's method is simpler than Casagrande's, this method can definitely be regarded as a useful and perhaps even favourable alternative to Casagrande's method.

The **work method** proposed by Becker et al. yielded much less convincing results, however. First of all, when trying to apply this method onto IL test data, stress-work curves were obtained (e.g. Appendix H2: Fig. 3) that all look nothing like they are supposed to look according to Becker et al. (Figure 4-5b). Since interpretation of these diagrams would be too ambiguous and doubtful, the work method was completely disregarded for IL test data.

When regarding the application of the work method onto CRS tests, curves were obtained (e.g. Appendix H3: Fig. 4) that look indeed similar to those produced by Becker et al. However drawing the tangent lines was again found to be ambiguous, especially at the beginning of the curve, due to the curve's unneglectable nonlinearity. To some degree this was already expected, as mentioned in subsection 4.2.2.8, yet it was found to be even more pronounced than in [Becker et al., 1987]. Furthermore, the results deviate considerably from values obtained with Butterfield's method, which was previously found to correspond very well with Casagrande's method.

The **pore pressure method** had to be disregarded completely. For IL test data this was logically because no pore water pressure measurements were available. However for CRS test data this was because the resulting diagrams turned out to be downright uninterpretable. This is illustrated by Figure 4-14 on the next page, for example. Recall from Figure 4-6 how such a pore pressure diagram is supposed to look like approximately.

Note from Figure 4-14 that the excess pore pressure fluctuates between just ±1 kPa, which is very low and in fact might just represent the (in)accuracy of the pore pressure sensor. Excess pore pressure is calculated by subtraction of the back pressure from the total pore pressure measurements. In case the back pressure is *not* subtracted, another extremity would occur: the total pore pressure would increase rapidly until 300 kPa and then remain constant throughout most of the test, which is uninterpretable as well.

These very peculiar pore pressure conditions might have serious implications for the reliability of the test results, however. Recall from section 3.1.2 that the excess pore pressure during a CRS test should remain between at least 7 kPa and at most 50% of the total vertical stress. Considering that the excess pore pressure was less than 1 kPa at any time, this implies that all CRS test results are unreliable. Admittedly the pore pressure method was tried just for additional verification in a very late stage of research, after all the settlement predictions were performed partly based on CRS test results. Therefore the CRS test results will not be simply discarded at once. When the soil compressibility parameters that were personally obtained from raw CRS test data, are compared with the parameters obtained from K_0-CRS tests by a professional laboratory [Deltares, 2015], then the results are very similar and not at all unrealistic in general. Therefore it is indeed thought to be tolerable to use the CRS test results for settlement prediction, despite the questionable pore pressure conditions.

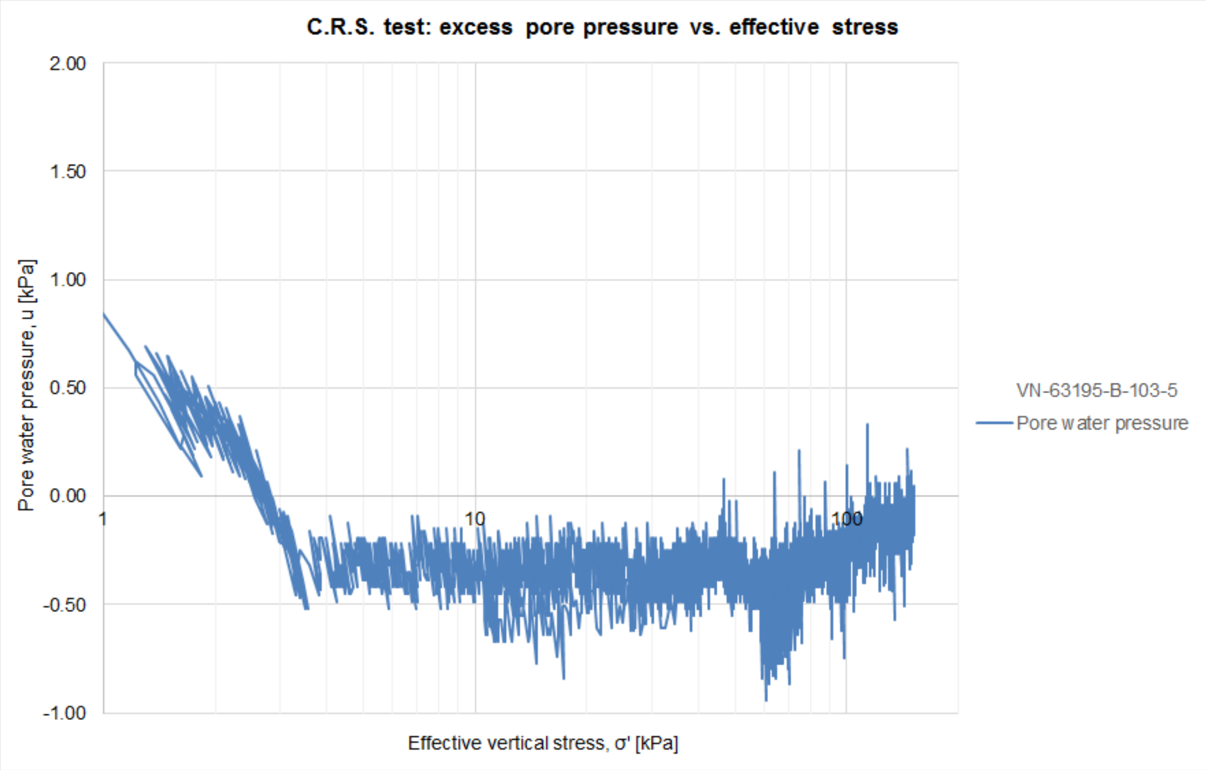

Figure 4-14: Excess pore pressure during CRS test on sample B105-5 (Leendert de Boerspolder). All CRS pore pressure diagrams looked similar. The preconsolidation pressure for this soil type and location is expected to be between 10 and 30 kPa, however this is clearly impossible to derive from this graph. Excess pore pressure was calculated by subtraction of the back pressure from the total pore pressure measurements.

Since it is known from literature review (subsection 3.3.3.5) that a very gradually curving compression curve is indicative of some form of sample disturbance, leading to *under*estimation of the preconsolidation stress, it might be argued that methods that tend to yield a higher value than Casagrande's method give a more realistic estimate of the actual preconsolidation. However none of the methods reviewed shows such a tendency of significance, from what can be observed on the basis of this limited dataset. However even if there would be a recognisable tendency, it is hardly possible to assess quantitatively which method in fact is the best, since there is no way of verification by directly "measuring" the preconsolidation stress of a soil, other than the approximate graphical methods that were regarded already.

Penultimately, the calculated values of **OCR** and **POP** are evaluated (refer again to Table 4-6). It is known that an OCR of less than 1, as well as a negative POP, is physically impossible. Hence it is apparent that in some cases an error has been made. Recall from equations (2-5) and (2-6) in subsection 2.2.2.1 that OCR and POP depend on the estimated in-situ effective stress. So when neglecting a possible error in the preconsolidation stress itself, the error source must lie in the estimated in-situ effective stress. This can have multiple causes, since the in-situ stress is based on the *estimated* and *average* value of unit weight of overburden soil at a certain location, along with an average or interpolated phreatic water level, all of which have a certain level of uncertainty, in particular anywhere below the dike body.

Finally, in all technical laboratory test reports composed by *Deltares* (2015) another, slightly different, method of determining the preconsolidation pressure was encountered. Apparently they use to determine the preconsolidation stress at the intersection between a horizontal line drawn through the point of in-situ effective stress at the ε-log(σ') curve, and the tangent to the virgin compression line, as shown in Figure 4-15. One advantage of this method is that the probability of obtaining physically impossible values of OCR and POP is nearly zero, since the intersection point will practically always lie to the right of, or at the in-situ stress point.

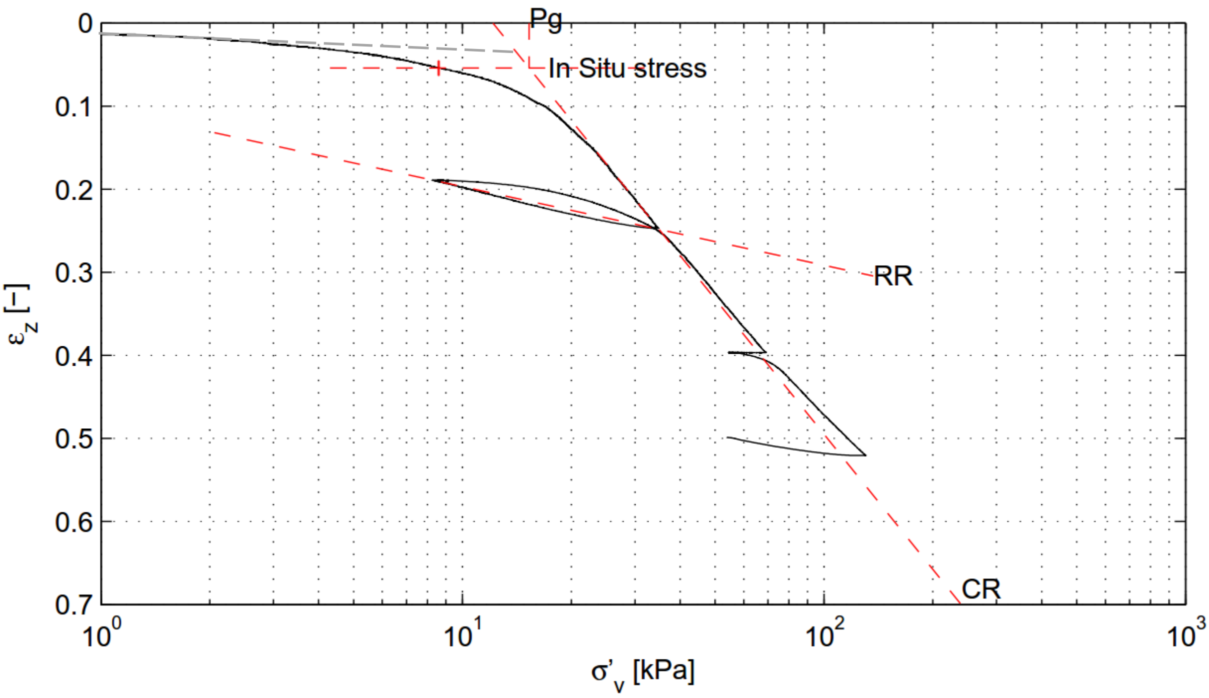

Figure 4-15: Illustration of the Deltares method of determining the preconsolidation pressure ('Pg'). Pg in the example above reportedly amounts to 15.3 kPa [Deltares, 2015]. Butterfield's method (intersection between the light grey dashed line and the CR-line) gives a similar result: about 14.5 kPa (-5%).

However an important point of attention and potential source of error has to be highlighted: the Deltares method strongly relies on the in-situ stress, the estimation of which can be difficult and prone to errors, as was already mentioned shortly before. Note that Deltares gives no indication of how they estimate or measure the in-situ stress for this purpose.

After visual comparison of the Deltares method and Butterfield's method (both for ε-log(σ')), regarding multiple soil compression graphs [Deltares, 2015], it is found that the results are generally very similar with deviations within 15%. The Deltares method appears to show a very weak tendency to yield slightly higher values on average than Butterfield's method and thus also than Casagrande's method (for e-log(σ')).

4.4.2.4 Consolidation properties from compression tests

First of all, it should be said that the consolidation or permeability properties are more important for short- and medium-term than for long-term settlement predictions, since consolidation may be expected to be completed in an "early" stage of the total period of settlement considered (order of decades). Nevertheless, it was desired to evaluate different methods of testing and parameter determination, which for settlement predictions naturally includes soil consolidation properties.

The determination of the coefficient of consolidation as well as the hydraulic conductivity was found to be difficult and very subjective. The latter concerns IL tests in particular, where application of the root time method after Taylor (refer to subsection 2.2.2.2) was by far not always unequivocal, especially towards higher stress levels, because the supposedly linear initial part of the curve most often is *not* linear. Therefore it is very difficult to draw objectively an initial tangent line and to determine the a_{60} and a_{90} points, as may become clear from the graphs depicting the settlement versus the (square) root of time in Appendix H2.

According to Head (1994), this nonlinearity of the early consolidation curve is indicative of incomplete saturation of the soil sample. Hence again the importance of ensuring full saturation of soil samples is highlighted. Yet the thesis author made his best effort to determine c_v and k_v on the basis of the available IL test data. The resulting values (Table 4-5, or Appendix H1) seem to be within possible range of peat soils, although somewhat on the high end, after comparison with laboratory values from e.g. Bloemendalerpolder and Amstelhoek (Appendices G1 and G2).

However also the calculation of consolidation properties from CRS test data, by means of equations (4-17) to (4-20), posed some unexplained difficulties. After the equations (4-17) and (4-18) were found to yield very unrealistic results, equations (4-19) and (4-20) seemed to yield very reasonable values. However later on during the data analysis it was noticed that, although the order of magnitude of the values is correct (in comparison with other case study data), the values of c_v and k_v steadily *increase* with increasing stress and strain – the exact opposite should be the case though. For this remarkable finding no adequate explanation could be found.

Another issue that possibly influenced the calculations for determining c_v and k_v from CRS test data, is the fact that at small time scales striking fluctuations in the effective stress reading occur. This behaviour was observed for every test at all times and is illustrated by Figure 4-16, based on actual CRS test data from the Leendert de Boerspolder. Since the effective stress is directly related to excess pore pressure, the fluctuations are likely also a direct consequence of the previously addressed peculiar pore pressure conditions (Figure 4-14), which were believed to be related to the (in)accuracy of the sensorical hardware. This complicates the calculation of differentials or increments along the curve considerably, though. So it was deliberately tried to circumvent this issue by calculating any differentials or increments not between adjacent cells, but by taking at least 10 time steps forward and 10 time steps backward from the actual point of interest. However this method might still have been insufficient; perhaps additionally averaging around the considered points might have been appropriate as well.

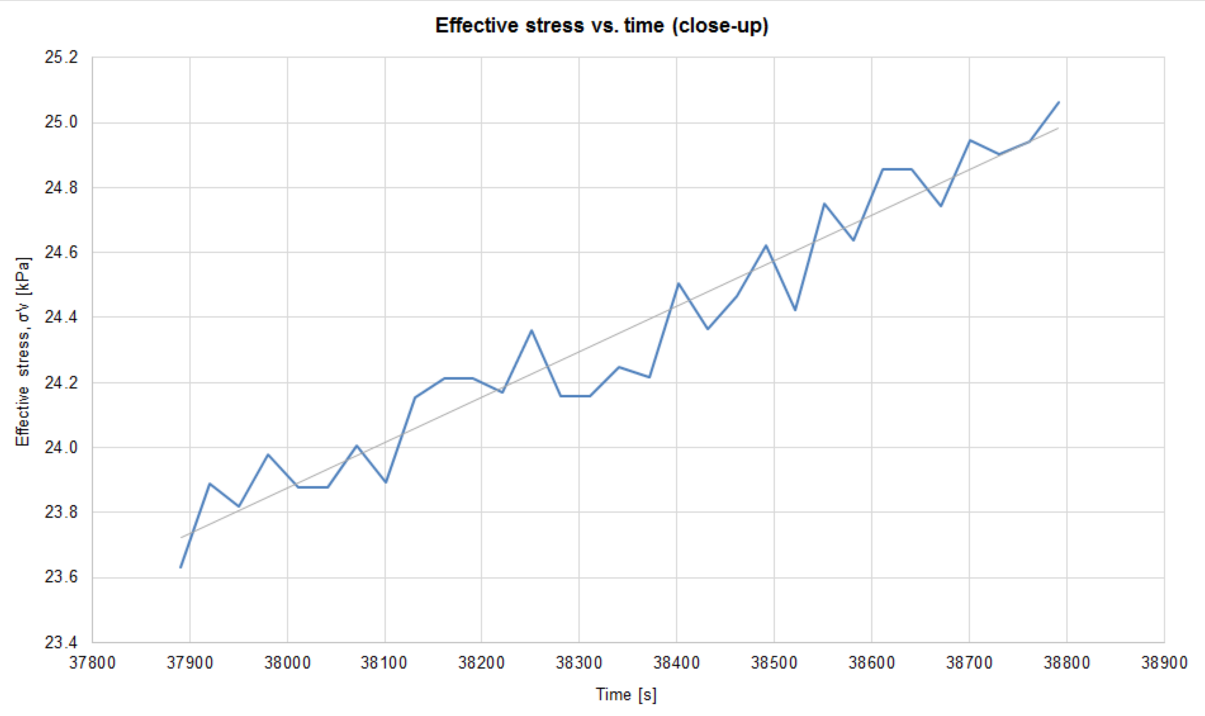

Figure 4-16: Fluctuations in effective stress ($\Delta\sigma' \leq 0.3$ kPa) during CRS testing, making incremental calculations very unreliable without correction or circumvention.

4.4.3 Settlement predictions

4.4.3.1 De Glopper

The correlation-obtained Koppejan coefficients were validated by means of settlement predictions with *D-Settlement* (Koppejan linear strain, which the relationship was based on). The location and soil considered were Bloemendalerpolder and peat, respectively. Although the deviations were not as large as could be expected from the observed parameter deviations, it was found that the final settlement predictions (Table 4-8) are generally more than 20% higher than the best fit settlement curve extrapolation. Moreover, the Koppejan model using coefficients obtained via De

Glopper's method also performs worse than predictions using laboratory-obtained Koppejan coefficients (whilst using the same consolidation properties and preconsolidation pressure in both cases). Considering moreover the several other limitations of De Glopper's method as previously addressed, it is strongly discouraged to use this method in engineering practice.

4.4.3.2 Fokkens

Fokkens: a case apart. Existing in six different formulations, every formula has also been tested and validated in the course of this research. Results are presented in Tables 4-10, 4-11 and 4-12, the analysis of which can be kept relatively brief, though. It follows from these tabulated results that the "analytical" versions of Fokkens' method, i.e. equations (3-13.1) and (3-14.1), are downright useless, since they yield final settlement estimations that are all more than 100% too high. Because this is very exceptional, it was triple-checked that the formulas were written and used exactly as proposed in the original article [Fokkens, 1970]. The input values used were in general the same for all formulas; it was just assured that units of gf/cm^2 for pressures were used where required, which was found to influence only the "empirical" formula.

Secondly, it has no doubt that the Fokkens method is unreliable for non-peat soils, which was to be expected and which was subsequently validated on the Amstelhoek case (Table 4-10), yielding final settlement estimations that are 28% too high at best, however mostly much higher.

Thirdly, the "updated" Fokkens formulas proposed by TAW and CUR, i.e. equations (3-15.1) and (3-15.2), both did not perform very well either, with final settlements being overestimated by 15-30%. This is deemed to be practically of no use – in any case certainly not advantageous in comparison with more modern, more complete and more universally applicable settlement prediction models.

Fourthly and surprisingly, the "empirical" versions of the Fokkens method, i.e. equations (3-13.2) and (3-14.2), performed not bad at all, provided that pure peat soil is considered (validated at the Bloemendalerpolder). Their worst result is an overestimation of 18.5%, however mostly the estimations are just about 0-10% too high. An additional benefit is that for using the "empirical" formulas it is not necessary to know the compression index C_c, which otherwise still would have required conducting compression tests. Nevertheless, even when considering solely the best performing formulation of the Fokkens method, it has so many practical limitations (refer to section 3.2.5) that it might best be disregarded for use in engineering practice.

One final remark concerns the practical question of submersion and subsequent effective weight reduction. It proved difficult to take into account or estimate the final submersion below the phreatic water level in advance. This may be possible to be found iteratively, which was tried, but overall the best results were found by simply assuming a final submersion of 100% (which is unrealistic, yet closer to reality than assuming no submersion at all).

4.4.3.3 Case-specific findings Amstelhoek

The case of Amstelhoek was partly chosen because there was a desire to investigate the causes of deviations between predicted and observed settlements at certain locations. For this, two different locations were considered, namely: 1300 m (in comparison with initial prediction at 1400 m) and 2000 m (in comparison with initial prediction at 2100 m). At the former location the extrapolated final settlement (based on settlement curve-fit) would be 33% larger than predicted, whereas at the latter location the extrapolated final settlement would be 22% smaller than predicted. Refer also to Table 4-9.

First of all, the laboratory test data and subsequently chosen representative values were critically reviewed. Given the limitation that soil compressibility properties from relatively far distance had to be used, there was no further reason to doubt the selection and attribution of soil parameters to soil types and layers in the subsurface. Next, the subsurface geometry was critically reviewed and compared with site investigation data. As a result, it was believed that improvements could be made in this regard, which were minor at 2000 m, but substantial at 1300 m. At the latter location it was found that in particular the amount of peat in the subsurface should be increased with respect to location 1400 m, as follows from the geological cross section in Appendix D3 as well as from CPT profiles and borings [Van der Valk, 2007].

The new revisited subsurface geometry of location 1300 m can be found in the according *D-Settlement* "Input View" in Appendix J, and can be compared with the original geometry of location 1400 m that is also to be found in Appendix J. Not only the total thickness of peat at 1300 m is more than twice the thickness at 1400 m, but more importantly most of this is in the *shallow* subsurface, namely 1.5 m of peat topsoil, which is clay at 1400 m.

The settlement predictions were subsequently performed again (Table 4-9: "revisited") and the results are remarkable in two ways. Firstly, the prediction at 1300 m indeed improved considerably to within 5.2% of the best fit extrapolation, proving that the initially underestimated, or wrongly extrapolated, thickness of the peat layer was indeed the main reason for unexpectedly high settlements at that location.

However at 2000 m, small changes in soil parameters, layer distributions and respective thicknesses with best efforts did *not* yield an improvement – instead, the prediction even deviated slightly more from the best fit extrapolation. The *possible* causes for this are threefold. Firstly, local spatial variability in subsurface structure and soil properties may have remained undetected and unquantified due to the large probing and sampling intervals (refer back to section 4.4.1). Secondly, this location was at furthest distance (more than a kilometre) from the area where soil samples for compressibility parameter determination were taken. Thirdly, especially considering that the soil was less compressible than expected, it cannot be excluded that the soil might have experienced some preloading in the past: since it is an agricultural area, it is possible that a farmer has had stored machinery, hayballs, or just a heap of soil for fill purposes on that location.

4.4.3.4 Case-specific findings Leendert de Boerspolder

Ultimately, the Leendert de Boerspolder is evaluated. After having gone through the process of soil parameter determination from compression tests, the geometry was designed in *D-Settlement*, and the settlement predictions – or rather reconstructions – over the past 365 years were performed using the NEN-Bjerrum and a,b,c-Isotachs models. Both models were used with and without the "maintain profile" function, requiring a different dike height, as explained in section 4.2.4. Furthermore, the peat properties were distinguished based on their test method, back then erroneously thought to both originate from the polder – however IL tests turned out to be conducted on material from below the slope of the dike.

Regarding the two different models separately, it is observed that the NEN-Bjerrum model generally gives a surprisingly accurate reconstruction of the actual final settlement, with a slight overestimation of only 8.6 to 12.3% after 365 years. The a,b,c-Isotachs model, on the other hand, generally gives not very accurate results, with an overestimation of 12.8% at best, up to 28.1%.

From a theoretical viewpoint, this is somewhat startling, since the a,b,c-Isotachs model is considered to be theoretically more sound, for large part due to the natural strains formulation. However these findings are in agreement with settlement predictions and analyses performed in the course of the Geo-Impuls research programme [Ammerlaan & Hoefsloot, 2012], which also found that a,b,c-Isotachs predictions tend to overestimate the settlements.

Regarding the different modelling approaches of whether or not using the practically very convenient "maintain profile" function, it is seen that for the same boundary conditions and knowing the final settlement on beforehand, the "maintain profile" function in *D-Settlement* tends to slightly overestimate the settlement and thus the required surplus height. For the predictions without "maintain profile", the total dike height was derived from CPT profiles as mentioned previously (section 4.2.5). By doing so, however, it is implicitly assumed that the dike body itself has not compacted, which is known to be unrealistic in particular for a man-made clay/peat/sand soil mixture. However the *settlement* was validated with respect to the dike's *bottom* profile, i.e. at the original polder ground surface, and the final surcharge load (total weight of the dike) would not have been much different either way or the other: the *unit* weight may have increased due to compaction, the *total* weight however would have not changed much except from the expelled pore water.

As a final remark, from the *D-Settlement* "Time-History" curves in Appendix J it can be observed that primary settlement is finished after merely a few months, i.e. within a fraction of the dike's total lifetime, and that the settlement during all of the remaining time is governed by creep. The (decreasing) creep rate can be estimated from these settlement curves and is in that way found to amount between 0.4 and 0.5 cm per decade *at present*.

5 Summary and conclusions

The final part of this thesis comprises a general comprehensive summary of the work done and the findings obtained, followed by the conclusions stating pointwise how and to what extent the research goal and objectives are met.

5.1 Summary

Organic soft soils pose technical challenges in construction industry due to their extraordinary compressibility and deformability, which is an issue of particular relevance in the densely populated Netherlands, of which more than half of the land surface is covered by such soft soils. Uncertainty and variability in settlement predictions for constructions on soft soils are very large, however. Therefore it was desired to assess the accuracy of different settlement prediction methods, as well as to investigate the possible causes of uncertainty and variability, in order to designate the best performing one-dimensional settlement prediction method with an optimum balance between accuracy, usability and time investment.

In the course of this research, a total of seven models or methods for the prediction of settlements were thoroughly reviewed by literature study in chapter 3.2. It has become clear that some methods can be considered obsolete (Terzaghi, Buisman), whereas others are still commonly used despite significant shortcomings (Koppejan). Some seem to be promising but are widely unknown and lacked validation (Fokkens), and others do not offer a full settlement prediction capability, but rather provide simpler ways of determining soil parameters for existing models (De Glopper). The most recently developed models theoretically provide the most complete and universal descriptions of soil compression behaviour, especially on the long term (Bjerrum, Den Haan).

Subsequently also a literature review regarding the reliability of settlement predictions, considering all phases from early desk study until construction and monitoring, was performed (chapter 3.3). This was as a whole mainly based on an earlier publication by CROW (2004), expanded with additional relevant remarks and findings from other literature. In the course of this literature review many possible sources of error and uncertainty have been identified, which were addressed per sequential phase in the settlement prediction process. One of the most essential phases appears to be the investigation phase, comprising site investigation, sampling, testing and data interpretation. Special attention regards the amount of site investigation points and geological features to be expected or potentially being overlooked, as well as the importance of ensuring soil sample saturation and limiting sample disturbance (subsection 3.3.3.5). Several considerable pitfalls were furthermore identified in the schematisation phase, partly related to data interpretation based on inadequate site investigation, and in the calculation and modelling phase, including personal judgement, choices and assumptions, and model limitations with regard to one-dimensional vs. multi-dimensional deformations. Shortcomings in site investigation and schematisation errors were also encountered in the course of the case study and the settlement analysis of Amstelhoek.

A number of settlement prediction methods and models were selected to investigate and validate in detail on the basis of actual field measurements. These include in particular: De Glopper (in combination with Koppejan) and Fokkens. The Koppejan model on itself has been validated already in a previous study regarding a trial mounds research project in the Boemendalerpolder (section 4.1.1). It was found that De Glopper's empirical correlation to determine the Koppejan coefficients can be considered as much too unreliable for practical use, for peat and even more for other soil types. The Fokkens method was validated and found to mostly have a (very) poor accuracy – depending on the specific variation of the formula used. Only two (related) versions of the formula yielded acceptable results, however considering its general practical limitations, this method is deemed of very little practical value in present time.

In addition, also several natural unit weight correlations for a,b,c-isotachs compression parameters of peat were validated with respect to both laboratory values and settlement measurements (subsection 4.4.2.2). The a,b,c parameter correlations were found to be of variable accuracy. Parameter *b* could on average be very accurately estimated on the basis of the natural unit weight. The results of the correlations for parameter *c* showed slightly more variation and uncertainty, but after cleaning of laboratory data outliers and proposition of a correction formula were still found to be practically useful. Parameter *a*, in contrast, showed very large deviations (overestimations up to 52% for averaged parameter sets) with respect to laboratory values, the latter which on themselves also showed remarkable mutual variations. Settlement predictions using these parameters, validated on field measurements, confirmed that these parameters also caused significant overestimations of settlements. It appears that not just by correlations, but also by laboratory testing, determination of parameter *a* is difficult and has a limited reliability. In any case the correlations for parameter *a* can best be disregarded. Apart from the variable accuracy, unit weight compressibility correlations cannot be used standalone for settlement predictions due to the lack of knowledge of preconsolidation and hydraulic properties.

Finally, the isotache models of Bjerrum and Den Haan were put to the test by back-analysis of the settlement of a more than 350 years old dike in the Leendert de Boerspolder, on the basis of soil compressibility parameters that were mostly personally determined from raw soil compression test data. In advance of the laboratory test interpretation and soil parameter determination, a critical review of the different soil compression test methods, their requirements, limitations and advantages was done (chapter 3.1). Subsequently, difficulties were encountered with the determination of the coefficient of consolidation (subsection 4.4.2.4) and the preconsolidation pressure, the latter of which was tried to be determined by four different methods that were evaluated and compared mutually (subsection 4.4.2.3). It was found that Butterfield’s method yields results that are most similar to the common Casagrande method, but the former is slightly easier to apply and therefore definitely worth being taken into consideration.

With these parameters, a settlement reconstruction of the aforementioned dike at the Leendert de Boerspolder was performed by modelling in *D-Settlement*. It was found that the NEN-Bjerrum model produced the most accurate and in fact absolutely acceptable results with a slight overestimation of merely 8-12%. The a,b,c-Isotachs model in contrast produced significantly larger overestimations of 13-29%. Although some peculiarities in the test data and results raised questions about the reliability of soil parameters, the used compression coefficients at least were in close agreement with professionally obtained (K_0-CRS) parameters.

Regarding soil compression tests, three different test methods were reviewed and compared: the conventional “incremental loading” (IL) oedometer test, the constant-rate-of-strain (CRS) test and the K_0-CRS test. The main advantages of IL oedometer tests are that the equipment is relatively simple and cheap, and the fact that only with this device the Koppejan compression coefficients can be determined. On the other hand, CRS test setups offer better control of the test process, pore pressure measurement and hence the possibility to calculate directly the consolidation and/or permeability properties, and last but not least a much shorter total test duration, potentially reducing costs on the long term. The K_0-CRS test is a further development of the CRS test providing additionally measurement of the neutral lateral earth pressure coefficient, which is not directly of use in 1D settlement predictions, however.

5.2 Conclusions

In the following paragraphs first the six research objectives, as presented in chapter 1.2, are addressed pointwise in order to finally provide answer to the main goal.

1) Of the seven settlement prediction methods that were reviewed and compared, the methods of Terzaghi and Keverling Buisman can be considered obsolete, having too many known limitations and shortcomings. The method of **Koppejan**, although still frequently applied, also has several considerable limitations, such as the fact that unloading cannot be modelled correctly. The use of a natural strain “correction” makes little sense as long as the compression coefficients were determined on the basis of linear strain. Furthermore, determination of the Koppejan coefficients can be done only on the basis of conventional (IL) oedometer tests and requires more calculation steps than parameters for other contemporary settlement prediction models. The other methods were selected for further analysis and validation, to be addressed at the next point.
2) **De Glopper**’s method is not a settlement prediction method on itself, but merely an empirical correlation for determining the Koppejan coefficients of peat soil – however with a very low reliability and with several other limitations, which is why use of De Glopper’s relationship is strongly discouraged. The method of **Fokkens** exists in six different variations, or formulas, of which only two (related) formulas yielded reasonable final settlement estimations for peat – for other soil types unsurprisingly their performance was very poor. However considering the general practical limitations associated with this method, it is deemed of very little practical value in present time.
   Bjerrum and **a,b,c-Isotachs** models were validated on the Leendert de Boerspolder based on compressibility parameters that were mostly personally obtained from raw laboratory test data. Considering a total settlement time period of 365 years, the final settlement modelled with NEN-Bjerrum was most accurate within just +12% of the actual final settlement, whereas the a,b,c-Isotachs model yielded an overestimation of 13-29%. Significant initial overestimation of settlements by the a,b,c-Isotachs was also found during previous settlement prediction validations as part of the Geo-Impuls research programme.
3) Although correlations and empirical formulas (e.g. De Glopper, Fokkens and unit weight correlations) are relatively quick and easy to use, they mostly have such significant practical limitations, apart from their variable or downright poor accuracy, that the use of such methods is generally discouraged. Merely the most “empirical” formulation of **Fokkens**’ method was found to offer a rough yet still practically useful *indicative* method of estimating the *final* settlement (considering a period of about 30 years) for fibrous to pseudo-fibrous *peat* – and for such soil only. In regular engineering projects, however, applicability to different soil types and to complex geometries, loading and unloading scenarios, and creep settlement are must-have functionalities, for which only more comprehensive stress- *and* time-dependent settlement prediction models can be used. As of now, only the models of **Bjerrum** and Den Haan (**a,b,c-Isotachs**) provide such full functionality in 1D, which are very similar with regard to their practical usability and which are also theoretically related.
4) Many sources of error, uncertainty and variability were identified on the basis of a comprehensive literature review regarding specifically the reliability of settlement predictions. The most important error-prone phases or processes identified are: **site investigation**, **sampling and testing** (with special emphasis on sample disturbance and the need of ensuring full saturation of soil samples to be tested), **data interpretation** (e.g. parameter determination), **schematisation** (subsurface structure and general geometry, material properties attribution) and **calculation and modelling** (including simplifying assumptions and the choice of 1D vs. 2D or 3D calculation models).
   From experience gained with soil parameter determination in the course this research, is was found that in particular the determination of the **preconsolidation pressure** as well as of the **coefficient of consolidation** were ambiguous, subjective and prone to errors, both known to influence strongly the modelled soil compression behaviour and thus settlement

predictions. In general, soil parameter determination is a meticulous task, results of which are strongly dependent also on the quality of the data and the quality of the tested soil specimens, both which can vary a lot but which are difficult to assess in retrospect.

5) The conventional "incremental loading" (IL) oedometer is technically relatively simple and cheap, and only with this device the Koppejan compression coefficients can be determined. On the other hand, constant-rate-of-strain (CRS) test setups offer better control of the test process, short-interval pore pressure measurement and hence the possibility to calculate directly the consolidation and/or permeability properties, and last but not least a much shorter total test duration (2-3 days, versus 1-2 weeks for IL tests), potentially reducing costs on the long term. The K_0-CRS test is a further development of the CRS test providing additionally measurement of the neutral lateral earth pressure coefficient, which is not directly of use in 1D settlement prediction models, however.
   Determination of consolidation and hydraulic properties is possible for all types of tests, albeit with different methods, but was found in all cases to be a likely source of errors and uncertainties due to subjectivity or due to formulas yielding peculiar results.
6) Key to the **improvement** of accuracy of settlement predictions is **quality assurance and control** of all steps in the geotechnical design. This follows in particular from a literature study regarding the reliability of settlement predictions, as well as from case studies and from experience gained with soil compression test data analysis and interpretation. In particular the investigation phase, from desk study to data interpretation, forms the basis which all subsequent geotechnical calculations and design decisions rely on. Integrity of soil specimens and adequate and consistent testing procedures are an integral part of this. However time and money are often the primary factors putting a limit on the thoroughness and quality of work during phases of which the results and value are not directly "visible" or do not immediately pay off within a project. Still, allocating more resources to geotechnical investigation can only decrease uncertainty and risk in later stages of a project.
   It may as well help to update existing or to develop new standards for laboratory testing equipment, procedures *and* interpretation. The latter concerns for example CRS tests, which are described neither in NEN nor in Eurocode standards yet.

Finally, the best performing 1D settlement prediction method with an optimum balance between accuracy, usability and time investment, is to be designated. This cannot be done without some reservation, however, since the information and data that were used are acknowledged to have limitations, shortcomings and even errors that could not always be resolved or circumvented.

After disregarding the soil compressibility parameter correlations and the method of Fokkens because of their unreliability or limitations, just the Bjerrum and a,b,c-Isotachs models remain. The Koppejan method on itself is not validated during this research, but based on literature review and case studies cannot be considered to be of advantage with regard to either accuracy, usability or time investment, in comparison to Bjerrum or a,b,c-Isotachs.

Theoretically, the a,b,c-Isotachs model provides the most sound and versatile description of soil behaviour upon compression as well as unloading, as a function of time and stress, in a natural strain formulation. The a,b,c-Isotachs is based on the Bjerrum model, which both are very similar with regard to their practical usability and functionality.

However based on the results obtained during this research, focussing on long-term final settlements, the (NEN-) **Bjerrum** model yielded better results in practice. Although the final settlement includes the contribution of the primary or consolidation settlement, the time-development of this phase could not be validated for the Leendert de Boerspolder.

5.3 Recommendations

Ultimately some recommendations for further research are given in this chapter.

First of all, the observed differences between settlement predictions using a,b,c-Isotachs and Bjerrum (both from own and from previous research) have raised questions about why these significant differences occur and why just the a,b,c-Isotachs model gives the largest overestimations of settlement, whereas due to the use of natural strains the contrary may be expected. It would be valuable to know in more detail the theoretical and practical causes for the differences between these two models.

Secondly, the difference between 1D vs. 2D and 3D settlement analysis is hardly investigated in detail yet. It is desired to know precisely to what extent (quantitatively) the geometrical dimensions of earth fills or embankments are related to 2D and 3D effects of soil deformation, in order to find the dimensions for which 2D and 3D effects can be neglected, and the dimensions for which it is more appropriate to use a 2D or 3D model.

Thirdly, settlement predictions would benefit from a (better) quantification of the influence of sample disturbance on soil strength and compressibility parameters. Additionally, the designation or new development of an easy-to-use, widely acceptable and validated method of assessing and correcting for such disturbance is needed.

Fourthly, there is a need to make geotechnical laboratory testing more reliable, which might partly relate to soil sample integrity and partly to test procedures and operation themselves. It can also be thought of developing or updating standards by addition of descriptions or guidelines for the most modern testing methods *and* subsequent data interpretation.

Lastly, from this research and after discussions with colleagues at *Sweco Nederland* it was found that there is desire to have a correlation for preconsolidation properties, such as OCR, of *peat* on the basis of Cone Penetration Tests, which so far is known to exist only for clay.

References

Adams, A.L. (2011). *Laboratory evaluation of the Constant Rate of Strain and Constant Head techniques for measurement of the hydraulic conductivity of fine grained soils* (MSc thesis). Retrieved from https://dspace.mit.edu/handle/1721.1/66859.

Alink, E. (2012). *Rapport betreffende Proefterpen Project Bloemendalerpolder te Weesp: Grondonderzoek, laboratoriumonderzoek en plaatsing van instrumentatie* (report No. 3009-0261-000.R02v3). Leidschendam, The Netherlands: Fugro GeoServices.

Ammerlaan, P.R.M. (2011). *Zettingspredicties betreffende Proefterpen Project Bloemendalerpolder te Weesp* (report No. 3009-0261-000.R03v1). Leidschendam, The Netherlands: Fugro GeoServices.

Ammerlaan, P.R.M. & Hoefsloot, F.J.M. (2012). *Rapport betreffende Evaluatie zettingsmodellen project Bloemendalerpolder te Weesp* (report No. 3009-0261-000.R04 c1). Leidschendam, The Netherlands: Fugro GeoServices.

ASTM D4186 (1989). *Standard test method for one-dimensional consolidation properties of soils using controlled-strain loading*. Philadelphia, Pennsylvania, USA: American Society for Testing and Materials.

Bartlett, S.F. (2005). *Constant rate of strain (CRS) consolidation tests* (lecture notes). Salt Lake City, Utah, USA: University of Utah.

Bartlett, S.F. & Alcorn, P. (2004). *Estimation of preconsolidation stress and compression ratio from field and laboratory measurements from the I-15 reconstruction project, Salt Lake City, Utah* (report No. UT-03.20). Salt Lake City, Utah, USA: University of Utah.

Becker, D.E., Crooks, J.H.A., Been, K. & Jefferies, M.G. (1987). Work as a criterion for determining in situ and yield stresses in clays. *Canadian Geotechnical Journal*, 24, pp. 549-564.

Bell, F.G. (2007). *Engineering Geology* (2nd ed.). Oxford, UK: Butterworth-Heinemann.

Berendsen, H.J.A. (2008). *De vorming van het land: inleiding in de geologie en morfologie* (5th ed.). Assen, The Netherlands: Van Gorcum B.V.

Bjerrum, L. & Lo, K.Y. (1963). Effect of aging on the shear-strength properties of a normally consolidated clay. *Norwegian Geotechnical Institute Publication*, (57), pp. 147-157.

Bjerrum, L. (1967). Engineering geology of Norwegian normally-consolidated marine clays as related to settlements of buildings. *Géotechnique*, 17(2), pp. 83-118.

Boekhorst, C. (2010). *N201 Omlegging Amstelhoek: Monitoringsplan Aardebaan* (internal report, project No. 10018). Woerden, The Netherlands: VWS Geotechniek.

Booltink, M., De Haas, G., Jak, S., Jaspers, H., Van Voorden, H. & Voskens, M. (2005). *Milieueffectrapportage N201 Utrecht, Passage Amstelhoek* (report No. 13/99052528/HO rev.D1). Houten, The Netherlands: Grontmij Nederland B.V.

Buisman, A.S.K. (1940). *Grondmechanica*. Delft, The Netherlands: Waltman.

Butterfield, R. (1979). *A natural compression law for soils (an advance on e-log p')* (Technical Note). Southampton, UK: Southampton University.

CBS: Centraal Bureau voor de Statistiek (2016). *Figures*. Retrieved 6 April 2016, from https://www.cbs.nl/en-gb/figures.

Chakrabarti, S. & Horvath, R.G. (1986). Conventional consolidation tests on two soils. *Consolidation of Soils: Testing and Evaluation. ASTM Special Technical Publication 892*, pp. 451-464.

CIA: Central Intelligence Agency (2016). *The World Factbook: Netherlands*. Retrieved 6 April 2016, from https://www.cia.gov/library/publications/the-world-factbook/geos/nl.html.

Clayton, C.R.I. & Hight, D.W. (2007). Laboratory testing of natural soils – Some factors affecting performance. *Characterisation and Engineering Properties of Natural Soils*, Vol. 3, pp. 1535-1599.

Cools, P.M.C.B.M. (2011). Geo-Impuls: 'Halvering geotechnisch falen in projecten in 2015'. *Geotechniek*, October 2011, pp. 24-28.

CROW (2004). *Betrouwbaarheid van zettingsprognoses* (report No. 204). Ede, The Netherlands: CROW.

CUR: Civieltechnisch Centrum Uitvoering Research en Regelgeving (1996). *Building on soft soil*s (English translation of CUR report No. 162). Rotterdam, The Netherlands: Balkema.

CUR: Civieltechnisch Centrum Uitvoering Research en Regelgeving (2003). *Bepaling geotechnische parameters* (report No. 2003-7). Gouda, The Netherlands: CUR.

De Glopper, R.J. (1979). Het verband tussen de samendrukkingsconstanten en het poriëngehalte in de afzettingen in het IJsselmeergebied. *Cultuurtechnisch Tijdschrift*, 19(2), pp. 73-80.

Deltares (2014). *D-Settlement. Embankment design and soil settlement prediction. User Manual Version 14.1.34525*. Delft, The Netherlands: Deltares.

Deltares (2015). *LdB proeven K0-CRS measurement* (internal laboratory test reports, project No. 1210215). Delft, The Netherlands: Deltares.

Den Adel, H. & Van, M.A. (2002). *Uitwerking K_0-CRS-proef, bepaling abc-parameters* (report No. 01.04.02-58). Delft, The Netherlands: Delft Cluster.

Den Haan, E.J. (1992). Denkraam voor samendrukking van verknede en natuurlijke klei: Nieuw a-b-c-vereenvoudigt berekening zetting. *Land+Water*, March 1992, pp. 25-29.

Den Haan, E.J. (1994). *Vertical compression of soils* (Dissertation). Retrieved from http://repository.tudelft.nl/view/ir/uuid:b8dc88e0-f400-4d86-9a2e-4e00b68d0472/.

Den Haan, E.J. (1996). A compression model for non-brittle soft clays and peat. *Géotechnique*, 46(1), pp. 1-16.

Den Haan, E.J. (2001). *Interpretatie meetdata K_0-C.R.S. - apparaat* (report No. CO-710203/22). Delft, The Netherlands: GeoDelft.

Den Haan, E.J. (2003). Het a,b,c-isotachenmodel: hoeksteen van een nieuwe aanpak van zettingsberekeningen. *Geotechniek*, October 2003, pp. 28-35.

Den Haan, E.J. (2008). De intrinsieke tijd in het isotachenmodel. *Geotechniek*, January 2008, pp. 34-38.

Den Haan, E.J. & Kamao, S. (2003). Obtaining isotache parameters from a C.R.S. K_0-oedometer. *Soils and Foundations*, 43(4), pp. 203-214.

Den Haan, E.J. & Kruse, G.A.M. (2007). Characterisation and engineering properties of Dutch peats. *Characterisation and Engineering Properties of Natural Soils*, Vol. 3, pp. 2101-2133.

Den Haan, E.J. & Molendijk, W.O. (2002). *Voorspelling restzettingen met het a,b,c isotachenmodel Betuweroute* (report No. 071.04.02-76). Delft, The Netherlands: Delft Cluster.

Den Haan, E.J., The, B.H.P.A.M. & Van, M.A. (2001). De K_0-C.R.S. samendrukkingsproef. *Geotechniek*, October 2001, pp. 55-63.

Den Haan, E.J., Van Essen, H.M., Visschedijk, M.A.T. & Maccabiani, J. (2004). Isotachenmodellen: help, hoe kom ik aan de parameters? *Geotechniek*, January 2004, pp. 62-69.

De Ronde Venen (2014). *Vrijdag 16 mei aquaduct Amstelhoek N201 open (15-05-2014)*. Retrieved 31 March 2016, from http://www.derondevenen.nl/actueel/nieuwsberichten_253/item/vrijdag-16-mei-aquaduct-amstelhoek-n201-open_26806.html.

Fokkens, B. (1970). Berekening van de samendrukking van veenlagen uit het gehalte aan organische stof en water. *De Ingenieur: Bouw- en Waterbouwkunde*, 82(13), pp. 23-28.

Freed, A.D. (1997). *Natural strain*. Cleveland, Ohio, USA: NASA Glenn Research Center.

Fröhlich, O.K. (1934). *Druckverteilung im Baugrunde mit besonderer Berücksichtigung der plastischen Erscheinungen*. Vienna, Austria: Verlag von Julius Springer.

Garlanger, J.E. (1972). The consolidation of soils exhibiting creep under constant effective stress. *Géotechnique*, 22(1), pp. 71-78.

Geonet (2016a). *Over Geo-Impuls*. Retrieved 8 March 2016, from http://www.geonet.nl/geoimpuls2.

Geonet (2016b). *Pilotproject: Proefterpen*. Retrieved 8 March 2016, from http://www.geonet.nl/684.

Gorman, C.T., Hopkins, T.C., Deen, R.C. & Dmevich, V.P. (1977). *Constant-Rate-of-Strain and Controlled-Gradient Consolidation Testing* (report No. 478). Frankfort, Kentucky, USA: Kentucky Department of Transportation.

Head, K.H. (1994). *Manual of Soil Laboratory Testing. Volume 2: Permeability, Shear Strength and Compressibility Tests* (2nd ed.). New York, USA: John Wiley & Sons, Inc.

Heemstra, J. (2013). Met Buisman naar de isotachen. *Geotechniek*, April 2013, pp. 30-33.

Hoefsloot, F. (2011). GeoImpuls - Langetermijnmetingen en modelvalidatie Proefterpen Bloemendalerpolder. *Geotechniek*, December 2011, pp. 36-39.

Hoefsloot, F.J.M. & Schadee, L.W. (2013). *Rapport betreffende Meetresultaten Proefterpen Bloemendalerpolder te Weesp* (report No. 3009-0261-000.R05_v2). Leidschendam, The Netherlands: Fugro GeoServices.

Huat, B.B.K, Prasad, A., Asadi, A. & Kazemian, S. (2014). *Geotechnics of organic soils and peat*. Leiden, The Netherlands: CRC Press/Balkema.

Jommi, C., Muraro, S, Ponzoni, E. & Zhao, H (2015). *Leendert de Boerspolder. Preliminary characterisation of the site: summary of main data from the laboratory tests performed at TU Delft* (internal report, rev.1). Delft, The Netherlands: TU Delft.

Knappett, J.A. & Craig, R.F. (2012). *Craig's Soil Mechanics* (8th ed.). Abingdon, UK: Spon Press.

Koppejan, A.W. (1948). A formula combining the Terzaghi load-compression relationship and the Buisman secular time effect. *Proceedings of the 2nd International Conference on Soil Mechanics and Foundation Engineering*, Rotterdam, Vol. 3, pp. 32-37.

Kulhawy, F.H. & Mayne, P.W. (1990). *Manual on estimating soil properties for foundation design* (report No. EL-6800). Ithaca, New York, USA: Cornell University.

La Fors, G. & Dercksen, B. (2006). *Bestemmingsplan Omlegging N201 De Ronde Venen; voorontwerp* (report No. 13/99070946/RJ rev.D1). Waddinxveen, The Netherlands: Grontmij Nederland B.V.

Luyten, B. (2011). *Algemeen Tijd Schema N201+ 'Omlegging Amstelhoek', Bestek 2496* (internal report No. 4106000-ATS-20110408). The Netherlands: Combinatie KWS – vH&B.

Mesri, G. & Godlewski, P.M. (1977). Time and stress-compressibility interrelationship. *Journal of the Geotechnical Engineering Division, ASCE*, 103(5), pp. 417-430.

Mesri, G., Stark, T.D., Ajlouni, M.A. & Chen, C.S. (1997). Secondary compression of peat with or without surcharging. *Journal of Geotechnical and Geoenvironmental Engineering*, 123(5), pp. 411-421.

Mesri, G. & Ajlouni, M.A. (2007). Engineering properties of fibrous peats. *Journal of Geotechnical and Geoenvironmental Engineering*, 133(7), pp. 850-866.

Meulblok, C.M. & Forger, L.R. (2009). *N201 Omlegging Amstelhoek: Geotechnisch advies wegen DO* (internal report, project No. 232592). De Bilt, The Netherlands: Grontmij Nederland B.V.

Monker, E. (2008a). *N201 Omlegging Amstelhoek Situatietekening: Definitief Ontwerp, Blad 1* (plan No. N201-21661-41-11-01_B). De Bilt, The Netherlands: Grontmij Nederland B.V.

Monker, E. (2008b). *N201 Omlegging Amstelhoek Situatietekening: Definitief Ontwerp, Blad 2* (plan No. N201-21661-41-11-02_B). De Bilt, The Netherlands: Grontmij Nederland B.V.

Neher, H.P. (2008). *Zeitabhängiges Materialverhalten und Anisotropie von weichen Böden – Theorie und Anwendung* (Dissertation). Retrieved from http://www.uni-stuttgart.de/igs/content/publications/IGS_Dissertationen/Diss-Neher.pdf.

NEN 5104 (1989). *Geotechniek - Classificatie van onverharde grondmonsters*. Delft, The Netherlands: Nederlands Normalisatie Instituut.

NEN 5118 (1991). *Geotechniek - Bepaling van de een-dimensionale samendrukkingseigenschappen van de grond*. Delft, The Netherlands: Nederlands Normalisatie Instituut.

NEN 6740 (2006). *Geotechniek - TGB 1990 - Basiseisen en belastingen*. Delft, The Netherlands: Nederlands Normalisatie Instituut.

NEN-EN-ISO 14688-1+A1+C11 (2016). *Geotechnisch onderzoek en beproeving - Identificatie en classificatie van grond - Deel 1: Identificatie en beschrijving*. Delft, The Netherlands: Nederlands Normalisatie Instituut.

NEN-EN-ISO 14688-2+A1+C11 (2016). *Geotechnisch onderzoek en beproeving - Identificatie en classificatie van grond - Deel 2: Grondslagen voor een classificatie*. Delft, The Netherlands: Nederlands Normalisatie Instituut.

Ngan-Tillard, D.J.M., Brinkgreve, R.B.J., Huisman, D.J., Van Meerten, H., Müller, A. & Van Kappel, K. (2016). *Tools for predicting damage to archaeological sites caused by one-dimensional loading. Conservation and management of archaeological sites*. Manuscript submitted for publication.

Papadaki, E. (2013). *Modelling of peat compressed under sand bodies: Experimental and numerical approach* (MSc thesis). Retrieved from http://repository.tudelft.nl/view/ir/uuid:faf79020-4c07-4931-9bf6-dcdbe491bca8/.

Pons, L.J. & Zonneveld, I.S. (1965). *Soil ripening and soil classification: Initial soil formation in alluvial deposits and a classification of the resulting soils*. Wageningen, The Netherlands: H. Veenman & Zonen N.V.

Prasad, K.N., Triveni, S., Schanz, T. & Nagaraj, L.T.S (2007). Sample disturbance in soft and sensitive clays: Analysis and assessment. *Marine Georesources and Geotechnology*, 25, pp. 181-197.

Provincie Noord-Holland (1999). *Omlegging N201 om Aalsmeer: Startnotitie MER* (report No. P1019-02). Haarlem, The Netherlands: Provincie Noord-Holland.

Provincie Noord-Holland (2001). *De Milieueffectrapportages in de corridor N201: Samenhang en actualisatie* (report No. P1019-95). Haarlem, The Netherlands: Provincie Noord-Holland.

Reddy, B.K., Sahu, R.B. & Ghosh, S. (2015). Constant rate of strain consolidation of organic clay: in Kolkata region. *International Journal of Geotechnical Engineering*, 9(5), pp. 471-482.

Robertson, P.K. & Cabal, K.L. (2015). *Guide to Cone Penetration Testing for Geotechnical Engineering* (6th ed.). Signal Hill, California, USA: Gregg Drilling & Testing, Inc.

Rocscience Inc. (2009). *Settle3D. Settlement and consolidation analysis. Theory Manual*. Toronto, Canada: Rocscience Inc. Retrieved from http://rocscience.com/help/settle3d/webhelp/pdf_files/theory/Settle3D_Theory.pdf.

Rohe, A. (2010). Lange termijn meting van zettingen Proefterpen Bloemendalerpolder. *'D'*, December 2010, pp. 12-13.

Saint-Exupéry, de A. (1999). *Le Petit Prince*. Paris, France: Éditions Gallimard.

Schadee, L.W. (2012). *Paalfundaties onderworpen aan tijdsafhankelijke horizontale belastingen door zachte bodems* (MSc thesis). Retrieved from http://repository.tudelft.nl/view/ir/uuid:ef8b8914-a3cd-4cbc-a5c0-d3ced832580e/.

Schothorst, C.J. (1977). Subsidence of low moor peat soils in the western Netherlands. *Geoderma*, 17(4), pp. 265-291.

Siderius, K. (2011). *Tijdsafhankelijke effecten bij door grond horizontaal belaste palen* (MSc thesis). Retrieved from http://repository.tudelft.nl/view/ir/uuid:8e8a92a8-42e1-4cec-92e4-5f34c149fcf8/.

Sipkema, D. (2006). *a,b,c-Isotachenmodel: van a,b,c tot zetting* (MSc thesis). Retrieved from http://repository.tudelft.nl/view/ir/uuid:93945e99-10dc-4e9b-9658-3c467e819c3f/.

Sipkema, D. (2012). *Tussentijdse zettingsprognose / evaluatie daadwerkelijk zettingsgedrag* (report No. 10018-r05). Woerden, The Netherlands: VWS Geotechniek.

Skempton, A.W. & Petley, D.J. (1970). Ignition loss and other properties of peats and clays from Avonmouth, King's Lynn and Cranberry Moss. *Géotechnique*, 20(4), pp. 343-356.

Solanki, C.H. & Desai, M.D. (2008). Preconsolidation from soil index and plasticity properties. *The 12th International Conference of International Association for Computer Methods and Advances in Geomechanics*, Goa, India, pp. 1475-1479.

Soudijn, B.J.J. & De Kock, R.A.J. (1977). *Compendium Geo-Tubomechanica: Deel I Grondmechanica*. 's-Gravenhage, The Netherlands: Provinciale Waterstaat van Zuid-Holland.

STOWA: Stichting Toegepast Onderzoek Waterbeheer (2012). *Onderzoek naar de invloed van veen op de stabiliteit van regionale waterkeringen* (report No. 45). Amersfoort, The Netherlands: STOWA.

STOWA: Stichting Toegepast Onderzoek Waterbeheer (2016). *Leendert de Boerspolder: Achtergronden*. Retrieved 11 May 2016, from http://www.leendertdeboerspolder.stowa.nl/Achtergronden/index.aspx.

Šuklje, L. (1957). The analysis of the consolidation process by the isotaches method. *Proceedings of the 4th International Conference on Soil Mechanics and Foundation Engineering*, London, Vol. 1, pp. 200-206.

TAW: Technische Adviescommissie voor de Waterkeringen (1987). *Veen, een grondmechanisch probleem*. Delft, The Netherlands: TAW.

TAW: Technische Adviescommissie voor de Waterkeringen (1996). *Technisch rapport geotechnische classificatie van veen*. Delft, The Netherlands: TAW.

Terzaghi, K. (1925). *Erdbaumechanik auf bodenphysikalischer Grundlage*. Leipzig und Wien: Franz Deuticke.

Terzaghi, K. & Fröhlich, O.K. (1936). *Theorie der Setzung von Tonschichten*. Leipzig und Wien: Franz Deuticke.

TNO – Geologische Dienst Nederland (2014a). *Diktekaart Holocene slappe lagen Nederland*. Retrieved 8 April 2016, from http://www.cob.nl/kennisbank/webshop/artikel/diktekaart-holocene-slappe-lagen-nederland.html.

TNO – Geologische Dienst Nederland (2014b). *Zettingskaart Nederland*. Retrieved 8 April 2016, from http://www.cob.nl/kennisbank/webshop/artikel/zettingskaart-nederland.html.

Van, M.A., Molendijk, W.O. & Den Haan, E.J. (1997). *Construction on peat and organic soils* (report No. CO-369400/36). Delft, The Netherlands: Delft Geotechnics.

Van Baars, S. (2003). Soft soil creep modelling of large settlements. *2nd International Conference on Advances in Soft Soil Engineering and Technology*, Putrajaya, Malaysia.

Van Essen, H. (2013). *Monsterverstoring: Invloed op geotechnische parameters* (presentation). Geotechniekdag 2013, Breda: Deltares. Retrieved from http://www.sbrcurnet.nl/uploads/attachment_file/368/7_Monsterverstoring_Harry_van_Essen.pdf.

Van Essen, H. (2014). *Monsterverstoring ten gevolge van boortechnieken* (presentation). Deltares. Retrieved 12 January 2016, from http://www.votb.nl/wordpress/wp-content/uploads/2014/05/140422-Monsterverstoring-ten-gevolge-van-boortechnieken-door-Harry-van-Essen-Deltares.pdf.

Van der Valk, M.J.H.T. (2007). *Bijlage C betreffende Geotechnisch Onderzoek N201 Deelproject Omlegging Amstelhoek* (report No. 1006-0181-000.R01; Volume C1, C2 & C3). Leidschendam, The Netherlands: Fugro GeoServices.

Van Veen, A.E. (2015). *Leendert de Boerspolder 4.0. Van landbouwpolder naar waterbergingspolder*. Retrieved 11 May 2016, from http://www.leendertdeboerspolder.stowa.nl/Publicaties/Beheerplan_Leendert_de_Boerspolder__Van_landbouwpolder_naar_waterbergingslocatie.aspx.

Vermeer, P.A. & Neher, H.P. (1999). A soft soil model that accounts for creep. *Proceedings of the International Symposium Beyond 2000 in Computational Geotechnics – 10 Years of PLAXIS International*, Amsterdam, pp. 249-261.

Verry, E.S., Boelter, D.H., Paivanen, J., Nichols, D.S., Malterer, T. & Gafni, A. (2011). Physical properties of organic soils. In: *Peatland Biogeochemistry and Watershed Hydrology at the Marcell Experimental Forest*, pp. 135-176. Boca Raton, Florida, USA: CRC Press.

Visschedijk, M. (2010). Isotachen berekeningen op een sigarendoosje. *Geotechniek*, July 2010, pp. 30-33.

Vos, P. & De Vries, S. (2013). *2e generatie palaeogeografische kaarten van Nederland (versie 2.0)*. Utrecht: Deltares. Retrieved 8 April 2016, from http://archeologieinnederland.nl/bronnen-en-kaarten/paleogeografische-kaarten.

Zwanenburg, C. (2013). Monsterverstoring, de laatste onbekende schakel? *Geotechniek*, April 2013, pp. 14-18.

Master thesis
MSc Applied Earth Sciences

Review and validation of settlement prediction methods for organic soft soils, on the basis of three case studies from the Netherlands

By

Christian Bernhard Houkes

Appendices

APPENDIX A – Palaeogeography of the Netherlands

A1 Palaeogeography and soil maps (1/2)

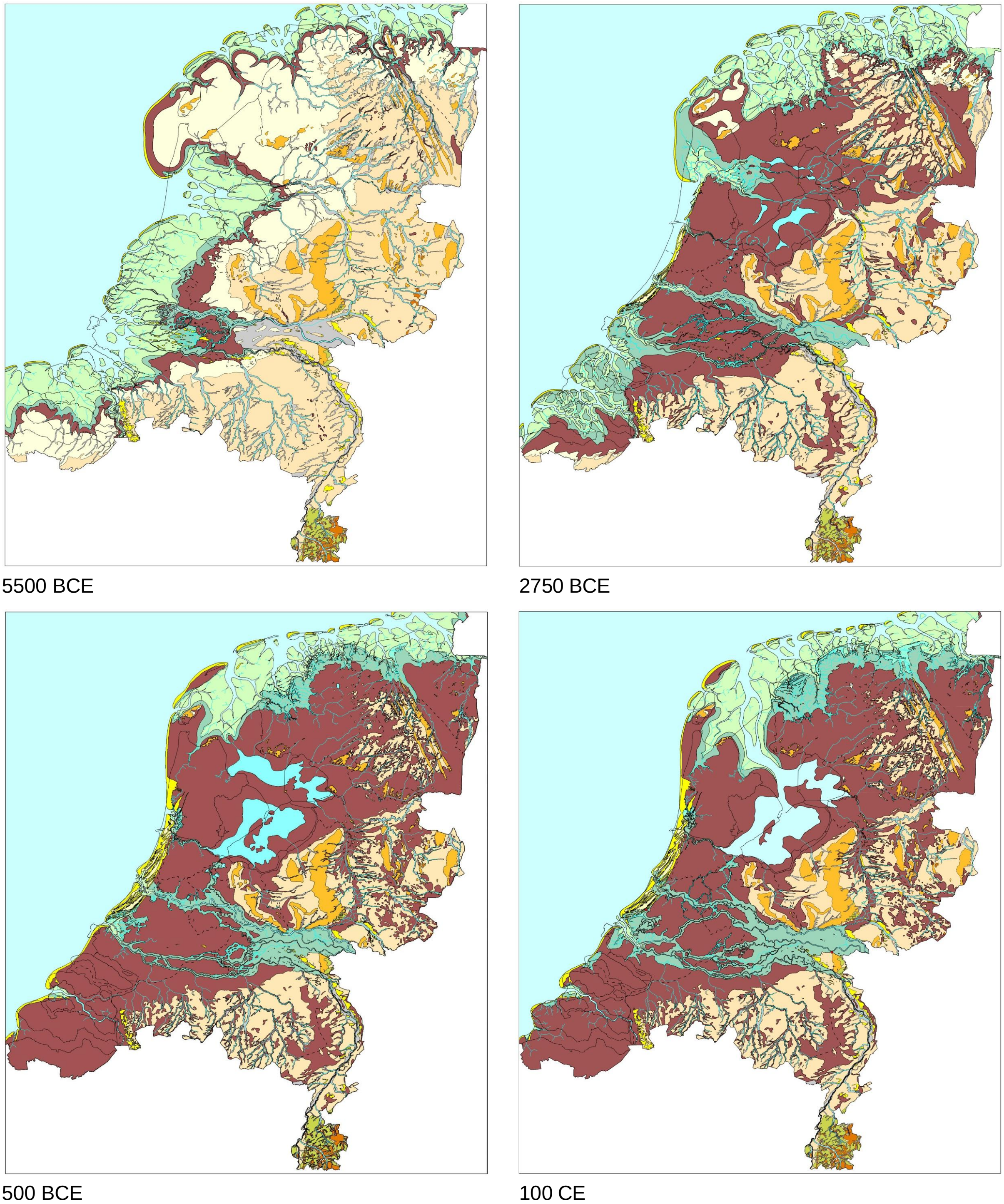

Figure A-1: Series of Holocene palaeogeography and soil maps of the Netherlands, depicting the change in top soil composition over time, from 5500 BCE until 100 CE [Vos & De Vries, 2013]. Brown coloured areas represent peat; the green colour tones indicate tidal or fluvial (flood plain) environments resulting in the deposition of clays. A full legend of colour codes is provided in Appendix A2.

A1 Palaeogeography and soil maps (2/2)

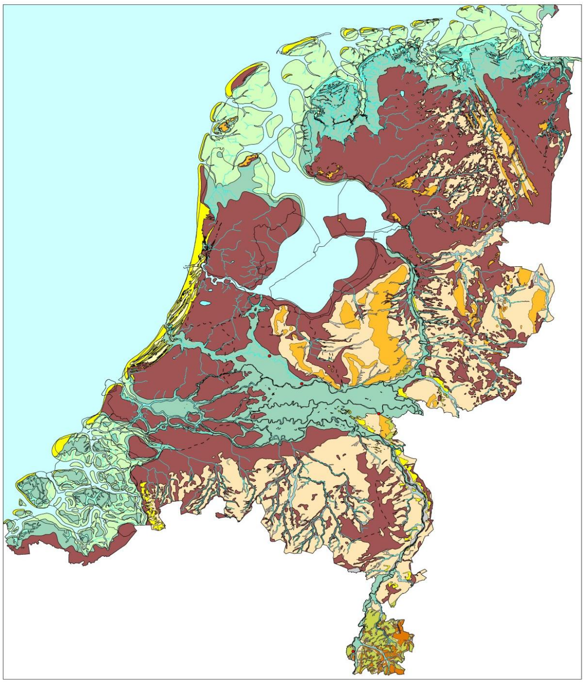

800 CE

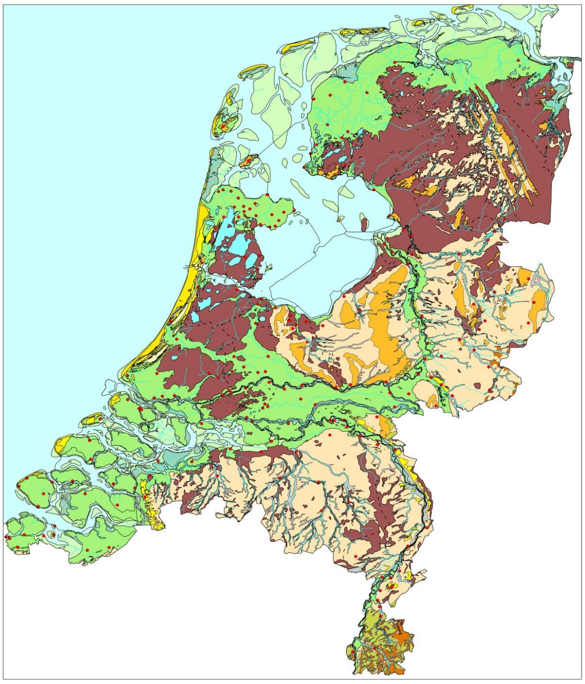

1500 CE

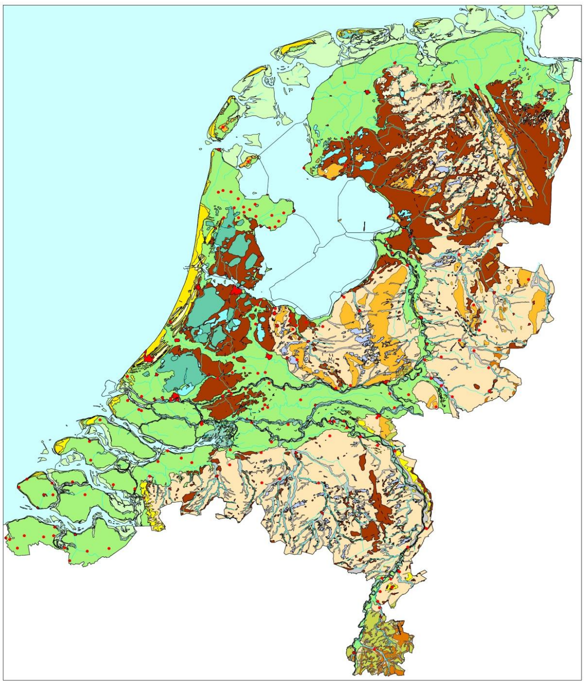

1850 CE

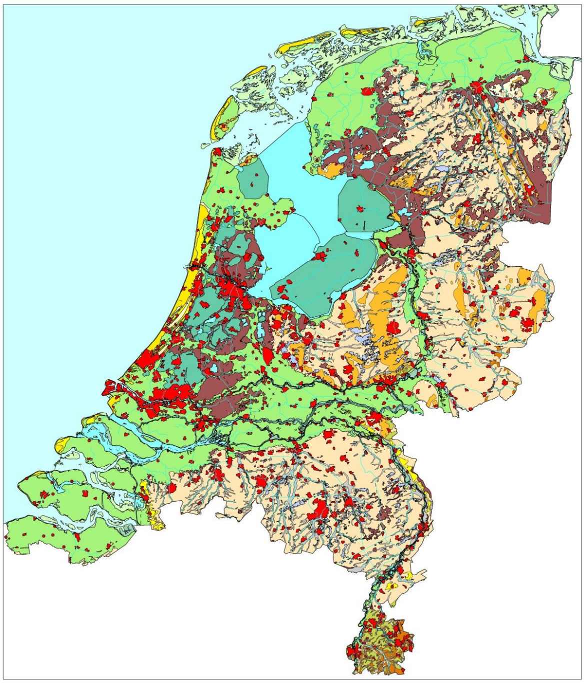

2000 CE

Figure A-2: Series of Holocene palaeogeography and soil maps of the Netherlands, depicting the change in top soil composition over time, from 5500 BCE until 2000 CE (about present day) [Vos & De Vries, 2013]. Brown coloured areas represent peat; the green colour tones indicate deposits of clay. The bright green areas appearing from 1500 CE onward indicate previous flood plains now being protected from flooding by mankind by means of dikes. A full legend of colour codes is provided in Appendix A2.

Note the gradual decrease and fragmentation of peat areas in recent times, which is mainly due to the practice of peat cutting for heating purposes, and due to changes in water management and land use. However this apparent decrease is only surficial, as older and deeper Holocene peat layers most often still exist in these areas.

A2 Legend of colour codes

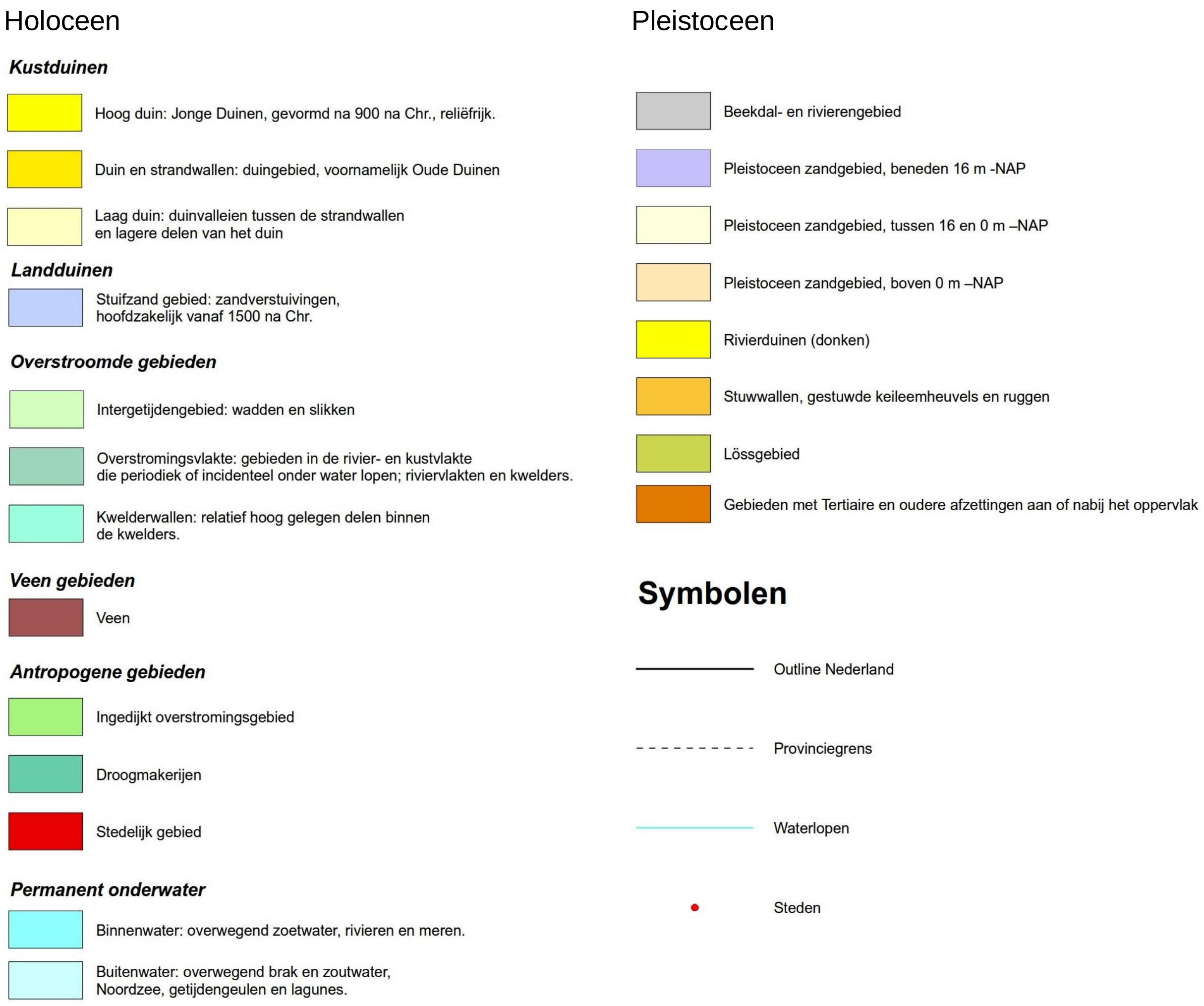

Legend of colour codes concerning the maps in Appendix A1 [Vos & De Vries, 2013].

APPENDIX B – Settlement analysis terminology

B1 Explanatory illustrations

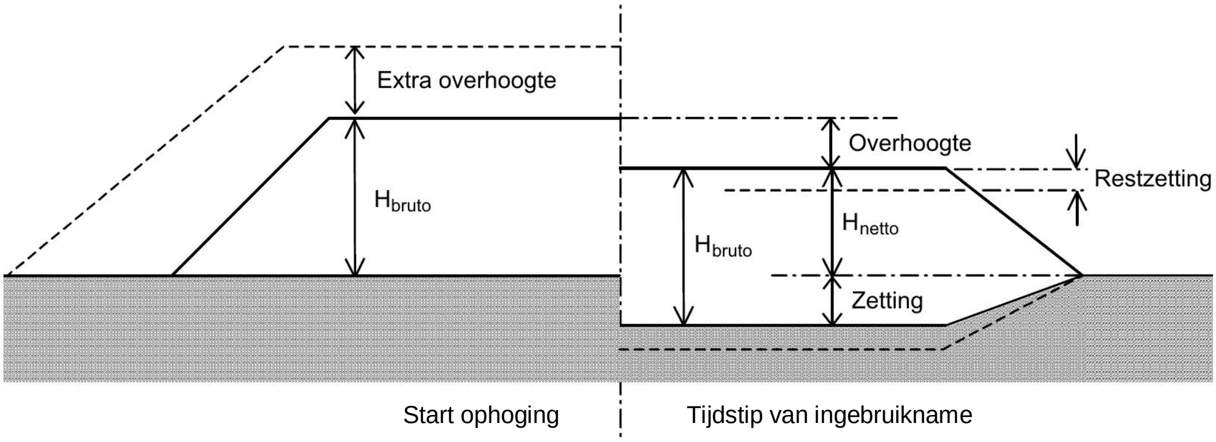

Figure B-1: Embankment construction geometry schematisation, illustrating the terminology used in settlement analysis in the Netherlands [CROW, 2004]. Translations of the Dutch terms are provided on the next page.

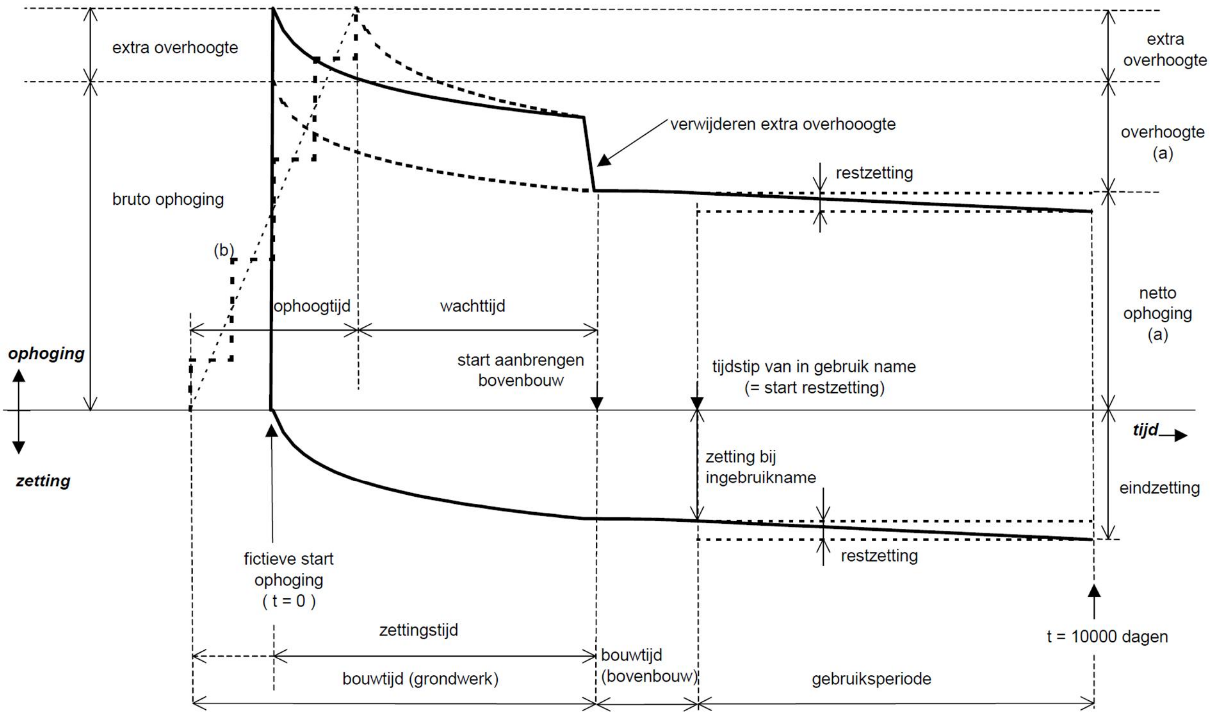

Figure B-2: Embankment construction time-line schematisation, also illustrating the terminology used in settlement analysis in the Netherlands [CROW, 2004]. Translations of the Dutch terms are provided on the next page.

B2 Dutch-English translation of settlement analysis terminology

Bruto ophoging (= netto ophoging + overhoogte)	**Gross fill** (= net fill + surplus height): amount of earth fill needed to achieve the desired effective (net) fill height, including the fill needed to compensate settlements, at the *start* of the period of use.
Bouwtijd bovenbouw	**Construction period** of the ‘**above-ground works**’, such as roadbed and pavement, technical installations and buildings.
Bouwtijd grondwerk	**Construction period** of the ‘**earth works**’, including (staged) construction of the fill or embankment as well as the waiting period.
Eindzetting	**Final settlement**: total settlement of the fill or embankment at the *end* of the considered period of use. The end time is commonly arbitrarily chosen to be 10,000 days after the start of fill and construction works, but may differ depending on the client’s requirements, purpose of the structure etc.
Extra overhoogte	**Extra surplus height**: *temporary* additional earth fill surcharge, in order to speed up and increase the settlement in an early phase of construction and hence to limit residual settlements.
Fictieve start ophoging	**Fictitious start of fill**: imaginary discrete starting time (t = 0) of fill and settlement process, in order to simplify the calculation/modelling of staged (and thus temporally indiscrete) construction of an earth fill.
Gebruiksperiode	**Period of use**: period during which the embankment and/or structure is functionally available and being used, and at the end of which the final settlement should remain within predefined limits.
$\mathbf{H_{bruto}}$	Refer to “Bruto ophoging”.
$\mathbf{H_{netto}}$	Refer to “Netto ophoging”.
Ingebruikname / **Tijdstip van ingebruikname**	**Moment of putting into use**: moment at which all construction works are completed, i.e. the start of the period of use.
Netto ophoging (= bruto ophoging – overhoogte)	**Net fill** (= gross fill – surplus height): the desired effective height of the fill or embankment, regardless of losses due to settlements, at the *start* of the period of use.
Ophoging	**Increase of the ground surface level** (in general), or: the amount of fill needed to achieve such an increase.
Ophoogtijd	**Fill time**: time needed to put in place the total amount of fill (gross fill + extra surplus height), which is usually done step-wise (staged construction) as to allow for consolidation and to avoid instability.
Overhoogte	**Surplus height**: amount of earth fill needed to compensate the settlements occurring from the start of the embankment construction until the start of the period of use.
Restzetting	**Residual settlement**: settlement that occurs *during* the period of use; mainly secondary (creep) settlements. Usually contractually limited.
Start aanbrengen bovenbouw	**Start** of the **above-ground works**; refer to “Bouwtijd bovenbouw”.
Verwijderen extra overhoogte	**Removing extra surplus height**; refer to “Extra overhoogte”.
Wachttijd	**Waiting period**: period between the last fill stage and the start of the above-ground works (“bovenbouw”), in order to allow the earth fill or embankment to consolidate and settle.
Zetting	**Settlement** in general.

APPENDIX C – Case Bloemendalerpolder

C1 Overview maps

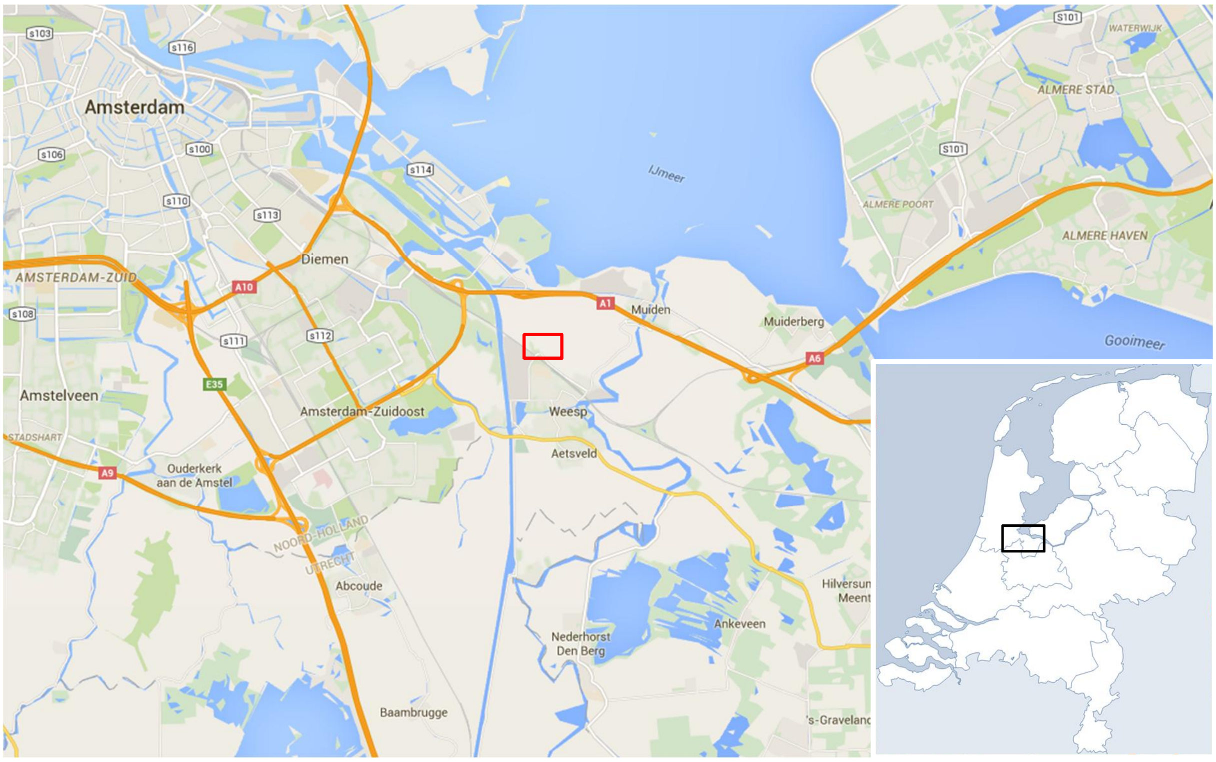

Figure C-1: Regional overview map of the area around Weesp (in the centre of the map). The rural (blank) area north of Weesp is the Bloemendalerpolder, in which the red rectangle indicates the outline of the close-up satellite image shown below. Field of view (width): 27.4 km. Source: Google Maps (2016).

Figure C-2: Close-up satellite image of the test site with the trial embankments in the Bloemendalerpolder north of Weesp. Field of view (width): 560 m. Source: Google Maps (2016).

C2 Site plan

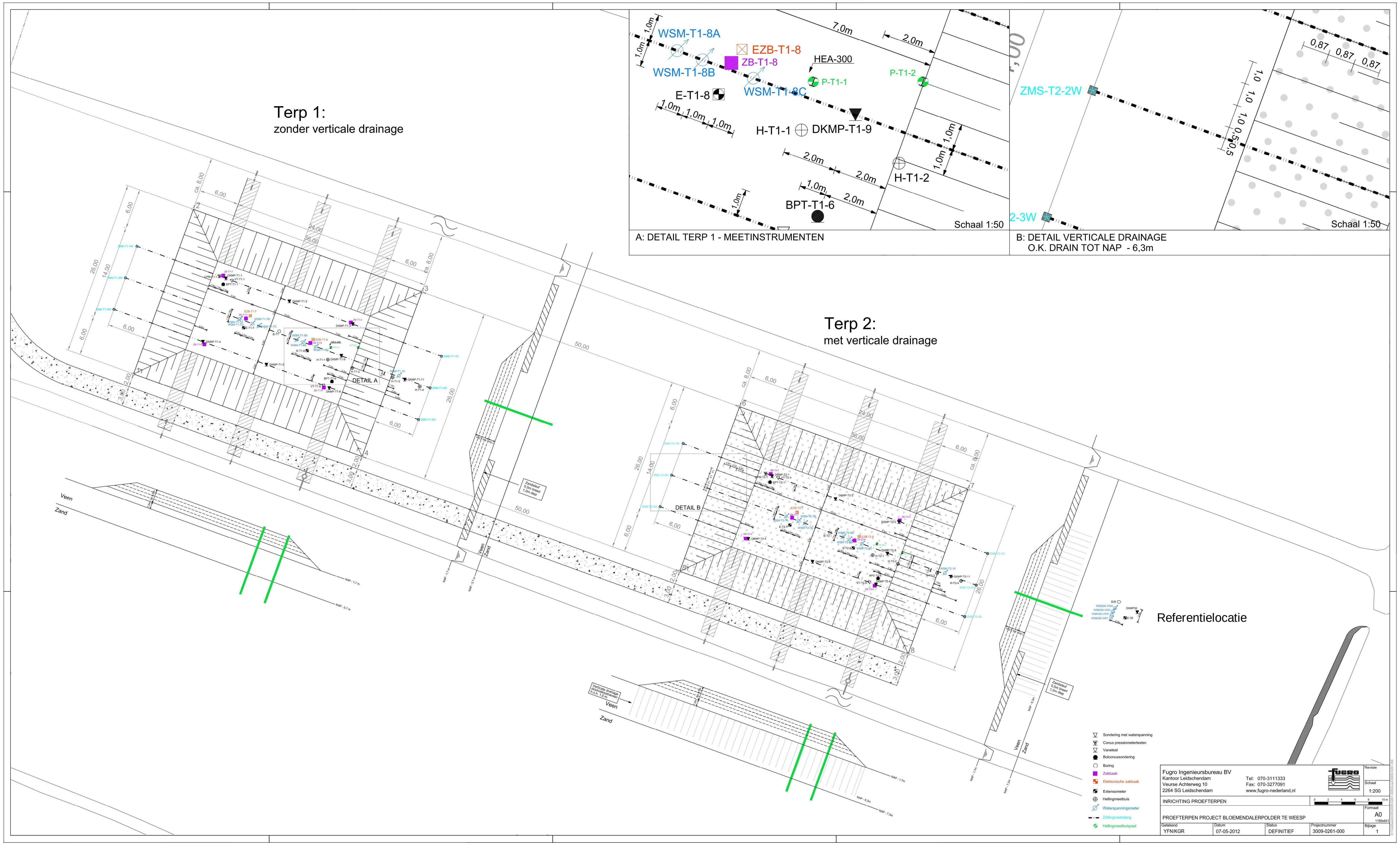

Figure C-3: Detailed site plan of the trial embankments in the Bloemendalerpolder north of Weesp, including all ground investigation and monitoring equipment locations, adapted from [Alink, 2012].
Note: it is recommended to view this map on a computer screen with digital zooming possibility, since otherwise a readable print would require a paper size of *at least* A2.

APPENDIX D – Case Amstelhoek

D1 Overview maps (1/2)

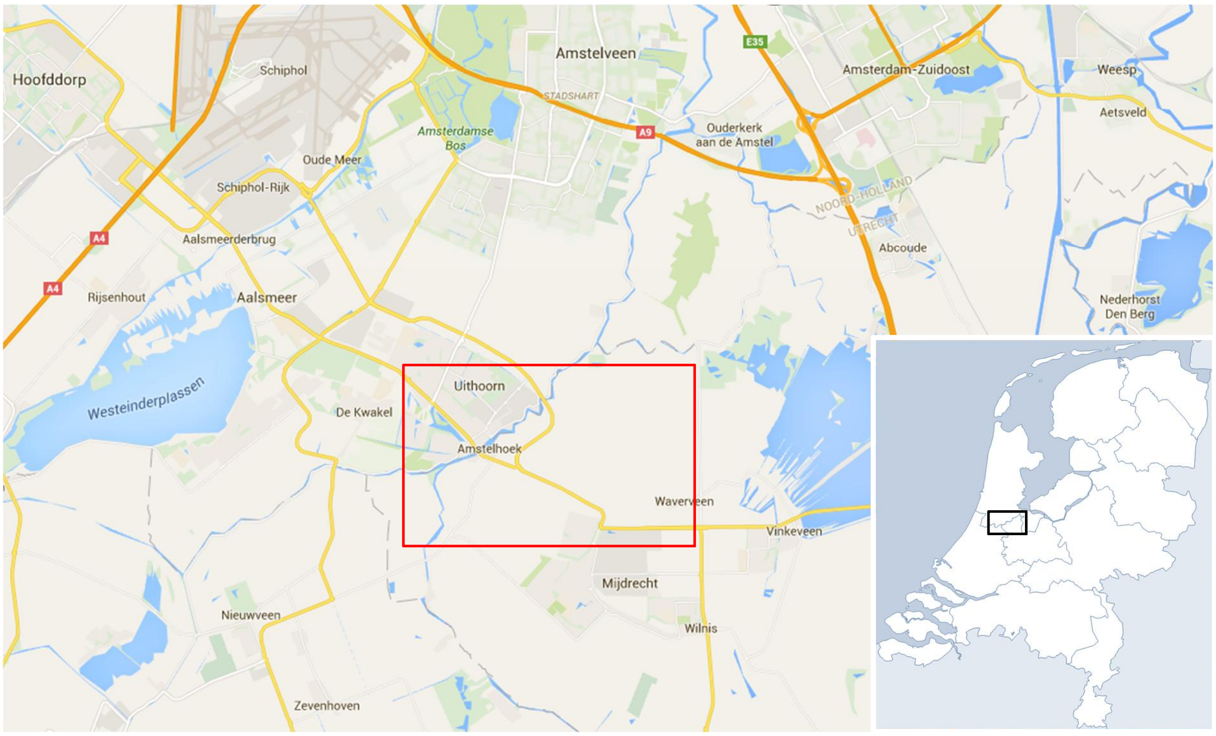

Figure D-1: Regional overview map of the area around Amstelhoek. The *old* N201 (presently N196) is the yellow coloured road that runs straight through Aalsmeer, then south along Uithoorn and finally through Amstelhoek, whereas the *new* N201 (also yellow) runs through Schiphol-Rijk and then north along Uithoorn. The red rectangle indicates the outline of the local map shown below. Field of view (width): 27.0 km. Source: Google Maps (2016).

Figure D-2: Local map of the N201 bypass east of Amstelhoek. The orange coloured dashed curve indicates the original preferred trace, which was discarded because of financial reasons. The economised trace plan alternatives are coloured yellow, green and red, and labelled B, R and A, respectively [Booltink et al., 2005]. Alternative B was accepted and realised finally. Field of view (width): 6.6 km. Source: Google Maps (2016).

D1 Overview maps (2/2)

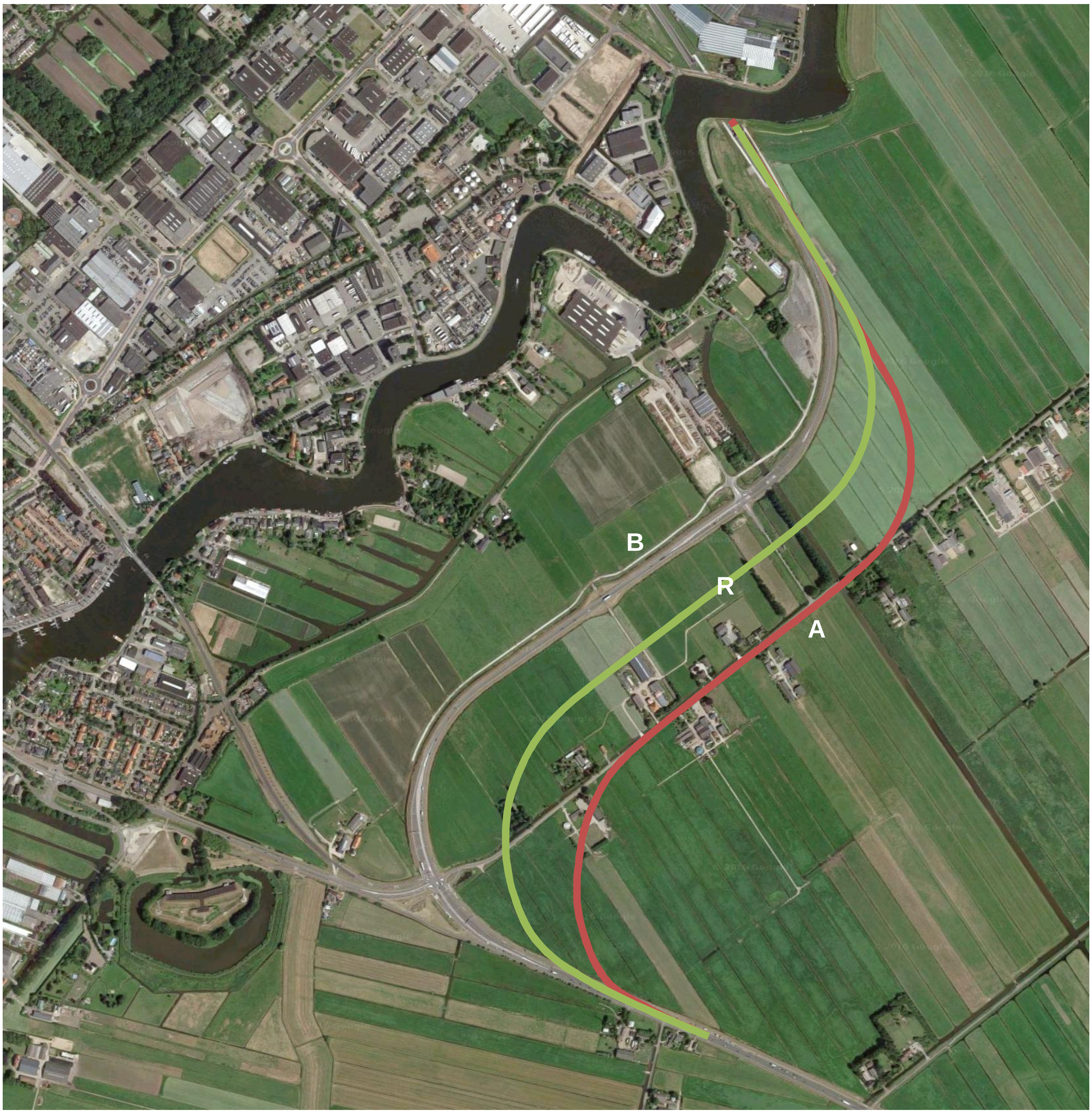

Figure D-3: Close-up satellite image of the new N201 bypass east of Amstelhoek. Indicated are all three economised trace plan alternatives B, R and A. Alternative B was accepted and realised finally. Field of view (width): 6.6 km. Source: Google Maps (2016).

D2 Site plans (1/3)

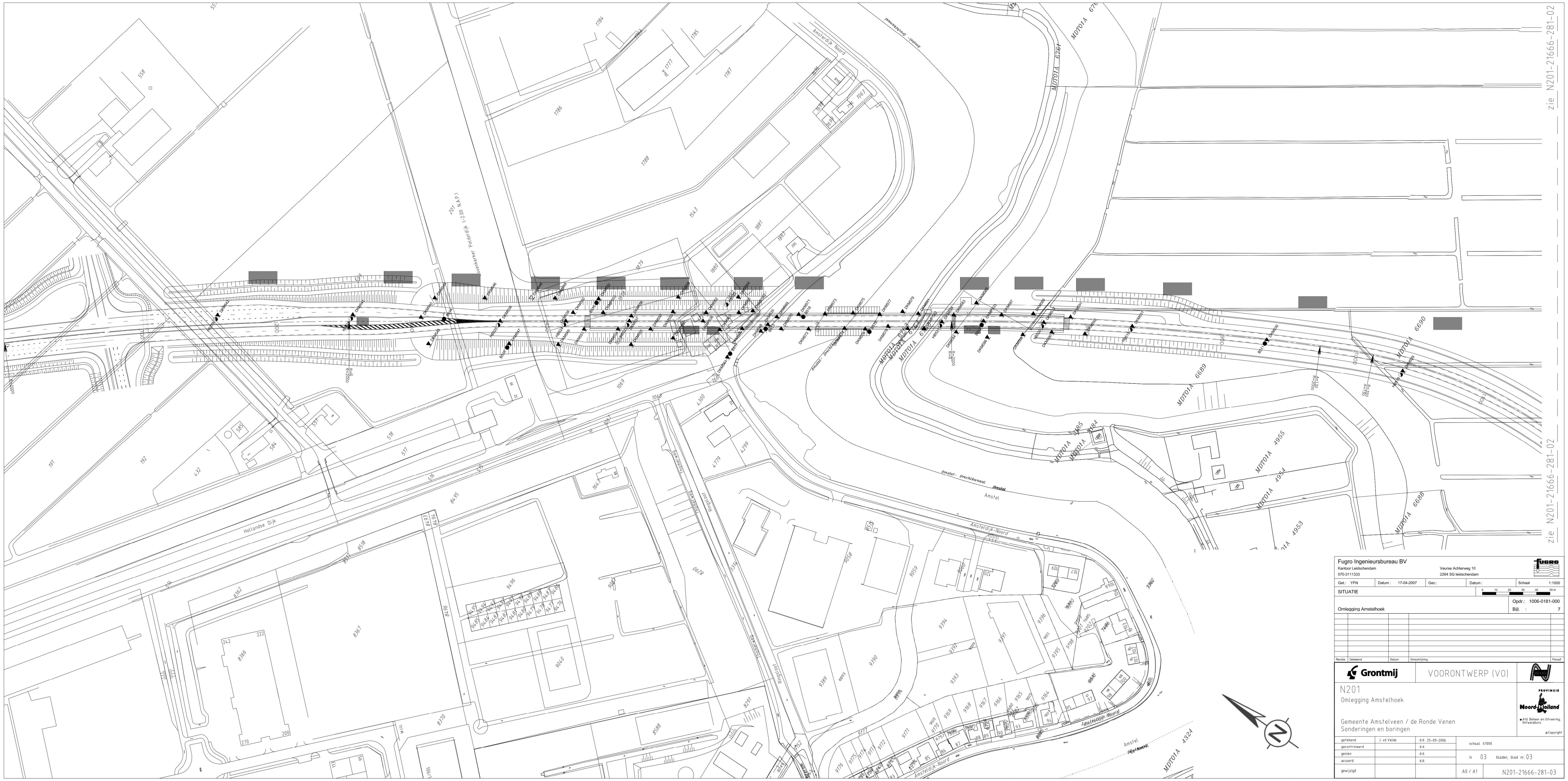

Figure D-4: Detailed site plan including ground investigation locations, of the northern third (0-1150 m) of the N201 bypass, northeast of Amstelhoek [Van der Valk, 2007]. Although the depicted plan is based on a pre-design, by comparison this was found to not differ significantly from the final design [Monker, 2008a+b].
Note: it is recommended to view this map on a computer screen with digital zooming possibility, since otherwise a readable print would require a paper size of at least A2.

D2 **Site plans** (2/3)

Figure D-5: Detailed site plan including ground investigation locations, of the middle third (1100-2300 m) of the N201 bypass, east of Amstelhoek [Van der Valk, 2007]. Although the depicted plan is based on a pre-design, by comparison this was found to not differ significantly from the final design [Monker, 2008a+b]. The red dotted line indicates the location of the perpendicular cross section at 1800 m, which is presented in Appendix D4.
Note: it is recommended to view this map on a computer screen with digital zooming possibility, since otherwise a readable print would require a paper size of at least A2.

D2 Site plans (3/3)

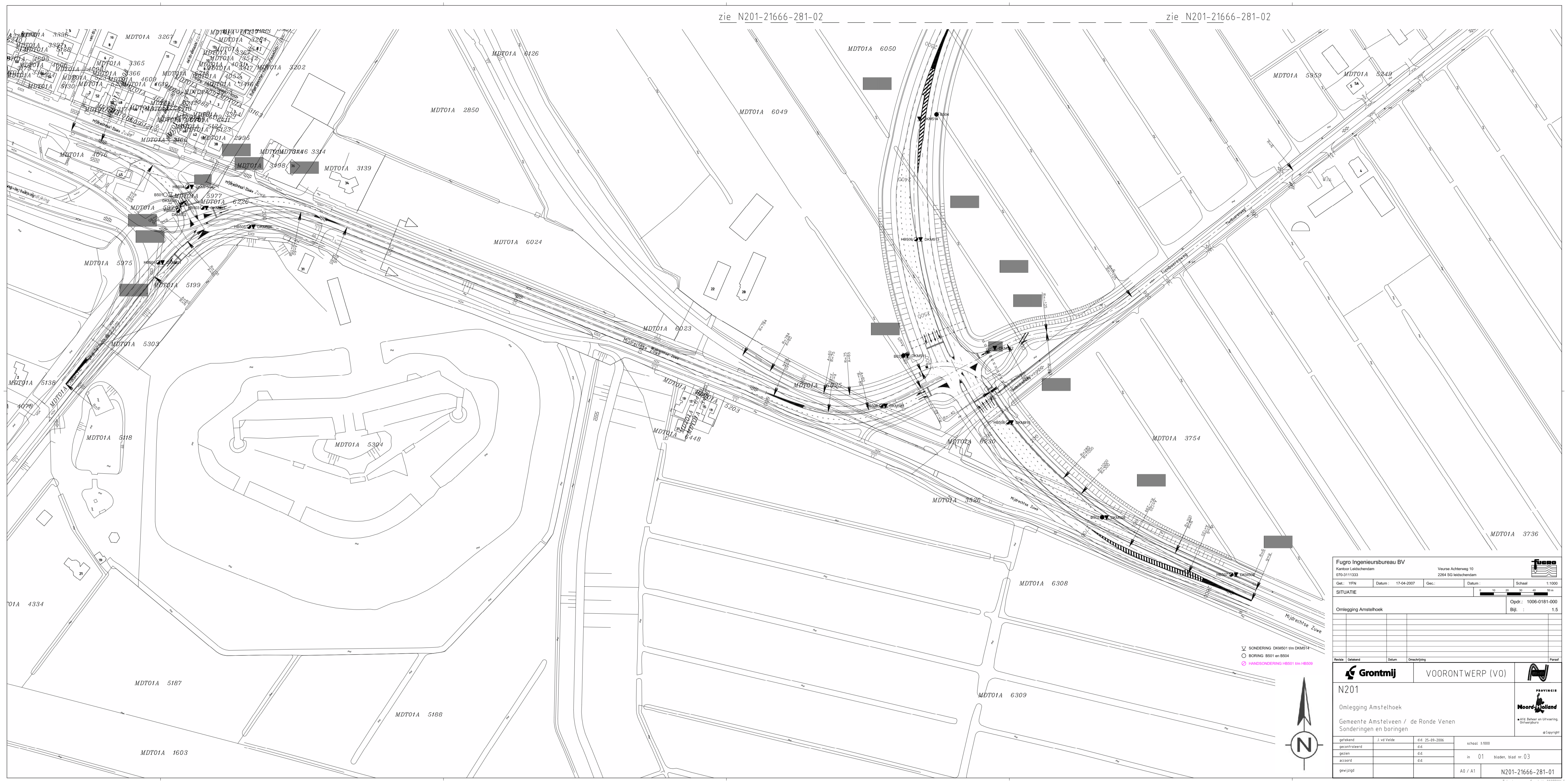

Figure D-6: Detailed site plan including ground investigation locations, of the southern third (2300-2850 m) of the N201 bypass, east of Amstelhoek [Van der Valk, 2007]. Although the depicted plan is based on a pre-design, by comparison this was found to not differ significantly from the final design [Monker, 2008a+b].
Note: it is recommended to view this map on a computer screen with digital zooming possibility, since otherwise a readable print would require a paper size of at least A2.

D3 Geological cross section

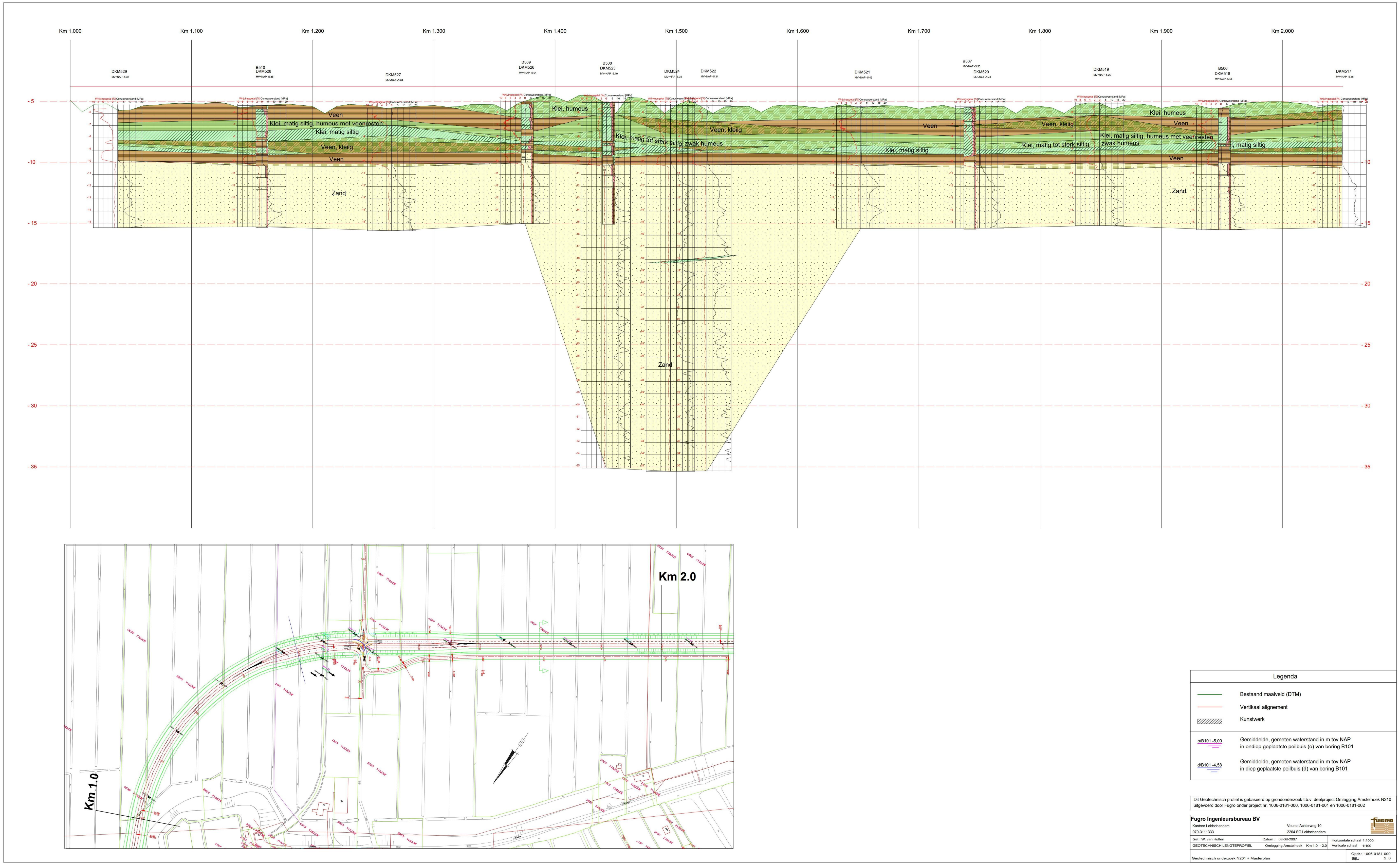

Figure D-7: Longitudinal geological cross-section from km 1.0 to km 2.0 along the trace of the N201 bypass east of Amstelhoek, providing insight into the local subsurface geology [Van der Valk, 2007].

D4 Road embankment cross-section and geometry

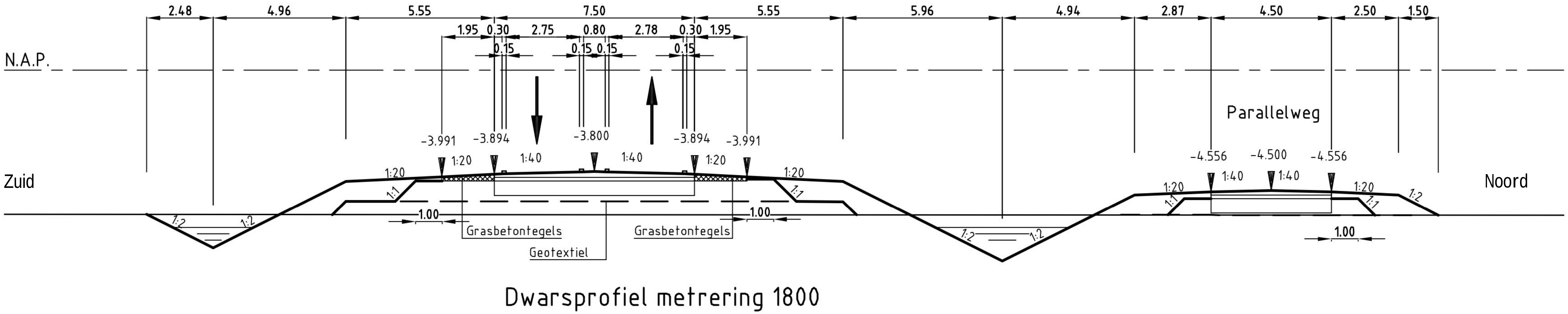

Figure D-8: Perpendicular cross-section with geometrical dimensions for the new N201 road embankment at location 1800 m, according to the final design [Monker, 2008b]. For information, the original polder ground surface level is on average -5.3 m NAP. Note, that in the original sketch North and South were erroneously switched, which is corrected in the copy above.

APPENDIX E – Case Leendert de Boerspolder

E1 **Overview maps** (1/2)

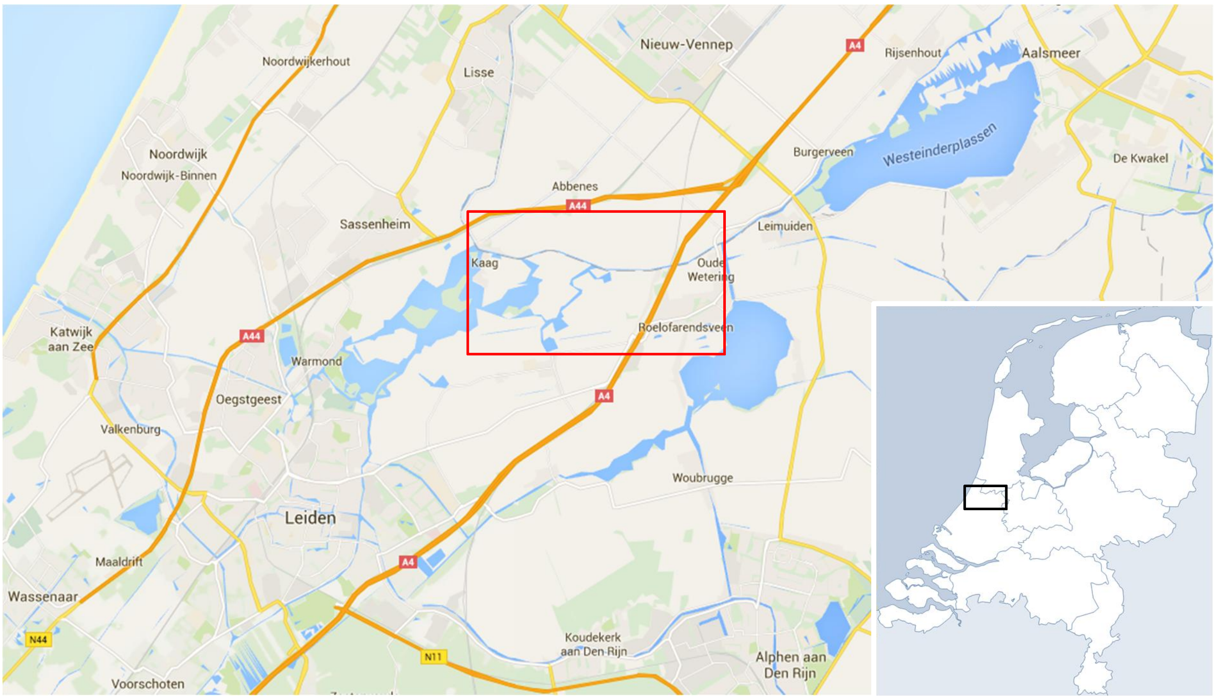

Figure E-1: Regional overview map of the wider area around the Leendert de Boerspolder, in which the red rectangle indicates the outline of the local map shown below. Field of view (width): 29.6 km. Source: Google Maps (2016).

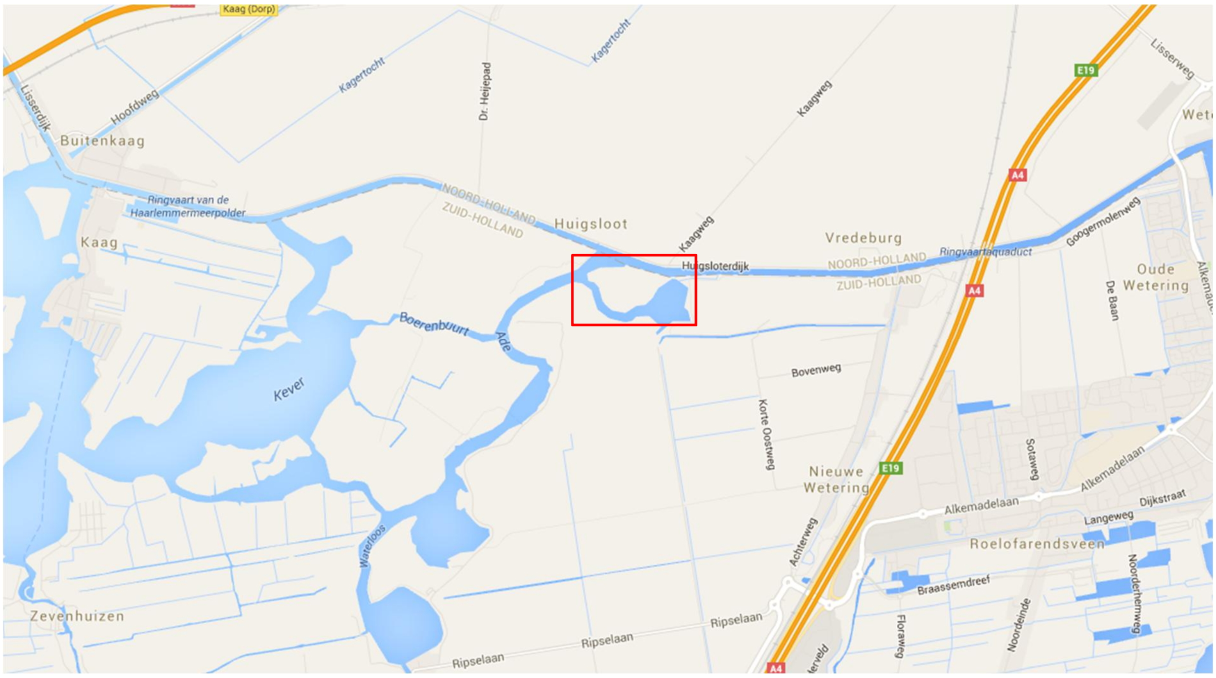

Figure E-2: Local map of the area around the Leendert de Boerspolder (in the centre of the map). The red rectangle indicates the outline of the close-up satellite image on the next page. Field of view (width): 6.3 km. Source: Google Maps (2016).

E1 Overview maps (2/2)

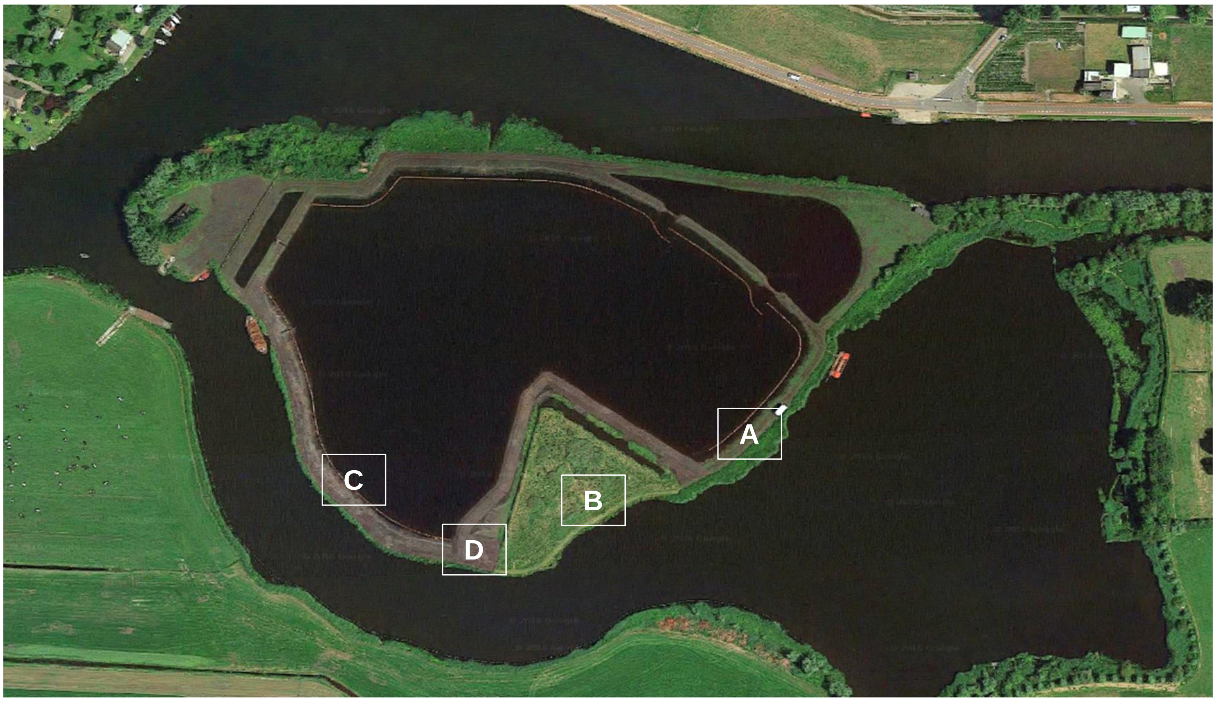

Figure E-3: Close-up satellite image of the Leendert de Boerspolder in its current (flooded) state. Indicated are also the site investigation areas, noting that data considered in this research originated mostly from area B.
Field of view (width): 630 m. Source: Google Maps (2016).

E2 **Site plans** (1/2)

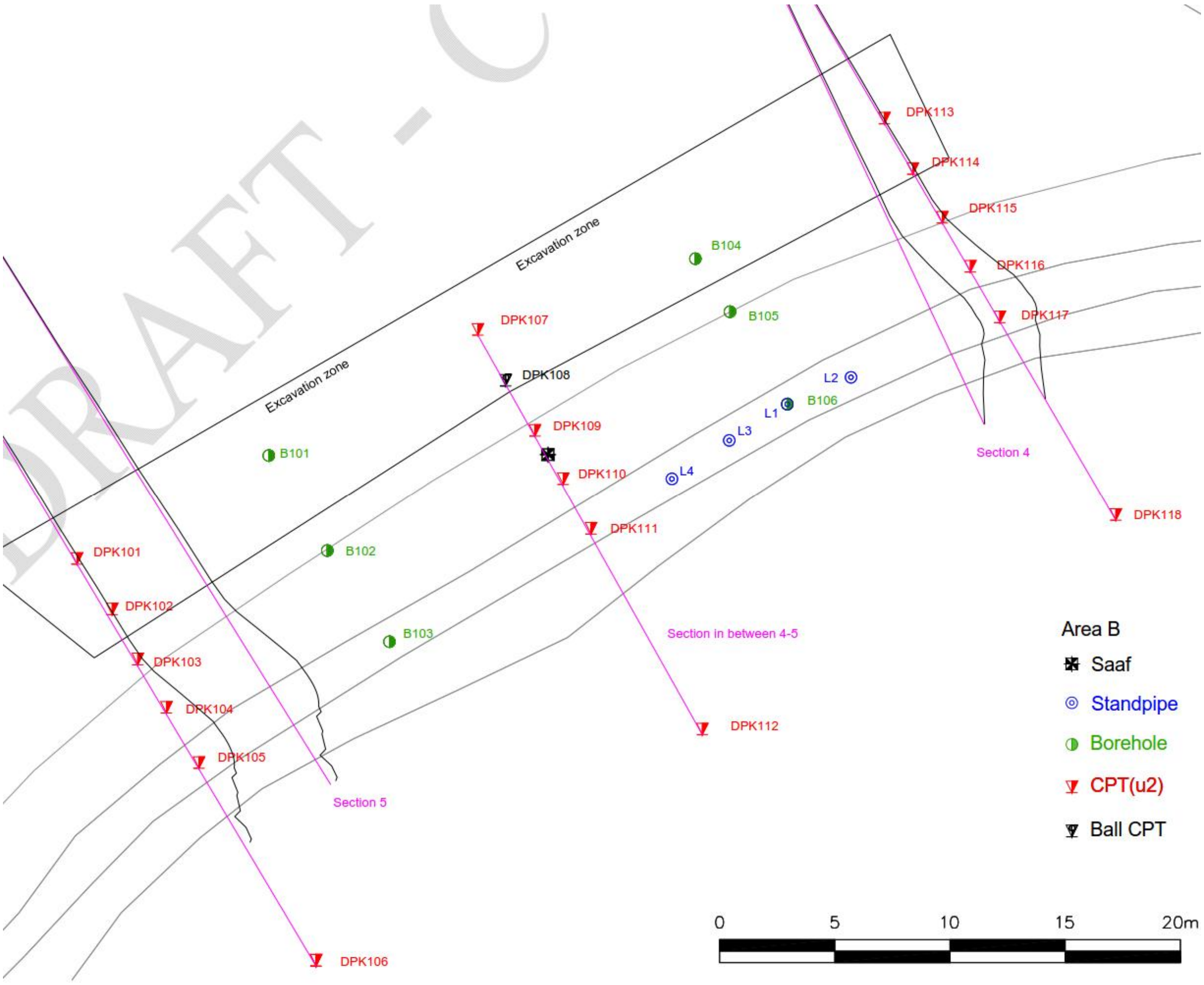

Figure E-4: Site plan with site investigation points in area **B** of the Leendert de Boerspolder. Adapted from [Jommi et al., 2015].

E2 **Site plans** (2/2)

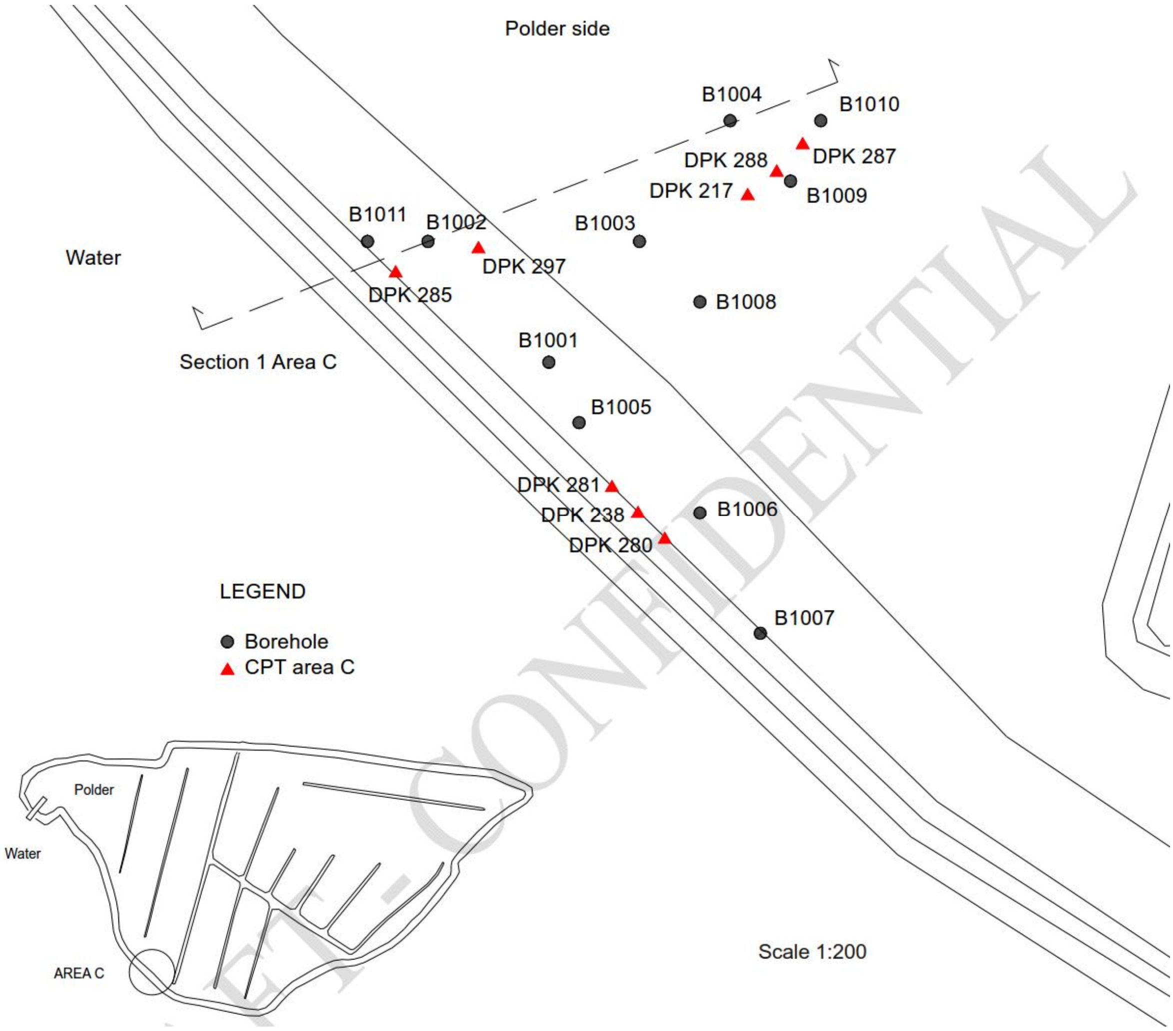

Figure E-5: Site plan with site investigation points in area **C** of the Leendert de Boerspolder. Adapted from [Jommi et al., 2015].

E3 CPT profile & subsurface interpretation

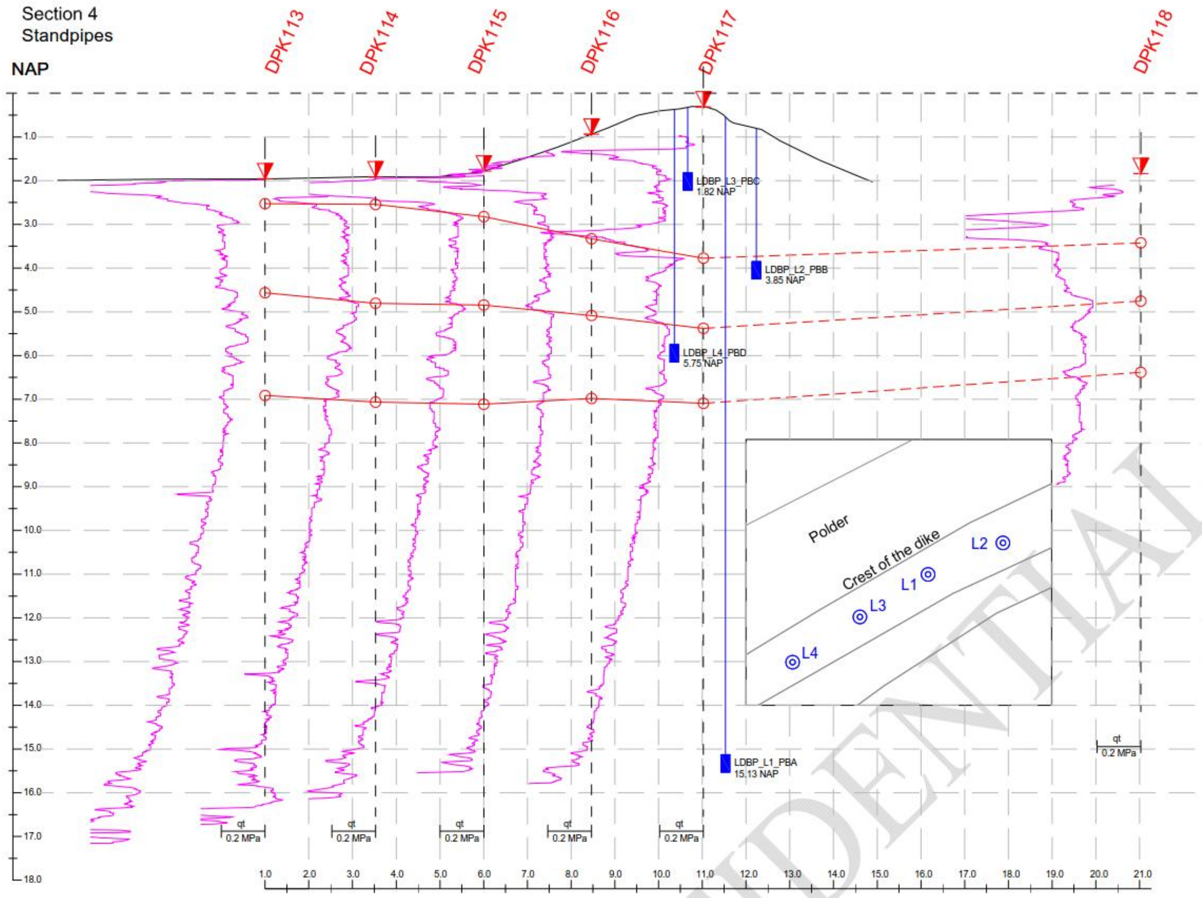

Figure E-6: Example of CPT profile in area **B** of the Leendert de Boerspolder [Jommi et al., 2015].

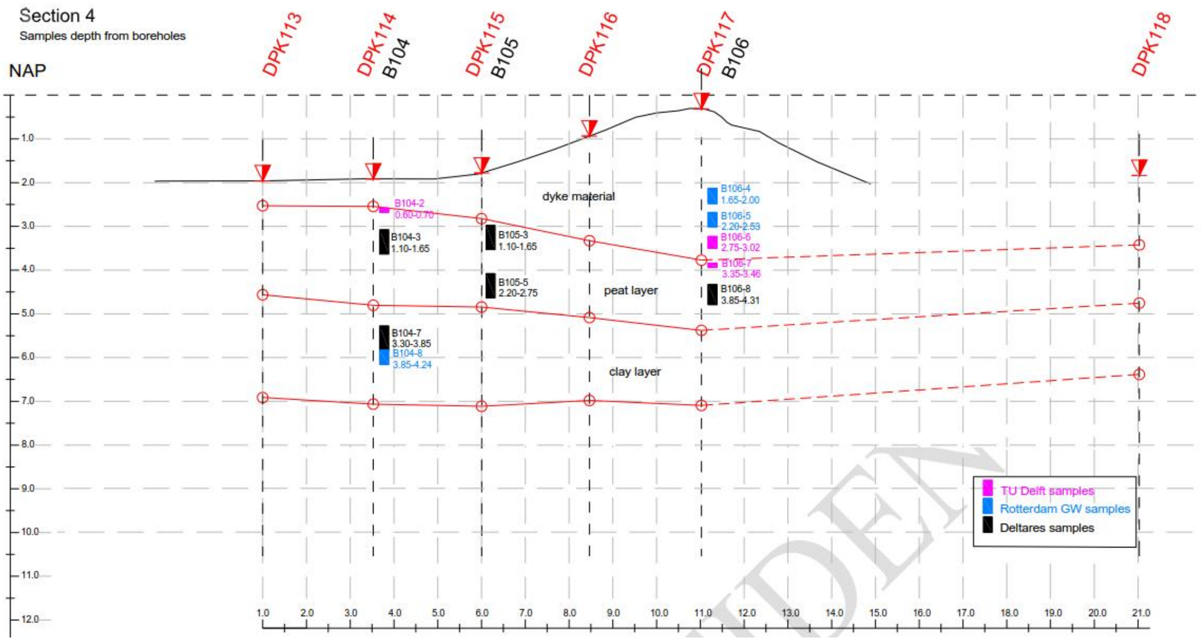

Figure E-7: Example of subsurface structure interpretation in area **B** of the Leendert de Boerspolder, based on CPT, borings and sampling. Adapted from [Jommi et al., 2015].

APPENDIX F – Legend of site plan and borehole log symbols

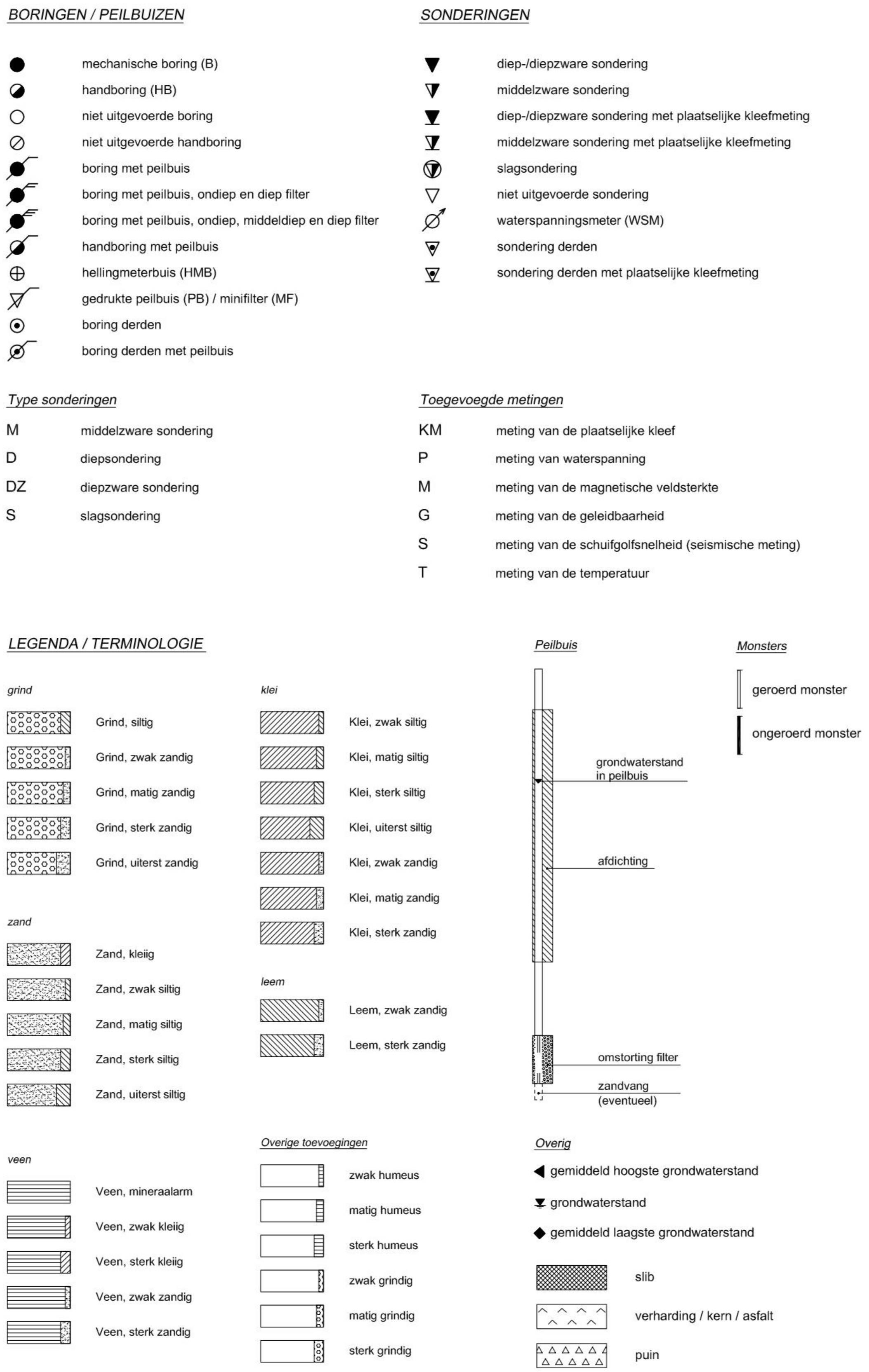

Legend of all site plan and borehole log symbols or abbreviations, as applied by Fugro GeoServices [Alink, 2012].

APPENDIX G – Soil parameters provided or derived from laboratory test reports

G1 Bloemendalerpolder

DATA IN GROUND INVESTIGATION REPORT [Alink (Fugro), 2012]

From K0-CRS test reports & graphs

	2012	2012	2012	2012						
Boring No.	B30	B30	B30	B30	BT1	BT1	BT1	BT2	BT2	BT2
Sample No.	5B	6D	2C	4C	2B	3D	4D	8B	11B	12B
Depth NAP [m]	-6.04	-7.04	-3.08	-5.04	-3.05	-4.35	-5.35	-2.65	-6.35	-6.90
Soil class.	Peat, low mineral content (all the same)									
Nat. unit wgt. [kN/m3]	9.2	10.8	10.2	10.0	10.0	9.9	9.6	10.1	10.0	9.9
Dry unit wgt. [kN/m3]	0.6	2.2	1.3	0.8	1.3	0.9	0.7	1.4	1.1	1.0
Init. grav. water content [%]	1380.2	392.9	667.5	1142.0	677.3	971.5	1258.6	609.8	795.3	932.0
Init. saturation	0.91	1.02	0.99	0.99	0.97	0.97	0.95	0.98	0.98	0.97
Init. void ratio e0 (1)	24.62	6.27	11.01	18.88	11.21	15.96	21.23	10.01	13.05	15.36
Disturbance index [%]	6.2	4.1	1.5	4.7	2.5	2.4	1.9	0.4	5.7	5.4
Init. water content: NEN 5112	1433.3	390.9	684.6	1150.0	669.2	1000.0	1271.4	621.4	809.1	890.0
Porosity n (1) from e0 (1)	0.96	0.86	0.92	0.95	0.92	0.94	0.96	0.91	0.93	0.94
Porosity n (2) from unit wgt.	0.96	0.86	0.92	0.95	0.91	0.95	0.95	0.90	0.93	0.94
e0 (2) from n (2)	26.29	6.12	10.96	17.97	10.67	17.45	21.22	9.52	12.47	14.46
Test method	K0-CRS (all the same)									
RR	4.10E-2	3.60E-2	5.50E-2	6.50E-2	7.57E-2	5.67E-2	5.69E-2	5.78E-2	3.98E-2	5.36E-2
CR	5.40E-1	4.30E-1	4.60E-1	5.60E-1	5.18E-1	4.90E-1	5.96E-1	4.72E-1	4.31E-1	4.20E-1
Cα	5.10E-2	3.30E-2	3.10E-2	3.70E-2	-	-	-	-	-	-
Pg (NEN-B.) [kPa]	6.3	8.3	11.7	7.9	11.9	7.5	7.6	12.2	8.2	7.9
a	3.30E-2	2.20E-2	3.10E-2	4.60E-2	4.48E-2	3.78E-2	4.35E-2	3.25E-2	2.60E-2	3.44E-2
b	4.30E-1	2.50E-1	3.20E-1	3.60E-1	2.94E-1	3.08E-1	4.10E-1	2.87E-1	3.08E-1	3.22E-1
c	4.00E-2	1.90E-2	2.20E-2	2.40E-2	2.40E-2	2.51E-2	3.64E-2	2.25E-2	2.46E-2	2.08E-2
Pg (abc) [kPa]	10.6	9.6	18.4	10.0	10.0	10.0	9.8	15.0	12.9	14.2
Kv init. permeability [m/s]	3.6E-6	4.7E-8	1.7E-8	3.4E-7	-	-	-	-	-	-

Note: all light grey coloured values were personally determined, for verification or other purposes.

From oedometer test reports & graphs

Boring No.	BT1	BT1	BT2	BT2	BT2
Sample No.	L3	L4	L10	L11	L12
Depth NAP [m]	-4.14	-5.14	-4.90	-6.19	-7.34
Soil class.	Peat, low mineral content				
Nat. unit wgt. [kN/m3]	9.2	9.4	9.8	9.6	13.2
Dry unit wgt. [kN/m3]	1.1	0.8	0.9	0.9	6.3
Init. grav. water content [%]	818.6	1059.7	994.1	1017.4	109.7
Init. saturation					
Init. void ratio e0 (1)	13.40	18.48	16.18	18.18	2.43
Disturbance index [%]					
Init. water content: NEN 5112	736.4	1075.0	988.9	966.7	109.5
Porosity n (1) from e0 (1)	0.93	0.95	0.94	0.95	0.71
Porosity n (2) from unit wgt.	0.85	0.90	0.93	0.91	0.72
e0 (2) from n (2)	5.61	9.10	13.80	10.29	2.61
LOI [%]	79.9	73.0	77.3	64.8	24.5
Test method	IL (all the same)				
C	9.2	4.6	4.9	6.1	25.2
C'	3.4	3.5	3.8	4.9	8.0
Pg1 (Kop.)	14	8	8	13	30
Cp	14.7	7.1	8.3	9.1	35.5
Cs	97.2	51.9	48.3	76.4	348.4
C'p	4.9	4.9	5.7	4.9	11.6
C's	43.6	47.5	45.5	0.0	102.4
Pg2 (Cas.)	21	11	20	25	40
Cc<Pg2	2.33	6.51	4.93	5.03	0.23
Cc>Pg2	6.96	9.40	7.44	9.48	0.79
Csw	1.022	1.219	0.984	0.182	0.076

From summary tables in Appendix 3c

Boring No.	BT1	BT1	BT2	BT2	BT2
Sample No.	L3	L4	L10	L11	L12
Depth NAP [m]	-4.14	-5.14	-4.90	-6.19	-7.34
Soil class.	Peat, low mineral content				
Nat. unit wgt. [kN/m3]	9.4	9.4	9.8	9.6	13.2
Dry unit wgt. [kN/m3]	1.0	0.8	0.9	0.9	6.3
Init. grav. water content [%]	818.6	1059.7	994.1	1017.4	109.7
Init. saturation					
Init. void ratio e0 (1)	13.9	18.47	16.19	18.18	2.43
Disturbance index [%]					
Init. water content: NEN 5112	840.0	1075.0	988.9	966.7	109.5
Porosity n (1) from e0 (1)	0.93	0.95	0.94	0.95	0.71
Porosity n (2) from unit wgt.	0.88	0.90	0.93	0.91	0.72
e0 (2) from n (2)	7.34	9.10	13.80	10.29	2.61
Test method	IL (all the same)				
RR	0.082	0.068	0.063	0.050	0.030
CR	0.496	0.487	0.469	0.562	0.228
Cα	0.019	0.019	0.021	0.021	0.007
Pg (NEN-B.)	15.77	8.14	12.88	21.31	38.60
a	0.055	0.065	0.052	0.010	0.012
b	0.315	0.356	0.319	0.354	0.119
c	0.0128	0.0156	0.0157	0.0165	0.0034
Pg (abc)	19.0	15.0	17.0	20.0	36.0
Cp	15.3	7.4	8.3	9.2	35.4
Cs	98.8	128.2	52.6	127.4	340.8
C'p	5.2	5.7	5.9	-	11.8
C's	77.0	126.2	102.0	-	138.4
Pg (Kop.)	14.1	3.4	8.4	16.7	30.5

Note: Source of orange coloured values unclear

Note: Red coloured values were found to deviate by more than 5% from actual lab results.

VALUES USED FOR SETTLEMENT PREDICTIONS [Ammerlaan (Fugro), 2011]

Results of sample L12 were disregarded due to odd values (reported explanation: possibly more clayey)

	Peat	Clay	Sand	Sand, fill	↓ *Real* averages from 'BT' samples (negl. L12)	
Nat. unit wgt. [kN/m3]	10.3	14	20	19	9.8	
Dry unit wgt. [kN/m3]	-	14	16	17		
						↓ Averages from Appendix 3c
RR	0.061	0.100	1E-6		0.060	0.066
CR	0.493	0.310	2E-6		0.494	0.504
Cα	0.020	0.014	1E-6		0.020	0.020
a	0.040	0.013	0.001		0.040	0.046
b	0.327	0.160	0.004		0.327	0.336
c	0.014	0.008	0.000		0.021	0.015
Cp	10	28	9E+99		9.8	10.1
Cs	102	320	9E+99		68.5	101.8
C'p	6	7	9E+99		5.1	5.6
C's	102	80	9E+99		45.5	101.7
					↓ (Casagrande)	↓ (Taylor)
cv	1.0E-7	7.9E-8	1.0E-7		5.3E-8	2.3E-7
ch	2 x cv	cv	cv			
Kv	5.0E-8				1.0E-6	(from 'B30' peat samples)
POP	7	7	7			

Note: Compression and consolidation coefficients for non-peat soils were reportedly based on NEN 6740, or on unit weight correlation (abc)

Note: Intrinsic times were reportedly calculated, but due to variability of results, use of a constant POP was preferred.

G2 **Amstelhoek** (1/2)

DATA IN GROUND INVESTIGATION REPORT [Van der Valk (Fugro), 2007]												
From laboratory test report: Vol. C3												
Boring No.	**B511**	**B514**	**B515**	**B515**	**B516**	**B516**	**B517**	**B518**	**B518**	**B518**	**B519**	**B519**
	(p.53)	(p.54)	(p.135)	(p.135)	(p.135)	(p.135)	(p.135)	(p.88)	(p.88)	(p.88)	(p.88)	(p.88)
Depth [m]	-9.48 NAP	-10.18 NAP	-1.7	-7.2	-1.1	-7.9	-4.6	-2.7	-6.0	-6.7	-0.7	-6.3
Soil class.	Peat, low mineral content	Peat, low mineral content	Peat, low mineral content	Clayey peat	Peat, low mineral content	Clayey-silty peat	Clayey peat	Clay, silty	Clay, slightly silty, slightly organic	Peat, low mineral content	NA	NA
LOI [% mass]	27.4	87.4	71.9	67.7	3.5	0.6	75.7	2.9	6.2	6.2	37.7	63.1

Boring No.	**B511**	**B515**	**B515**	**B515**	**B515**	**B516**	**B516**	**B516**	**B516**	**B517**	**B517**	**B517**	**B517**	**B518**	**B518**	**B518**	**B518**	**B519**	**B519**	**B519**	**B519**
Sample No.	4	3	7	13	19	3	8	12	20	2	9	15	16	1	2	5	6	1	3	5	7
Depth NAP [m]	-6.63	-4.20	-5.70	-7.50	-10.40	-3.46	-5.46	-7.06	-10.26	-4.08	-7.18	-9.48	-9.88	-4.90	-5.90	-8.90	-9.90	-4.10	-6.15	-8.20	-9.60
Soil class.	Clay, slightly silty, slightly organic	Peat, low mineral content	Clayey peat	Clay, slightly silty, slightly organic	Peat, low mineral content	Clay, slightly silty, strongly organic	Clay, silty, organic	Clay, silty, strongly organic	Peat, low mineral content	Peat, low mineral content	Clay, silty, organic	Peat, low mineral content	Peat, low mineral content	Clay, silty, strongly organic	Clay, slightly silty	Clay, slightly silty & sandy	Peat, low mineral content	Peat, slightly clayey	Clay, slightly silty, slightly organic	Clay, slightly silty, slightly organic	
Nat. unit wgt. [kN/m3]	11.6	9.6	11.5	12.1	10.2	15.6	11.1	15.5	9.8	10.5	14.3	10.1	10.6	14.6	14.0	14.8	10.3	10.4	13.5	12.4	9.9
Dry unit wgt. [kN/m3]	4.6	1.4	2.9	4.2	1.6	9.4	7.6	4.8	2.0	2.1	7.5	2.2	2.4	8.3	7.1	8.1	1.9	2.2	6.4	4.9	2.1
Init. grav. water content [%]	174.6	605.6	296.5	188.9	542.1	65.5	46.9	223.8	399.3	406.6	89.8	363.1	339.7	77.1	98.5	82.9	445.8	367.8	110.4	155.9	369.3
Init. water content: NEN 5112	152.2	585.7	296.6	188.1	537.5	66.0	46.1	222.9	390.0	400.0	90.7	359.1	341.7	75.9	97.2	82.7	442.1	372.7	110.9	153.1	371.4
Porosity from unit weights	0.75	0.88	0.92	0.85	0.92	0.67	0.38	0.70	0.84	0.90	0.73	0.85	0.88	0.68	0.74	0.72	0.90	0.88	0.76	0.80	0.84
Init. void ratio from porosity	3.02	7.32	11.95	5.57	11.95	1.99	0.60	2.33	5.13	9.14	2.70	5.57	7.32	2.09	2.85	2.56	9.14	7.32	3.20	4.12	5.13
C	14.0	14.4	10.7	7.0	10.2	37.9	32.8	6.6	8.2	11.5	10.8	17.8	25.6	21.8	14.3	20.1	30.5	5.2	30.6	22.5	23.2
C'	3.3	6.1	4.4	5.3	2.4	9.3	10.1	4.9	3.0	2.9	5.0	2.4	3.6	6.3	6.6	3.8	6.4	4.0	5.6	4.2	5.9
Pg (Koppejan)	21	8	13	31	48	10	28	29	54	56	62	90	98	10	10	45	44	10	13	29	40
Cp	26.7	32.4	20.6	12.9	16.3	66.7	59.1	11.8	16.3	21.0	19.6	27.7	41.7	39.1	25.8	34.0	48.7	10.0	51.4	36.1	44.0
Cs	117.5	103.8	88.7	60.6	108.6	351.6	293.7	59.0	65.4	101.6	96.2	198.8	264.3	196.3	129.5	197.0	326.0	44.1	302.1	239.2	196.4
C'p	6.3	7.4	6.6	8.6	4.4	13.0	16.7	8.1	6.0	5.8	9.9	5.8	8.1	14.2	15.1	8.7	12.2	8.0	13.0	9.4	14.1
C's	27.6	138.1	51.2	55.4	21.5	129.8	102.8	49.9	23.6	23.1	40.5	16.5	25.3	44.9	46.6	26.9	53.6	32.5	39.3	30.1	41.1
Consolidation coefficients [m2/s]																					
trap 3	3.80E-8	1.40E-6	8.60E-9	8.80E-9	3.90E-7	1.90E-8	7.00E-8	1.10E-8	7.50E-8	8.40E-8	1.90E-8	9.80E-8	1.10E-7	2.00E-8	1.30E-8	5.40E-8	1.00E-7	2.70E-8	5.50E-8	5.60E-8	6.10E-7
trap 4	1.50E-8																				
trap 5	1.30E-8																				

Notes:
- All relevant laboratory tests (compression, LOI, triaxial) were performed only on B511-B519 (i.e. around the aqueduct)
- Else only some basic soil physical properties were determined on B502 and B510
- Test results from samples taken directly at or below Amstel dike were disregarded
- Orange coloured entries indicate data whose correctness and general validity is doubted.
- Light grey coloured values were personally determined, for verification or other purposes.

G2 **Amstelhoek** (2/2)

VALUES USED FOR SETTLEMENT PREDICTIONS [Meulblok & Forger (Grontmij), 2009]								
	Peat, Hollandveen	Peat top	Clay top	Clay, organic	Peat, clayey	Peat, basisveen	Sand, Pleist.	Sand, fill
	11	10.5	14.5	13.5	10	10	20	20
	11	10.5	14.5	13.5	10	10	18	18
Avg. nat. unit wgt.	10.2	10.2	13.8	13.2	11.0	10.0		
Avg. Cp	21.1	21.1	42.3	40.8	15.3	32.2		
Avg. Cs	83.2	83.2	215.5	205.2	66.4	190.9		
Avg. C'p	7.1	7.1	11.8	12.6	7.3	8.7		
Avg. C's	64.6	64.6	88.0	79.8	41.9	31.7		
Avg. **Pg**	24.7	24.7	14.5	29.8	11.5	54.5		
Cp	35	60	150	50	45	45	1800	9E+99
Cs	175	400	800	275	150	150	9E+99	9E+99
C'p	7	12	30	10	9	9	600	9E+99
C's	35	80	160	55	30	30	9E+99	9E+99
POP	10	10	10	10	10	10	10	10
	(in D-Settlement, Pg instead of POP was used)							
cv	2E-7	9E+99	9E+99	3.5E-8	2E-7	2E-7	9E+99	9E+99
Avg. cv (3)	5.04E-7	5.04E-7	3.00E-8	3.73E-8	1.78E-8	2.24E-7		

Notes:
- Light grey coloured values were personally determined based on revisit and re-averaging of test results. These are also the values that were used for the “revisited” Amstelhoek settlement predictions. ‘Avg’ = ‘Average’.
- Orange coloured entries indicate values whose correctness and general validity is doubted.

G3 Leendert de Boerspolder

K0-CRS test results obtained by Deltares

Boring No.	**B101**	**B101**	**B102**	**B102**	**B102**	**B103**	**B104**	**B105**	**B105**	**B105**	**B106**
Sample No.	**t3-3**	**t3-6**	**t5-3**	**t5-4**	**t8-3**	**t8-3**	**t3-2**	**t3-2**	**t5-2**	**t5-3**	**t8-3**
Depth NAP [m]	3.25	3.40	4.10	4.15	5.80	4.00	3.35	3.25	4.35	4.40	4.60
	polder	polder	dike toe	dike toe	dike toe	dike crest	polder	dike toe	dike toe	dike toe	dike crest
Soil class.	Peat, low mineral content	Peat, low mineral content	Peat, low mineral content	Peat, low mineral content	Clay, silty	Clay, slightly silty	Peat, low mineral content	Peat, low mineral content	Peat, low mineral content	Peat, low mineral content	Peat, low mineral content
Nat. unit wgt. [kN/m3]	9.8	9.8	10.1	9.8	14.0	9.8	9.7	9.7	9.7	9.4	10.0
Dry unit wgt. [kN/m3]	1.0	1.0	1.4	1.2	7.4	1.3	1.1	1.2	1.1	1.1	1.2
Init. grav. water content [%]	891.7	850.1	629.1	698.8	89.5	650.0	804.7	733.5	767.0	760.7	723.7
Init. void ratio	9.21	8.08	8.16	6.85	2.05	6.58	7.02	6.58	6.78	5.64	8.6
Disturbance index [%]	3.2	3.8	3.6	6.2	1.6	8.7	2.8	2.7	3.9	4.6	**20.6**
Test method	K0-CRS	K0-CRS	K0-CRS	K0-CRS	K0-CRS	K0-CRS	K0-CRS	K0-CRS	K0-CRS	K0-CRS	K0-CRS
a	5.90E-2	5.20E-2	5.00E-2	5.30E-2	8.00E-3	5.00E-2	5.60E-2	3.50E-2	5.00E-2	4.90E-2	5.40E-2
b	3.90E-1	3.50E-1	3.50E-1	3.50E-1	1.50E-1	3.40E-1	3.40E-1	3.70E-1	3.50E-1	3.90E-1	3.90E-1
c		2.60E-2	1.70E-2	2.10E-2	8.70E-3	2.10E-2	3.00E-2	2.90E-2	2.40E-2	2.60E-2	2.40E-2
RR	9.60E-2	8.40E-2	9.60E-2	9.50E-2	1.80E-2	9.40E-2	8.90E-2	6.40E-2	8.90E-2	8.40E-2	1.10E-1
CR	6.60E-1	5.30E-1	5.30E-1	5.40E-1	2.90E-1	5.30E-1	5.60E-1	6.00E-1	5.30E-1	5.90E-1	6.60E-1
Cαε		3.90E-2	2.50E-2	3.20E-2	1.70E-2	3.30E-2	4.80E-2	4.80E-2	3.60E-2	3.80E-2	4.00E-2
In-situ eff. stress	6.0	4.0	9.0	8.5	9.0	13.0	3.0	5.0	5.5	6.0	40.0
Pg (abc):	14.7	14.7	23.7	19.3	42.2	25.3	12.2	21.3	16.8	19	40.3
Pg (Bj):	13.2	10.7	18.3	15.3	39.8	21.1	10.3	18.2	13.2	15.2	39.9
OCR (abc):	2.5	3.7	2.6	2.3	4.7	1.9	4.1	4.3	3.1	3.2	1.0
POP (abc):	8.7	10.7	14.7	10.8	33.2	12.3	9.2	16.3	11.3	13.0	0.3
OCR (Bj):	2.2	2.7	2.0	1.8	4.4	1.6	3.4	3.6	2.4	2.5	1.0
POP (Bj):	7.2	6.7	9.3	6.8	30.8	8.1	7.3	13.2	7.7	9.2	-0.1
Kv0	1.30E-6	2.30E-7	1.00E-8	1.30E-8	2.90E-8	2.10E-8	1.70E-7	1.90E-8	1.30E-8	2.40E-7	2.10E-8

Notes:
- Light grey coloured values were personally determined based on provided data.
- Orange coloured entries indicate values whose correctness and general validity is doubted.
- No soil compressibility parameters from below the dike *crest* were used in settlement predictions

APPENDIX H – Soil parameters determined from raw compression test data (Leendert de Boerspolder)

H1 Tabular overview of soil parameters

Boring No.	**B1002**	**B1002**	**B1002**	**B1002**	**B1002**	**B1002**		**B103**	**B103**	**B104**	**B106**	**B106**
Sample No.	**6-2**	**6-4**	**6-7**	**7-2**	**7-4**	**8-1**		**5**	**6**	**8**	**4**	**5**
Depth below gr.surface [m]	2.92	3.05	3.27	3.66	3.79	4.02		1.85	2.25	4.20	1.95	2.45
	dike slope	dike slope	dike slope	dike slope	dike slope	dike slope		dike crest	dike crest	polder	dike crest	dike crest
Soil class.	Peat	Peat	Peat	Peat	Peat	Peat						
Sat. unit wgt. [kN/m3]	9.64	9.91	9.31	9.83	9.54	9.35						
Dry unit wgt. [kN/m3]	1.32	1.34	1.41	1.41	1.11	1.00						
Init. grav. water content [%]	628.2	639.8	561.0	596.9	757.2	838.3						
Init. void ratio	9.20	9.18	9.21	8.97	11.14	12.73						
Test method	IL	IL	IL	IL	IL	IL		CRS	CRS	CRS	CRS	CRS
a	1.02E-01	8.64E-02	6.34E-02	7.20E-02	8.58E-02	9.99E-02		2.71E-03	2.95E-03	7.89E-03	4.08E-03	4.18E-03
b	3.82E-01	3.66E-01	3.11E-01	3.24E-01	3.38E-01	4.10E-01		4.40E-02	4.66E-02	1.75E-01	6.57E-02	7.09E-02
c	1.16E-02	1.71E-02	1.63E-02	1.68E-02	1.74E-02	2.05E-02		2.18E-03	2.37E-03	1.03E-02	3.36E-03	3.92E-03
RR	1.15E-01	1.01E-01	7.79E-02	8.82E-02	9.88E-02	9.32E-02		6.00E-03	6.40E-03	1.73E-02	9.12E-03	9.10E-03
CR	5.40E-01	5.42E-01	4.74E-01	4.87E-01	4.73E-01	4.88E-01		9.31E-02	9.65E-02	3.25E-01	1.39E-01	1.44E-01
$C_{\alpha\varepsilon}$	2.01E-02	2.61E-02	2.57E-02	2.14E-02	2.07E-02	1.97E-02		4.79E-03	5.15E-03	2.10E-02	7.36E-03	8.42E-03
Cp	115.2	73.3	69.7	76.7	62.1	54.7						
C'p	4.1	4.1	5.0	4.6	4.6	4.3						
Cs	702.1	699.7	541.5	665.7	689.2	516.6						
C's	24.8	19.1	19.4	23.3	24.0	25.3						
Pg (Casagrande)	23.0	26.0	23.0	25.5	22.0	17.5		-	-	-	-	-
Pg (Butterfield)	26.0	26.0	25.0	25.5	22.0	17.5		23.0	18.5	38.0	38.0	25.5
Pg (Becker et al.)	-	-	-	-	-	-		34	20	33.5	34	24
OCR (Casagrande)	1.2	1.5	1.1	1.4	1.1	0.6		-	-	-	-	-
POP (Casagrande)	4.2	8.6	2.4	7.7	2.6	-9.5		-	-	-	-	-
OCR (Butterfield)	1.4	1.5	1.2	1.4	1.1	0.6		1.0	0.7	4.2	1.5	0.9
POP (Butterfield)	7.2	8.6	4.4	7.7	2.6	-9.5		-0.8	-8.5	29.0	13.4	-3.2
OCR (Becker et al.)	-	-	-	-	-	-		1.4	0.7	3.7	1.4	0.8
POP (Becker et al.)	-	-	-	-	-	-		10.3	-7.0	24.5	9.4	-4.7
Consolidation coefficients [m2/s] & hydraulic conductivity [m/s]												
cv trap 2	1.16E-05	1.19E-05	2.62E-05	1.79E-05	1.67E-05	2.84E-05	**cv** 9 kPa			6.60E-07		
cv trap 3	1.18E-05	1.02E-05	6.83E-06	6.43E-06	4.56E-06	5.69E-06	**cv** 25 kPa	9.88E-07	1.11E-06	7.94E-07	1.25E-06	6.44E-07
cv trap 7	3.43E-07	6.86E-08	2.53E-07	2.05E-07	3.03E-07	1.88E-08	**cv** 50 kPa	1.49E-06	1.53E-06	3.16E-07	1.59E-08	5.09E-06
Kv 2	5.71E-07	6.10E-07	1.41E-06	8.22E-07	9.36E-07	1.82E-06	**Kv** 9 kPa			7.52E-06		
Kv 3	5.12E-07	3.59E-07	3.48E-07	2.46E-07	1.95E-07	3.84E-07	**Kv** 25 kPa	9.55E-06	8.03E-06	8.06E-06	1.21E-05	9.77E-06
Kv 7	1.40E-08	2.78E-09	8.54E-09	6.91E-09	1.03E-08	6.91E-10	**Kv** 50 kPa	8.67E-06	8.41E-06	6.71E-06	1.06E-05	7.01E-06

Notes:
- Red coloured values are acknowledged to be incorrect.
- Orange coloured values indicate results whose correctness and general validity is doubted (Kv ought to be lower than cv)
- The subsequent Sub-Appendices H2 and H3 contain each for *one* tested specimen, par example, the relevant compression and consolidation diagrams that the above displayed parameters were derived from.

H2 Example compression diagrams (IL: B1002 6-2)

The following graphs and line constructions were drawn each for **all 6** tested samples, in order to determine all required compressibility or consolidation parameters.

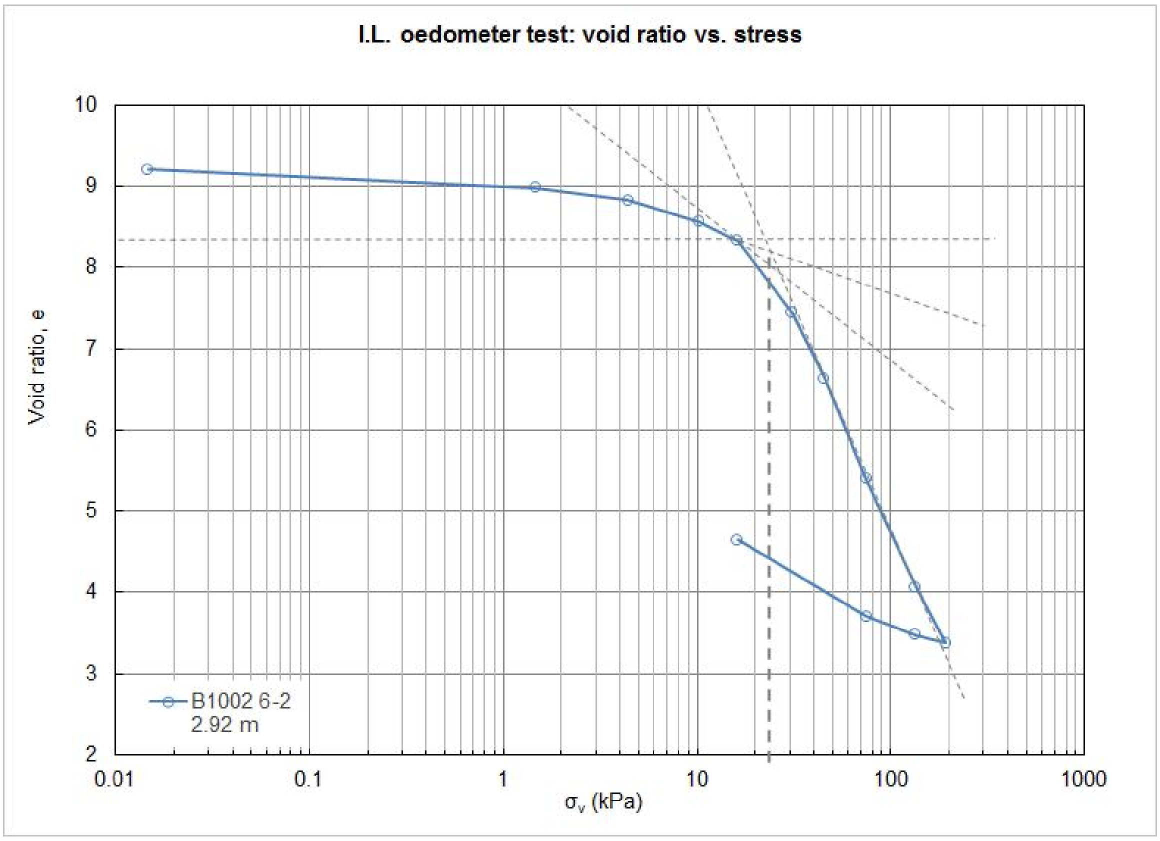

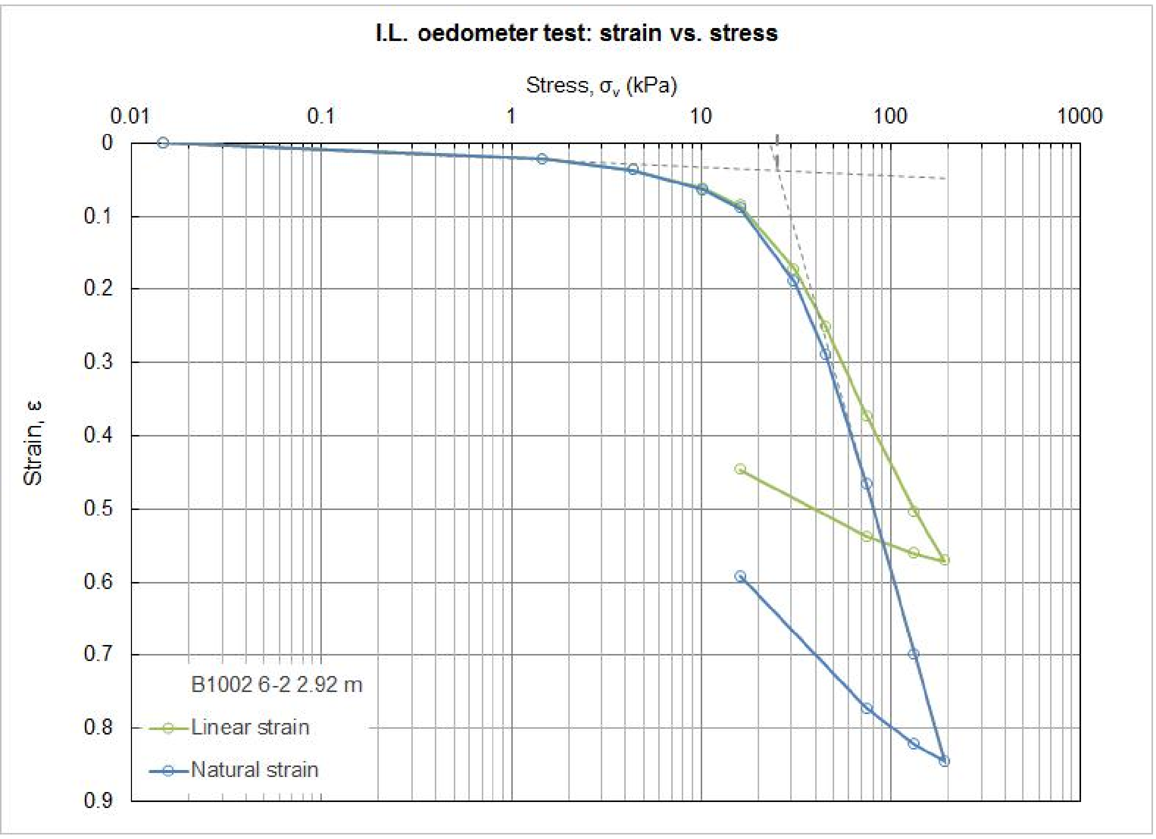

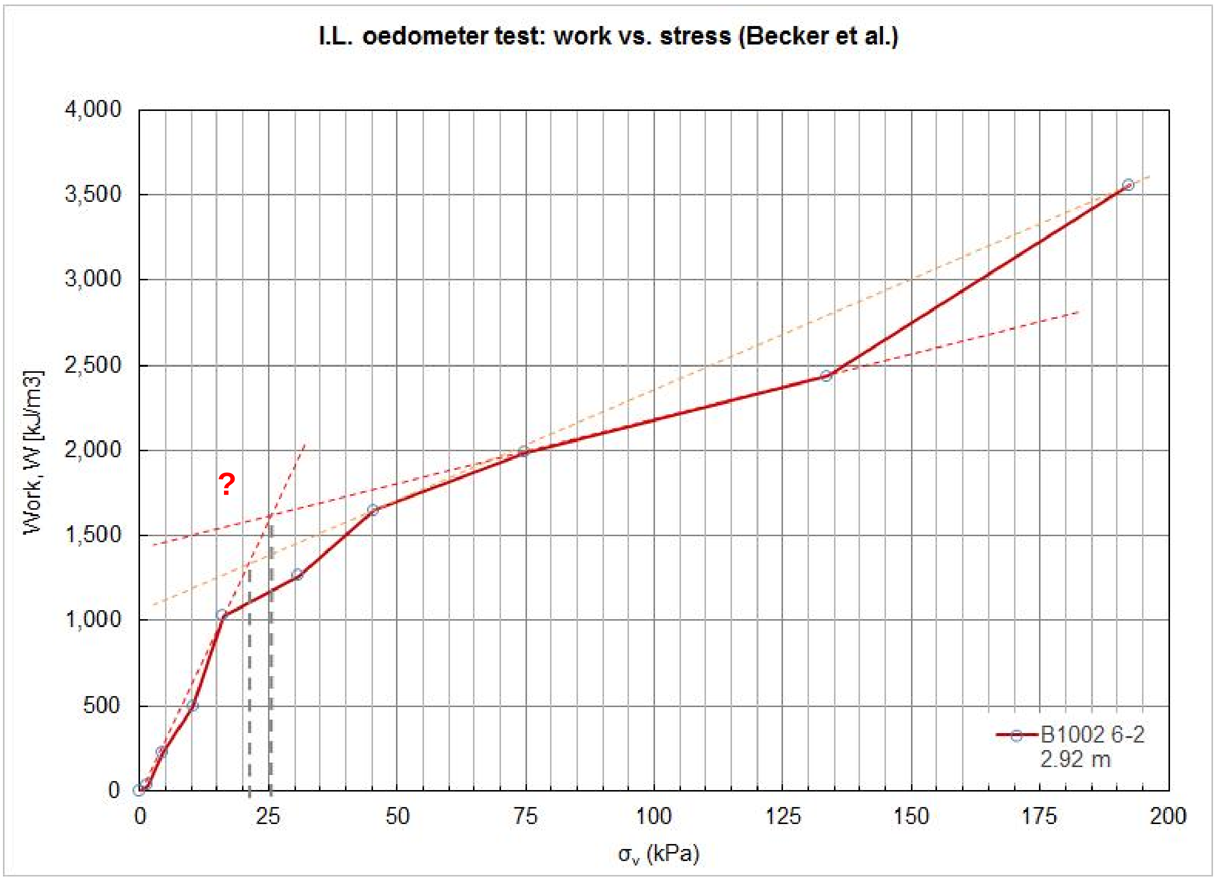
I.L. oedometer test: work vs. stress (Becker et al.)
Work, W [kJ/m3]
4,000
3,500
3,000
2,500
2,000
1,500
1,000
500
0
0
25
50
75
100
125
150
175
200
σv (kPa)
?
B1002 6-2
2.92 m

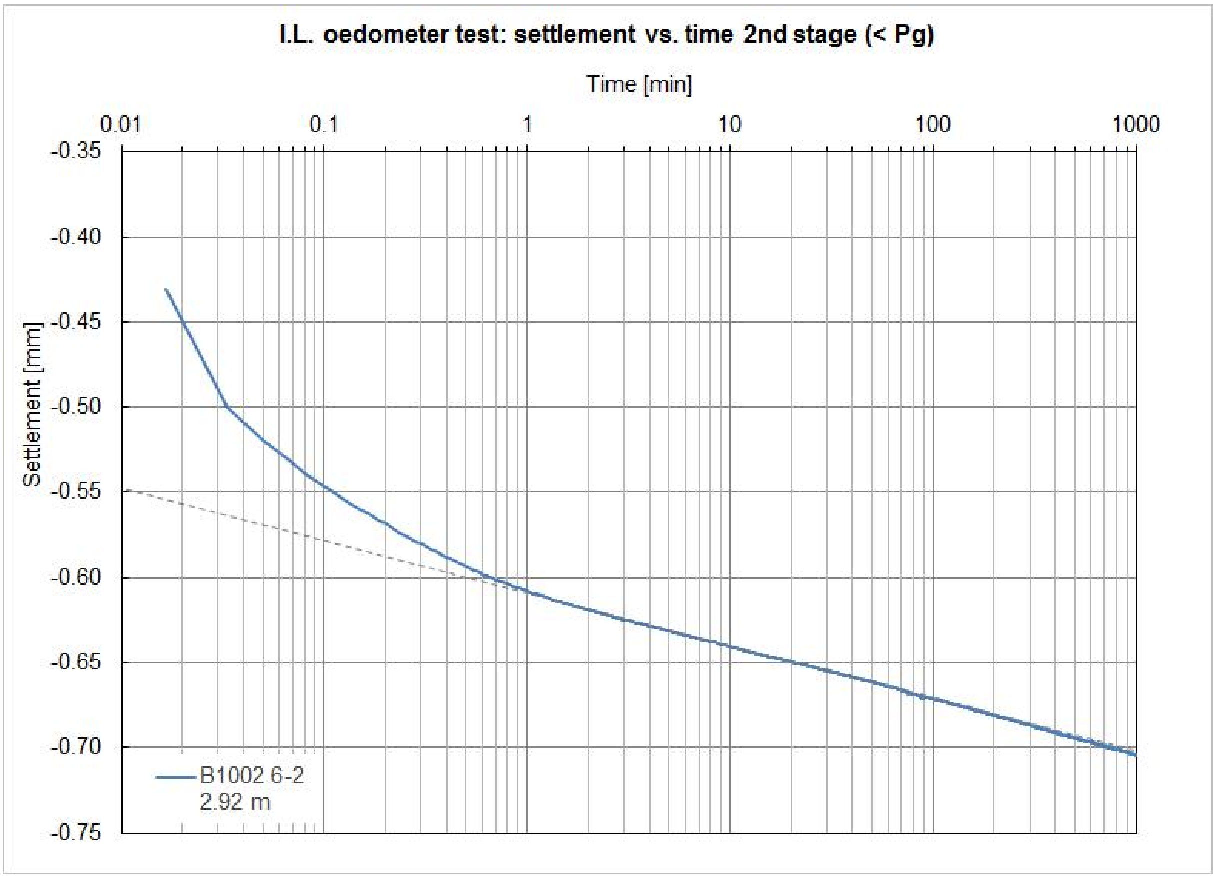
I.L. oedometer test: settlement vs. time 2nd stage (< Pg)
Time [min]
0.01
0.1
1
10
100
1000
Settlement [mm]
-0.35
-0.40
-0.45
-0.50
-0.55
-0.60
-0.65
-0.70
-0.75
B1002 6-2
2.92 m

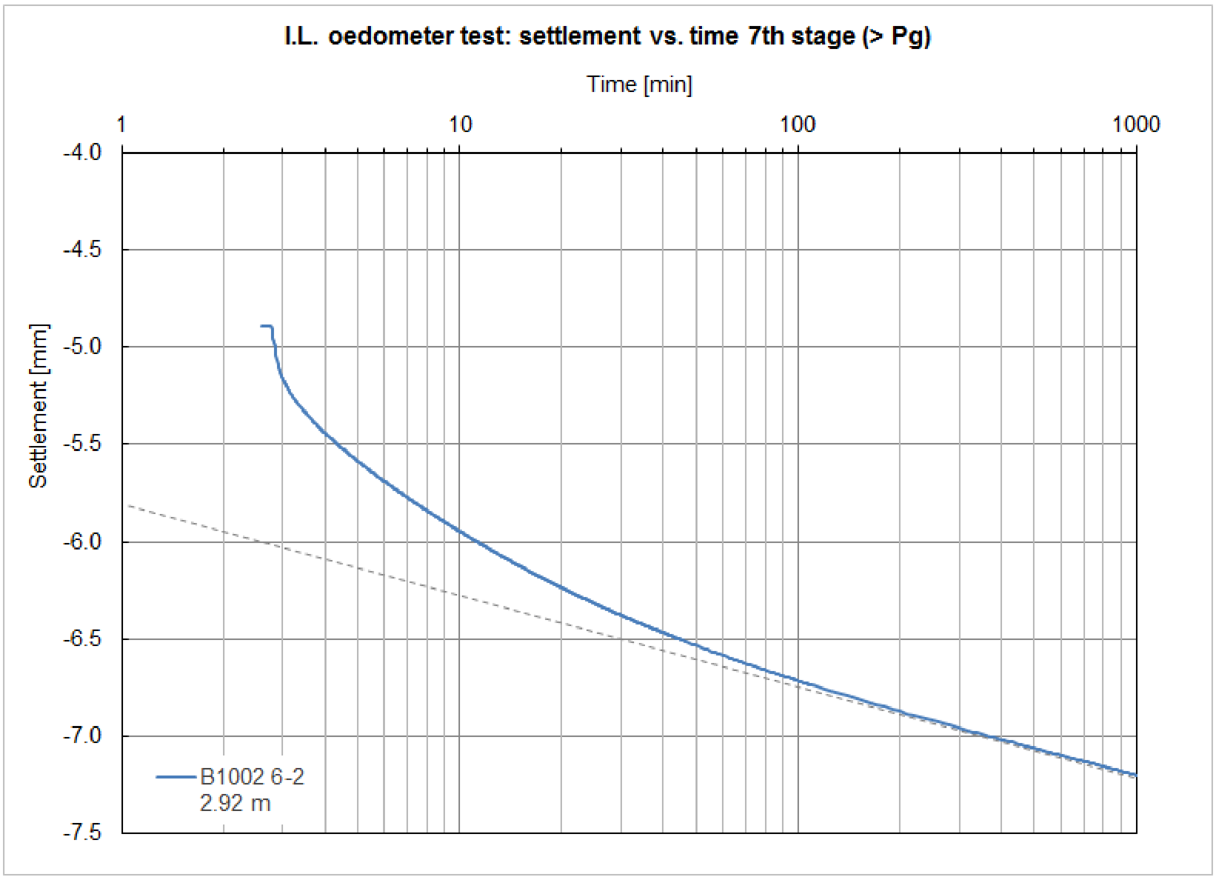
I.L. oedometer test: settlement vs. time 7th stage (> Pg)
Time [min]
1
10
100
1000
Settlement [mm]
-4.0
-4.5
-5.0
-5.5
-6.0
-6.5
-7.0
-7.5
B1002 6-2
2.92 m

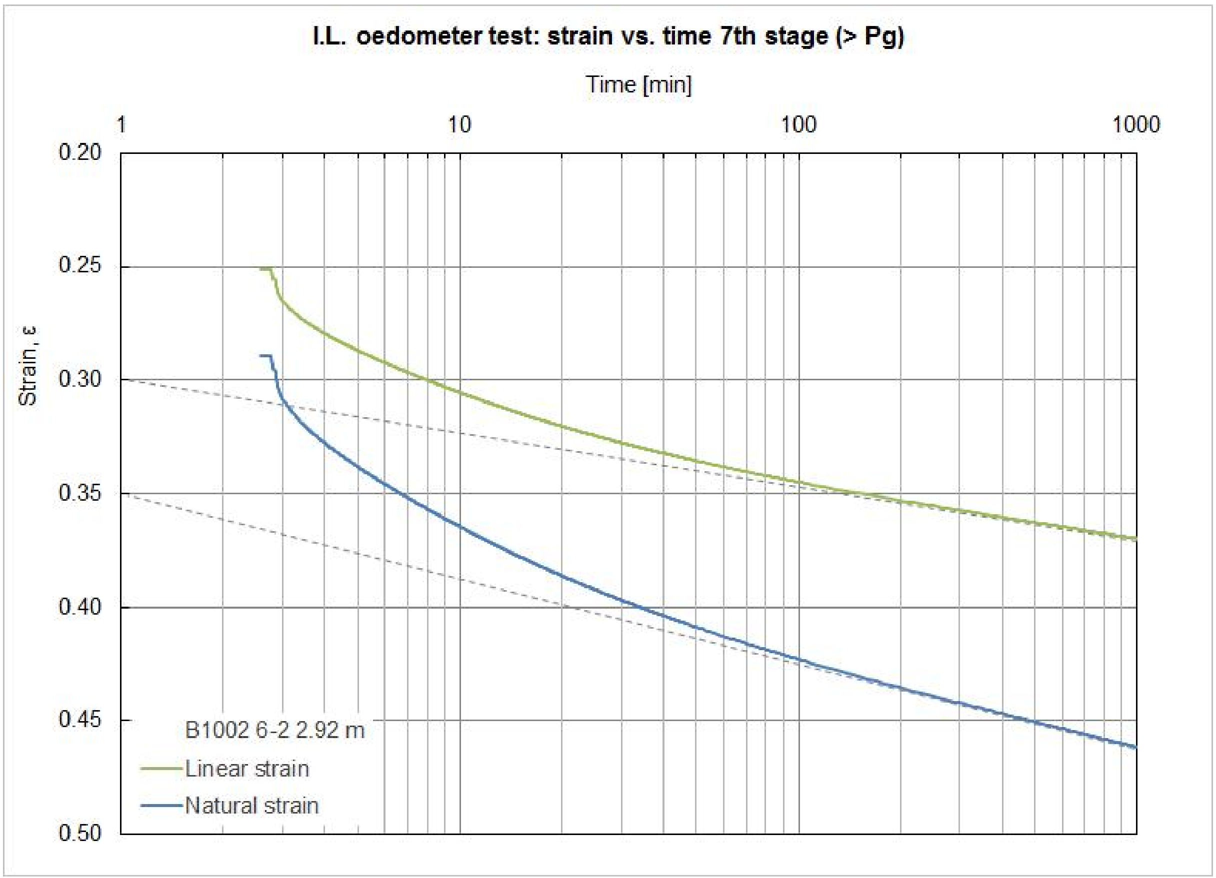
I.L. oedometer test: strain vs. time 7th stage (> Pg)
Time [min]
1
10
100
1000
Strain, ε
0.20
0.25
0.30
0.35
0.40
0.45
0.50
B1002 6-2 2.92 m
Linear strain
Natural strain

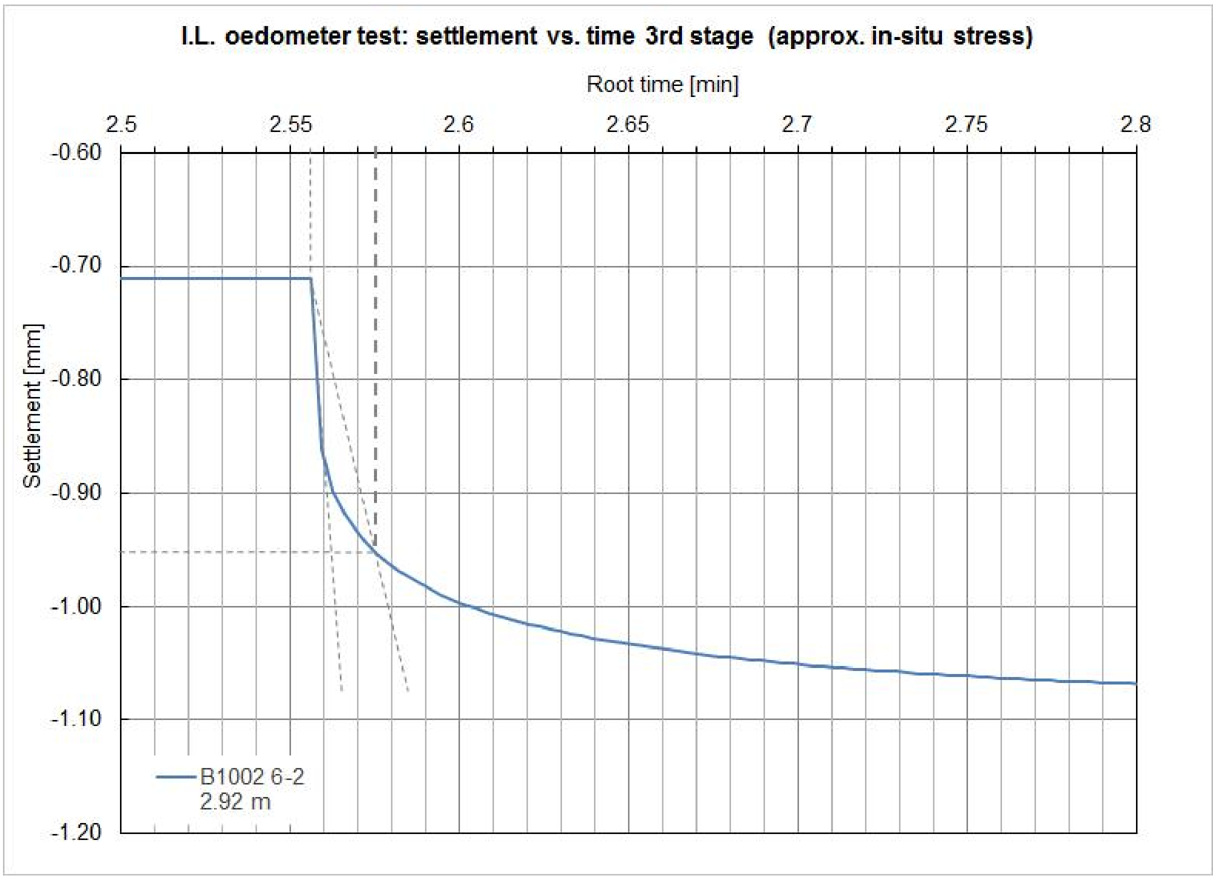
I.L. oedometer test: settlement vs. time 3rd stage (approx. in-situ stress)
Root time [min]
2.5
2.55
2.6
2.65
2.7
2.75
2.8
-0.60
-0.70
-0.80
-0.90
-1.00
-1.10
-1.20
Settlement [mm]
B1002 6-2
2.92 m

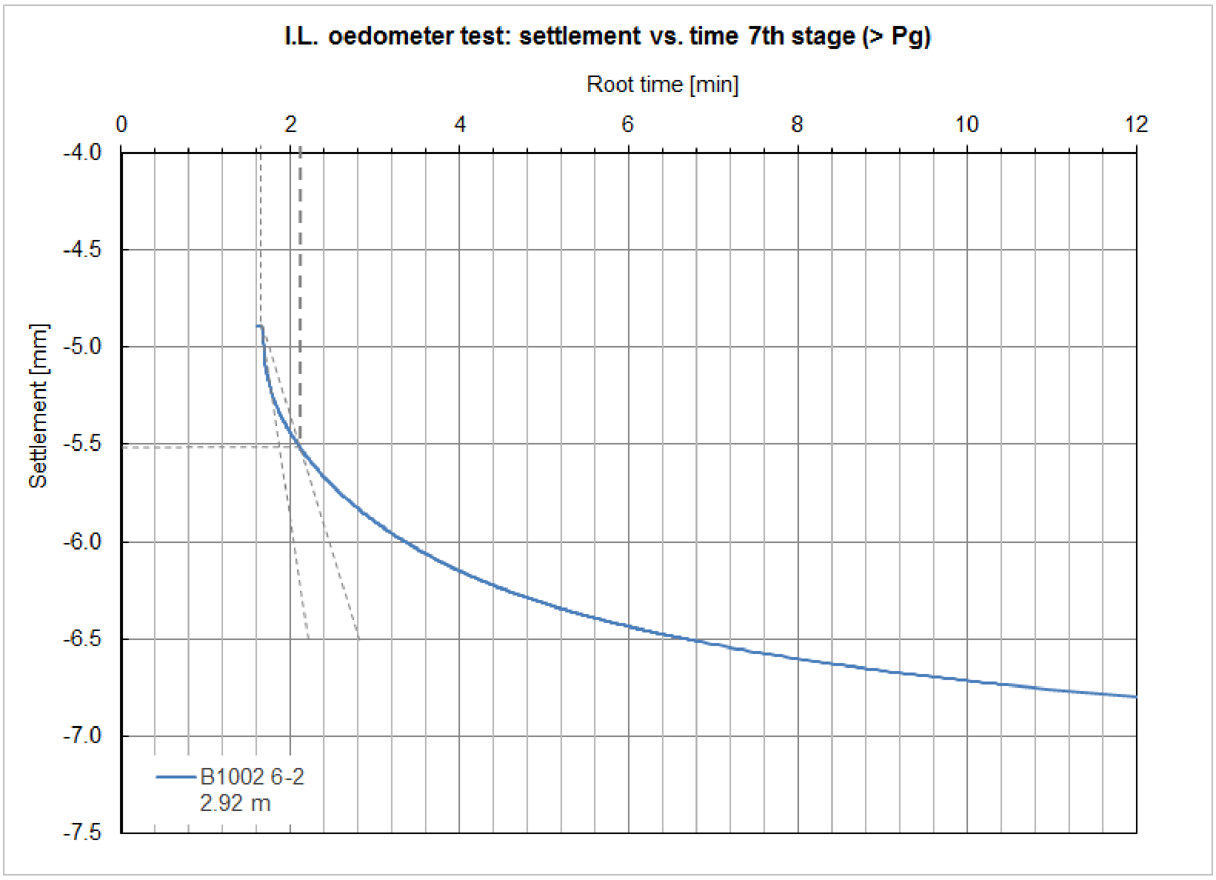
I.L. oedometer test: settlement vs. time 7th stage (> Pg)
Root time [min]
0
2
4
6
8
10
12
-4.0
-4.5
-5.0
-5.5
-6.0
-6.5
-7.0
-7.5
Settlement [mm]
B1002 6-2
2.92 m

H3 Example compression diagrams (CRS: B103 5)

The following graphs and line constructions were drawn each for **all 5** tested samples, in order to determine all required compressibility or consolidation parameters.

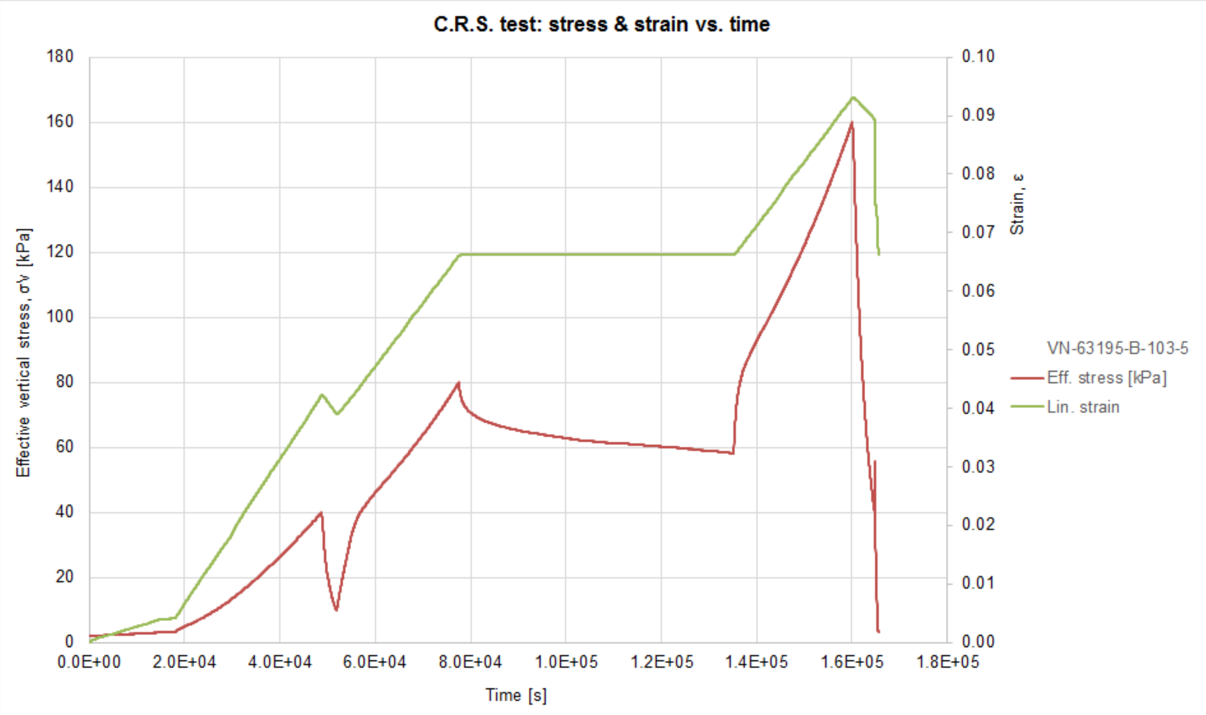

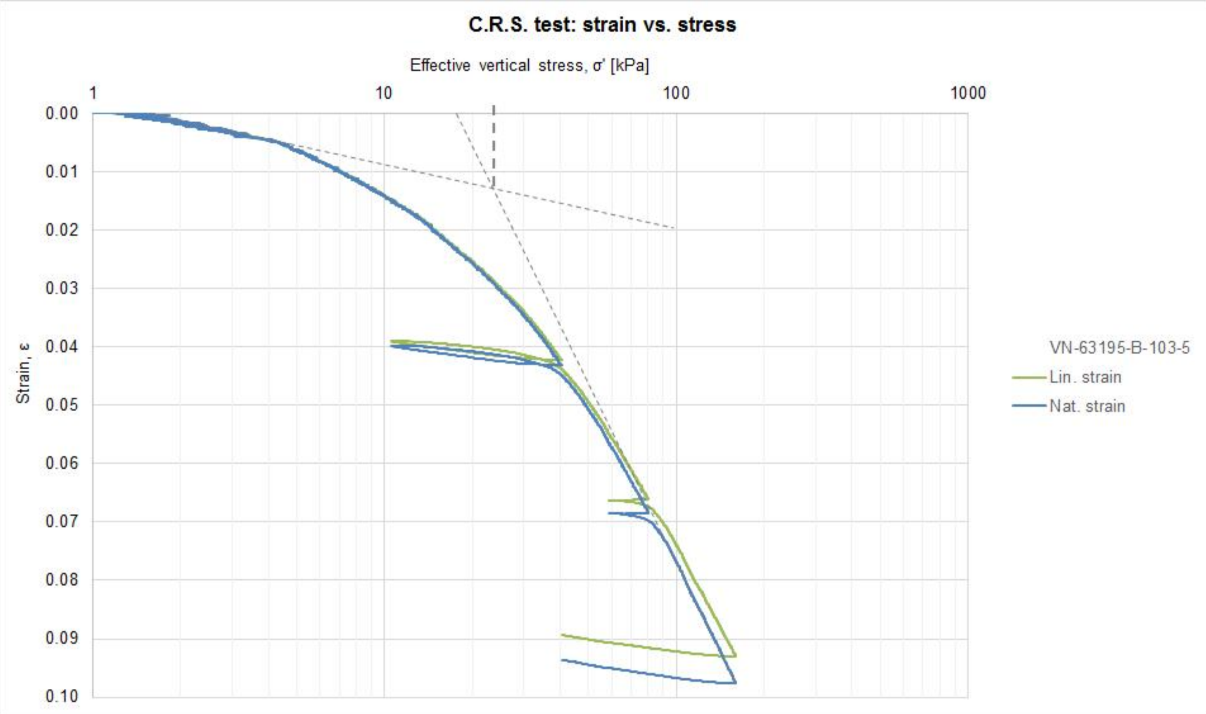

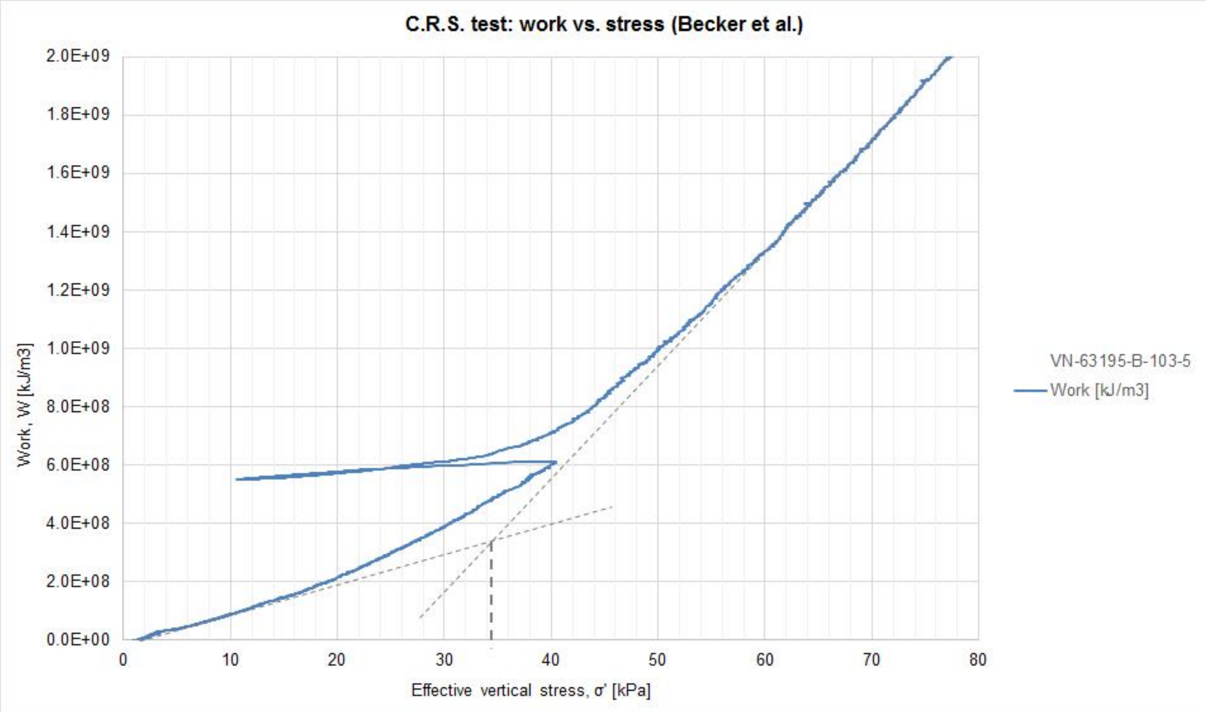
C.R.S. test: work vs. stress (Becker et al.)
Work, W [kJ/m3]
Effective vertical stress, σ' [kPa]
VN-63195-B-103-5
Work [kJ/m3]
0.0E+00
2.0E+08
4.0E+08
6.0E+08
8.0E+08
1.0E+09
1.2E+09
1.4E+09
1.6E+09
1.8E+09
2.0E+09
0
10
20
30
40
50
60
70
80

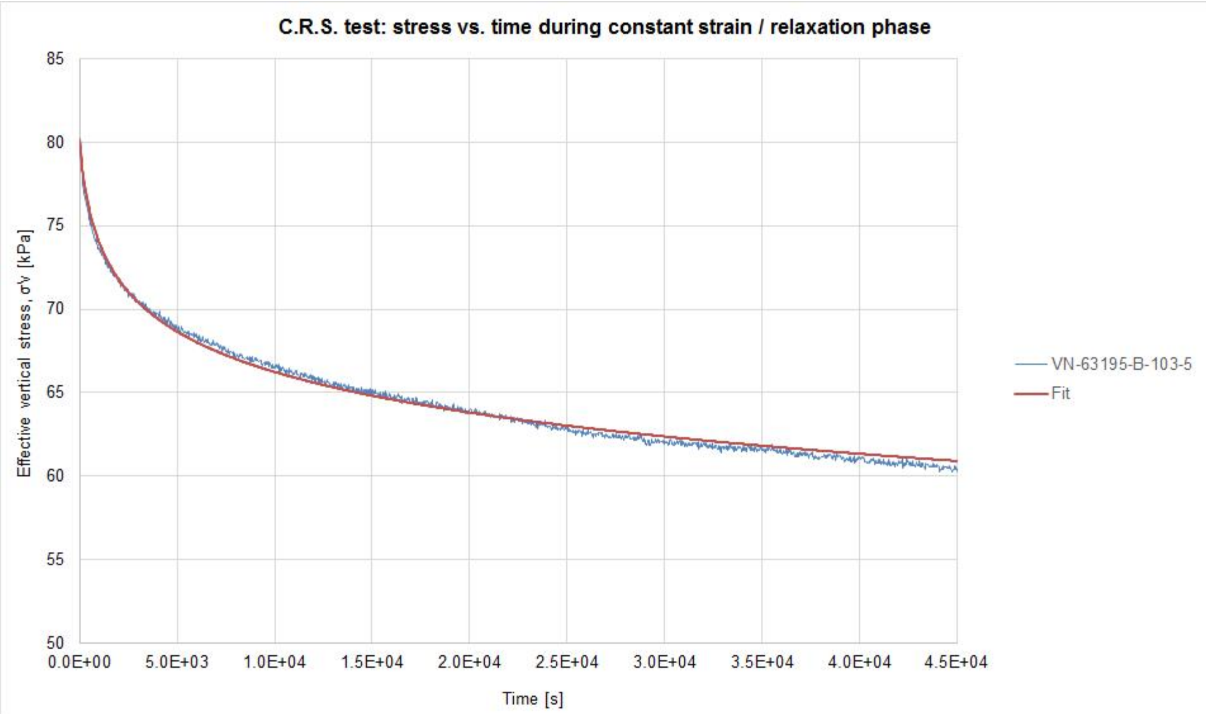
C.R.S. test: stress vs. time during constant strain / relaxation phase
Effective vertical stress, σ'v [kPa]
Time [s]
VN-63195-B-103-5
Fit
50
55
60
65
70
75
80
85
0.0E+00
5.0E+03
1.0E+04
1.5E+04
2.0E+04
2.5E+04
3.0E+04
3.5E+04
4.0E+04
4.5E+04

APPENDIX I – Settlement predictions: Fokkens

I1 Bloemendalerpolder

	Analytical formula				Empirical formula				TAW (1996) adaptation				CUR (1996) adaptation			
	T1	T2	T1 (avg)	T2 (avg)	T1	T2	T1 (avg)	T2 (avg)	T1	T2	T1 (avg)	T2 (avg)	T1	T2	T1 (avg)	T2 (avg)
ΔZ, Δh [m] (NC)	**3.61**	**5.03**	**3.63**	**5.00**	**1.65**	**2.46**	**1.72**	**2.36**	**1.88**	**2.94**	**2.01**	**2.77**	**1.96**	**3.03**	**2.09**	**2.87**
Rel. error [%]	125.8	109.5	127.2	108.3	2.8	2.5	7.3	-1.6	17.7	22.4	25.9	15.4	22.3	26.4	30.4	19.5
ΔZ, Δh [m] (OC)	**3.60**	**4.95**	**3.60**	**4.95**	**1.76**	**2.79**	**1.90**	**2.61**								
Rel. error [%]	124.9	106.3	125.2	106.4	9.9	16.1	18.5	8.6								
Z, h0 [m]	4	5.5	4	5.5	4	5.5	4	5.5	4	5.5	4	5.5	4	5.5	4	5.5
n1	0.91	0.92	0.92	0.92	0.91	0.92	0.92	0.92	0.91	0.92	0.92	0.92	0.91	0.92	0.92	0.92
Cv (< pg)	0.23	0.20	0.21	0.21	0.23	0.20	0.21	0.21	0.23	0.20	0.21	0.21	0.23	0.20	0.21	0.21
Cv (> pg)	0.12	0.12	0.12	0.12	0.12	0.12	0.12	0.12	0.12	0.12	0.12	0.12	0.12	0.12	0.12	0.12
A1, w0	939.2	1005.8	972.5	972.5	939.2	1005.8	972.5	972.5	939.2	1005.8	972.5	972.5	939.2	1005.8	972.5	972.5
N	76.5	71.1	73.8	73.8	76.5	71.1	73.8	73.8	76.5	71.1	73.8	73.8	76.5	71.1	73.8	73.8
H	79.5	73.9	76.7	76.7	79.5	73.9	76.7	76.7	79.5	73.9	76.7	76.7	79.5	73.9	76.7	76.7
p1	57.1	57.1	57.1	57.1	57.1	57.1	57.1	57.1	5.6	5.6	5.6	5.6	5.6	5.6	5.6	5.6
p2	327.8	327.8	327.8	327.8	327.8	327.8	327.8	327.8	32.2	32.2	32.2	32.2	32.2	32.2	32.2	32.2
pm	163.1	229.4	196.2	196.2	163.1	229.4	196.2	196.2	16.0	22.5	19.3	19.3	16.0	22.5	19.3	19.3
G	1.50	1.50	1.50	1.50	1.50	1.50	1.50	1.50	1.50	1.50	1.50	1.50	1.50	1.50	1.50	1.50
yw	9.81	9.81	9.81	9.81	9.81	9.81	9.81	9.81	9.81	9.81	9.81	9.81	9.81	9.81	9.81	9.81

Reference values being validated with: **1.60 m for T1**, and **2.40 m for T2**, according to best fit [Ammerlaan & Hoefsloot, 2012]

Note (1): “avg” means that the input soil properties were averaged from both locations, except for the layer thickness Z or h0.
Note (2): Orange coloured values are values that exceed a relative error of ±15%, or that make no sense at all.
Note (3): Repetitive values are greyed out in order to keep better overview.

I2 Amstelhoek

	Analytical formula				Empirical formula				TAW (1996) adaptation				CUR (1996) adaptation			
	Peat, basis	Clay, middle	Peat top	TOT	Peat, basis	Clay, middle	Peat top	TOT	Peat, basis	Clay, middle	Peat top	TOT	Peat, basis	Clay, middle	Peat top	TOT
ΔZ, Δh [m] (NC)	1.08	1.66	0.60	**3.35**	0.19	0.89	0.14	**1.22**	-0.36	1.26	-0.01	**0.89**	-0.31	1.28	0.01	**0.98**
Rel. error [%]				415.6				87.1				36.9				51.5
ΔZ, Δh [m] (OC)	1.16	2.04	0.55	**3.75**	-0.38	1.23	-0.02	**0.83**								
Rel. error [%]				477.0				27.6								
Z, h0 [m]	1.3	2.5	0.7		1.3	2.5	0.7		1.3	2.5	0.7		1.3	2.5	0.7	
n1	0.87	0.68	0.89		0.87	0.68	0.89		0.87	0.68	0.89		0.87	0.68	0.89	
Cv (< pg)	0.20	0.50	0.20		0.20	0.50	0.20		0.20	0.50	0.20		0.20	0.50	0.20	
Cv (> pg)	0.10	0.25	0.10		0.10	0.25	0.10		0.10	0.25	0.10		0.10	0.25	0.10	
A1, w0	422.6	98.6	460.0		422.6	98.6	460.0		422.6	98.6	460.0		422.6	98.6	460.0	
N	87.4	4.6	71.9		87.4	4.6	71.9		87.4	4.6	71.9		87.4	4.6	71.9	
H	90.9	4.7	74.7		90.9	4.7	74.7		90.9	4.7	74.7		90.9	4.7	74.7	
p1	91.8	82.6	82.6		91.8	82.6	82.6		9.0	8.1	8.1		9.0	8.1	8.1	
p2	292.0	282.8	282.8		292.0	282.8	282.8		28.6	27.7	27.7		28.6	27.7	27.7	
pm	555.6	303.3	251.4		555.6	303.3	251.4		54.5	29.8	24.7		54.5	29.8	24.7	
G	1.50	2.60	1.50		1.50	2.60	1.50		1.50	2.60	1.50		1.50	2.60	1.50	
γw	9.81	9.81	9.81		9.81	9.81	9.81		9.81	9.81	9.81		9.81	9.81	9.81	

Reference value being validated with: **0.65 m**, according to best fit based on settlement beacon ZB181 at 2000 m [Sipkema, 2012]

Note (1): “TOT” indicates the total (cumulative) final settlement estimation from the 3 preceding components.
Note (2): Orange coloured values are values that exceed a relative error of ±15%, or that make no sense at all.
Note (3): Repetitive values are greyed out in order to keep better overview.

APPENDIX J – Settlement predictions: D-Settlement

The following and altogether last pages of this thesis comprise all relevant D-Settlement "Input View" subsurface geometries, as well as "Time-History" settlement curves resulting from subsequent settlement predictions.

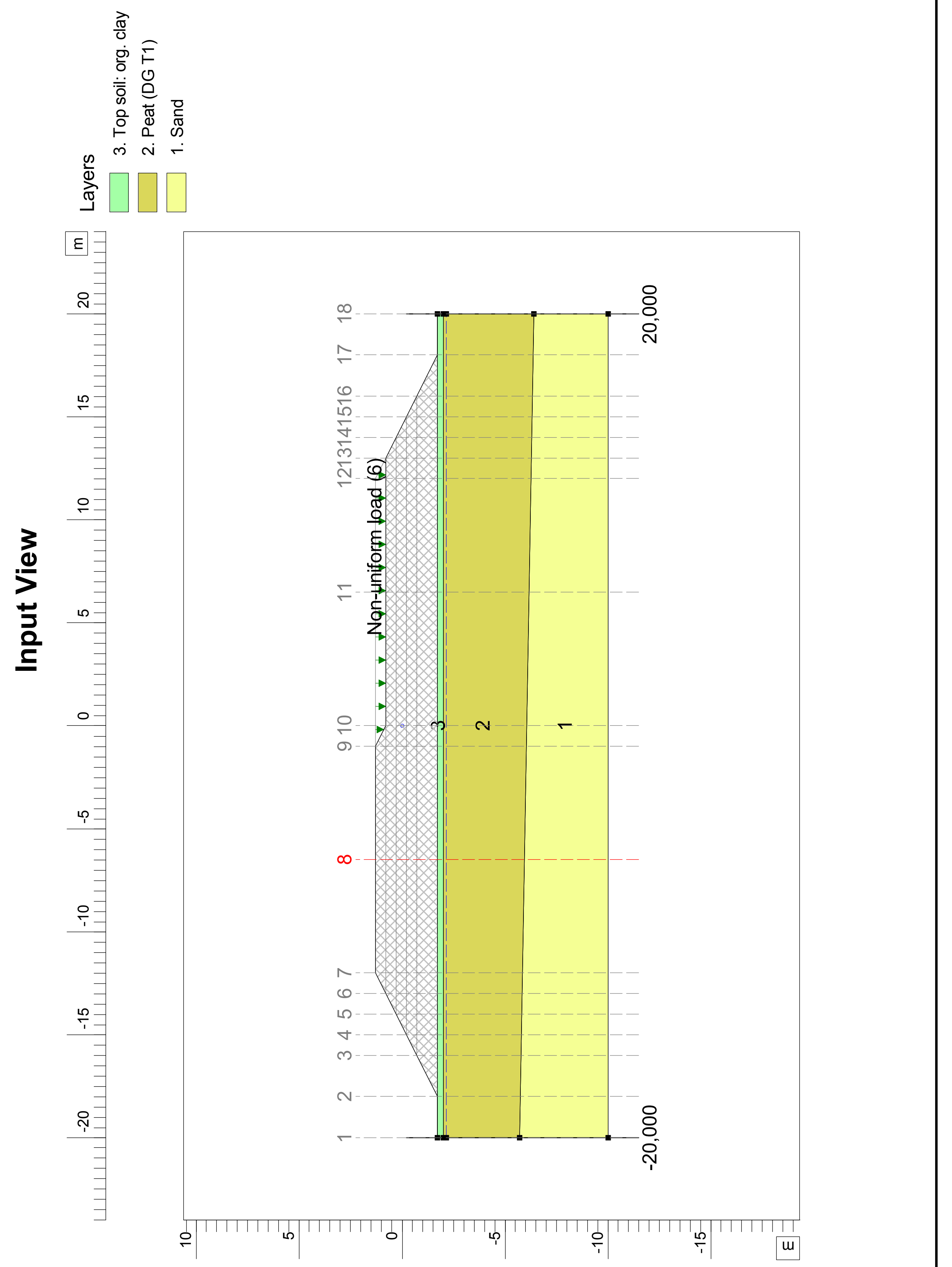

D-Settlement 15.1 : Blp Koppejan+Glopper.sli

Grontmij	Phone Fax	date 2016	drw. CBH
Bloemendalerpolder trial embankment 1 Koppejan parameters from De Glopper's correlations		- Annex -	ctr. form. A4

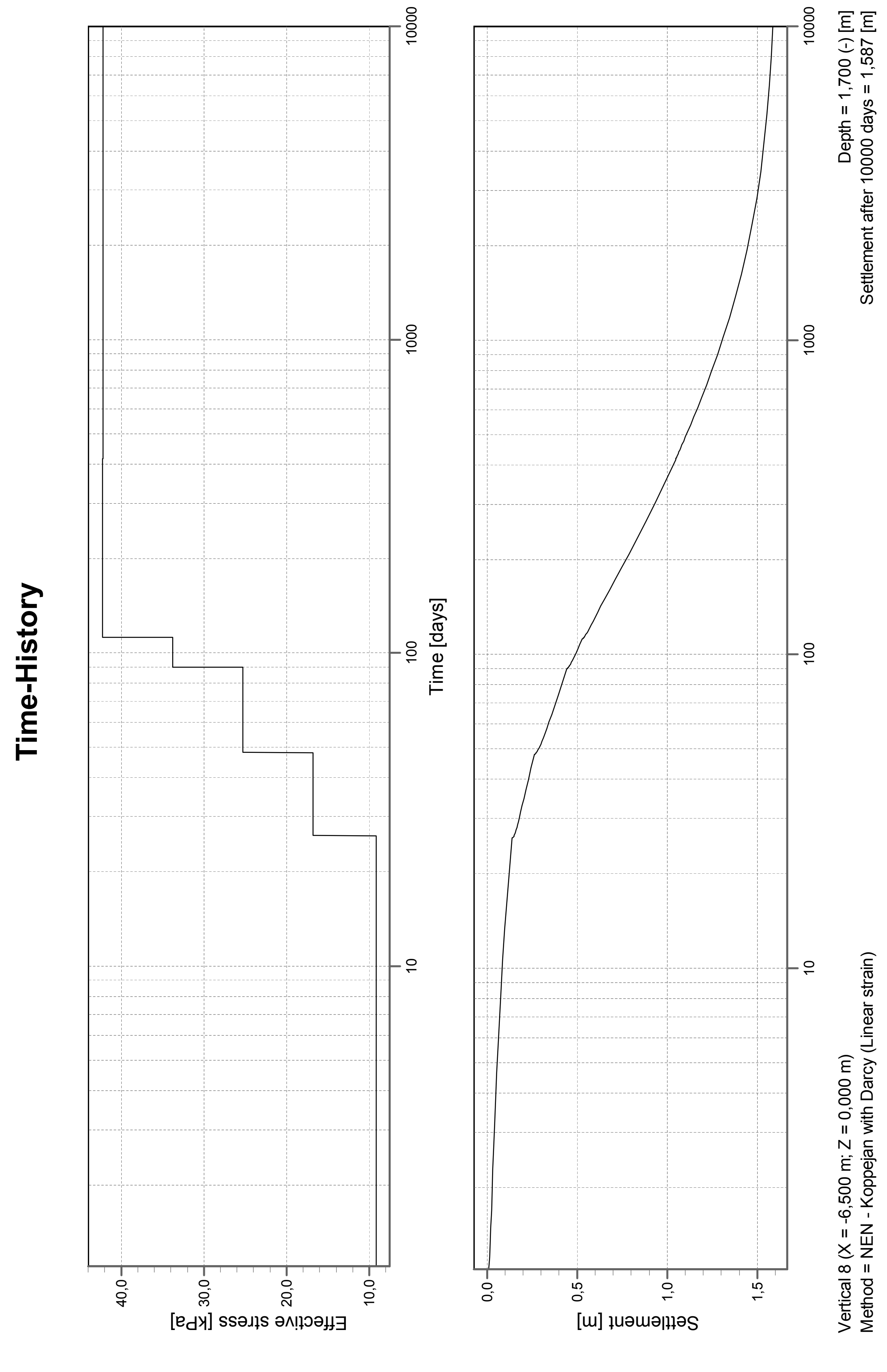

D-Settlement 15.1 : Blp Koppejan+Glopper.sli

Grontmij	Phone Fax	date 2016	drw. CBH
Bloemendalerpolder trial embankment 1 Koppejan parameters ~~from De Glopper's correlations~~ original (lab) parameters		-	ctr.
		Annex -	form. A4

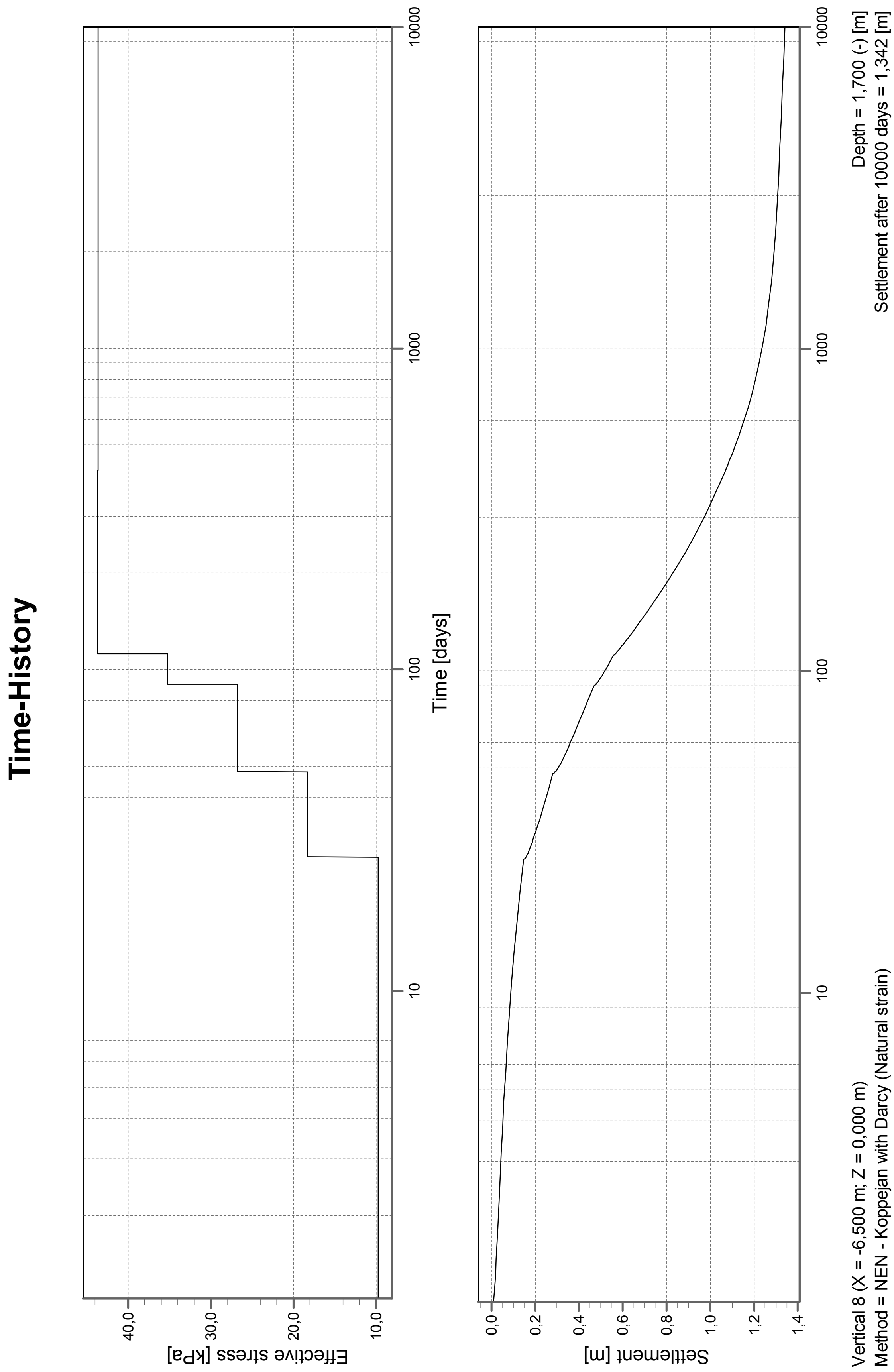

D-Settlement 15.1 : Blp Koppejan+Glopper.sli

Grontmij	Phone Fax	date 2016	drw. CBH
Bloemendalerpolder trial embankment 1 Koppejan parameters ~~from De Glopper's correlations~~ original (lab) parameters		-	ctr.
		Annex -	form. A4

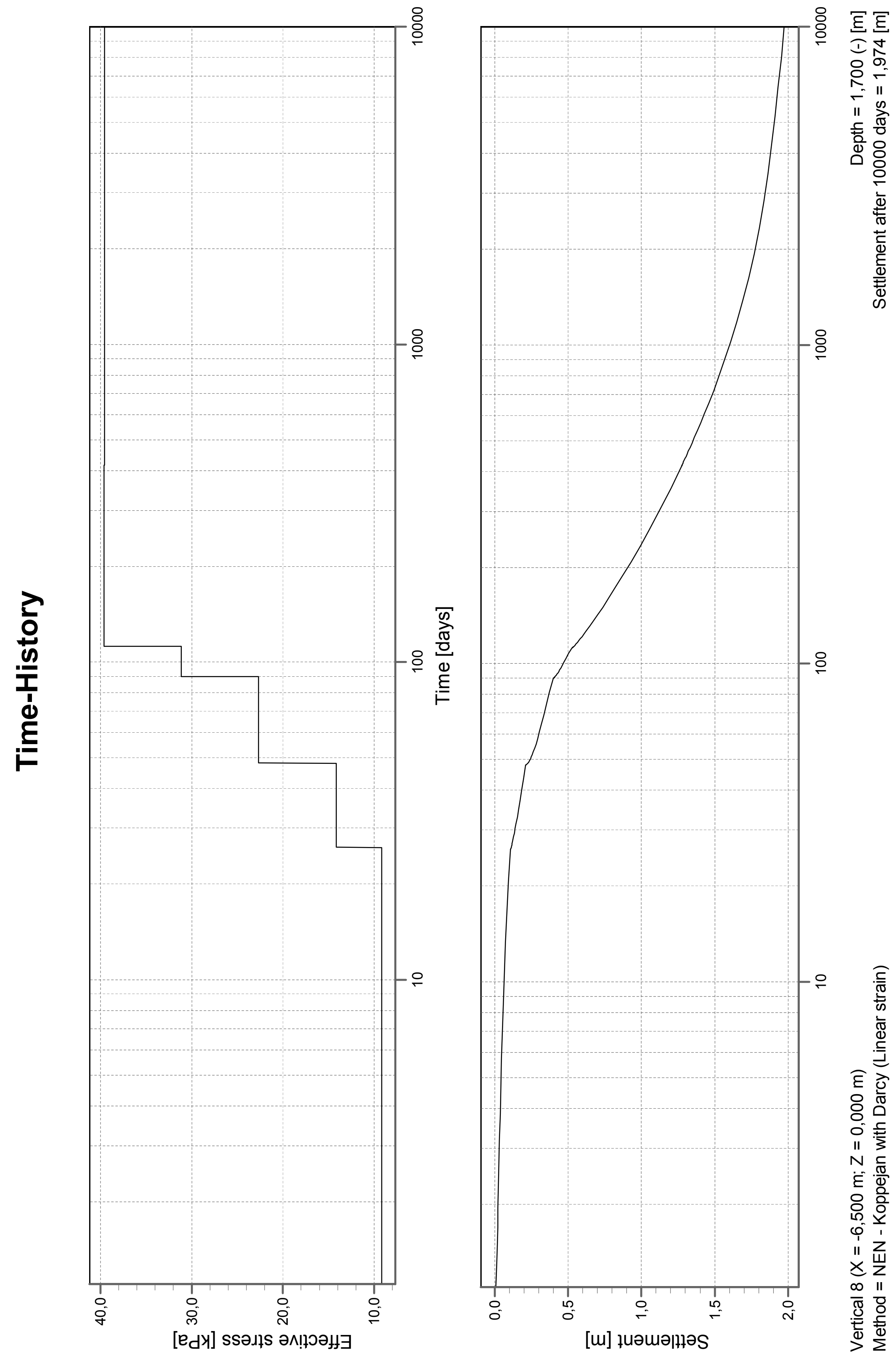

D-Settlement 15.1 : Blp Koppejan+Glopper.sli

Grontmij	Phone Fax	date 2016	drw. CBH
Bloemendalerpolder trial embankment 1 Koppejan parameters from De Glopper's correlations (T1 properties only)		- Annex -	ctr. form. A4

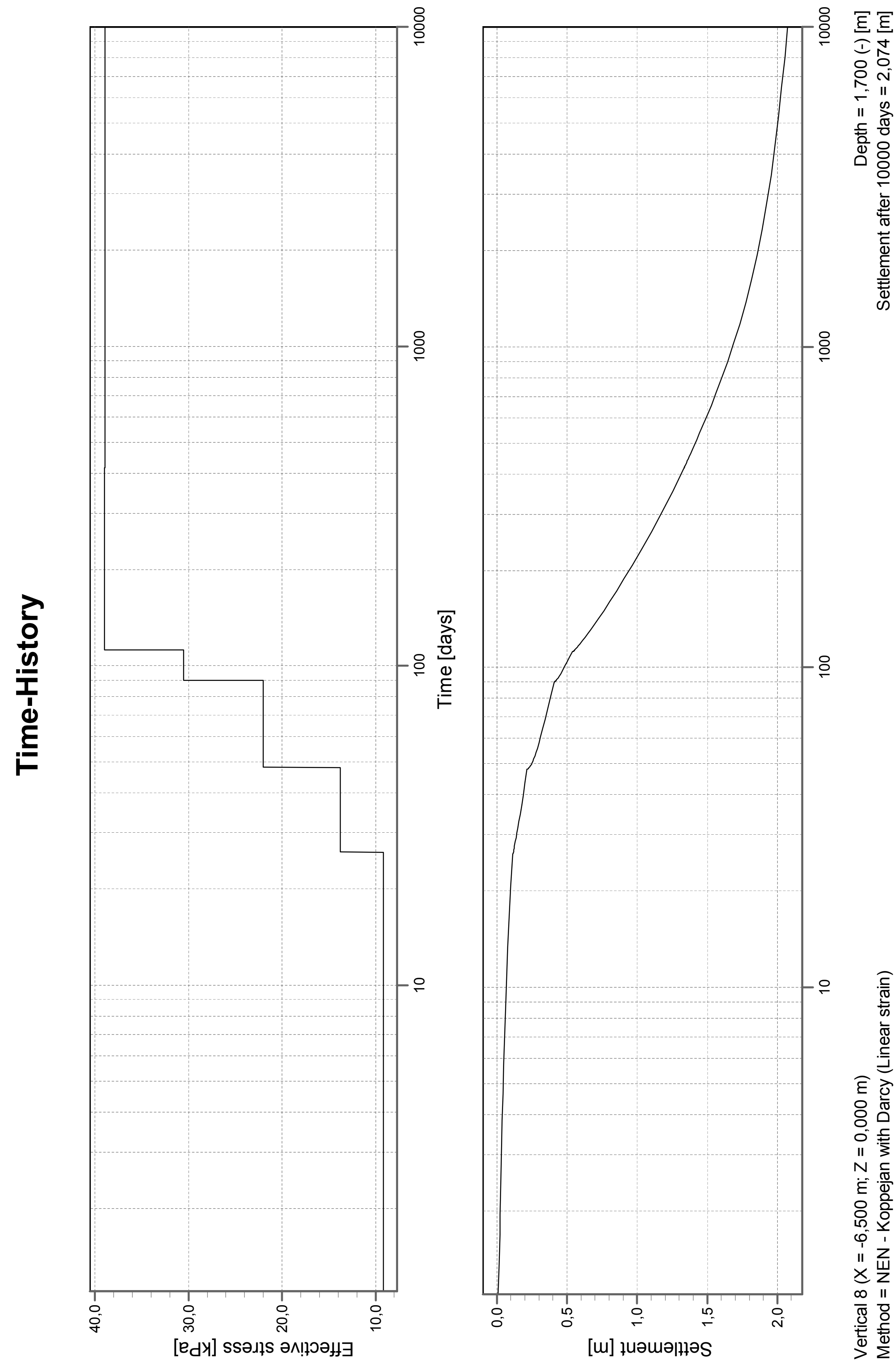

D-Settlement 15.1 : Blp Koppejan+Glopper.sli

Grontmij	Phone Fax	date 2016	drw. CBH
Bloemendalerpolder trial embankment 1 Koppejan parameters from De Glopper's correlations (T1+T2 average properties)		- Annex -	ctr. form. A4

Time-History

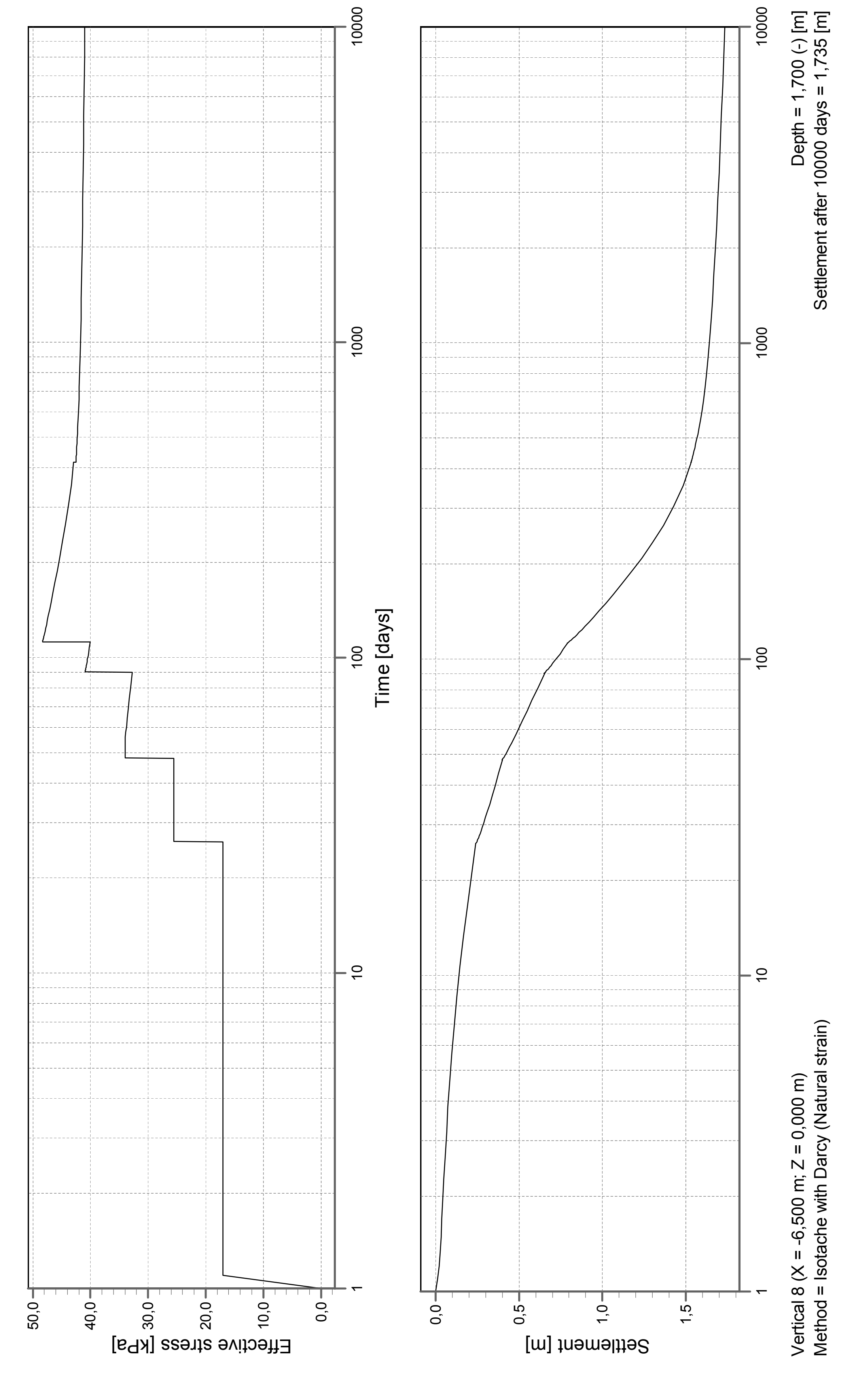

D-Settlement 15.1 : Blp abc.sli

Grontmij	Phone Fax	date 2016	drw. CBH
Bloemendalerpolder trial embankment 1 abc-Isotachs ~~parameters from correlations~~ original (lab) parameters		-	ctr.
		Annex -	form. A4

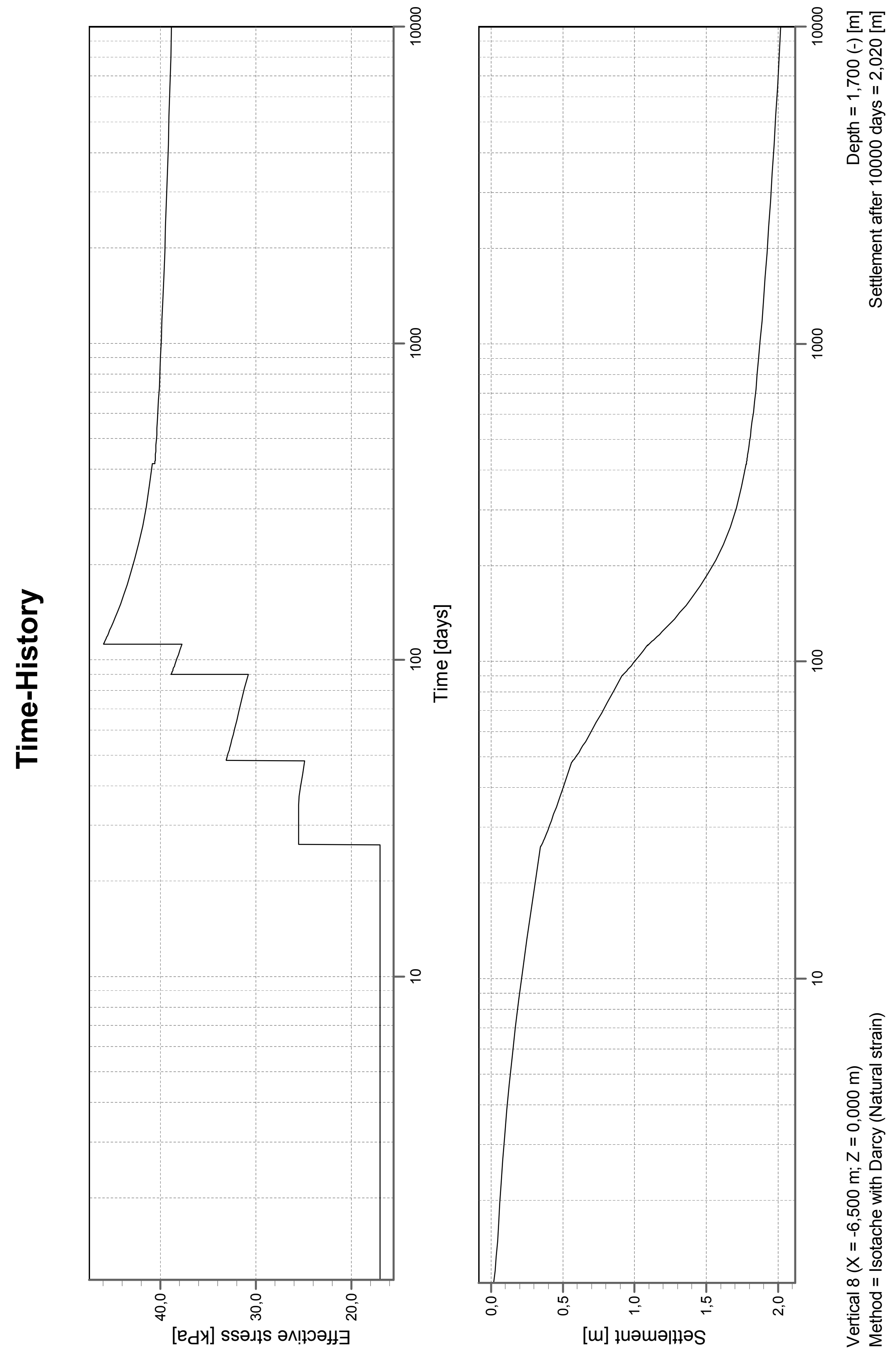

D-Settlement 15.1 : Blp abc.sli

Grontmij	Phone Fax	date 2016	drw. CBH
Bloemendalerpolder trial embankment 1 abc-Isotachs parameters from correlations (set 1)		-	ctr.
		Annex -	form. A4

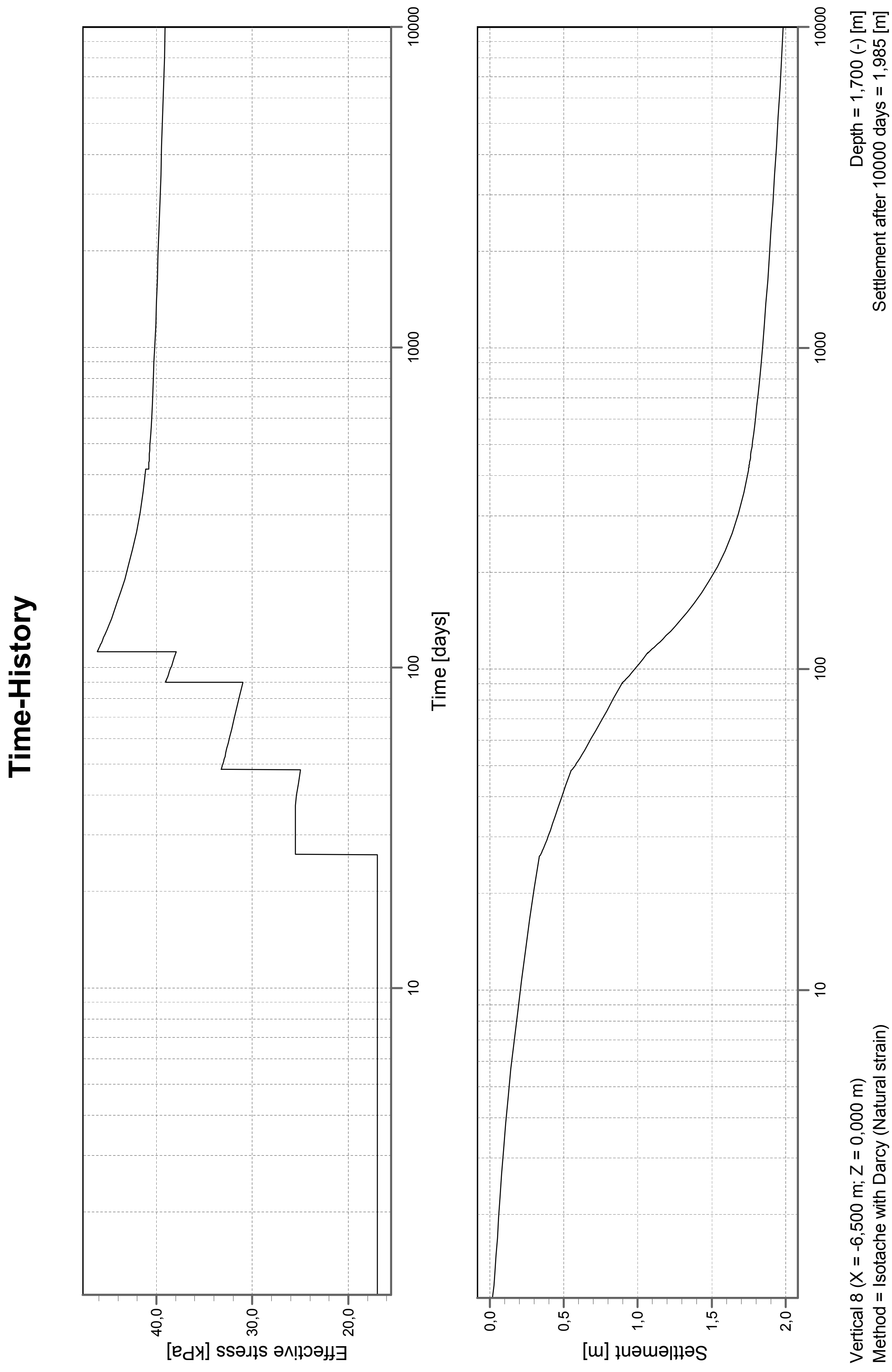

D-Settlement 15.1 : Blp abc.sli

Grontmij	Phone Fax	date 2016	drw. CBH
Bloemendalerpolder trial embankment 1 abc-Isotachs parameters from correlations (set 2)		-	ctr.
		Annex -	form. A4

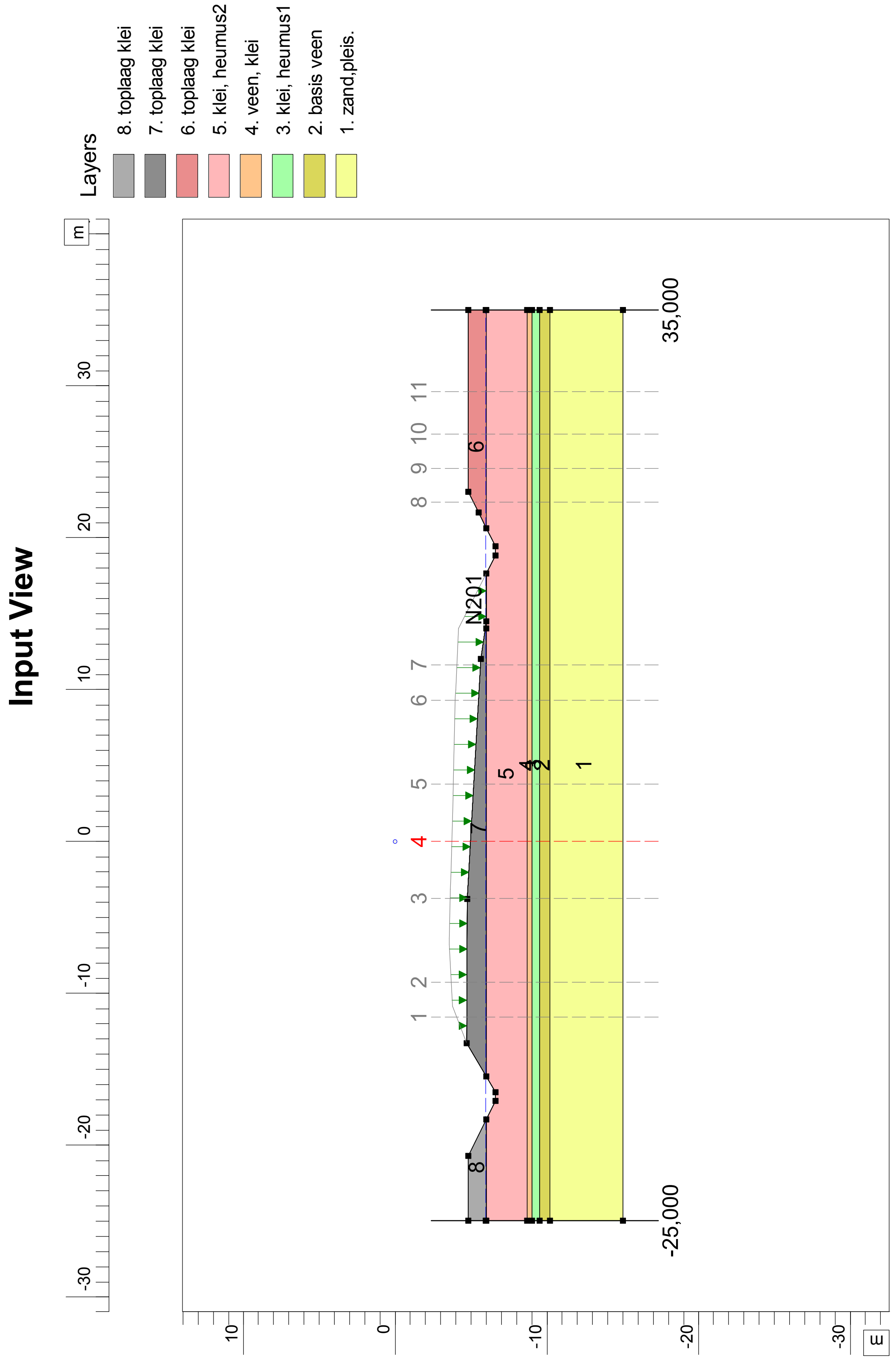

D-Settlement 15.1 : Metrering 1400.sli

Grontmij	Phone Fax	date 2008	drw. MM
N201 Amstelhoek Grondopbouw volgens B508 / DKM523		232592	ctr.
Eindzetting metrering 1400		Annex	form. A4

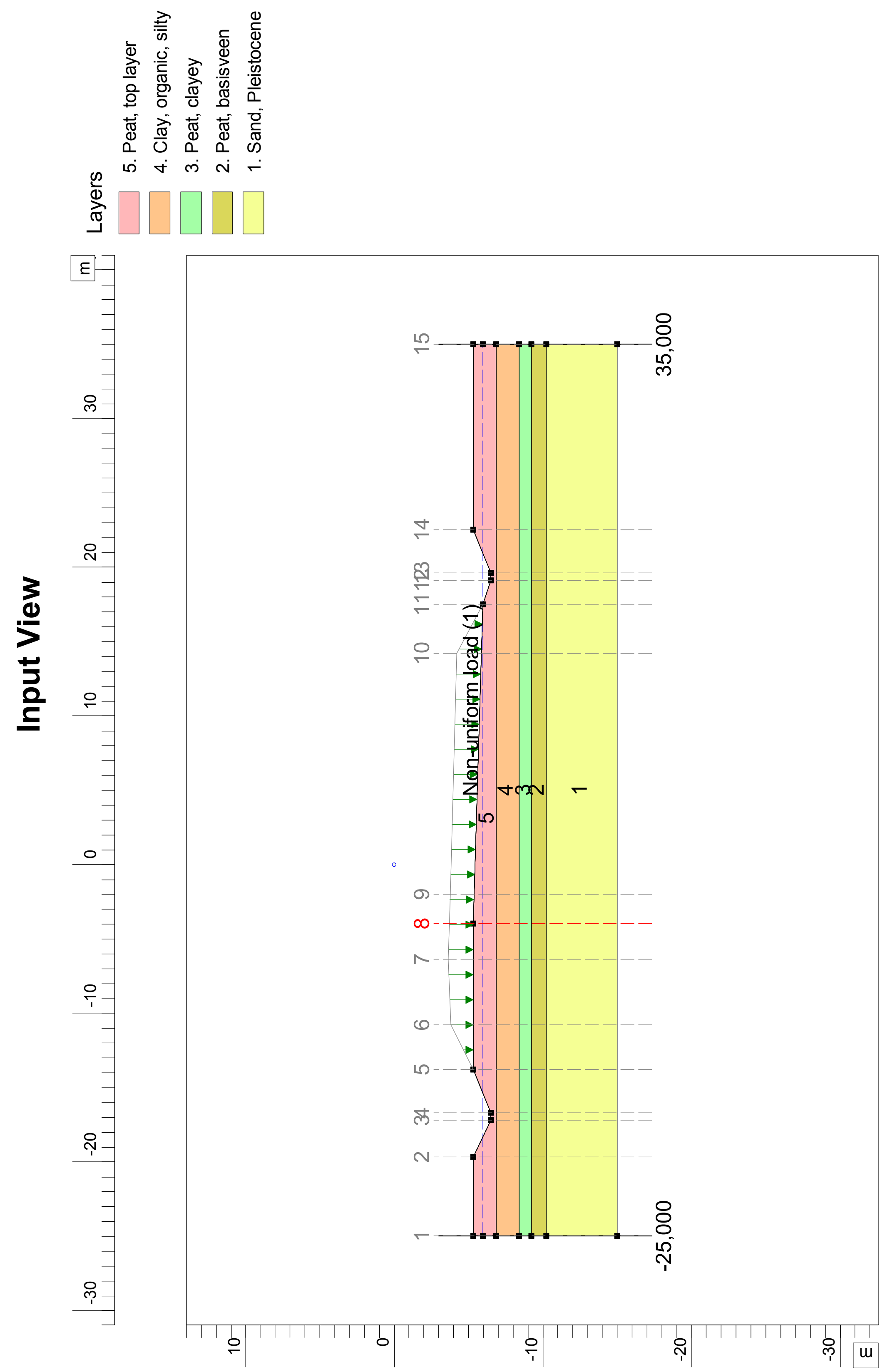

D-Settlement 15.1 : Ahk 1300m +mp.sli

Grontmij	Phone Fax	date 2016	drw. CBH
N201 bypass Amstelhoek 1300m Revisited stratigraphy & parameters 10000d, Koppejan n.s. + 'maintain profile'		- Annex -	ctr. form. A4

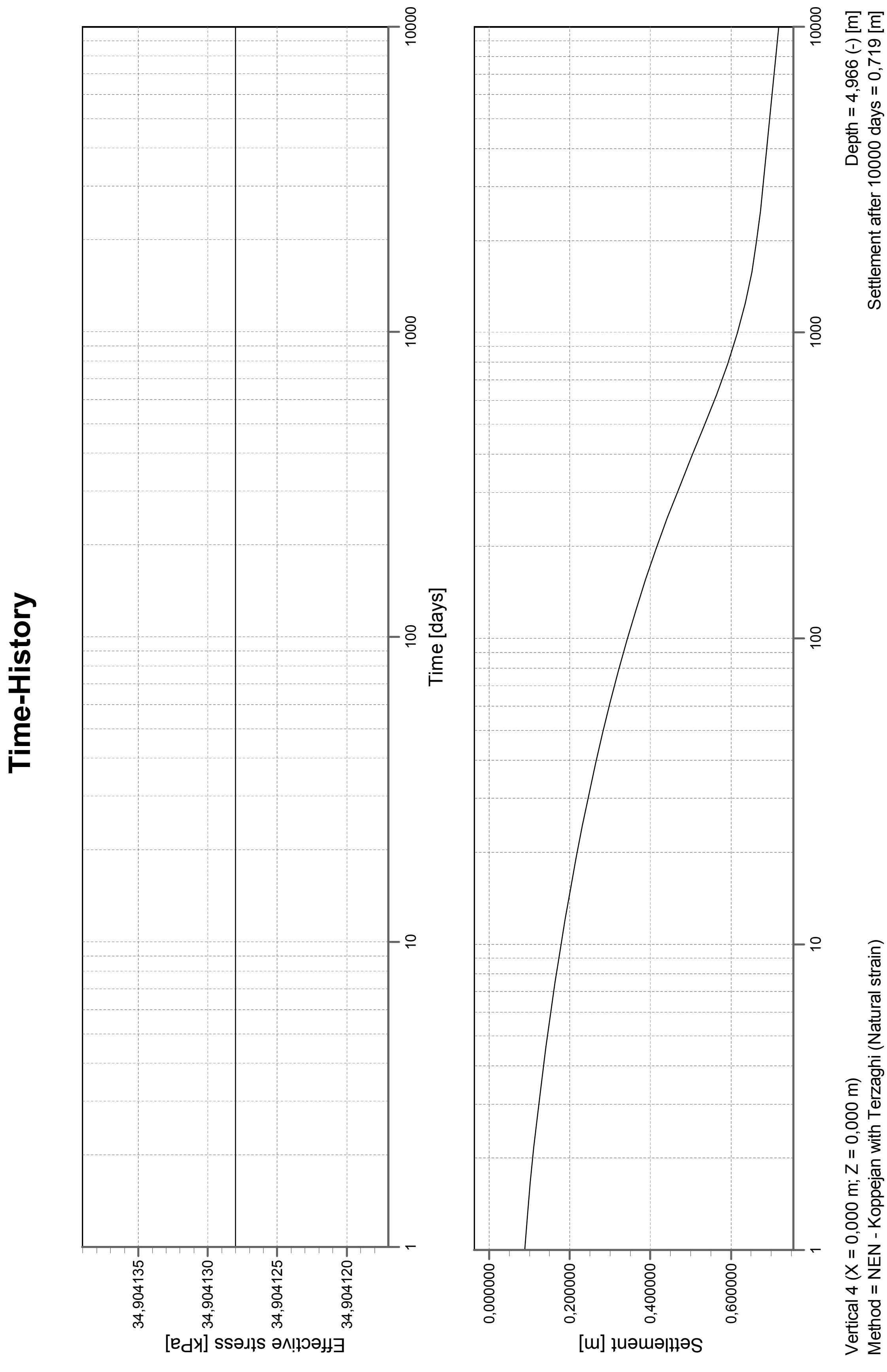

D-Settlement 15.1 : Metrering 1400.sli

Grontmij	Phone Fax	date 2008	drw. MM
N201 Amstelhoek Grondopbouw volgens B508 / DKM523		232592	ctr.
Eindzetting metrering 1400		Annex	form. A4

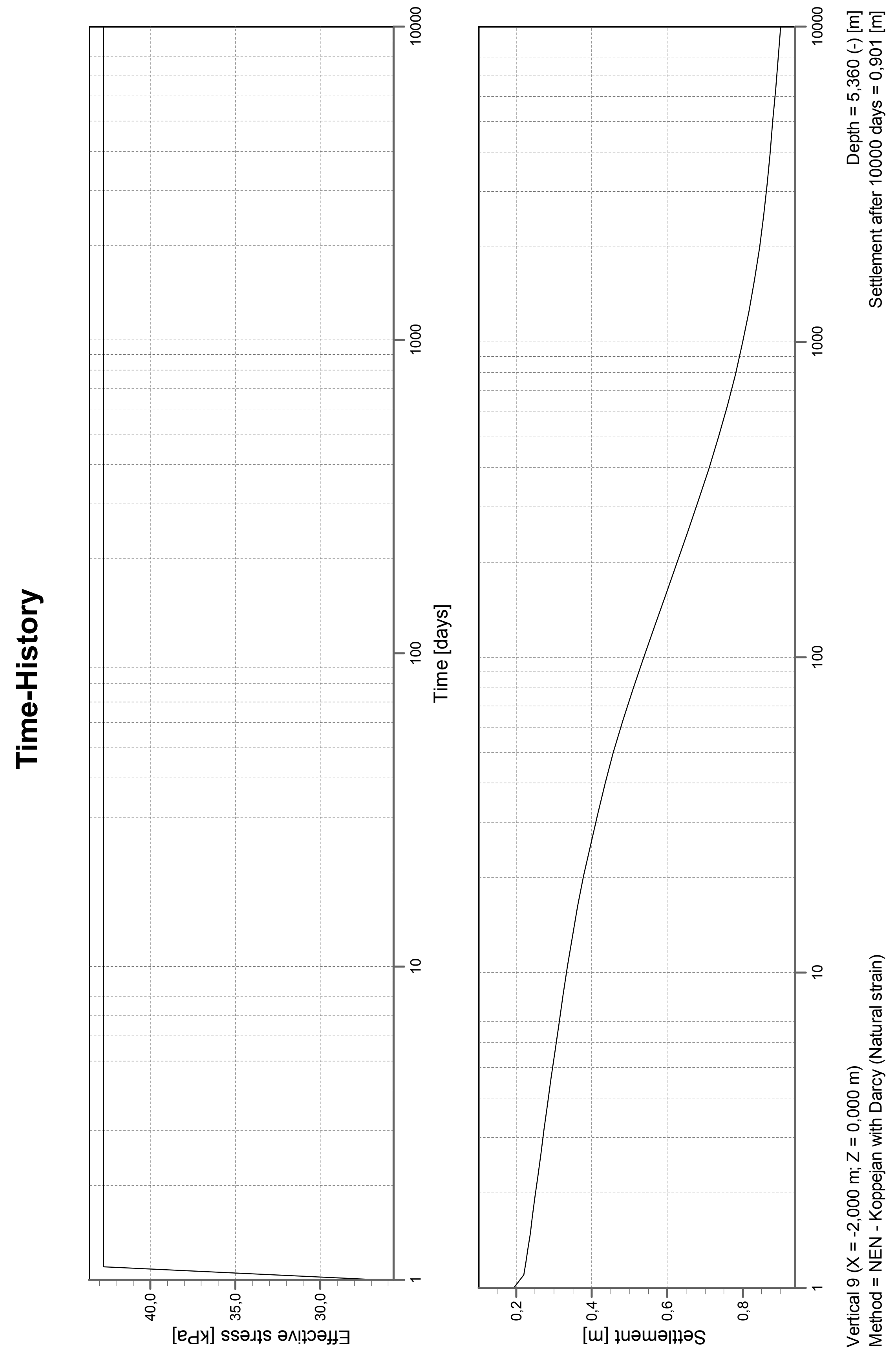

D-Settlement 15.1 : Ahk 1300m +mp.sli

Grontmij	Phone Fax	date 2016	drw. CBH
N201 bypass Amstelhoek 1300m Revisited stratigraphy & parameters		-	ctr.
10000d, Koppejan n.s. + 'maintain profile'		Annex -	form. A4

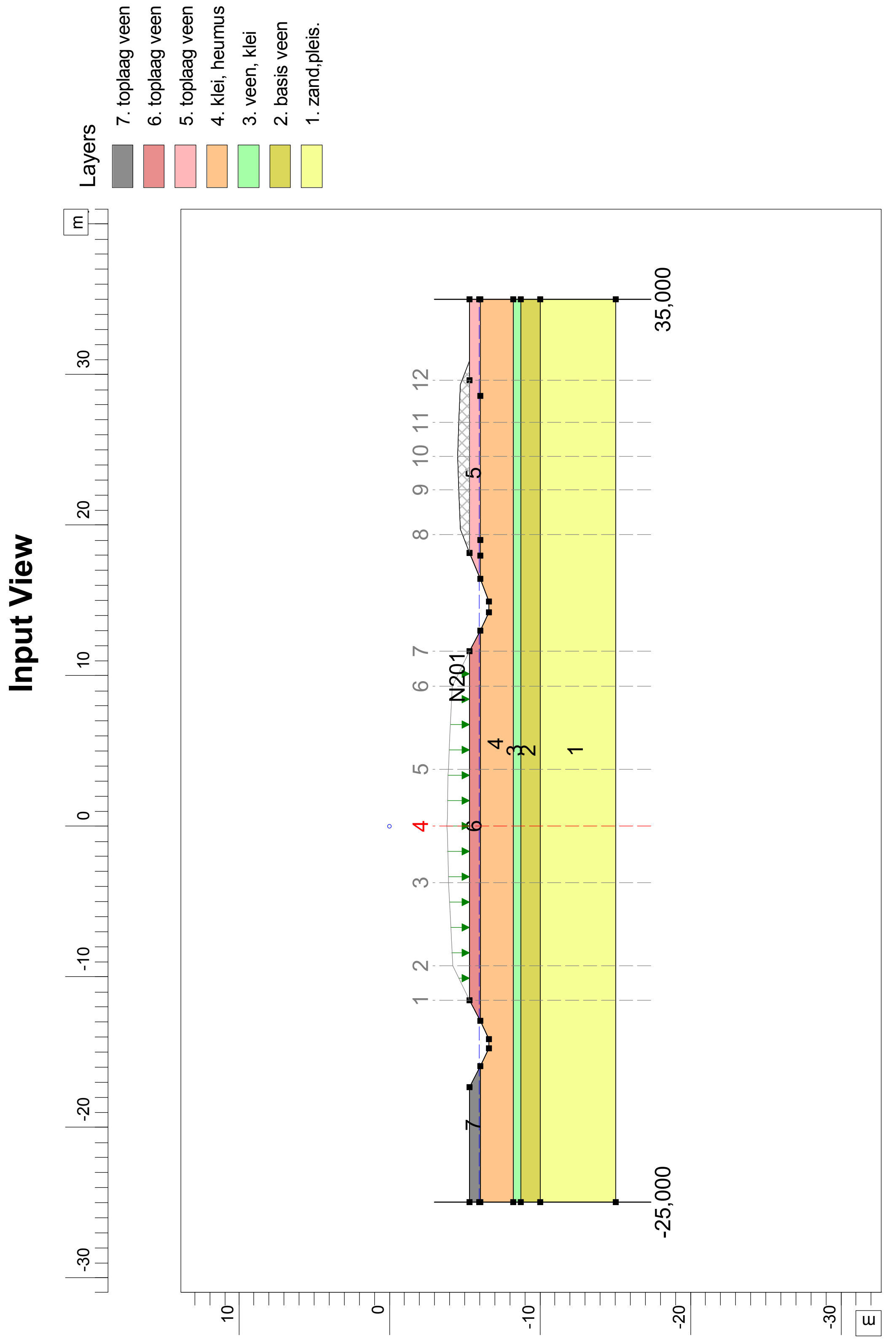

D-Settlement 15.1 : Metrering 2100.sli

Grontmij	Phone Fax	date 2008	drw. MM
N201 Amstelhoek Grondopbouw volgens B505 / DKM516		232592	ctr.
Eindzetting metrering 2100		Annex	form. A4

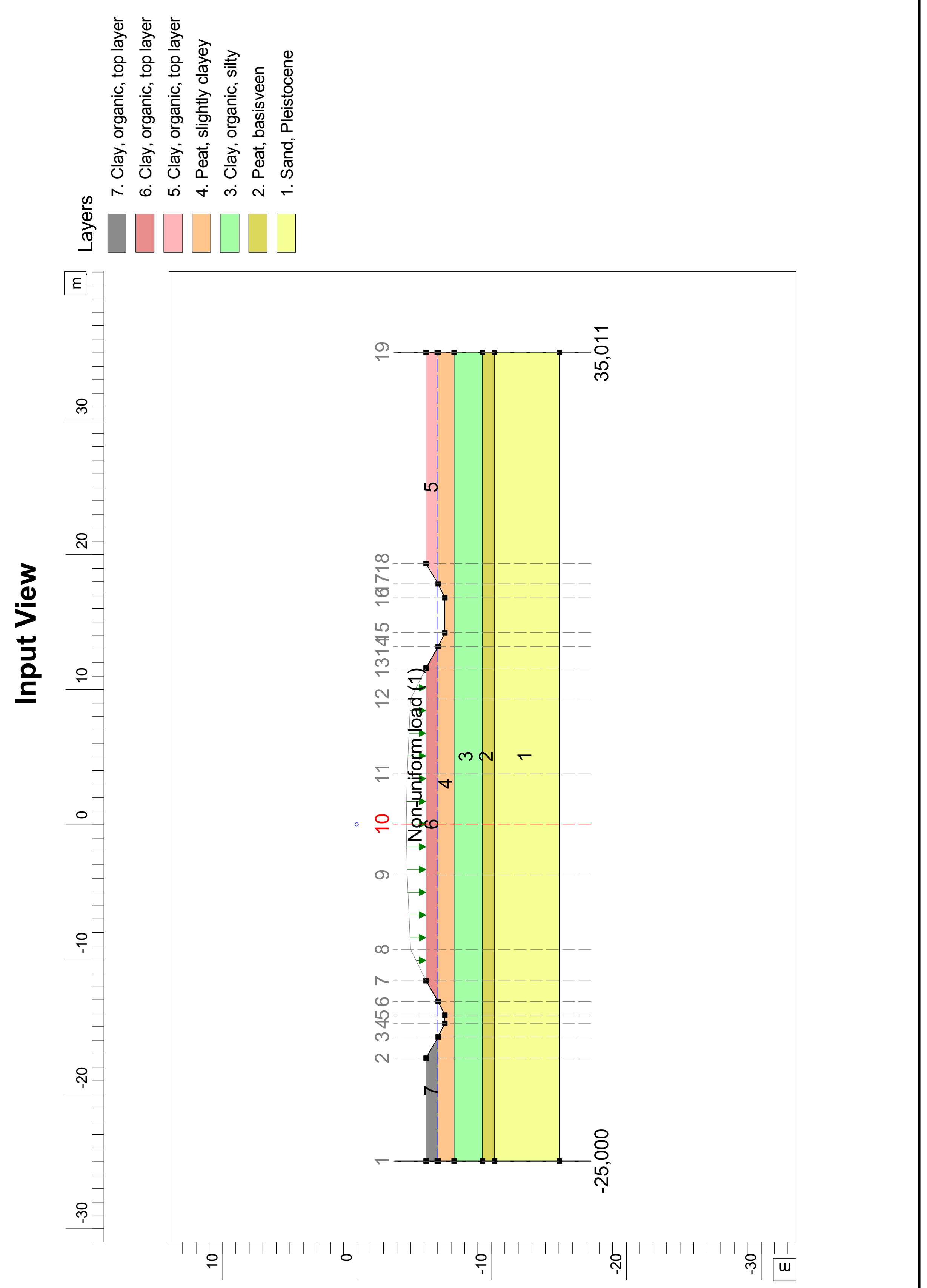

D-Settlement 15.1 : Ahk 2000m +mp.sli

Grontmij	Phone Fax	date 2016	drw. CBH
N201 bypass Amstelhoek 2000m Revisited stratigraphy & parameters 10000d, Koppejan n.s. + 'maintain profile'		- Annex -	ctr. form. A4

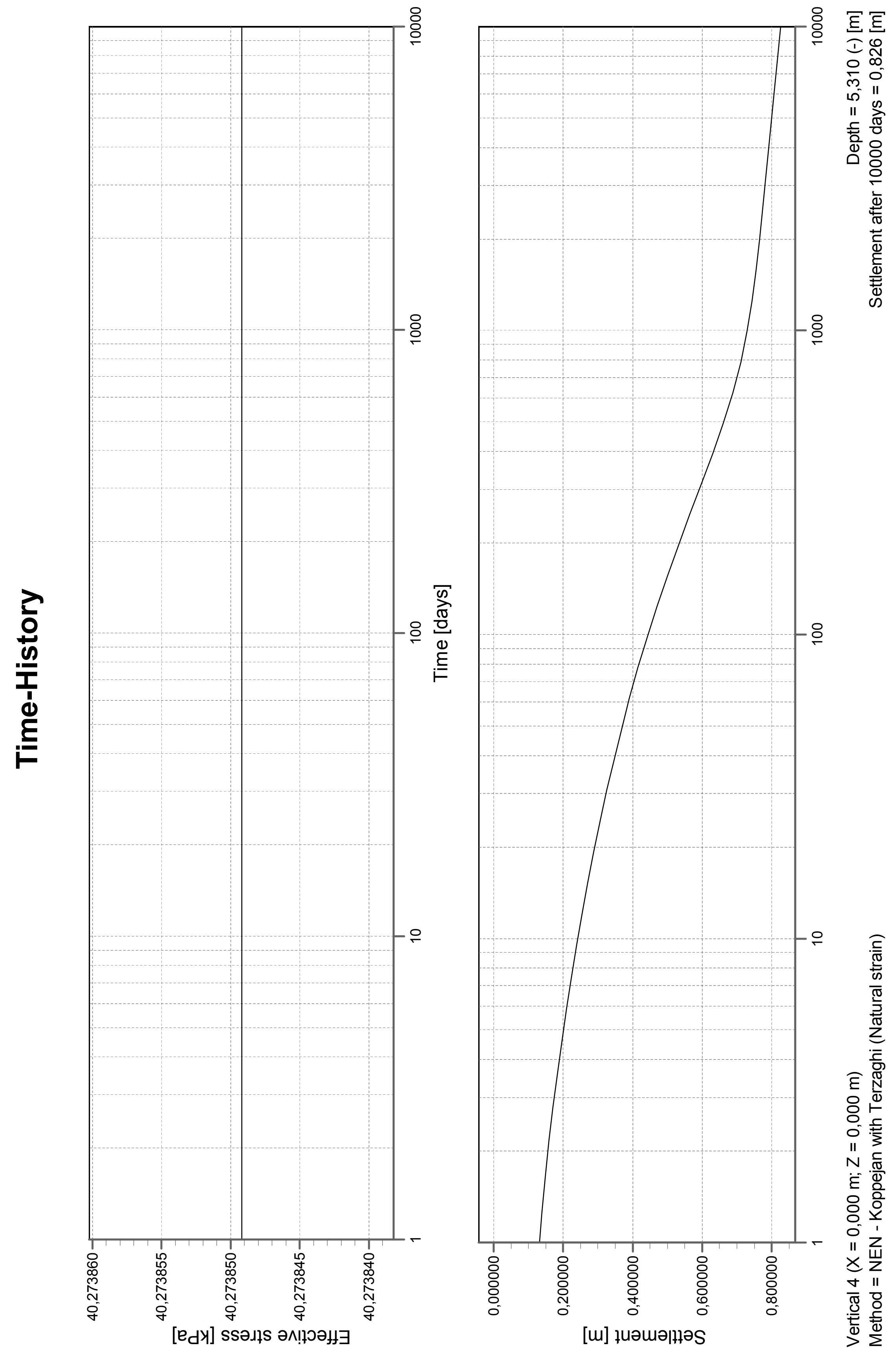

D-Settlement 15.1 : Metrering 2100.sli

Grontmij	Phone Fax	date 2008	drw. MM
N201 Amstelhoek Grondopbouw volgens B505 / DKM516		232592	ctr.
Eindzetting metrering 2100		Annex	form. A4

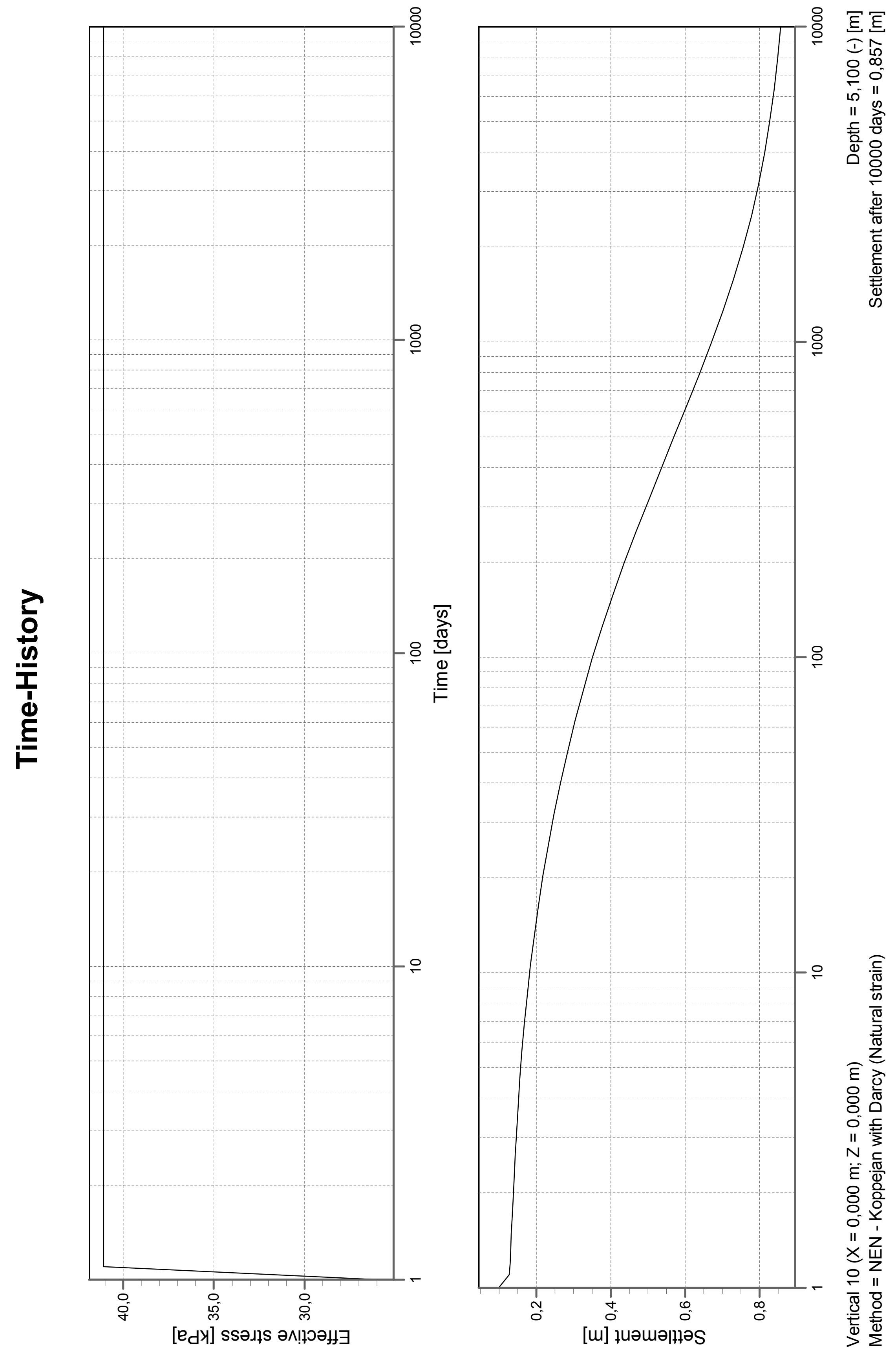

D-Settlement 15.1 : Ahk 2000m +mp.sli

Grontmij	Phone Fax	date 2016	drw. CBH
N201 bypass Amstelhoek 2000m Revisited stratigraphy & parameters		-	ctr.
10000d, Koppejan n.s. + 'maintain profile'		Annex -	form. A4

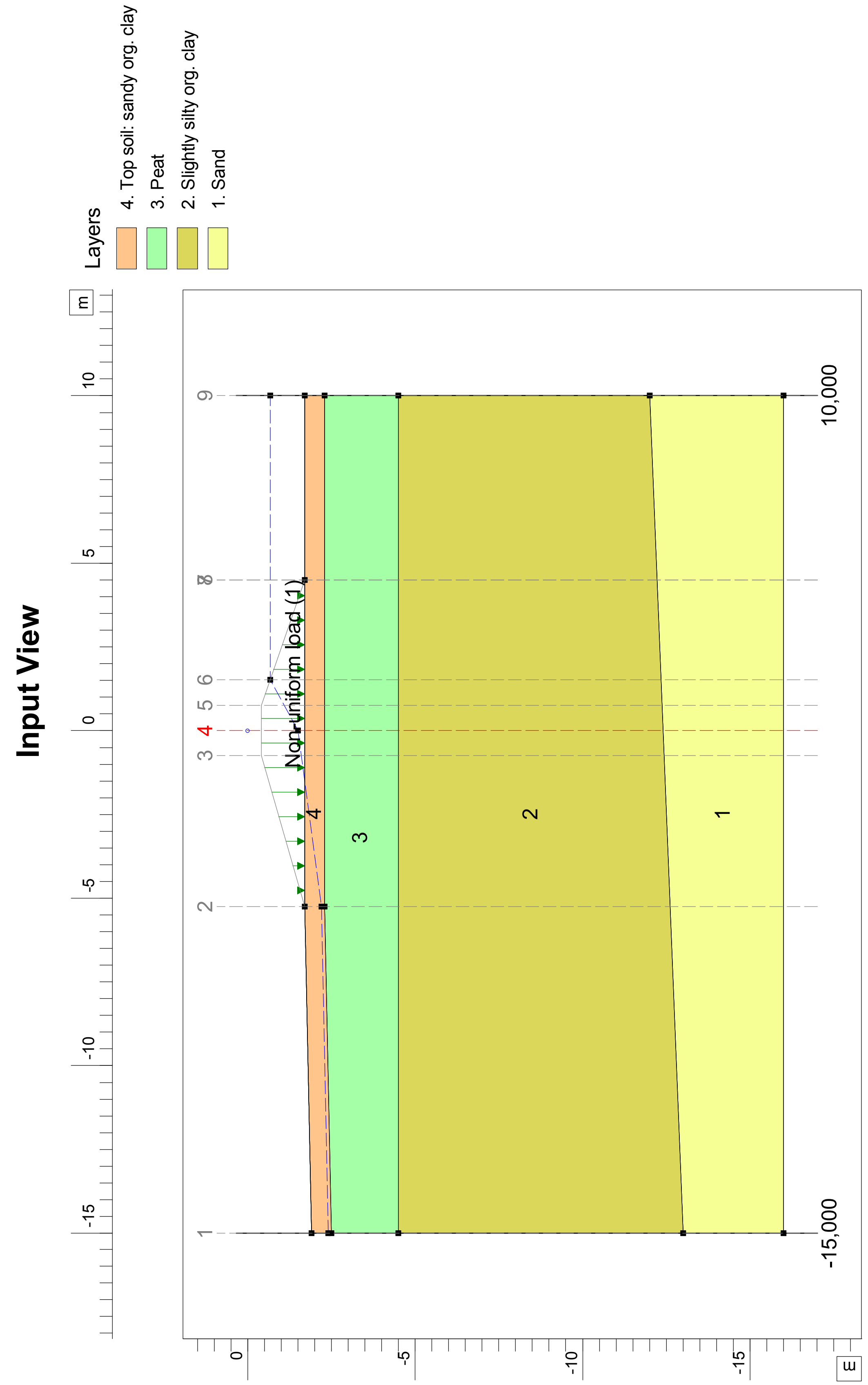

D-Settlement 15.1 : LdB NB +peat IL +mp.sli

Grontmij	Phone Fax	date 2016	drw. CBH
Leendert de Boerspolder dike IL-based peat properties 350y, NEN-Bjerrum + 'maintain profile'		- Annex -	ctr. form. A4

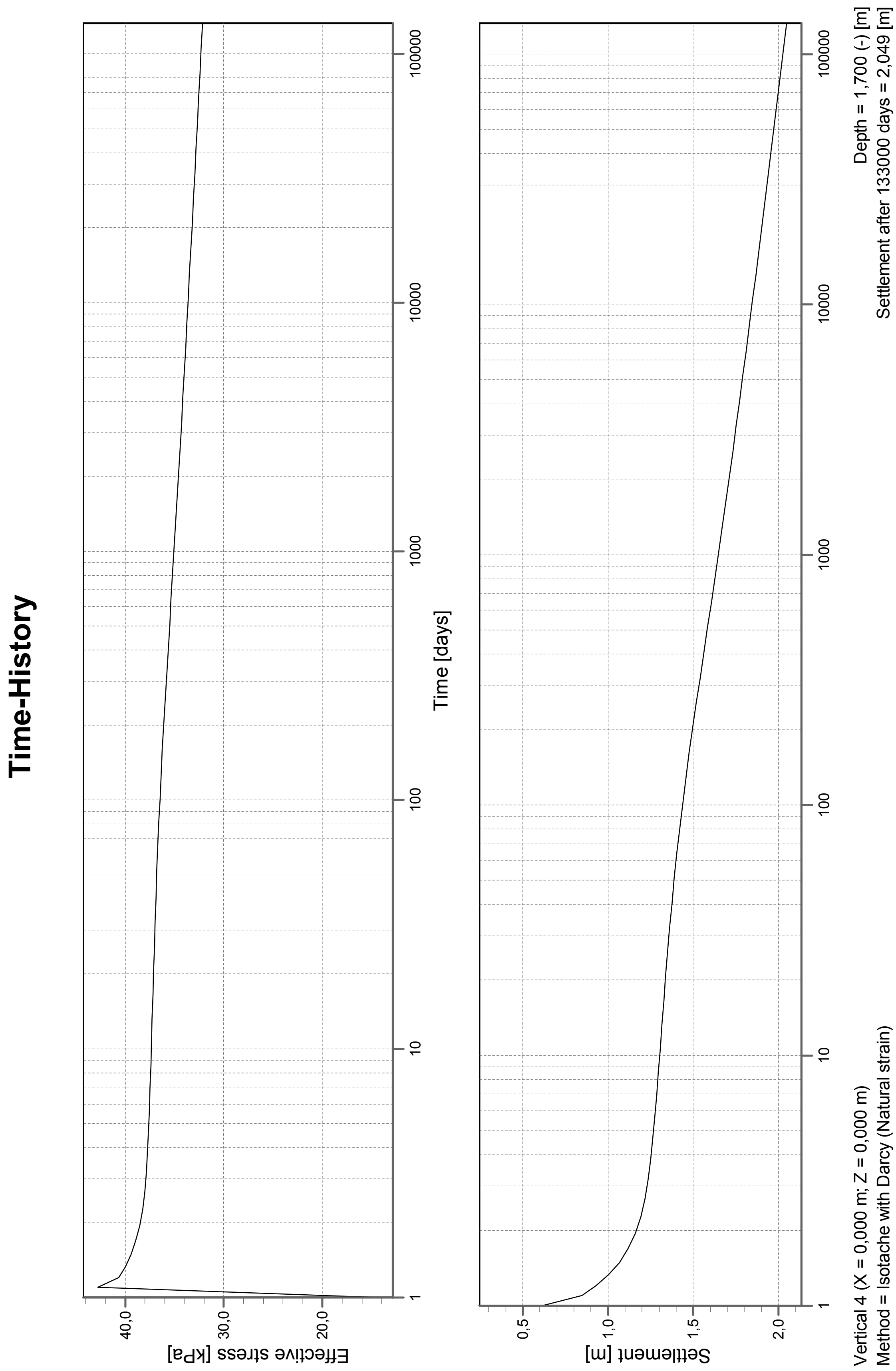

D-Settlement 15.1 : LdB abc +peat IL +mp.sli

		date	drw.
Grontmij	Phone Fax	2016	CBH
Leendert de Boerspolder dike IL-based peat properties		-	ctr.
350y, abc-Isotachs + 'maintain profile'		Annex -	form. A4

Time-History

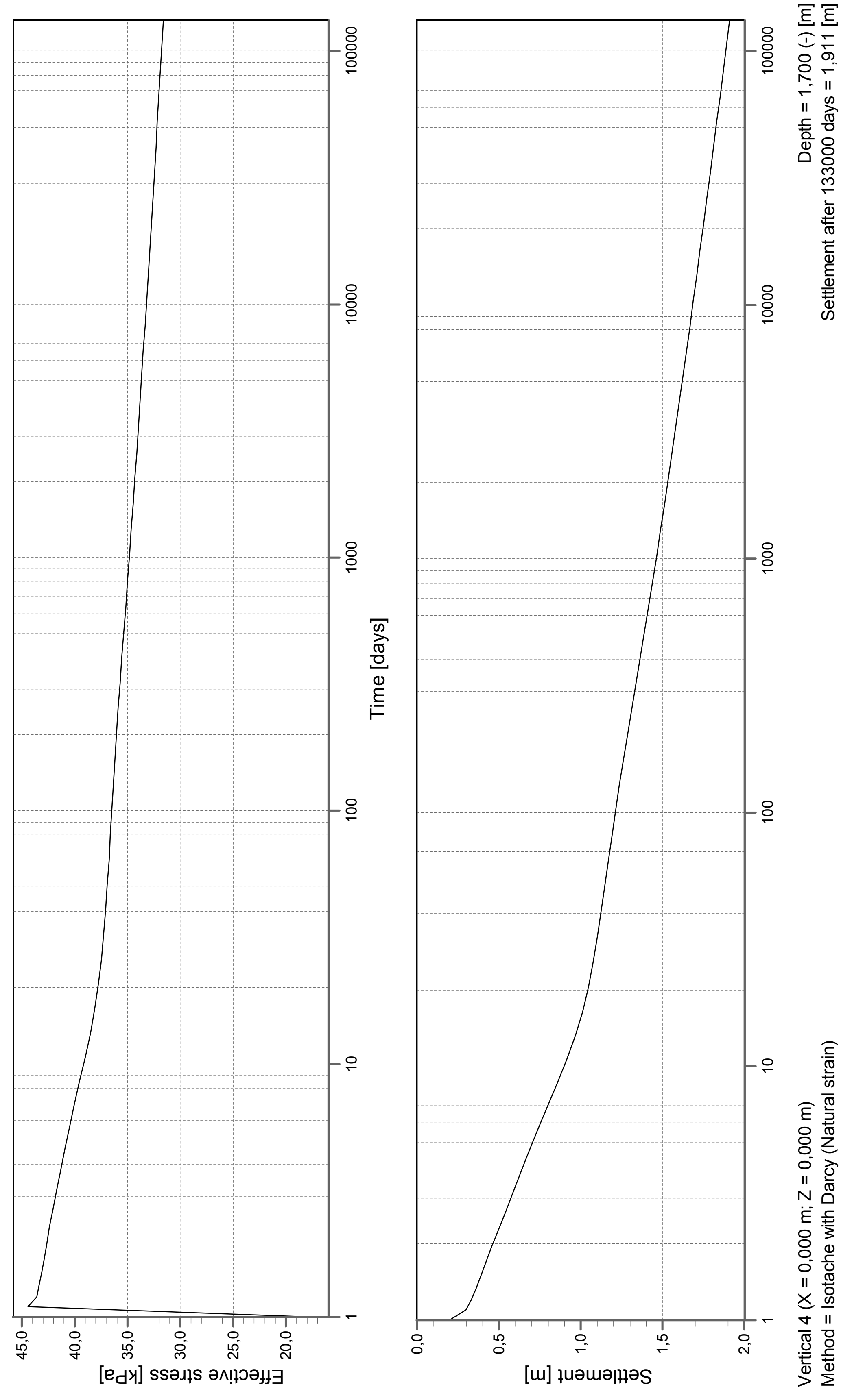

D-Settlement 15.1 : LdB abc +peat K0CRS +mp.sli

Grontmij	Phone Fax	date 2016	drw. CBH
Leendert de Boerspolder dike K0-CRS-based peat properties		-	ctr.
350y, abc-Isotachs + 'maintain profile'		Annex -	form. A4

Time-History

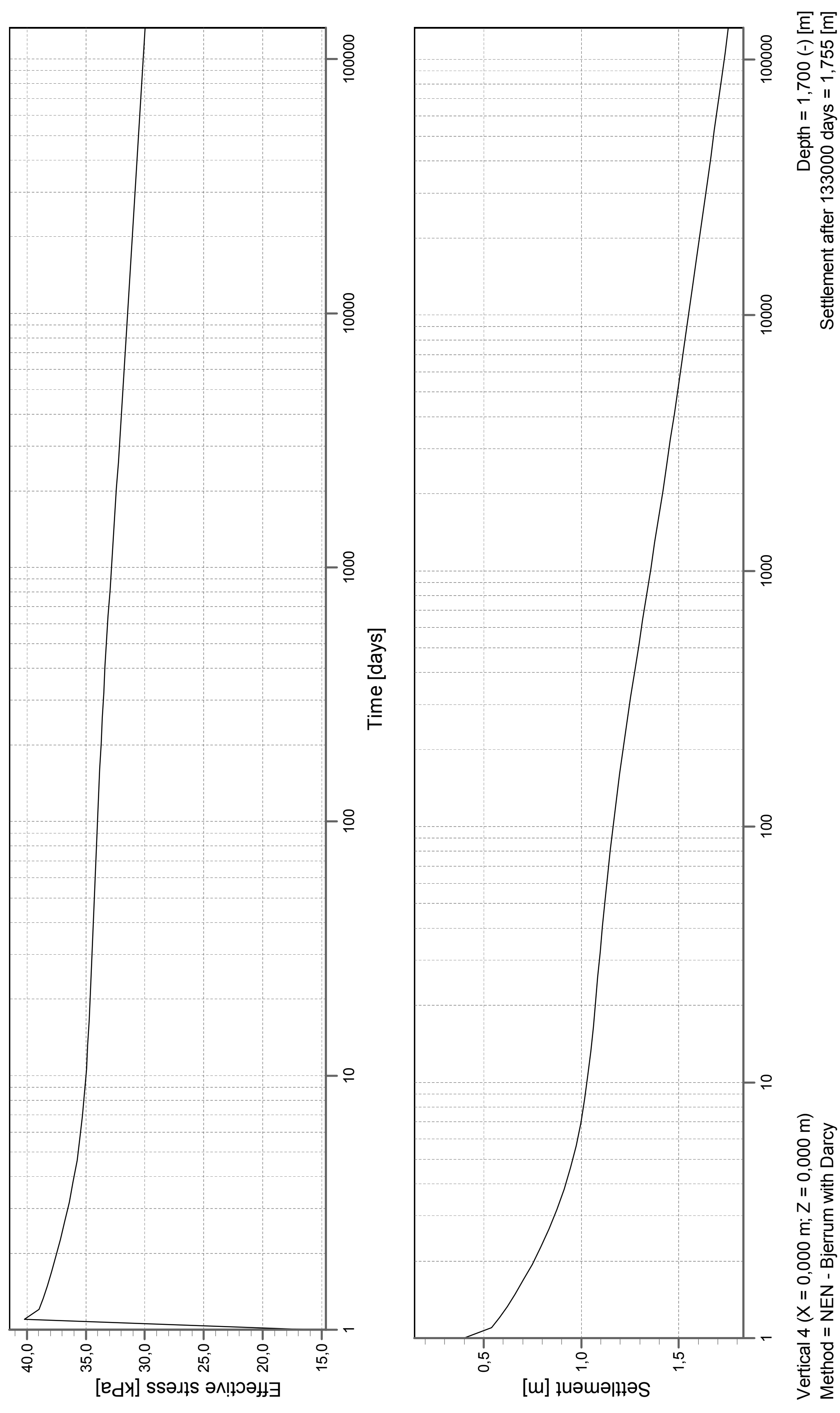

D-Settlement 15.1 : LdB NB +peat IL +mp.sli

		date	drw.
Grontmij	Phone Fax	2016	CBH
Leendert de Boerspolder dike IL-based peat properties		-	ctr.
350y, NEN-Bjerrum + 'maintain profile'		Annex -	form. A4

Time-History

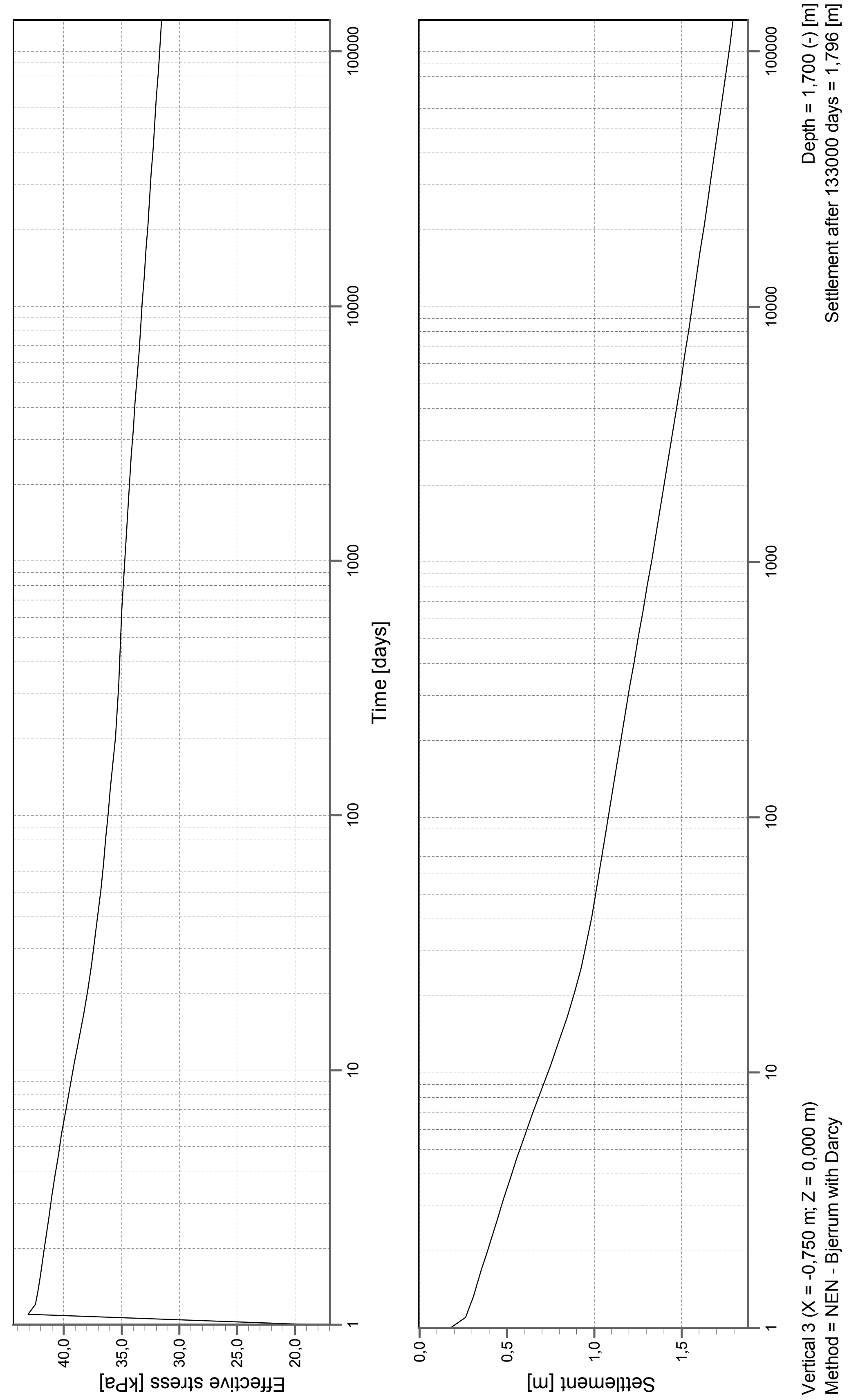

D-Settlement 15.1 : LdB NB +peat K0CRS +mp.sli

Grontmij	Phone Fax	date 2016	drw. CBH
Leendert de Boerspolder dike K0-CRS-based peat properties 350y, NEN-Bjerrum + 'maintain profile'		- Annex -	ctr. form. A4

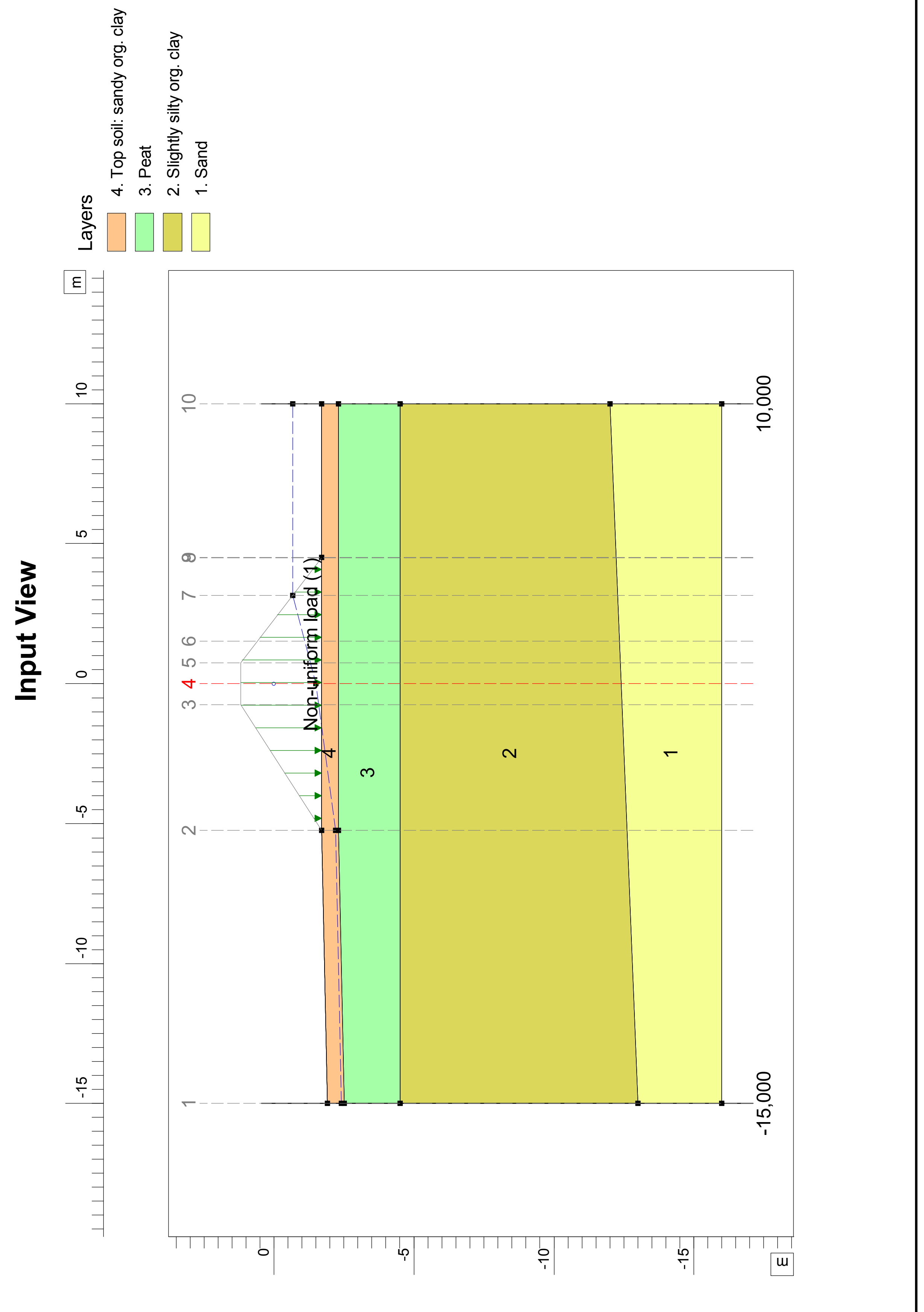

D-Settlement 15.1 : LdB abc +peat IL +without mp.sli

Grontmij	Phone Fax	date 2016	drw. CBH
Leendert de Boerspolder dike IL-based peat properties 350y, abc-Isotachs, no 'maintain profile'		-	ctr.
		Annex -	form. A4

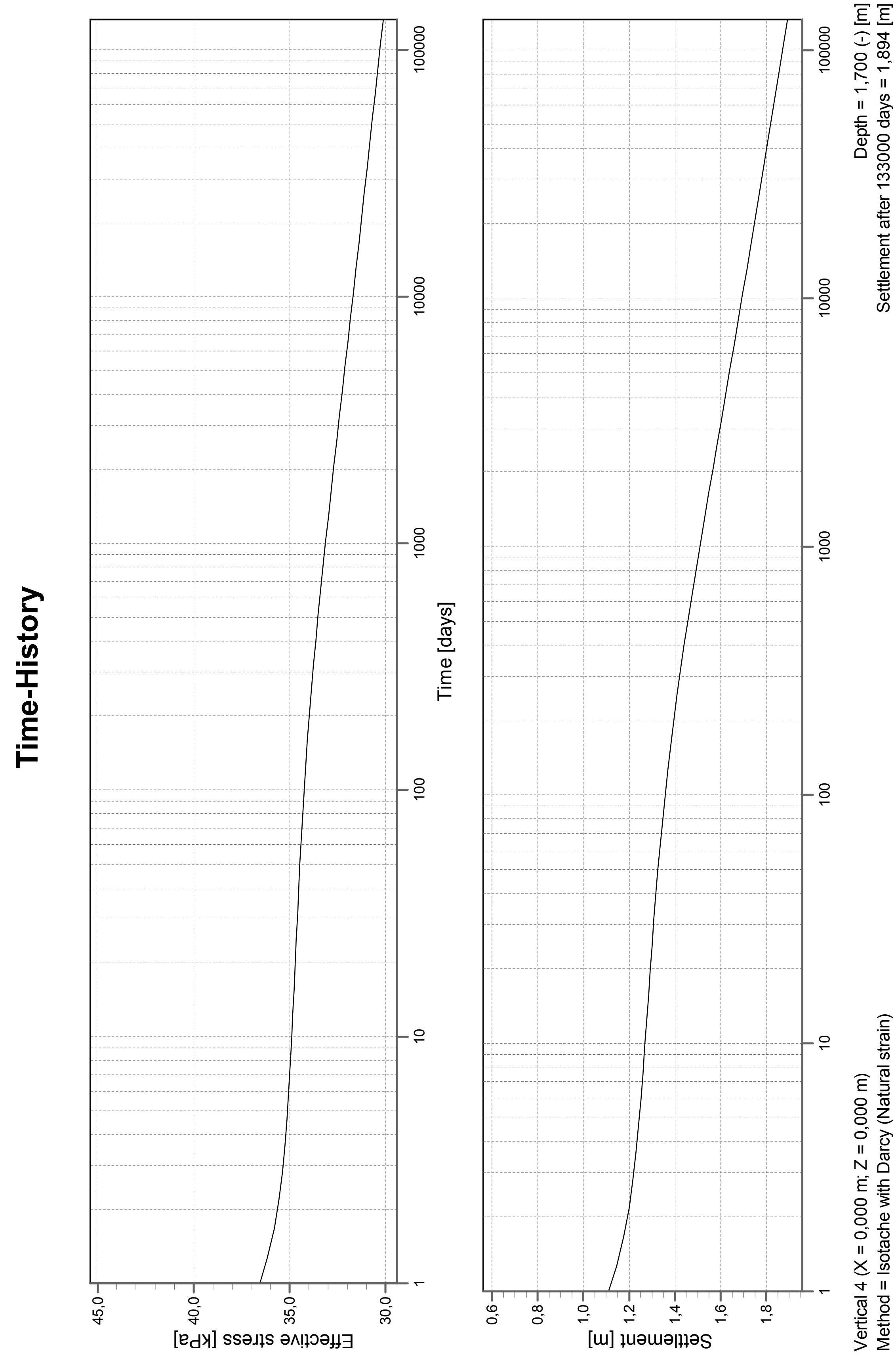

D-Settlement 15.1 : LdB abc +peat IL +without mp.sli

Grontmij	Phone Fax	date 2016	drw. CBH
Leendert de Boerspolder dike IL-based peat properties 350y, abc-Isotachs, no 'maintain profile'		- Annex -	ctr. form. A4

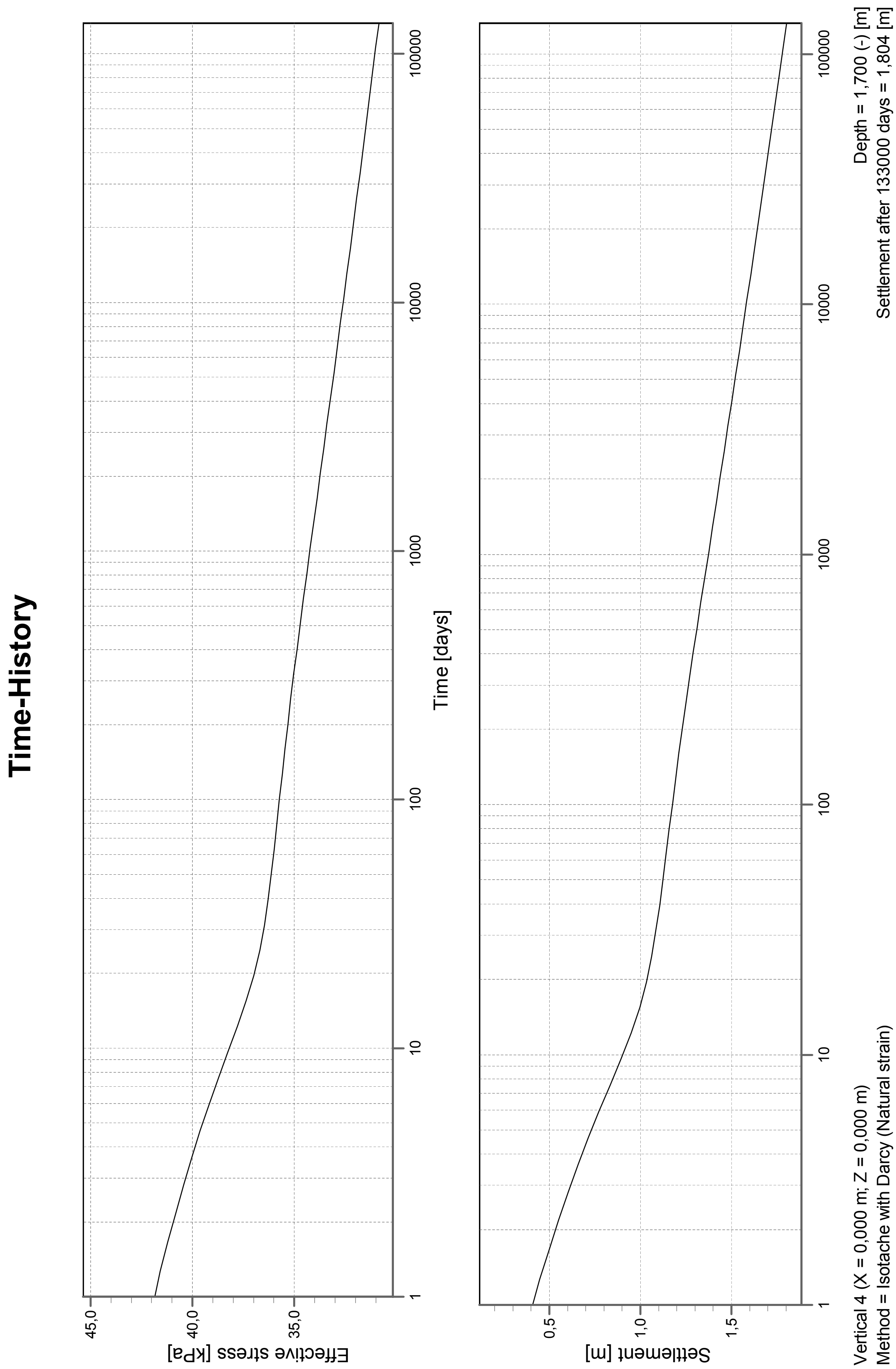

D-Settlement 15.1 : LdB abc +peat K0CRS +without mp.sli

Grontmij	Phone Fax	date 2016	drw. CBH
Leendert de Boerspolder dike K0-CRS-based peat properties 350y, abc-Isotachs, no 'maintain profile'		- Annex -	ctr. form. A4

Time-History

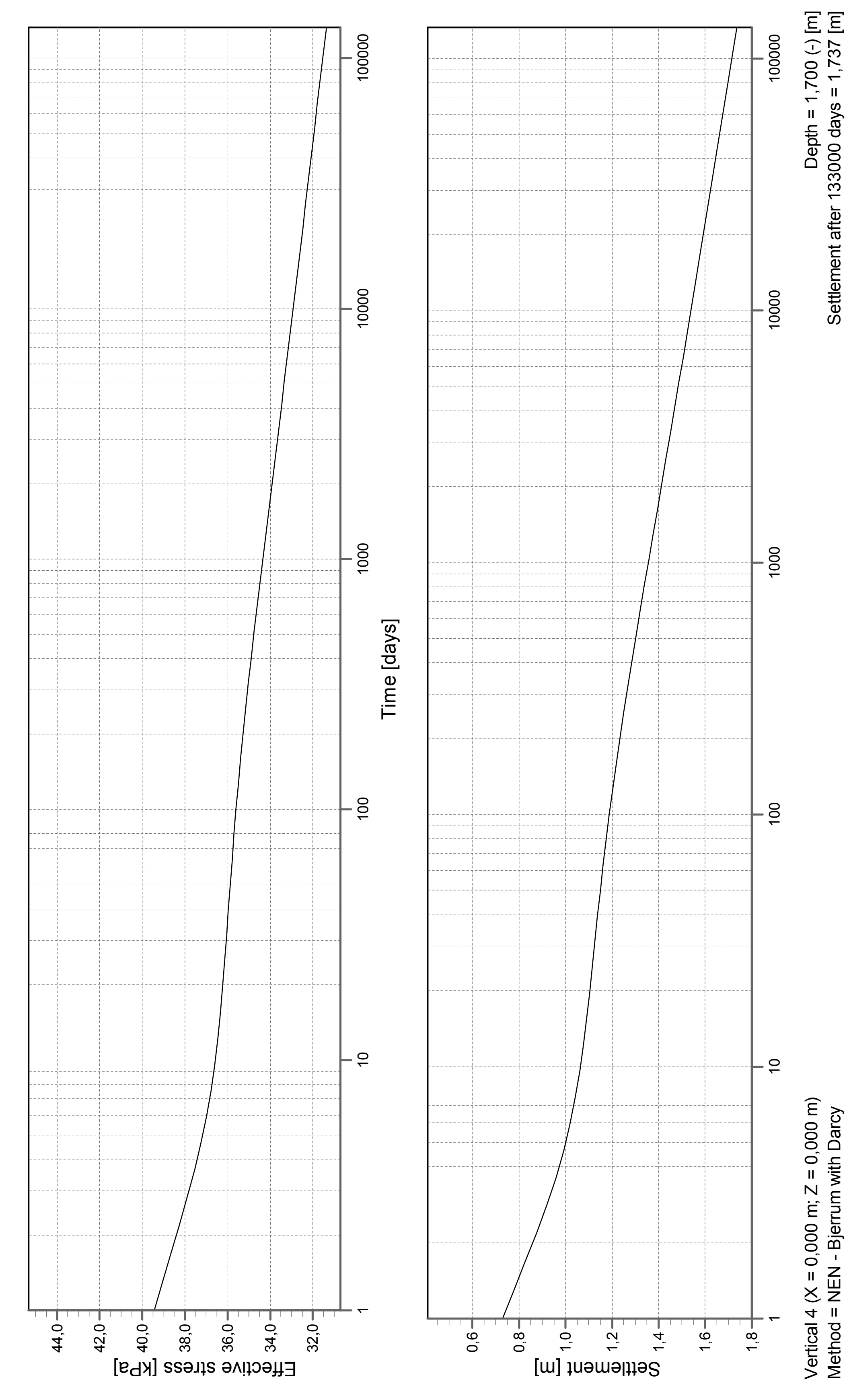

D-Settlement 15.1 : LdB NB +peat IL +without mp.sli

			date	drw.
Grontmij	Phone Fax		2016	CBH
Leendert de Boerspolder dike IL-based peat properties			-	ctr.
350y, NEN-Bjerrum, no 'maintain profile'			Annex -	form. A4

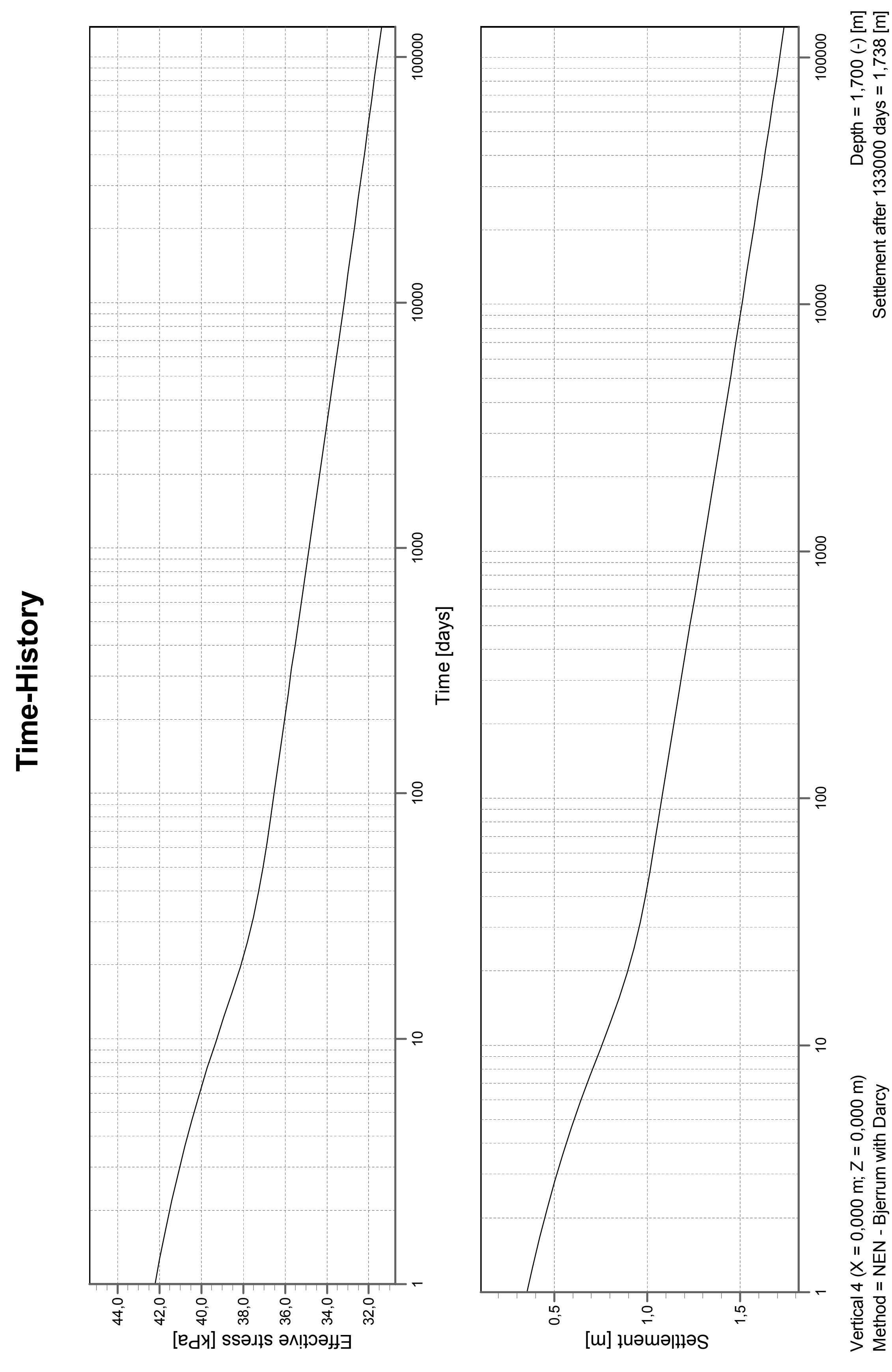

D-Settlement 15.1 : LdB NB +peat K0CRS +without mp.sli

Grontmij	Phone Fax	date 2016	drw. CBH
Leendert de Boerspolder dike K0-CRS-based peat properties		-	ctr.
350y, NEN-Bjerrum, no 'maintain profile'		Annex -	form. A4